Society of Skeletal Radiology

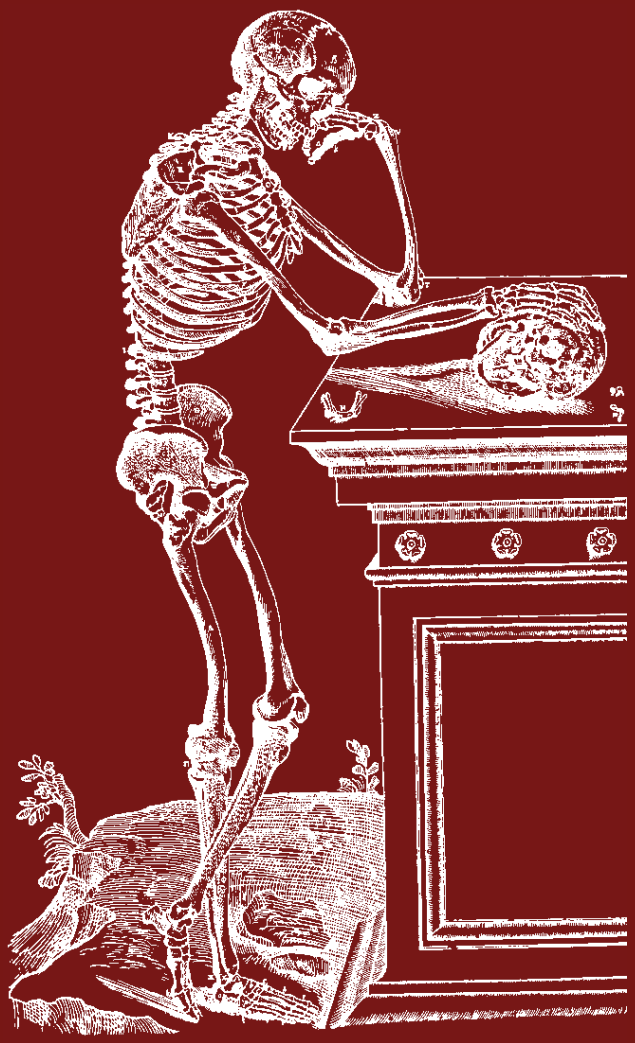

42ND ANNUAL MEETING

March 10 – 13, 2019

2019

JW Marriott Scottsdale Camelback Inn Resort & Spa
Scottsdale, AZ

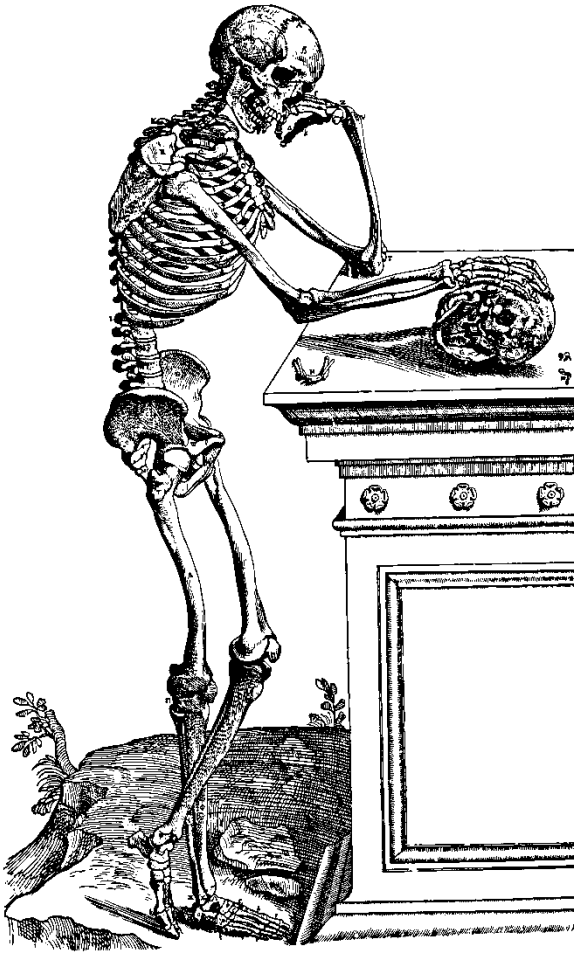

Society of Skeletal Radiology 42nd Annual Meeting

March 10-13, 2019

JW Marriott Scottsdale Camelback Inn Resort and Spa

Scottsdale, Arizona

Table of Contents

Welcome

Society of Skeletal Radiology

42nd Annual Meeting
March 10-13, 2019
JW Marriott Camelback Inn
Resort and Spa
Scottsdale, Arizona

Dear Colleagues and Friends,

Welcome to the 42nd Annual SSR Scientific Meeting at the JW Marriott Scottsdale Camelback in Scottsdale, Arizona! We hope that you are getting excited about another fantastic scientific program in the luxury oasis of the Sonoran Desert.

Our annual meeting is made possible only though the tireless efforts of our committee chairs, the executive committee, and our management team at Veritas Meeting Solutions. Although the meeting is the visible reward of that work, activities of the society leadership occur year-round. Thank you to all those who contribute.

I would like to specifically thank and acknowledge the efforts of this year's program committee members, Donna Blankenbaker, Catherine Roberts, David Rubin, and Mihra Taljanovic, as well as MK Jesse and Brian Petersen for coordinating this year's SAM sessions. Thanks also to Ben Levine for coordinating the Ultrasound Hands-On Session (this year focusing on the Foot & Ankle) and Daniel Wessel for coordinating the Case-of-the-Day presentations.

Abstract and Eposter submission quality were impressive again this year. As before, ePosters have been arranged into groups corresponding to the themes of the scientific sessions. In addition to the regular slate of selected podium scientific presentations, this year's program will feature two invited abstracts including the inaugural ESSR paper award presentation selected as best paper from the proceedings of the 2018 annual ESSR meeting, as well as an abstract pertaining to the 2018 SSR Seed Grant research award project. The SSR is proud to continue to offer the Seed Grant and Young Investigator Awards. Be sure to remind your Fellows / MIT members about this member benefit, as awards are selected by the Research Committee in January of the Meeting year.

Microphone, projected screen and Twitter interaction will be provided in order to maximize audience participation during the meeting. All podium and poster authors have been asked to set up Twitter conversations regarding their presentations, so that participants can continue discussion on each topic after the allotted general discussion period for each paper. Look for the "hashtag" identifier on the presentation slides.

The program committee invites you to relax and enjoy this year's offerings, both in and out of the meeting room.

Warmly,

Lawrence M. White, MD FRCPC
2019 Program Committee Chair

2018–2019 Committees

EXECUTIVE COMMITTEE

President
Laura Bancroft, MD, FACR

President-Elect
Lawrence White, MD

Secretary
Donna Blankenbaker, MD

Treasurer
Jon Jacobson, MD

Past President
Andrew Sonin, MD, FACR

Archive and History Committee
William Conway, MD (Committee Chair)
Carol Andrews, MD
Barbara Weissman, MD

Audit Committee
Thomas Lee Pope Jr., MD, FACR (Committee Chair)
Elaine Susan Gould, MD, FACR (Co-Chair)
Kirk Davis, MD

Electronic Learning Committee
Jeffrey M. Brody, MD, FACR (Committee Chair)
Theodore Miller, MD (Co-Chair)
Richard Barger, MD
Connie Chang, MD
Alex Chien, MD
Travis Hillen, MD
Matthew Larrison, MD
Ken Schreibman, MD

Electronic Exhibit Judge Committee
Kirkland Davis, MD
Russ Chapin, MD
Peter Evangelista, MD
Hakan IIaslan, MD
Linda Probyn, MD
Corrie Yablon, MD

Finance Committee
Jon Jacobson, MD (Committee Chair)
Eric Brandser, MD
Michael Tuite, MD

Health and Wellness Committee
Don Flemming, MD (Committee Chair)
Hailey Allen, MD
Eric Brandser, MD
Felix Chew, MD
Richard Daffner, MD, FACR
Derik Davis, MD
Zach Elliott, DO
Dave Fessell, MD
Alice Ha, MD
Corrie Yablon, MD

Membership Committee
Jon Baker, MD (Committee Chair)
Darus "Lee" Bennett, MD, MA, MBA (Co-Chair)
Michael Fox, MD
Jennifer Hinkle, MD
Rosemary Klecker, MD
Sarah Koles, MD

Nominating Committee
Corrie Yablon, MD (Committee Chair)
Laura Bancroft, MD, FACR (President)
Jim Wu, MD (Chair of Rules Committee)

Podium Presentation Judge Committee
David Rubin, MD (Committee Chair)
Jenifer Demertzis, MD
Laura Fayad, MD
MK Jesse, MD
Brian Petersen, MD

Practice Parameters and Technical Standards Committee
Mary Hochman, MD, MBA (Committee Chair)
Richard Walker, MD (Co-Chair)
Daniel Siegal, MD
Naveen Subhas, MD
Andrew Wilmont, MD
Tony Wong, MD

Program Committee
Lawrence M. White, MD (Committee Chair)
Donna Blankenbaker, MD
Catherine Roberts, MD
Mihra S. Taljanovic, MD
David Rubin, MD (ad-hoc)

Research Committee
Andrew Cordle, MD (Committee Chair)
Jordan Scotty Gross, MD (Co-Chair)
Avneesh Chhabra, MD
Leah Davis, MD
MK Jesse, MD
Nicola Refky, MD

Residency and Fellowship Education Committee
Jennifer Demertzis, MD (Committee Chair)
Bethany Casagranda, DO (Co-Chair)
Shivani Ahlawat, MD
Eric Goodman, MD
Soterios Gyftopoulos, MD
Alice Ha, MD
Sung Han Kim, MD
Kaushal Mehta, MD
Kurt Scherer, MD

Rules Committee
Jim Wu, MD (Committee Chair)
Kambiz Motamedi, MD (Co-Chair)
Shaifali Kaushik, MD
Jonathan Luchs, MD
Geoffrey Riley, MD
Dave Rubin, MD

Social Media AdHoc Committee
Soterios Gyftopoulos, MD (Co-Chair)
Naveen Subhas, MD (Co-Chair)

Socioeconomic Affairs Committee
Jonathan Flug, MD (Committee Chair)
Eric Friedberg, MD (Co-Chair)
Ian Amber, MD
Gregory Harkey, MD
David W. Tsai, MD
Stan Weiss, MD

SSR Representatives to Other Societies
Jonathan Flug, MD (ACR Councilor)
Christopher Hanrahan, MD (ACR Alternate Councilor)
Miriam A. Bredella, MD (AAR)
Jon Jacobson, MD (ESSR Liaison/ISS Liaison)
Jon Jacobson, MD (AIUM/AMSSM Nomenclature Task Force)
Joseph Craig, MB, ChB (AIUM Liaison)

Sponsor and Vendor Relations (Ad Hoc)
William Morrison, MD

Executive Office
Veritas Meeting Solutions
Sue O'Sullivan, Executive Director
1061 East Main Street, Suite 300
East Dundee, IL 60118
Email: admin@skeletalrad.org
Phone: 847-752-6626

Accreditation

Sponsored for Continuing Medical Education credit by Rush University Medical Center

Learning objectives

At the conclusion of this activity, the learner will be able to:

1. Apply real life situations to clinical practice;
2. Integrate knowledge and performance in the assessment and diagnosis of musculoskeletal sports injury, tumors, trauma and degenerative disease;
3. Identify the anatomy of normal MSK tissues, variants and mimicker of disease;
4. Identify morphologic, histologic and imaging characteristics of MSK disease;
5. Describe the specific pathology that accounts for the appearance of osseous and soft tissues in the setting of trauma, overuse, degeneration, inflammatory/autoimmune and neoplastic conditions on various imaging modalities;
6. Recognize the relationship of specific biomechanical activities, injuries and treatments to the appearance of joints, bone, and soft tissues on imagine, arthroscopic, and pathologic assessment;
7. Review the optimal role of imaging, surgery and histopathology in the diagnosis and management of musculoskeletal disease and health;
8. Identify the complementary role of emerging imaging techniques, modalities, and interventional/therapeutic procedures in the diagnosis and management of specific musculoskeletal conditions;
9. Illustrate competency in Ultrasound, MRI, and therapeutic approaches in the assessment and management of the musculoskeletal system.

To obtain credit you must be present for the session, complete the program evaluation which will be emailed to you the last day of the meeting. Certificates of participation will be sent by e-mail 7-10 days after the closing of the Society of Skeletal Radiology Annual Meeting.

Rush University Medical Center is accredited by the Accreditation Council for Continuing Medical Education to provide continuing medical education for physicians. Rush University Medical Center designates this live activity for a maximum of 20.25 AMA PRA Category 1 Credit(s)™ Physicians should claim only credit commensurate with the extent of their participation in the activity.

It is the policy of the Rush University Medical Center Office of Interprofessional Continuing Education to ensure that its CE activities are independent, free of commercial bias and beyond the control of persons or organizations with an economic interest in influencing the content of CE. Everyone who is in a position to control the content of an educational activity must disclose all relevant financial relationships with any commercial interest (including but not limited to pharmaceutical companies, biomedical device manufacturers, or other corporations whose products or services are related to the subject matter of the presentation topic) within the preceding 12 months. If there are relationships that create a conflict of interest, these must be resolved by the CE Course Director in consultation with the Office of Interprofessional Continuing Education prior to the participation of the faculty member in the development or presentation of course content.

Specific Planner and Faculty disclosures can be found on the CME handout in your registration packet.

In accordance with requirements of the FDA, the audience is advised that information presented in this continuing medical education activity may contain references to unlabeled or unapproved uses of drugs or devices. Please refer to the FDA approved package insert for each drug/device for full prescribing/utilization information.

Self-Assessment Module (SAM)

This module (or activity) meets the ABR's criteria for a self-assessment activity in the ABR Maintenance of Certification program:

Focus Session / Self-Assessment Module I: **Spine Intervention** *1.5 credits*
Focus Session / Self-Assessment Module II: **Elbow and Forearm Imaging** *1.5 credits*

Musculoskeletal Ultrasound Hands-On Workshop: Ankle/Foot

Needs

Achieving competence in ultra sound of the Foot/Ankle not only depends on knowledge of anatomy and pathology, but also familiarity with various techniques of acquiring ultrasound images including positioning, placement of the probe and methods for visualization of structures and avoiding artifact. Successful ultrasound of the Foot/Ankle is largely dependent on the skills of the individual performing the ultrasound. One of the most effective learning formats is a hands- on workshop supervised by experienced instructors.

Objectives

At the completion of the ultrasound workshop, the participant will able to:

Explain and perform ultrasound examination of the Foot/Ankle

SSR Paper Award Winners

2018
Miriam Bredella, MD
"Brown Adipose Tissue and Cancer Activity"
Selected for presentation at RSNA

Nicholas Rhodes, MD
"Pacinian Corpuscles: Bright Palmar Blind-Spots on MRI"
Selected for presentation at ISS

2017
Soterios Gyftopoulos, MD
"Cost-effectiveness of MRI Versus Ultrasound for the Detection of Full-thickness Rotator Cuff Tears"
Selected for presentation at RSNA

John Symanski, MD
"Diagnosis of Superior Glenoid Labral Tears Using MRI and MRA: A Systematic Review and Meta-Analysis"
Selected for presentation at ISS

2016
Naveem Subhas, MD
"A 5-minute shoulder MRI: Is it Good Enough?"
Selected for presentation at RSNA

MK Jesse, MD
"Radiculopathy Following Vertebral Body Compression Fracture: Is There a Role for Percutaneous Cement Augmentation?"
Selected for presentation at ISS

2015
Soterios Gyftopoulos, MD
"Rotator Cuff Tear Shape Characterization: A Comparison of 2D Imaging and 3D MR Reconstruction"
Selected for presentation at ISS

Ken Lee, MD
"Ultrasound-guided Treatment for Refractory Plantar Fasciopathy: A Randomized Controlled Pilot Study of Platelet-Rich Plasma Versus Standard of Care Corticosteroid Injections"
Selected for presentation at RSNA

2014
Mary Kristen Jesse, MD
"3D Morphologic Assessment of Normal and Abnormal Si Joints and the Potential Implications in the Development of Pain Syndrome"
Selected for presentation at ISS

Lawrence White, MD
"Femoroacetabular Impingement: Accuracy of Non-Arthrographic 3T MR Imaging in Evaluation of Intra-Articular Pathology of the Hip"
Selected for presentation at RSNA

2013
Lien Senchak, MD
"Imaging of Osteoblastoma of the Appendicular Skeleton with Pathologic Correlation:
Selected for presentation at ISS

Mary Kristin Jesse
"Morphology of Endplate Cement Estravasation Can Predict Adjacent Level Fracture in Osteoporotic Patients Undergoing Vertebroplasty and Kyphoplasty" *Selected for presentation at RSNA*

2012
Meredith Hayes, MD
"Phosphaturic Mesenchymal Tumors Imaging Features of a Rare Entity with Clinicopathologic Correlation"
Selected for presentation at ISS

Srinivasan Harish, FRCPC
"MRI of the Spine and Sacroiliac Joints for Spondyloarthropathy: Influence on Clinical Diagnostic Confidence and Patient Management"
Selected for presentation at RSNA

2011
Tal Laor, MD
"Juvenile Osteochondritis Dissecans (JOCD): Is It a Growth Disturbance of the Secondary Physis of the Epiphysis?"
Selected for presentation at ISS

Donna Blankenbaker, MD
"MR Arthrographic Appearance of the Post-Operative Acetabular Labrum"
Selected for presentation at RSNA

2010
Maxime Freire, MD
"MR Evaluation of Repair Tissue in Osteochondral Defects Following Treatment with Acellular Scaffolds: High Resolution MR-Histological Correlation in a Goat Model" *Selected for presentation at ISS*

Peter MacMahon, MD
"Injectable Corticosteroid Preparations: An Embolic RiskAssessment by Static and Dynamic Microscopic Analysis" *Selected for presentation at RSNA*

2009
Christopher J. Hanrahan, MD, PhD
"Temporal Evolution of MRI Findings after Rotator Cuff Repair" *Selected for presentation at ISS*

Kevin Johnson, MD
"Contrast-Enhanced Ultrasound Characterization of the Vascularity of the Repaired Rotator Cuff" *Selected for presentation at RSNA*

2008
Stephanie A. Bernard, MD
"Cartilage Cap Thickness Measurement on T2-Weighted MR Imaging and the Risk of Secondary Chondrosarcoma in Osteochondromas"
Selected for presentation at ISS

Kelley W. Marshall, MD
"Osteochondral Lesions of the Lateral Trochlea in the Pediatric Athlete with Elbow Pain"
Selected for presentation at RSNA

2007
Adam Zoga, MD
"The Sports Hernia: What Is It? How Do I image It? What Are Its Confounders?"
Selected for presentation at ISS

Tal Laor, MD
"The Effect of Childhood Growth on the Anterior and Posterior Cruciate Ligaments"
Selected for presentation at RSNA

2006
Eric T. Chou, MD
"Bifurcated Distal Biceps Brachii Tendon: Magnetic Resonance Imaging Appearances and Prevalence"
Selected for presentation at ISS

Lawrence M. White, MD
"Direct MR Arthrographic Assessment of Recurrent Symptoms Post Shoulder Instability Repair: Correlation with Second Look Surgical Evaluations in 40 Patients"
Selected for presentation at RSNA

2005
Steven S. Gerguis, MD
"Review of the Secondary Signs of Femoracetabular Impingement and Correlation with the Head-neck Angle Measured on the Frog-Leg Lateral View"
Selected for presentation at ISS

Suzanne E. Anderson, BMed
"Computer-assisted Software for Accurate Determination of Acetabular Coverage with Conventional Radiography"

2004
Mihra Taljanovic, MD, MS
"Bone Marrow Edema in Hip Osteoarthritis: Quantitative Assessment with MRI and Correlation with Clinical Exam, Radiographic Findings and Histopathology"

2003
Joseph R. DeMartini, MD
"Effects of MR Gradient Coil- Induced Vibration Artifacts and Inherent Pulse Sequence Imperfections on Phase"

2002
Derek R. Armfield, MD
"MRI of Posterior Medial Meniscal Root Avulsion"

2001
Patrick T. Liu, MD
"Improved Imaging of Osteoid Osteoma with Dynamic Gadolinium-Enhanced MRI"

2000
Timothy G. Sanders, MD
"MRI at Different Time Intervals Following Hamstring Harvest for ACL Reconstruction"

Patrick T. Liu Innovation in Research Award Recipient

2018
Robert Lopez, MD
"Intramuscular Botulism Toxin Type A (BTA) Injection Facilitates Abdominal Wall Reconstruction (AWR) Of Recurrent Large-Defect Hernias"

2017
Micah Cohen, MD
"X-ray and MRI of Diabetic Foot Osteomyelitis. Review of Pathologically Proven Surgically Treated Cases: MRI Shows Better but What Does It Mean?"

2016
Robert Boutin, MD
"CT of Hip Fracture Patients: Can Muscle Size & Attenuation Predict Clinical Outcomes?"

2015
David Melville, MD
"Diffusion Tensor MR Imaging of Quadriceps Musculature in the Setting of Clinical Fragility Syndrome"

Joshua M. Polster, MD
"Enhanced Detection of CT-Occult Bone Marrow Lesions In The Lumbar Spine Using Trabecular Suppression"

2014
Gandikota Girish, MD
"Photoacoustic Imaging of Joints"

2013
Douglas P. Beall, MD
"Tissue Distribution of Clondine Following Intraforminal Implantation of Biodegradablepellets: Potential Alternative to Epidural Steroid for Radiculopathy"

2012
Joshua M. Polster, MD
"Single Energy Post – Processing Technique for Bone Marrow Imaging on CT"

2011
Kenneth Lee, MD
"Treatment of Chronic Lateral Epicondylosis Using Hyperosmolar Dextrose Solution: CanAcoustoelastography Monitor Tissue Healing?"

AIRP Award – Best Poster

2018
Hailey Allen, MD; Megan Mills, MD; Miriam Peckham, MD; Lubdha Shah, MD; R. Kent Sanders, MD; Sarah Stilwill, MD
"MRI of the Lumbosacral Plexus: What the Practicing Radiologist Needs to Know"

2017
Xue Susan Bai, MD; Alice S. Ha, MD; Susan Ng, MS; Katelyn Nye, BS; John M. Sabol, PhD
"Not Your Grandma's X-ray: Utility of Advanced Reconstruction and Visualization Methods for Digital Tomosynthesis of Bone and Joint Pathology"

2016
Barrett Luce, MD; Michael Fox, MD; David Diduch, MD
"Assessment of Femoral Trochlear Morphology on Cross SectionalImaging: Comparing the Dejour Classification and Quantitative Measurements in Patients Later Treated with Deepening Trochleoplasty"

2015
Shefali Kothary MD
"Imaging Spectrum of Pectoralis Tears"

SSR Excellence Award

2013
Luke Scalcione, MD
"Hallux Valgus: Spectrum of Imaging, Surgical Procedures, and Complications"

2011
Luis Beltran, Jason Mayo, Jenny Bencardino, Zehava Rosenberg, Luis Neto Pecci, Maria Diaz de Tuesta, Olga Ruiz
"Diagnostic Evaluation of Hip Dysplasia in the Young Adult – Emphasis on Cross-Sectional Imaging"

ACR Education Award – Best Poster

2018
Gary LiMarzi, MD; Omar Khan, MD; Yashesh Shah, MD; Corrie Yablon, MD
"Imaging of Ankle Impingement"

2017
Pardeep Athwal, MD; Megan K. Mills, MD; Mark Mahan, MD; Kevin R. Moore, MD; Barry G. Hansford, MD; Chrish J. Hanrahan,MD; Anna K. McGow, MD; Sarah E. Stilwill, MD
"Traumatic and Non-Traumatic Brachial Plexus Imaging: What the Practicing Radiologist Needs to Know"

2016
Usman Anwer, MD
Corrie Yoblon, MD
"A Sound Approach to Peripheral Neuropathies"

2015
Kimia K Kani, MD
"MR Imaging of Soft Tissue Injuries of the Fingers"

2014
David Melville, MD
"Osteoarthritis of the Basal Joints of the Thumb: Imaging and Management"

Young Investigator Award Winners

2019

Amanda Crawford, MD
"The Role of Sarcopenia in Clinical Vertebral Augmentation Outcomes"

Michael Durst, MD
"The Role of Paraspinal Edema in Clinical Vertebral Augmentation Outcomes"

David Gimarc, MD
"Platelet-Rich Plasma for Treatment of Moderate-To-Severe Midsubstance Achilles Tendinopathy: A Pilot RCT With Conventional and Novel Ultrasound Imaging Correlation"

Natalie Gorelik, MD
"Comparison Between Radiography and Magnetic Resonance Imaging for The Detection of Sacroiliitis in The Initial Diagnosis of Axial Spondyloarthritis: A Cost-Effectiveness Study"

Alexander Grushky, MD
"Biopsy of Suspicious Osseous Lesions in Patients with a Known Primary Malignancy: Rate of Alternate Diagnosis and Complication Rate"

Brian Kennedy, MD
"Loss of Reduction is Common After Coracoclavicular Ligament Reconstruction"

2018

Hailey Allen, MD
"T2 Mapping of Articular Cartilage of The Normal Pediatric Knee At 3.0 T"

Kate Harrington, MD
"Textural 3T MRI Measures of Proximal Femur Bone Quality as Biomarkers of Fracture Risk"

Dana Lin, MD
"Diagnostic Utility of Lavage for Periprosthetic Joint Infection: Are the Culture Results Reliable?"

Palanan Siriwanarangsun, MD
"Carved in Bone: The Calcaneal Crescent in Patients with and Without Plantar Fasciitis"

Ramya Srinivasan, MD
"Optimizing Bone Marrow Lesion Detection Using Dual Energy CT: A Phantom Study"

Edward Yoon, MD
"Ultrasound-Guided Aspiration of Intramuscular Hematomas: Efficacy and Relationship to Sonographic Appearance "

2017

Timothy Dickson, MD
"Clinical Findings and Imaging Appearances of Angiomyomas"

Jennifer L. Favinger, MD
"Soft Tissue Sarcoma Response to Two Cycles of Neoadjuvant Chemotherapy: a Multi-Therapy Analysis of MRI Findings and Agreement Between RECIST Criteria and SUVmax"

Corey Ho, MD
"Temporal Assessment of the Ligamentization Process of Anterior Cruciate Ligament Graft Utilizing a Nevel Ultrashort T2* Sequence (UTE)"

O. Kenechi Nwawka, MD
"Ultrasound for Brachial Plexopathy: Prospective Correlation to MRI, EMG, and Surgical and Clinical Findings"

2016

Connie Y. Chang, MD
"Quantitative CT Density Evaluation of Osseous Metastases Following Chemotherapy"

Erin FitzGerald Alaia, MD
"Imaging Features on Ibalance, New High Tibial Osteotomy: What the Radiologist Needs to Know"

Elisabeth Garwood, MD
"Clinical Utility of Shoulder Imaging in the Outpatient Setting: A Pilot Study"

Tony Wong, MD
"Utility of 3D Print Models for Pre-Operative Planning in Femoroacetabular Impingement"

2015

Shivani Ahlawat, MD
"Traumatic Neuromas: Common MRI Features"

Kimia K Kani, MD
"Concepts of Operative Treatment in Scapholunate Instability: An Imaging Perspective"

Lauren M. Ladd, MD
"Quantitative and Qualitative Comparison of 3.0t versus 1.5t Warp Imaging of Hip Prostheses"

Daniel Siegal, MD
"Sonographic Evaluation of the Distal Biceps Tendon: Accuracy and Pitfalls in the diagnosis of Partial Thickness Tears"

Andrew Wilmot, MD
"Subchondral Insufficiency Fracture of the Knee: Revising the Epidemiology and Soft Tissue Edema Pattern"

2014

Luis Beltran
"Anatomy, Diagnostic Pitfalls and Variants of the Shoulder Joint in Abduction and External Rotation MR Arthrography"

Shadpour Demehri
"Accuracy of Conventional and Functional MRI in Diagnosing Indeterminate Peripheral Nerve Sheath"

Alice Ha
"Digital Tomosynthesis to Detect Bone Healing?: Comparison to Radiography and ComputedTomography"

Kaushal Mehta
"Superolateral Hoffa's Fat Pad Edema in Collegiate Volleyball Players"

2013

Gyftopoulos, Soterios, MD
"Correlation of MIR with Arthroscopy for the Diagnosis of Subscapularis TendonTears"

Raghavan, Meera, MD, BS
"Radiomics of Soft tissue Sarcoma-Comuter-Aided Image Analysis and Characterization of Tumor Heterogeneity"

Rantiolu Aro, Michael, MD
"Anatomic Variations of Femoral Nerves on High Resolution 3 Tesla Magnetic Resonance Neurography and Their Relation to Abnormal Nerve and Muscle Imaging Findings"

2012

Bethany Casagranda, DO
"Coronal Oblique Imaging of The Knee: Can It Increase Radiologists' Confidence in Diagnosing Posterior Root Meniscal Tears?"

Glenn Gaviola, MD
"Assessment of Fellowship Trainee Clinical Competency and Growth with an Objective Standardized Clinical Examination Within the Musculoskeletal Fellowship Program: Initial Experience"

Jonelle Petscavage, MD, MPH
"Magnetic Resonance Imaging Findings of Adverse Reactions to Metallic Debris (ARMD) of Metal-On-Metal Total Hip Replacements"

Naveen Subhas, MD
"Metal Artifact Reduction Using a Monoenergetic Dual Energy CTTechnique"

SSR Seed Grant Research Award

2018

Naveen Subhas, MD

"Highly Accelerated Knee MRI using a Novel Deep Convoluted Neural Network Algorithm: A Multi-Reader Comparison Study"

2017

Michael Fadell, MD

"Utilization of non-invasive MR imaging to differentiate between infectious and noninfectious fluid in septic arthritis"

2016

Kenneth S. Lee MD, Andrew B. Ross, MD

Rapid MRI protocol for the Evaluation of Potential Hip Fractures in the Elderly

Thank You to Our 2019 Exhibitors

Special thanks to the following companies for their support to the Society of Skeletal Radiology in 2019.

Gold
AprioMed Inc.

Silver
Envision Physician Services

Bronze
Canon Medical Systems USA, Inc.
Teleflex

SSR Past Presidents

William Bonner Guilford, MD
July 1978 – June 1980

Jeremy J. Kaye, MD
July 1980 – June 1982

Cosmo L. Haun, MD
July 1982 – June 1984

William W. Daniel, MD
July 1984 – June 1986

Anne C. Brower, MD
July 1986 – June 1988

Jeno I. Sebes, MD
July 1988 – June 1990

Murali Sundaram, MD
July 1990 – June 1992

Charles S. Resnik, MD
July 1992 – June 1994

William Bonner Guilford, MD
July 1994 – June 1996

Terry M. Hudson, MD
July 1996 – June 1998

William F. Conway, MD, PhD
July 1998 – June 2000

Arthur A. De Smet, MD
July 2000 – June 2002

B.J. Manaster, MD, PhD
July 2002 – June 2004

Arthur H. Newberg, MD
July 2004 – June 2006

Cheryl A. Petersilge, MD
July 2006 – June 2008

Mark J. Kransdorf, MD
July 2008 – March 2010

Carol L. Andrews, MD
April 2010 –March 2012

Kenneth Buckwalter, MD
April 2012 – March 2014

William Morrison, MD
April 2014 – March 2016

Andrew Sonin, MD, FACR
April 2016 – April 2018

Ultrasound Workshop Instructors

Organizer:

Benjamin Levine, MD - UCLA Medical Center
Santa Monica, CA

Lecturers:

Jon Jacobson, MD – University of Michigan
Ann Arbor, MI

Theodore Miller, MD – Hospital for Special Surgery
Mamaroneck, NY

Instructors:

Meg Chiavaras, MD, PhD – McMaster University
Hamilton, ON, CAN

Joseph Craig, MBChB – Henry Ford Hospital
Detroit, MI

Mark Cresswell, MD – University of British Columbia
Vancouver, BC, CAN

Girish Gandikota, MD – University of Michigan
Ann Arbor, MI

Jordan Gross, MD – Keck School of Medicine of USC
Los Angeles, CA

Robert Lopez, MD – Charlotte Radiology, PA
Charlotte, NC

Kevin McGill, MD – Henry Ford Hospital
Detroit, MI

Yoav Morag, MD – University of Michigan
Ann Arbor, MI

Linda Probyn, MD –University of Toronto
Toronto, ON, CAN

Andrew Ross, MD, MPH –University of Wisconsin
Madison, WI

Daniel Siegal, MD – Henry Ford Hospital
Detroit, MI

Thank You to the Following Companies for the In Kind Support of Ultrasound Equipment Loaned for this Workshop

Canon Medical Systems USA, Inc.
TBD

SSR RED FUND Donors

2018-2019 Contributors (as of 3/5/19)

Paul Morgan Aitchison, MD
Behrang Amini, MD
Carol L. Andrews, MD
Derek R. Armfield, MD
Laura W. Bancroft, MD, FACR
Donna G. Blankenbaker, MD
Robert Boutin, MD
Jeffrey M. Brody, MD
Arnold Cheung, MD
James J. Choi, MD
Robert Hanley Choplin, MD
Edgar Colon, MD
James M. Coumas, MD
Mark E Cresswell, MD
Peter G. D'Amour, MD
Ivan Christopher Davis, MD
Kirkland W. Davis, MD
Sukhvinder Dhillon, MD
William Rhey Dunfee, MD
Gregor Dunham, MD
Timothy R. Enright, MD
Peter Thomas Evangelista, MD
Eric James Feldmann, MD
Donald Joel Flemming, MD
Hillary Garner, MD
Jeffery Gronkiewicz, MD
W. Bonner Guilford, MD
Parlyn Denise Hatch, MD
Mary Gabriella Hochman, MD
James S. Jelinek, MD
Yazan Kaakaji, MD
Mark J. Kransdorf, MD
Manickam Kumaravel, MD
Lauren M. Ladd, MD
Robert G.W. Lambert, MD
Laurie M. Lomasney, MD
David Alan May, MD
Joshua M. McDonald, MD
Kevin McGill, MD
Drew Mcmenamin, MD
Jorge M. Medina, MD
Douglas N. Mintz, MD
Lacey F. Moore, MD
William Brian Morrison, MD
Erik N. Nelson, MD
Alan Patrick Northington, MD
Ogonna Kenechi Nwawka, MD
Seth O'Brien, MD
Cheryl A. Petersilge, MD
Thomas Lee Pope, MD
Cody Ryan Quirk, MD
Andres Rahal, MD
Faisal Rashid, MD
Trenton D. Roth, MD
Hamid Salamipour, MD
David C. Salonen, MD
Alex L. Sleeker, MD
Edward Smitaman, MD
John Michael Smith, MD
Andrew Sonin, MD, FACR
Charles E. Spritzer, MD
Troy F. Storey, MD
D. Dean Thornton, MD
Joseph Triolo, MD
Jorge Alberto Vidal, MD
Richard Edward Allan Walker, MD
William McCaleb Weathers, MD
Lawrence M. White, MD
Carl S. Winalski, MD
James Neal Wise, MD
Corrie M. Yablon, MD
Brian W Yue, MD
Vanessa M. Zayas, MD

***R**esearch, **E**ducation and **D**evelopment (RED) Fund*

Program Schedule Overview

*General Session will be located in the **Salon A-G** unless otherwise noted.*

Sunday, March 10, 2019

7:00 a.m.– 7:55 a.m.	CONTINENTAL BREAKFAST
7:00 a.m. – 5:00 p.m.	REGISTRATION/INFORMATION DESK OPEN
7:00 a.m. – 1:30 p.m.	EXHIBIT HALL OPEN
7:00 a.m. – 4:30 p.m.	*POSTER SESSION*
7:45 a.m. – 8:50 a.m.	**SSR ANNUAL BUSINESS MEETING**
9:00 a.m. – 9:15 a.m.	2018 SEED GRANT RESEARCH AWARD RECIPIENT PRESENTATION
9:15 a.m. – 10:15 a.m.	BEST PRACTICE & EMERGING TRENDS SESSION
10:15 a.m. – 10:20 a.m.	**CASE OF THE DAY**
10:20 a.m. – 10:45 a.m.	BREAK – VISIT EXHIBIT HALL
10:45 a.m. – 12:00 p.m.	TECHNOLOGIES AND TECHNIQUES SESSION
12:00 p.m. – 12:05 p.m.	**CASE OF THE DAY**
12:05 p.m. – 1:30 p.m.	LUNCH (in Exhibit Hall or Industry Sponsored Lunch Symposium)
12:05 p.m. – 1:30 p.m.	MATCH UPDATE LUNCH
1:30 p.m. – 3:00 p.m.	**FOCUS SESSION/SELF ASSESSMENT MODULE (SAM I) – Spine Intervention**
3:00 p.m. – 3:10 p.m.	SAM I EXAM
3:10 p.m. – 3:20 p.m.	BREAK
3:20 p.m. – 4:50 p.m.	**FOCUS SESSION/SELF ASSESSMENT MODULE (SAM II) – Elbow and Forearm Imaging**
4:50 p.m. – 5:00 p.m.	SAM II EXAM

Monday, March 11, 2019

7:00 a.m. – 7:55 a.m.	CONTINENTAL BREAKFAST
7:00 a.m. – 12:35 p.m.	REGISTRATION/INFORMATION DESK OPEN
7:00 a.m. – 12:30 p.m.	EXHIBIT HALL OPEN
7:00 a.m. – 12:30 p.m.	*EPOSTER SESSION*
7:45 a.m. – 8:00 a.m.	ESSR BEST PAPER AWARD PRESENTATION
8:00 a.m. – 10:00 a.m.	UPPER EXTREMITY SESSION
10:00 a.m. – 10:05 a.m.	**CASE OF THE DAY**
10:05 a.m. – 10:30 a.m.	BREAK – VISIT EXHIBIT HALL
10:30 a.m. – 12:30 p.m.	INTERVENTION SESSION
12:30 p.m. – 12:35 p.m.	**CASE OF THE DAY**
12:35 p.m. – 12:45 p.m.	**REVIEW OF OLA PROCESS**
1:00 p.m. – 3:00 p.m.	**MSK ULTRASOUND HANDS-ON WORKSHOP: Ankle/Foot** (*separate registration and fee required)*
6:00 p.m. – 9:30 p.m.	SSR ANNUAL BANQUET

Tuesday, March 12, 2019

7:00 a.m. – 7:55 a.m.	CONTINENTAL BREAKFAST
7:00 a.m. – 12:35 p.m.	REGISTRATION/INFORMATION DESK OPEN
7:00 a.m. – 12:30 p.m.	EXHIBIT HALL OPEN
7:00 a.m. – 12:30 p.m.	*EPOSTER SESSION*
8:00 a.m. – 10:00 a.m.	HIP / PELVIS SESSION
10:00 a.m. – 10:05 a.m.	**CASE OF THE DAY**
10:05 a.m. – 10:30 a.m.	BREAK – VISIT EXHIBIT HALL
10:30 a.m. – 12:30 p.m.	SPINE SESSION
12:30 p.m. – 12:35 p.m.	**CASE OF THE DAY**
1:00 p.m.	SSR Annual Golf Outing (*separate registration and fee required)*

Wednesday, March 13, 2019

7:00 a.m. – 7:55 a.m.	CONTINENTAL BREAKFAST
7:00 a.m. – 12:30 p.m.	REGISTRATION/INFORMATION DESK OPEN
7:00 a.m. – 10:30 a.m.	EXHIBIT HALL OPEN
7:00 a.m. – 10:30 a.m.	*EPOSTER SESSION*
8:00 a.m. – 10:00 a.m.	TUMOR / MARROW SESSION
10:00 a.m. – 10:05 a.m.	**CASE OF THE DAY**
10:05 a.m. – 10:30 a.m.	BREAK – VISIT EXHIBIT HALL
10:30 a.m. – 12:30 p.m.	LOWER EXTREMITY SESSION

SSR Hotel Floor Plan

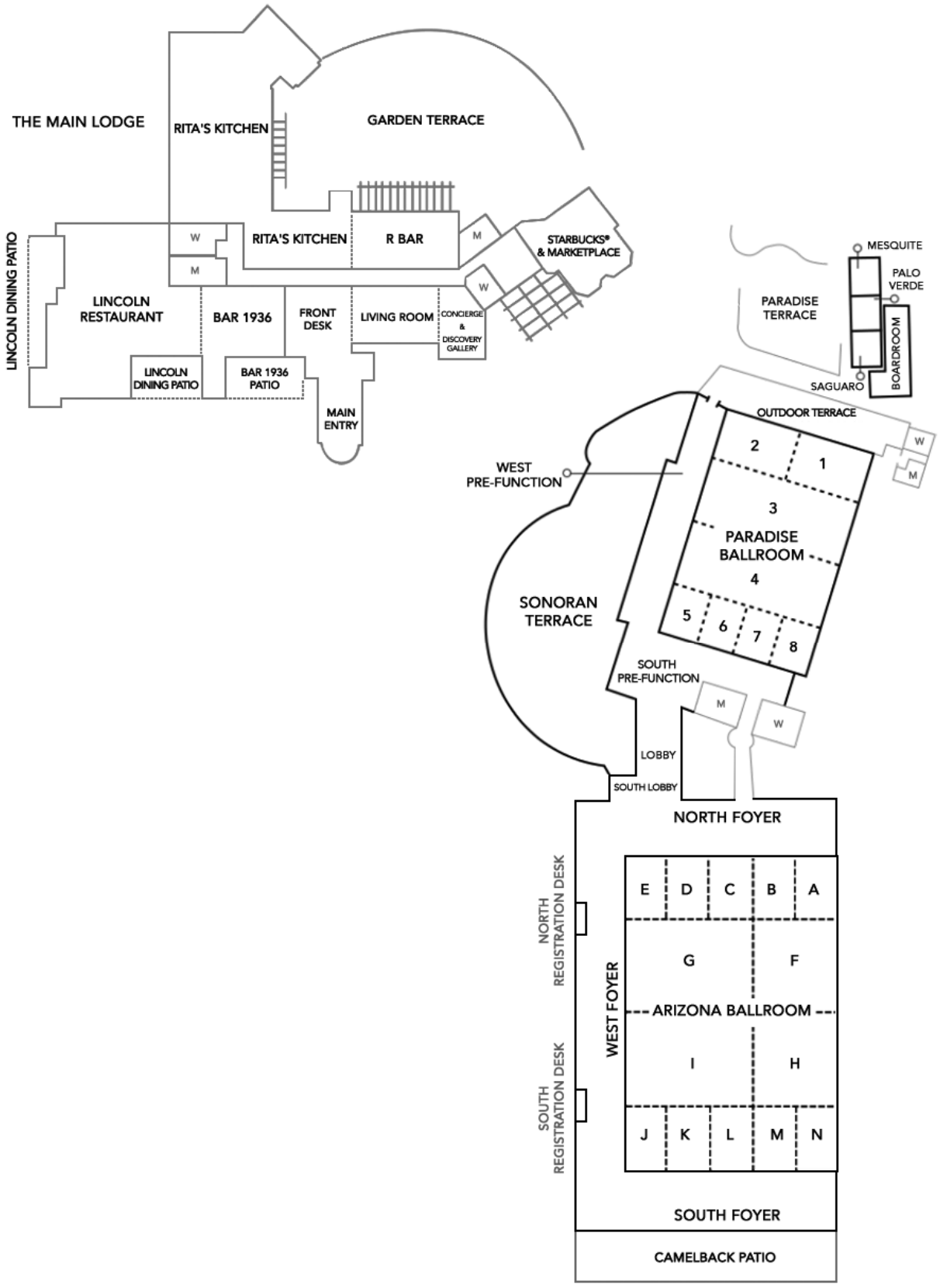

SUNDAY

Society of Skeletal Radiology

42nd Annual Meeting

March 10-13, 2019

Saturday, March 9, 2019

4:00 p.m.–6:00 p.m. Registration/Information Desk Open
Location: Salon A-G

Sunday, March 10, 2019

7:00 a.m.–7:55 a.m. **Continental Breakfast**

7:00 a.m.–5:00 p.m. **Registration/Information Desk Open**

7:00 a.m.–1:30 p.m. **Exhibit Hall Open**

7:00 a.m.–4:30 p.m. **ePoster Session**

7:45 a.m.–8:50 a.m. **SSR Annual Business Meeting**

9:00 a.m.–9:15 a.m. 2018 Seed Grant Research Award
HIGHLY ACCELERATED KNEE MRI USING A NOVEL DEEP CONVOLUTED NEURAL NETWORK ALGORITHM: A MULTI-READER COMPARISON STUDY
Moderators: Laura Bancroft, MD, FACR, Lawrence White, MD FRCPC

9:15 a.m.–10:15 a.m. **BEST PRACTICE & EMERGING TRENDS**
Moderators: Christine Chung, MD, Martin Torriani, MD, MMSc

9:15 a.m. #1 **NOMENCLATURE FOR SUBCHONDRAL NON-NEOPLASTIC BONE LESIONS**
Tetyana Gorbachova, MD[1]; Ian Amber, MD[2]; Nicholas Beckman, MD[3]; D. Lee Bennet, MD[4]; Eric Chang, MD[5]; Leah Davis, DO[6]; Felix Gonzalez, MD[7]; Barry Hansford, MD[8]; B. Matthew Howe, MD[9]; Leon Lenchik, MD[10]; Carl Winalski, MD[11]; Miriam Bredella[12]
[1]Albert Einstein College of Medicine Montefiore Medical Center, Philadelphia, PA, USA; [2]Medstar Georgetown University Hospital, Washington, DC, USA; [3]UT Houston- McGovern School of Medicine, Houston, TX, USA; [4]University of Iowa Hospital & Clinics, Iowa, IA, USA; [5]University of California, San Diego & Veterans Affairs Med Center, SD, San Diego, CA, USA; [6]Medical University of South Carolina, Charleston, SC, USA; [7]Emory University Dept. of Radiology, MSK Division, Atlanta, GA, USA; [8]Oregon Health Sciences University, Portland, OR, USA; [9]Mayo Clinic, Rochester, MN, USA; [10]Wake Forest University School of Medicine, Winston-Salem, NC, USA; [11]Cleveland Clinic, Cleveland, OH, USA; [12]Mass General Hospital, Boston, MA, USA
(Presented by: Tetyana Gorbachova, MD, Albert Einstein College of Medicine Montefiore Medical Center)

9:30 a.m. #2 **LOSS OF MUSCLE QUALITY IS CORRELATED WITH DECREASED BONE MINERAL DENSITY IN PATIENTS WITH SARCOMA**
Stephanie Jo, MD, PhD; Ronnie Sebro, MD, MS, PhD
Hospital of University of Pennsylvania, Philadelphia, PA, USA
(Presented by: Stephanie Jo, MD, PhD, Hospital of University of Pennsylvania)

9:45 a.m. #3 **DIAGNOSIS OF SARCOPENIA IN THE RADIOLOGY DEPARTMENT: FEASIBLE AND SAFE?**
Robert Boutin, MD[1]; Anahit Petrosyan, MD[1]; Praman Fuangfa, MD[1]; Lawrence Yao, MD[2]; John Brock[1]; Patrick Kortebein, MD[1]; Leon Lenchik, MD[3]
[1]University of California, Davis, Sacramento, CA, USA; [2]National Institutes of Health, Bethesda, MD, USA; [3]Wake Forest University School of Medicine, Winston-Salem, NC, USA
(Presented by: Robert Boutin, MD, University of California, Davis)

10:00 a.m. #4 **TRENDS OF FOLLOW UP RECOMMENDATIONS MADE ON MUSCULOSKELETAL MRI EXAMINATIONS**
Tony Wong, MD; John Nemer; Jonathan Kazam, MD
Columbia-Presbyterian Medical Center, New York, NY, USA
(Presented by: Tony Wong, MD, Columbia-Presbyterian Medical Center)

10:15 a.m.–10:20 a.m. **CASE OF THE DAY**
Presenting author: Andrew Erie, MD

10:20 a.m.–10:45 a.m. **Break - Visit the Exhibit Hall**

10:45 a.m.–12:00 p.m. **TECHNOLOGIES AND TECHNIQUES**
Moderators: Michael Recht, MD, Jan Fritz, MD

10:45 a.m. #5 **MRI SEGMENTATION OF THE GLENOID AND HUMERAL HEAD USING DEEP CONVOLUTIONAL NEURAL NETWORKS**
Tatiane Cantarelli Rodrigues, MD[1]; Cem Deniz, PhD[2]; Jared Dublin[2]; Natalia Gorelik, MD[1]; Soterios Gyftopoulos, MD, MS[1]
[1]NYU Medical Center/ Hospital for Joint Diseases Langone Medical Center, New York, NY, USA; [2]New York University School of Medicine, New York, NY, USA
(Presented by: Tatiane Cantarelli Rodrigues, MD, NYU Medical Center/ Hospital for Joint Diseases Langone Medical Center)

11:00 a.m. #6 **MACHINE LEARNING CLASSIFICATION OF SOFT TISSUE MASSES OF THE PELVIS**
James Cortez, MD[1]; Michael Richardson, MD[2]; Beth Vettiyil, MD[1]; Behrang Amini, MD, PhD[1]
[1]The University of Texas M.D. Anderson Cancer Center, Houston, TX, USA; [2]University of Washington / Harborview Medical Center, Seattle, WA, USA
(Presented by: James Cortez, MD, The University of Texas M.D. Anderson Cancer Center)

11:15 a.m. #7 **COMPARISON OF "STIR-CT" TO CONVENTIONAL CT IMAGES FOR DETECTION OF MUSCLE LESIONS IN A BEEF SHANK MODEL.**
Joshua Polster, MD; Jennifer Bullen, MS; Naveen Subhas, MD; Bradford Richmond, MD; Darlene Holden, MD; Jean Schils, MD
Cleveland Clinic, Cleveland, OH, USA
(Presented by: Joshua Polster, MD, Cleveland Clinic)

11:30 a.m. #8 **CT-GUIDED BONE MARROW ASPIRATIONS AND BIOPSIES: RETROSPECTIVE REVIEW AND COMPARISON WITH BLIND PROCEDURES**
Connie Chang, MD; Adriana Moreira; Nathaniel Mercaldo, MS; Jad Husseini, MD; Robert Hasserjian, MD
Mass General Hospital, Boston, MA, USA
(Presented by: Connie Chang, MD, Mass General Hospital)

11:45 a.m. #9 **ILIAC BONE MARROW BIOPSY AND ASPIRATION WITH FLUOROSOCOPIC GUIDANCE - EXPERIENCE WITH 775 CASES**
Jeremiah Long, MD[1]; James Stensby, MD[2]; Travis Hillen, MD[3]; Jack Jennings, MD, PhD[3]; Stephen Herrmann, MD[3]; Elizabeth Wiesner, BA[3]
[1]Mayo Clinic, Phoenix, AZ, USA; [2]University of Missouri, Columbia, MO, USA; [3]Mallinckrodt Institute of Radiology, Saint Louis, MO, USA
(Presented by: Jeremiah Long, MD, Mayo Clinic)

Sunday, March 10, 2019

12:00 p.m.–12:05 p.m.		**CASE OF THE DAY** **Presenting author: David Gimarc, MD**
12:05 p.m.–1:30 p.m.		**LUNCH (In Exhibit Hall or Industry Sponsored Lunch Symposium)**
1:30 p.m.–3:00 p.m.		**Focus Session/Self Assessment Module (SAM I) - Spine Intervention** **Chair: Brian Peterson, MD**
	1:30 pm	Injectable Choices and Avoiding Complications in Spine Injection *Brian Peterson, MD*
	1:50 pm	Neuro Ablative Techniques and Neuro Modulation *Douglas Beall, MD*
	2:10 pm	Vertebral Augmentation *MK Jesse, MD*
	2:30 pm	Tumor Thermoablation *Jack Jennings, MD, PhD*
3:00 p.m.–3:10 p.m.		**SAM I Exam**
3:10 p.m.–3:20 p.m.		**Break - Visit the Exhibit Hall**
3:20 p.m.–4:50 p.m.		**Focus Session/Self Assessment Module (SAM II) - Elbow Imaging** **Chair: MK Jesse, MD**
	3:20 pm	Elbow Imaging: Post-traumatic Fractures and Osteochondroses *Manickam Kumaravel, MD*
	3:40 pm	Elbow Tendon Pathology *Lynne Steinbach, MD*
	4:00 pm	Elbow Ligament Pathology *Mark Anderson, MD*
	4:20 pm	Nerve Impingement Syndromes of the Elbow and Forearm *Megan Mills, MD*
4:50 p.m.–5:00 p.m.		**SAM II Exam**

Related ePosters

BEST PRACTICE & EMERGING TRENDS

Poster #1 **CARTILAGE ICING AND CHONDROCALCINOSIS IN THE DIFFERENTIATION BETWEEN GOUT AND PSEUDOGOUT ON RADIOGRAPHS**
Anna Falkowski, MD, MHBA; Jon Jacobson, MD
University of Michigan Medical Center, Ann Arbor, MI, USA

Poster #2 **MUSCULOSKELETAL MANIFESTATIONS OF DIABETES MELLITUS: A REVIEW FOR THE PRACTICING RADIOLOGIST AND RADIOLOGIST IN TRAINING, WITH EMPHASIS ON CLINICAL PRESENTATION, PATHOGENESIS, AND IMAGING APPEARANCE.**
Alexander Grushky, MD[1]; David Marcantonio, MD[1]; Jonathan Im, MS[2]
[1]Beaumont Health System, Royal Oak, MI, USA; [2]Michigan State Univeristy College of Human Medicine, Grand Rapids, MI, USA

Poster #3 **PERIPROSTHETIC JOINT INFECTIONS**
Kimia Kani, MD[1]; Jack Porrino, MD[2]; Hyojeong Mulchay, MD[3]; Felix Chew, MD[3]
[1]University of Maryland School of Medicine, Baltimore, MD, USA; [2]Yale University School of Medicine, New Haven, CT, USA; [3]University of Washington / Harborview Medical Center, Seattle, WA, USA

Poster #4 **EXTERNAL FIXATORS: LOOKING BEYOND THE HARDWARE MAZE**
Kimia Kani, MD[1]; Jack Porrino, MD[2]; Hyojeong Mulcahy, MD[3]; Felix Chew, MD[3]
[1]University of Maryland School of Medicine, Baltimore, MD, USA; [2]Yale University School of Medicine, New Haven, CT, USA; [3]University of Washington / Harborview Medical Center, Seattle, WA, USA

Poster #5 **GUN VIOLENCE AND RADIOLOGY UTILIZATION AT A MAJOR CITY ACADEMIC CENTER**
William Morrison, MD; Ankit Gandhi, MD; Corbin Pomeranz, MD; Lauren Brown, MD; Kimberly Klinger, MD; Adam Zoga, MD; Johannes Roedl, MD; Jeffrey Belair, MD; Suzanne Long, MD
Thomas Jefferson University Hospital, Philadelphia, PA, USA

Poster #6 **DON'T MISS THE BULL'S-EYE: MRI APPEARANCE OF LYME DISEASE ARTHRITIS**
Sean Cleary, MD; Johnny Monu, MBBS, MD; Gregory Dieudonne, MD; Scott Schiffman, MD
The University of Rochester School of Medicine and Dentistry, Rochester, NY, USA

Poster #7 **MUSCULOSKELETAL MANIFESTATIONS OF SCLERODERMA ON MRI AND ULTRASOUND**
Emily Casaletto, BS; Ogonna Nwawka, MD; Alissa Burge, MD
Hospital for Special Surgery, New York, NY, USA

TECHNOLOGIES & TECHNIQUES

Poster #8 **HYBRID 18F-FDG PET/MR IN THE EVALUATION OF PEDAL OSTEOMYELITIS**
Margaret Kincaid, MD[1]; Stephen Broski, MD[1]; Drake McArthur, MD[2]; Erik Weiss, MD[3]
[1]Mayo Clinic, Rochester, MN, USA; [2]Tulane University Health Sciences Center, New Orleans, LA, USA; [3]Phoenix VA Medical Center, Phoenix, AZ, USA

Poster #9 **ULTRASOUND IMAGING OF NERVES IN THE NECK: CORRELATION TO MRI, ELECTRODIAGNOSTIC AND CLINICAL FINDINGS**
Ogonna Nwawka, MD; Emily Casaletto, BS
Hospital for Special Surgery, New York, NY, USA

Poster #10 **COMPRESSED SENSING MAGNETIC RESONANCE IMAGING (CS-MRI) OF THE KNEE: ASSESSMENT OF QUALITY, INTER-READER AGREEMENT, AND TIME SAVINGS**

George Matcuk, Jr., MD; Jordan Gross, MD; Brandon Fields, BA, BM; Steven Cen, PhD
KECK School of Medicine of USC, Los Angeles, CA, USA

Poster #11 **NEXT-GENERATION 5-MIN KNEE MRI WITH COMBINED SIMULTANEOUS MULTI-SLICE AND PARALLEL IMAGING ACCELERATION**

Jan Fritz, MD; Ali Rashidi, MD; Miho Tanaka, MD; Filippo Del Grande, MD
Johns Hopkins University, Baltimore, MD, USA

Poster #12 **PERIPHERAL NERVE IMAGING: A REVIEW OF ANATOMY, IMAGING TECHNIQUES, AND IMPORTANT PATHOLOGY**

Ryan Joyce, MD; Sarah Stilwill, MD; Richard Leake, MD; Megan Mills, MD; Patrick Kobes, DO; Hailey Allen, MD
University of Utah Medical Center / SOM, Salt Lake City, UT, USA

2018 Seed Grant Research Award

HIGHLY ACCELERATED KNEE MRI USING A NOVEL DEEP CONVOLUTED NEURAL NETWORK ALGORITHM: A MULTI-READER COMPARISON STUDY

Subhas Naveen, MD
Cleveland Clinic

Purpose: Previous work has shown the feasibility of reconstructing diagnostic quality images from a highly undersampled knee MRI acquisition to achieve a 6-fold acceleration with a novel machine learning algorithm using a 15-layer deep convolutional neural network (DCNN). The purpose of this study was to assess the interchangeability of highly accelerated images reconstructed using DCNN and a standard 3-layer CNN with standard non-accelerated images for evaluating internal derangement of the knee.

Materials and Methods: Highly accelerated 2D fat-saturated (fs) sagittal proton-density weighted (PD) and non-fs PD coronal sequences from knee MRIs in 40 patients were reconstructed with DCNN and CNN techniques. 3 MSK radiologists, blinded to the reconstruction technique, independently evaluated the menisci, ligaments, articular cartilage, bones and image quality on the DCNN, CNN and standard images. Interchangeability was measured by comparing the frequency of agreement between 2 readers both evaluating the standard images (intramodality agreement) with the frequency of agreement between 1 reader evaluating the accelerated images and the other reader evaluating the standard images (intermodality agreement). The mean difference in intramodality and intermodality agreement was calculated with 95% confidence intervals (CI). A non-inferiority margin of 10% excess disagreement when using accelerated images was used.

Results: Intramodality agreement between standard images and intermodality agreement between standard and DCNN and CNN images were very similar for all of the evaluated structures. The increased disagreement (mean, [95% CI])when standard images were replaced with DCNN and CNN images was, respectively,: medial meniscus tears -2.5% [-6.1,+1.1%] and 0% [-5.7%,+5.7%]; lateral meniscus tears +1.6% [-4.4%,+7.8%] and 0% [-5.7%,+5.7%]; ACL tears -0.8% [-2.4%, +0.8%] and -0.8% [-2.4%, +0.8%]; articular cartilage +2.2% [-0.7%,+5.1%], +3.0% [-0.1%, +6.1%]. The image quality using standard, DCNN, and CNN images was graded as excellent or acceptable in 97.5%, 95% and 60% of cases, respectively.

Conclusion: A highly accelerated knee MRI reconstructed using a novel machine learning DCNN is diagnostically interchangeable with a standard knee MRI with acceptable to excellent image quality in most cases.

Podium #1

NOMENCLATURE FOR SUBCHONDRAL NON-NEOPLASTIC BONE LESIONS

Tetyana Gorbachova, MD[1]; Ian Amber, MD[2]; Nicholas Beckman, MD[3]; D. Lee Bennet, MD[4]; Eric Chang, MD[5]; Leah Davis, DO[6]; Felix Gonzalez, MD[7]; Barry Hansford, MD[8]; B. Matthew Howe, MD[9]; Leon Lenchik, MD[10]; Carl Winalski, MD[11]; Miriam Bredella[12]
[1]Albert Einstein College of Medicine Montefiore Medical Center, Philadelphia, PA, USA; [2]Medstar Georgetown University Hospital, Washington, DC, USA; [3]UT Houston- McGovern School of Medicine, Houston, TX, USA; [4]University of Iowa Hospital & Clinics, Iowa, IA, USA; [5]University of California, San Diego & Veterans Affairs Med Center, SD, San Diego, CA, USA; [6]Medical University of South Carolina, Charleston, SC, USA; [7]Emory University Dept. of Radiology, MSK Division, Atlanta, GA, USA; [8]Oregon Health Sciences University, Portland, OR, USA; [9]Mayo Clinic, Rochester, MN, USA; [10]Wake Forest University School of Medicine, Winston-Salem, NC, USA; [11]Cleveland Clinic, Cleveland, OH, USA; [12]Mass General Hospital, Boston, MA, USA
(Presented by: Tetyana Gorbachova, MD, Albert Einstein College of Medicine Montefiore Medical Center)

Purpose: To provide an updated approach to the nomenclature of non-neoplastic conditions affecting the subchondral bone through a comprehensive review of the medical literature and the expert opinion of the Society of Skeletal Radiology (SSR) Subchondral Bone Nomenclature Committee.

Materials and Methods: A committee of 12 radiologists of the SSR was tasked with developing a consensus on nomenclature of subchondral non-neoplastic bone lesions. The committee was divided into subgroups assigned to specific sections and questions. Reviewers from each subgroup performed a literature review using a screening process based on article title and abstract, with predefined inclusion and exclusion criteria (original scientific papers that pertained to the key questions of each subgroup; study population of more than ten patients; English language abstract available). The subgroups reviewed the relevant literature and produced a draft of their respective sections, which were compiled by the committee chairs, and reviewed and edited by all committee members.

Results: Definitions of non-neoplastic abnormalities affecting the articular cartilage, subchondral bone and marrow, and descriptive terms pertaining to these lesions, such as osteochondral lesion, edema-like bone marrow lesion, osteochondral defect, bone contusion, subchondral fracture/insufficiency fracture, epiphyseal collapse and subchondral cyst, were provided. Recommendations for a nomenclature, based on literature review and consensus agreement, were performed. Clinicopathologic entities, such as osteochondritis dissecans, so-called transient osteoporosis of the hip and spontaneous osteonecrosis of the knee, avascular necrosis, and rapidly destructive osteoarthritis, were reviewed and recommendations on nomenclature were provided.

Conclusion: There is controversy on the nomenclature and pathophysiology of subchondral non-neoplastic bone lesions. This consensus statement is intended to summarize current understanding of the pathophysiology and imaging findings of these lesions, standardize and update the nomenclature and thereby improve patient management.

Modality % - Radiography / Fluoroscopy:	15
Modality % - CT:	15
Modality % - MRI:	65
Modality % - US:	0
Modality % - Nuclear Medicine:	5

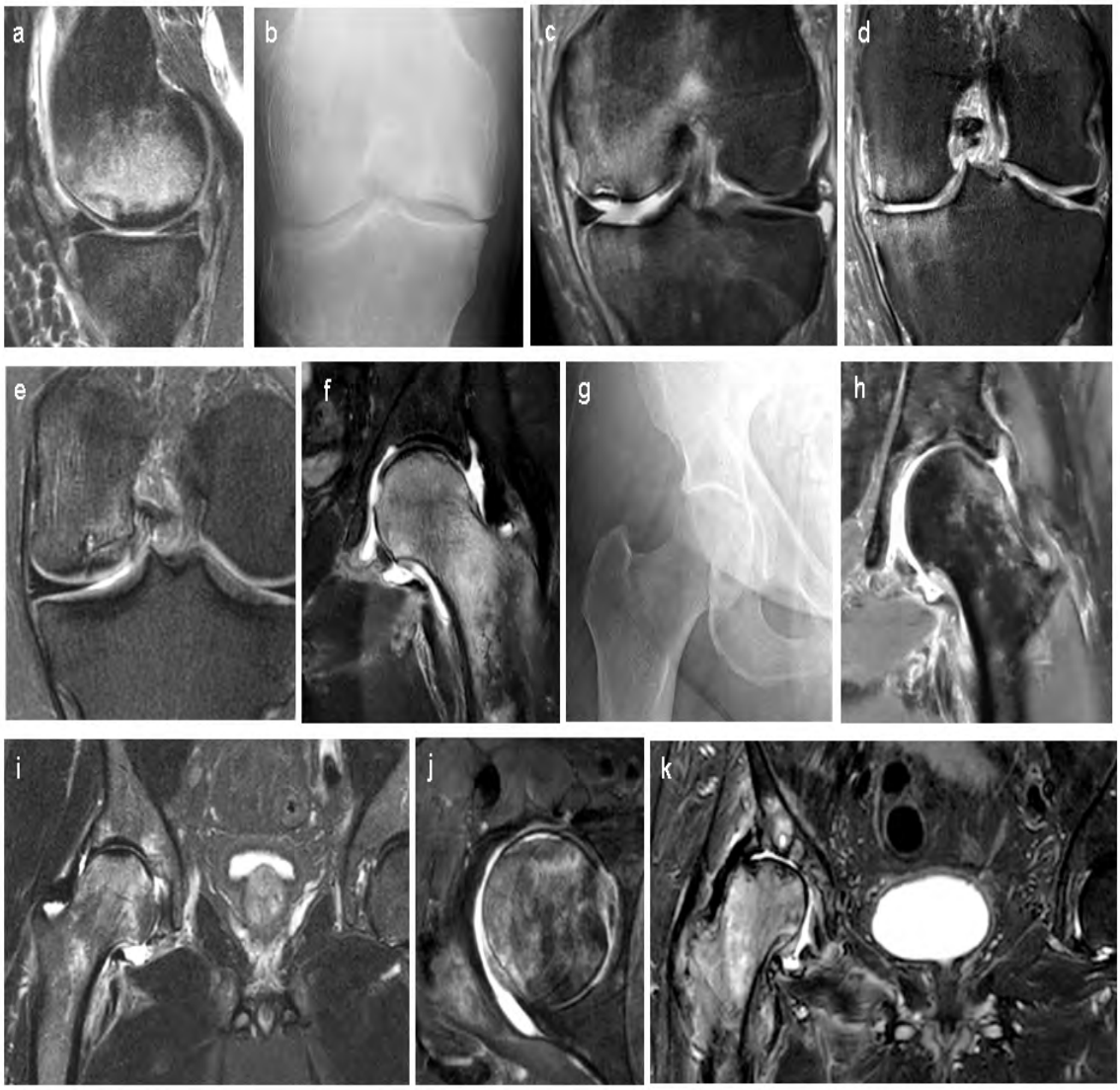

“Subchondral insufficiency fracture”(a,b,c,f,h,i),so called “spontaneous osteonecrosis of the knee”(b,c), “transient osteoporosis of the hip”(g),osteoarthritis(d,k), osteochondritis dissecans(e), “transient painful bone marrow edema”(f), avascular necrosis(j),“rapidly destructive osteoarthritis”(k).

Podium #2

LOSS OF MUSCLE QUALITY IS CORRELATED WITH DECREASED BONE MINERAL DENSITY IN PATIENTS WITH SARCOMA

Stephanie Jo, MD, PhD; Ronnie Sebro, MD, MS, PhD
Hospital of University of Pennsylvania, Philadelphia, PA, USA
(Presented by: Stephanie Jo, MD, PhD, Hospital of University of Pennsylvania)

Purpose: Sarcopenia has been shown as a poor prognostic factor for patients with malignancies. We hypothesized that decreasing muscle cross sectional area (CSA) and increasing muscle fat infiltration would be associated with decreased BMD in patients with sarcoma.

Materials and Methods: 76 patients with sarcoma were retrospectively identified. The 1 year change in the muscle computed tomography (CT) attenuation and CSA of the pectoralis major at the sternoclavicular joint, and the erector spinae at T12 was correlated with the change in CT attenuation of the T12 vertebral body. Measurements were obtained on chest CT studies at diagnosis and 1 year after diagnosis. Correlations were evaluated using Pearson's correlation coefficients. Multivariable linear regression was used adjusting for patient age, sex, and height.

Results: The 1 year decrease in BMD at T12 was positively associated with the decrease in the CT attenuation (r=0.46, $P=3.0x10^{-5}$, 95% CI (0.26, 0.62)) and CSA (r=0.30, P=0.008, 95% CI (0.08, 0.49)) of the pectoralis major, and positively correlated with the decrease in the CT attenuation of the erector spinae at T12 ($r=0.43,9x10^{-5}$, 95% CI (0.23, 0.60)). No association was seen between the change in BMD at T12 and the change in CSA of the erector spinae at T12 (r=0.08, P=0.51, 95% CI (-0.15, 0.30)). These results persisted in the multivariate analysis: the 1 year change in BMD at T12 was associated with the change in the CT attenuation ($P=8.6x10^{-5}$) and CSA (P=0.004) of the pectoralis major, and with the change in the CT attenuation of the erector spinae at T12 (P=0.0001), but not with the CSA of the erector spinae at T12 (P=0.23).

Conclusion: Increased fatty infiltration of the pectoralis major and erector spinae muscles was associated with decrease in spinal BMD at T12. This study shows the important interplay between muscles and BMD in patients with sarcoma.

Modality % - Radiography / Fluoroscopy:	0
Modality % - CT:	100
Modality % - MRI:	0
Modality % - US:	0
Modality % - Nuclear Medicine:	0

Podium #3

DIAGNOSIS OF SARCOPENIA IN THE RADIOLOGY DEPARTMENT: FEASIBLE AND SAFE?

Robert Boutin, MD[1]; Anahit Petrosyan, MD[1]; Praman Fuangfa, MD[1]; Lawrence Yao, MD[2]; John Brock[1]; Patrick Kortebein, MD[1]; Leon Lenchik, MD[3]

[1]University of California, Davis, Sacramento, CA, USA; [2]National Institutes of Health, Bethesda, MD, USA; [3]Wake Forest University School of Medicine, Winston-Salem, NC, USA

(Presented by: Robert Boutin, MD, University of California, Davis)

Purpose: Given that international consensus definitions of sarcopenia require assessment of both muscle function and muscle mass, our purpose was to examine the feasibility and safety of diagnosing sarcopenia at the point of care in the Radiology Department.

Materials and Methods: Consecutive patients $\geq$ 65 years of age undergoing clinical FDG-PET/CT scans were prospectively offered enrollment. *Functional evaluation* included: [a] SARC-F assessment, [b] Frailty Risk Assessment (FRAIL scale), [c] grip strength, and [d] gait speed. The duration of the functional evaluation and any adverse events associated with this evaluation were recorded. *CT evaluation* of muscle was performed opportunistically at the L3 level, yielding two metrics: skeletal muscle density (SMD, in HU) and skeletal muscle index (SMI, muscle area in cm2/patient height in m2). Sarcopenia was diagnosed and classified into three stages according to modified EWGSOP criteria. Functional and imaging metrics were compared using Spearman correlations.

Results: 92/100 (92%) patients (45 M, 47 F; mean age, 74.6 years; sd, 5.8) agreed to participate and completed the clinical assessment. The duration of the functional assessment ranged from 3.5 to 6.0 minutes. There were no adverse events. Positive screening results by individual measures were: SARC-F (21/92, 23%), FRAIL (32/92, 35%), grip strength (19/92, 21%), gait speed (11/92, 12%), SMD (80/92, 87%), SMI (69/92, 75%). SMD was significantly correlated with SARC-F, FRAIL, grip strength, and gait speed ($R=-0.30$, $p<0.01$; $R=-0.27$, $p<0.01$; $R=0.40$, $p<0.001$; $R=0.39$, $p<0.001$, respectively). SMI was significantly correlated only with grip strength and gait speed ($R=0.43$, $p<0.001$ and $R=0.29$, $p<0.01$, respectively). Based on SMD, the group incidences of pre-sarcopenia, sarcopenia, and severe sarcopenia were 56.5%, 27.2%, and 2.2%; based on SMI, these incidences were 50%, 20.7%, and 2.2%.

Conclusion: Prospective collection of functional data and opportunistic CT data is both feasible and safe. Such an integrated approach allows the diagnosis of sarcopenia to be established in Radiology departments.

Modality % - Radiography / Fluoroscopy:	0
Modality % - CT:	100
Modality % - MRI:	0
Modality % - US:	0
Modality % - Nuclear Medicine:	0

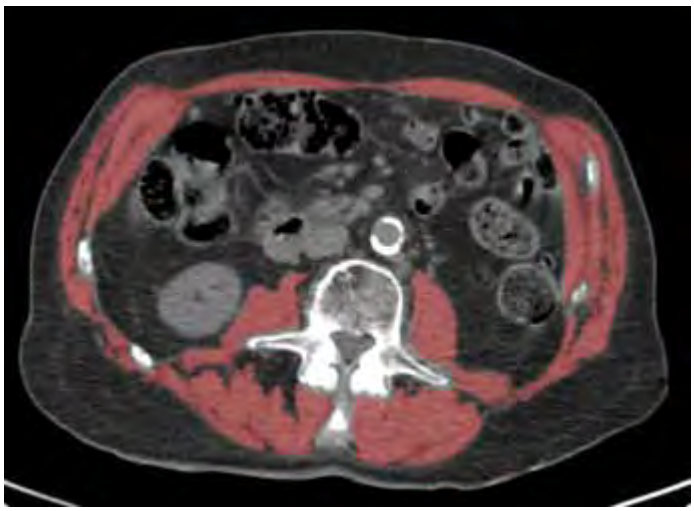

83-year-old man with a body mass index of 26, skeletal muscle density of 31 HU, and skeletal muscle index of 43.4 cm2/m2.

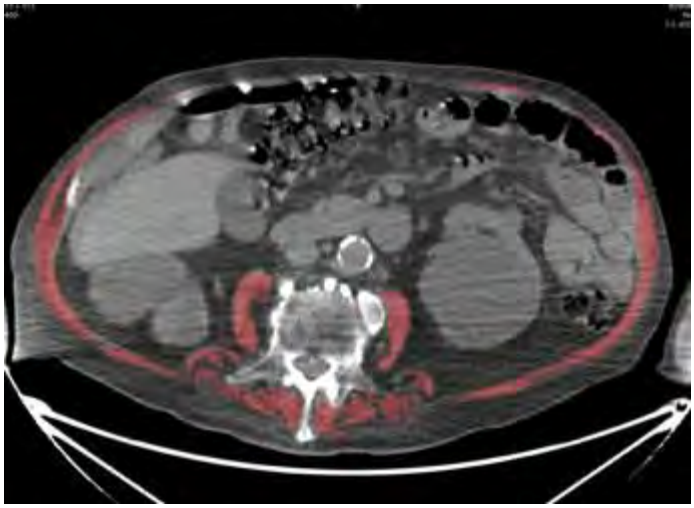

84-year-old man with a body mass index of 26, skeletal muscle density of 20 HU, and skeletal muscle index of 20.2 cm2/m2.

Podium #4

TRENDS OF FOLLOW UP RECOMMENDATIONS MADE ON MUSCULOSKELETAL MRI EXAMINATIONS

Tony Wong, MD; John Nemer; Jonathan Kazam, MD
Columbia-Presbyterian Medical Center, New York, NY, USA
(Presented by: Tony Wong, MD, Columbia-Presbyterian Medical Center)

Purpose: To analyze trends in the follow up recommendations made on musculoskeletal MRI reports

Materials and Methods: An IRB-approved retrospective search identified 790 separate musculoskeletal MRI reports containing follow up recommendations from 1/1/2016-12/31/2017. A total of 774 reports were analyzed (excluding 16 exams that were incomplete or contained artifact). Meta-data was automatically extracted and follow up recommendations were determined from manual review. Outcome data was determined by EHR and was available for 654 reports (120 were lost to follow up). Descriptive statistics and a chi-squared test were used for analysis.

Results: Types of recommendations: additional imaging (68%), obtain old studies (5%), clinical history/physical exam (14%), subspecialty consult (4%), lab-work (5%), intervention (7%) (Fig 1a)

Recommendation compliance by clinicians: followed (73%) vs. not followed (27%) (Fig 2a)

Recommendations followed by clinicians:

1. Inpatient (74%) vs. Outpatient (73%); $p = 0.77$
2. After direct communication (93%) vs. no direct communication (71%); $p < 0.001$
3. Based on pathology: neoplasm (73%), trauma (73%), infection/inflammation/degenerative disease (73%), hardware (71%), vascular abnormality (77%); $p = 1.0$
4. Based on recommendation: additional imaging (67%), obtain old studies (72%), clinical history/physical exam (92%), subspecialty consult (69%), lab-work (76%), intervention (98%); $p < 0.001$ (Fig 1b)

Recommendations acknowledged by clinicians: acknowledged (83%) vs. unacknowledged (17%) (Fig 2b)

73% of all unacknowledged recommendations were concern for neoplasm (locations: 41% abdomen/pelvis, 40% bone, 2% brain, 13% head/neck, 4% lung)

Acknowledged/followed by subspecialty: Ortho (76%/64%), Rehab (86%/77%), Internal medicine (92%/85%), Non-Ortho Surgery (83%/75%), Other (92%/82%); ($p < 0.001$/$p < 0.001$)

Conclusion: Many recommendations made on musculoskeletal MRIs are not followed independent of patient location and type of suspicious pathology. Requests for additional imaging are least likely to be followed.

The majority of unacknowledged recommendations are for suspicion of neoplasm.

Direct communication with clinicians can increase compliance for follow up recommendations, which may be helpful in particular for orthopedic referrers.

Modality % - Radiography / Fluoroscopy:	0
Modality % - CT:	0
Modality % - MRI:	100
Modality % - US:	0
Modality % - Nuclear Medicine:	0

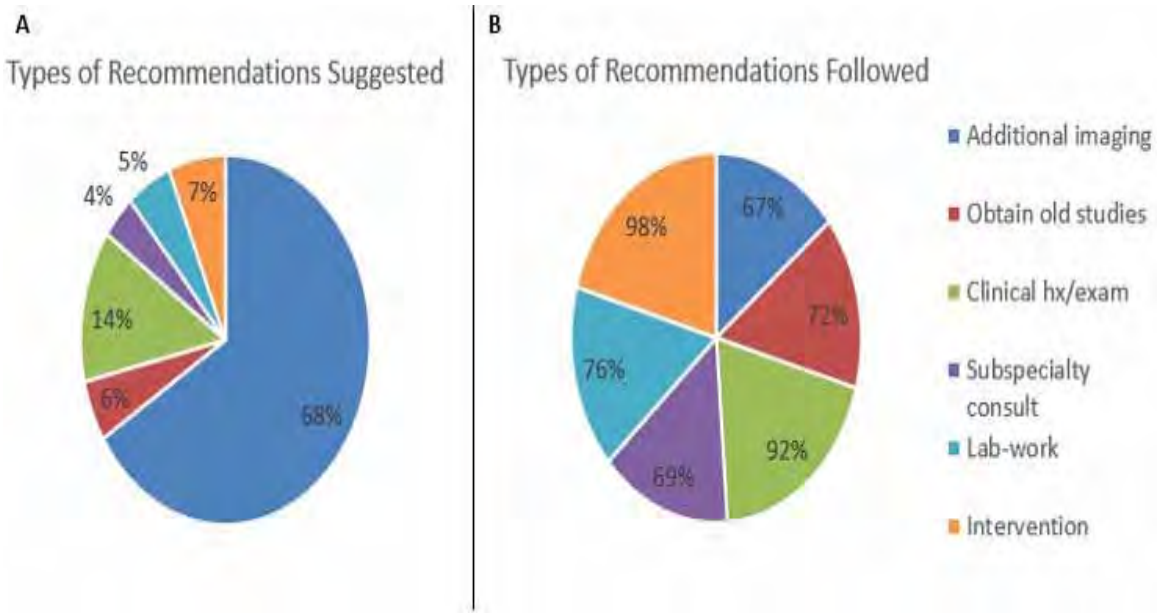

Types of Recommendations Suggested (A) and Followed (B)

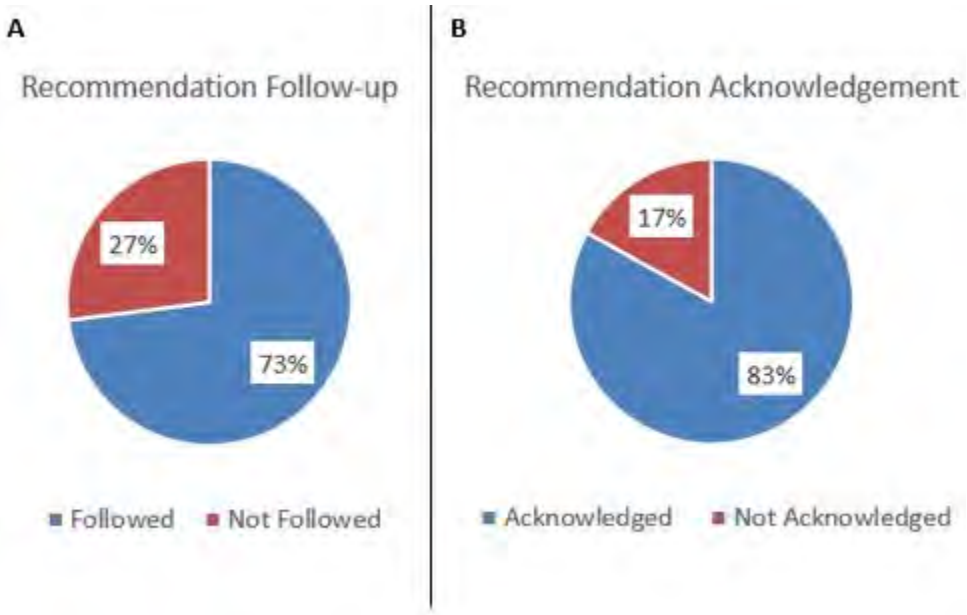

Recommendation Follow-up (A) and Acknowledgement (B)

Podium #5

MRI SEGMENTATION OF THE GLENOID AND HUMERAL HEAD USING DEEP CONVOLUTIONAL NEURAL NETWORKS

Tatiane Cantarelli Rodrigues, MD[1]; Cem Deniz, PhD[2]; Jared Dublin[2]; Natalia Gorelik, MD[1]; Soterios Gyftopoulos, MD, MS[1]
[1]NYU Medical Center/ Hospital for Joint Diseases Langone Medical Center, New York, NY, USA; [2]New York University School of Medicine, New York, NY, USA
(Presented by: Tatiane Cantarelli Rodrigues, MD, NYU Medical Center/ Hospital for Joint Diseases Langone Medical Center)

Purpose: To present an automatic humeral head and glenoid segmentation method based on two-dimensional deep convolutional neural networks (CNNs).

Materials and Methods: The study received institutional review board approval. A retrospective dataset of volumetric structural MR images of the shoulder from 100 subjects, including 73 normal cases and 27 cases with a Hill-Sachs lesion and/or anterior glenoid bone loss in the setting of anterior shoulder instability, were manually segmented by experts. A 2D CNN architecture was trained with multiple initial feature maps and layers. Its segmentation performance was then tested against the gold standard of manual segmentation using four-fold cross-validation. The time needed to manually segment each shoulder MRI was documented for each case.

Results: Automatic segmentation of the humeral head achieved a mean average precision for object detection of 0.99, a dice similarity score of 0.95, a segmentation precision of 0.95, and recall of 0.95. The Hausdorff distance was 26.9mm, the mean square distance of 0.5mm, and the residual mean square distance of 1.5mm. For the glenoid, automatic segmentation achieved a mean average precision for object detection of 0.92, a dice similarity score of 0.86, a segmentation precision of 0.88, and recall of 0.86. The Hausdorff distance was 20.7mm, the mean square distance of 0.8mm, and the residual mean square distance of 1.8mm. On average, the time for manual segmentation ranged between 90 to 120 minutes per imaging study.

Conclusion: Using CNNs, we were able to accurately segment the humeral head and glenoid on MRI. Our results serve as an important initial step towards the automatic diagnosis and quantification of Hill-Sachs lesions and glenoid bone loss and determination of on/off track status. This, in turn, has the potential to provide consistently accurate imaging information that can be used to guide the selection of the most appropriate initial treatment for the anterior shoulder instability patient population.

Modality % - Radiography / Fluoroscopy:	0
Modality % - CT:	0
Modality % - MRI:	100
Modality % - US:	0
Modality % - Nuclear Medicine:	0

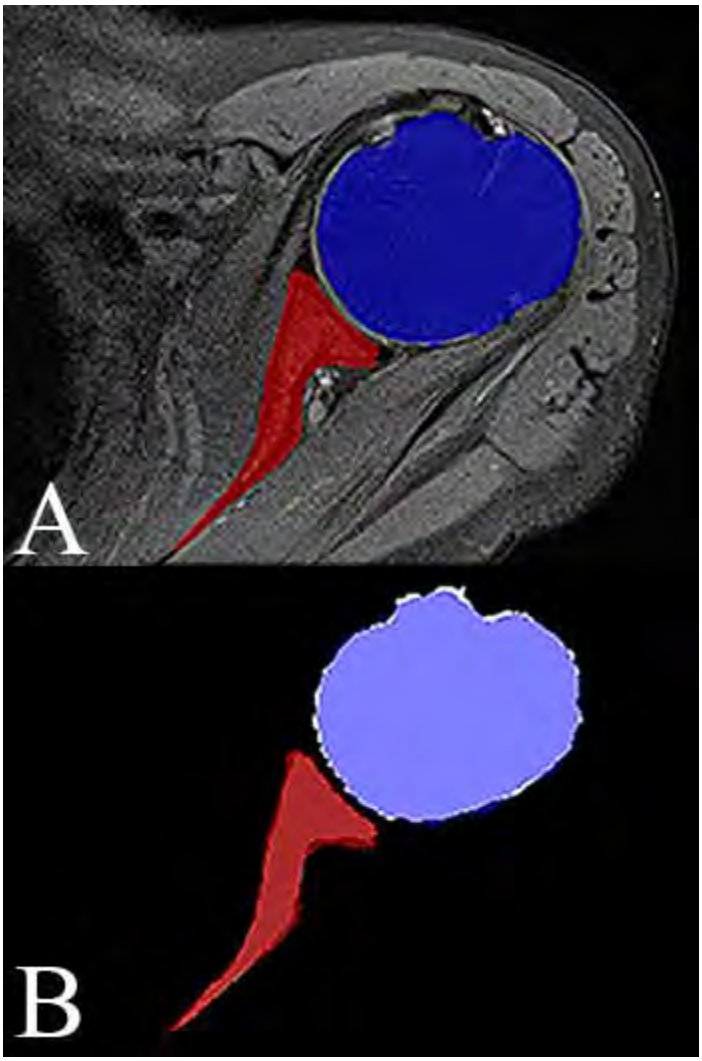

A. Automatic segmentation performed by CNN. B. Comparison between manual (white for humerus; grey for glenoid) and automatic segmentation (blue for humerus; red for glenoid).

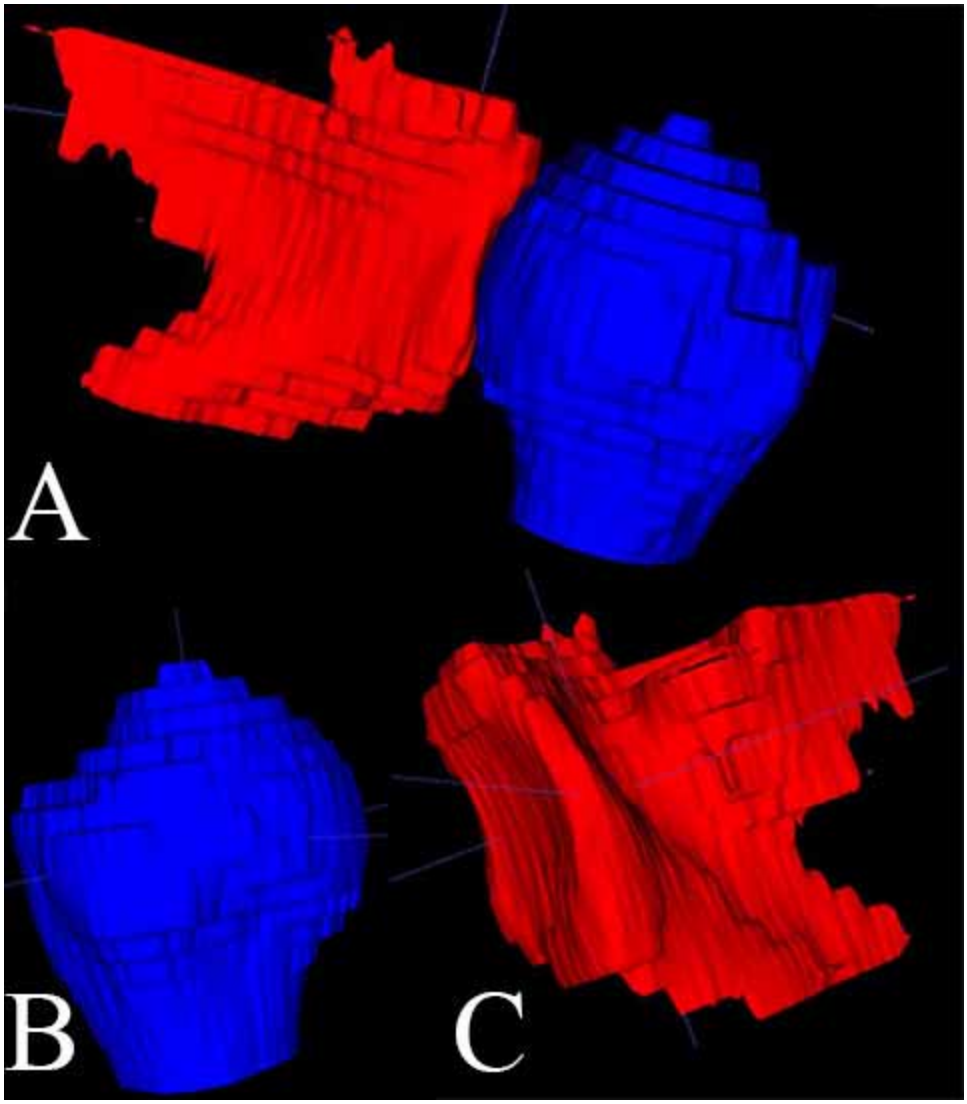

Three dimensional reconstructions of an automatically segmented humeral head (blue) and glenoid (red).

Podium #6

MACHINE LEARNING CLASSIFICATION OF SOFT TISSUE MASSES OF THE PELVIS

James Cortez, MD[1]; Michael Richardson, MD[2]; Beth Vettiyil, MD[1]; Behrang Amini, MD, PhD[1]
[1]The University of Texas M.D. Anderson Cancer Center, Houston, TX, USA; [2]University of Washington / Harborview Medical Center, Seattle, WA, USA
(Presented by: James Cortez, MD, The University of Texas M.D. Anderson Cancer Center)

Purpose: Prospective classification of a soft tissue mass as benign or malignant remains challenging. We sought to develop a machine learning-derived decision tree for classification of soft tissue masses about the pelvis.
Materials and Methods: 5,334 consecutive musculoskeletal pelvis MRIs performed between 12/1/2014 and 8/31/2018 were retrospectively reviewed. 71 studies met inclusion criteria (absence of significant artifact, imaging prior to therapy initiation, and presence of DWI and of post-contrast sequences). Images were reviewed by a single musculoskeletal imaging fellow, assisted when needed by a fellowship trained attending with 6 years' experience. Assessed variables were: age, sex, T1 heterogeneity, presence of low T2 signal areas, whether lesion was mostly T2 hyperintense, internal fat, myxoid appearance on T2 and post-contrast images, peri-lesional “edema,” longest dimension, and mean ADC of low-ADC, solid areas. Age, dimension, and ADC were continuous variables, and the remaining were binary. These data were used to build a decision tree for benign/malignant classification using the C4.5 algorithm (J48 classifier in Weka 3.8.2, University of Waikato, NZ) using 50% of the data for training, and the other 50% for validation. Results for the validation set are presented.
Results: The decision tree is shown in Fig 1. Addition of DWI produced identical diagnostic performance. Decision points were size (cutoffs: 6.7 cm and 8.7 cm), perilesional “edema,” lesion T1-heterogeneity, and age (cutoff: 55 years). Diagnostic performance was as follows. Sensitivity: 0.82 (95% CI: 0.48-0.98), specificity: 0.75 (95% CI: 0.53-.90), accuracy 0.77 (95% CI: 0.60-0.90) and positive and likelihood ratios: 3.3 (95% CI: 1.6-6.9) and 0.24 (95% CI: 0.07-0.87), respectively. Estimated area under the ROC curve: 0.790 (95% CI: 0.61-0.97).
Conclusion: We propose an algorithm for classification of soft tissue masses of the pelvis using standard, non-contrast MR imaging. The results would need to be validated in a larger data set.

Modality % - Radiography / Fluoroscopy:	0
Modality % - CT:	0
Modality % - MRI:	1
Modality % - US:	0
Modality % - Nuclear Medicine:	0

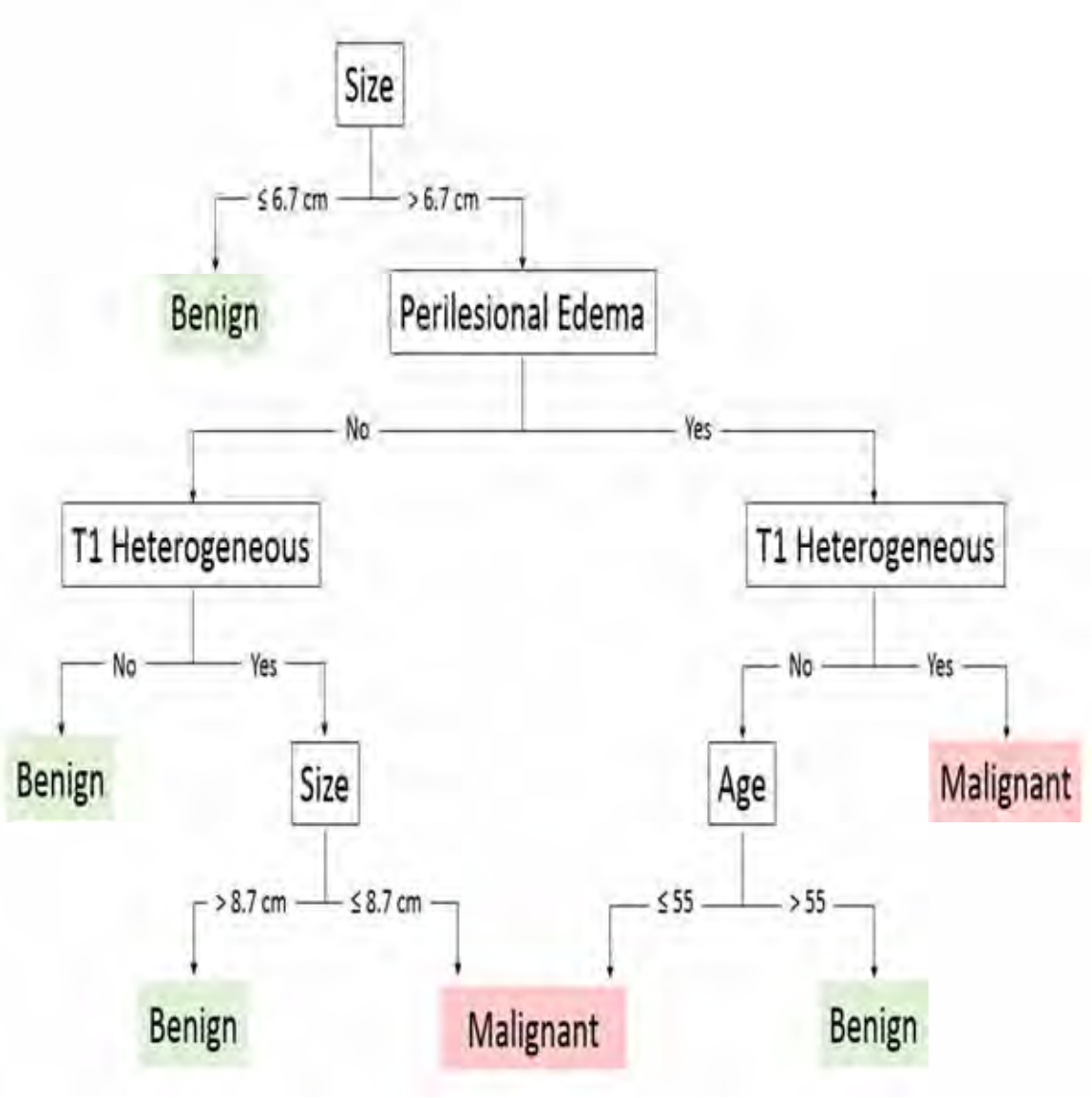

Proposed algorithm for classification of soft tissue masses about the pelvis

Podium #7

Comparison of "STIR-CT" to conventional CT images for detection of muscle lesions in a beef shank model.

Joshua Polster, MD; Jennifer Bullen, MS; Naveen Subhas, MD; Bradford Richmond, MD; Darlene Holden, MD; Jean Schils, MD
Cleveland Clinic, Cleveland, OH, USA
(Presented by: Joshua Polster, MD, Cleveland Clinic)

Purpose: To compare the accuracy and diagnostic confidence between conventional CT images and an experimental processing technique for CT images termed "STIR-CT" that mimics a fluid-sensitive MRI sequence.

Materials and Methods: A model to mimic muscle strains was created using injected water in beef shank specimens. 7 specimens were used. 0, 1 or 2 lesions was created in each specimen by injecting 3 to 5 cc of tap water using a 22G needle. CT data was acquired using routine clinical protocol and reconstructed using soft tissue reconstruction (B40) at 3 mm slice thickness per clinical protocol with standard clinical window and level. A second set of images was created employing a "fluid-peak" look-up table to mimic the appearance of STIR MRI yielding 14 image sets (7 standard,7 STIR-CT). 4 musculoskeletal radiologists interpreted each data set in randomized order blinded to the number of lesions injected. For each suspected lesion, the lesion was pointed out and a confidence score was given.

Results: Aggregating all 4 readers, 100% of lesions (24 of 24) were identified correctly using STIR-CT images and 95.8% (23 of 24) were identified using standard images. There were a total of 5 false positives on STIR-CT imaging and 4 false positives on standard imaging. There was one false negative on standard imaging. Median confidence scores for correctly identified lesions were higher using the STIR-CT technique for 2 readers (100 vs 95; 87.5 vs 75) and the same for the other 2 readers however this was not statistically significant. Median confidence scores for false positive cases was higher using standard technique for 2 readers (100 vs 70; 95 vs 80).

Conclusion: More lesions were correctly identified and confidence scores were higher for some readers using the STIR-CT technique than conventional CT technique however the differences were not statistically significant.

Modality % - Radiography / Fluoroscopy:	0
Modality % - CT:	100
Modality % - MRI:	0
Modality % - US:	0
Modality % - Nuclear Medicine:	0

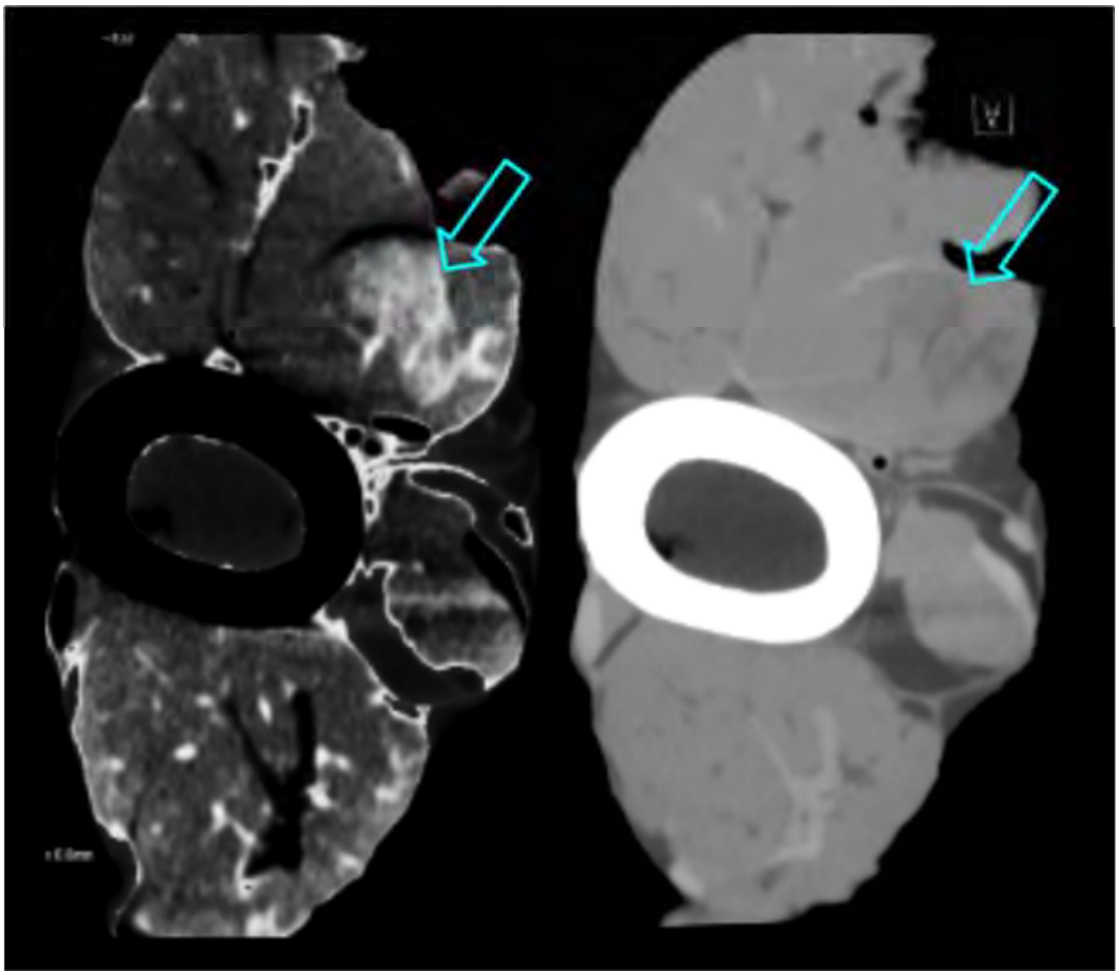

STIR CT (left image) and conventional CT (right image) with muscle lesion (arrows)

Podium #8

CT-guided bone marrow aspirations and biopsies: retrospective review and comparison with blind procedures

Connie Chang, MD; Adriana Moreira; Nathaniel Mercaldo, MS; Jad Husseini, MD; Robert Hasserjian, MD
Mass General Hospital, Boston, MA, USA
(Presented by: Connie Chang, MD, Mass General Hospital)

Purpose: To compare the pathology results of CT-guided and blind bone marrow aspirations and biopsies.

Materials and Methods: This study was IRB-approved and HIPAA-compliant. 76 consecutive CT-guided and 70 blind posterior iliac crest bone marrow aspirations and biopsies performed between 1/2017-10/2017 were reviewed. All CT-guided biopsies used an 11-gauge battery-powered drill-assisted device. Blind biopsies used either the drill-assisted device or a 13-gauge manual biopsy device. Pathology reports were reviewed for adequacy of aspirate smears and biopsy samples (categorized as adequate, suboptimal, and not adequate) and core length. Patient age, gender, and body mass index (BMI), and core length were compared using Mann-Whitney (continuous) or chi-square/Fisher's Exact (categorical) tests.

Results: No significant difference was detected in the age (CT: median [25 and 75th percentile] 65 [56, 72] years; blind: 69 [57, 76] years; P = 0.1) or BMI (CT: 26.6 [23.1, 29.6]; blind: 27.3 [24.8, 32]; P =0.1) of the CT-guided and blind biopsy groups. The blind biopsy group (48 M, 22 F) had a higher proportion of males than the CT-guided biopsy group (38 M, 38 F; P = 0.02).

More CT-guided aspirate smears than blind aspirate smears were categorized by the pathologist as adequate (CT: 72 (97%) adequate, 2 (3%) suboptimal, 0 inadequate, 2 no smear; blind: 58 (85%) adequate, 5 (7%) suboptimal, 5 (7%) inadequate, 2 no smeard; P = 0.02).

More CT-guided biopsy samples than blind biopsy samples were categorized as adequate (CT: 72 (95%) adequate, 4 (5%) suboptimal, 0 inadequate; blind: 54 (77%) adequate, 9 (13%) suboptimal; 7 (10%) inadequate; P = 0.002).

The CT-guided biopsies had longer aggregate core lengths (CT: 1.3 [0.9, 1.8] mm; blind: 1.0 [0.6, 1.2] mm; P = 0.001).

Conclusion: CT-guided bone marrow procedures were more likely to result in both adequate aspirate smears and biopsy samples when compared to blind bone marrow procedures.

Modality % - Radiography / Fluoroscopy:	0
Modality % - CT:	100
Modality % - MRI:	0
Modality % - US:	0
Modality % - Nuclear Medicine:	0

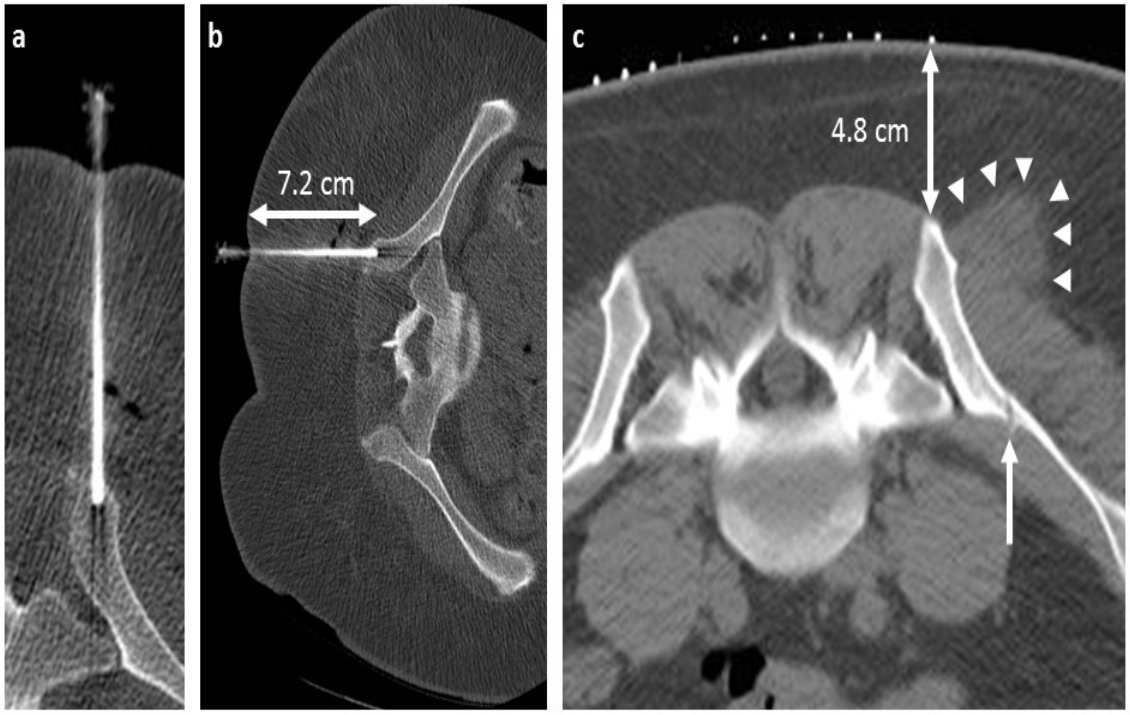

a) Many marrow biopsies can be accomplished by a vertical trajectory. At first glance, CT-guidance does not appear to be necessary.

b) In reality, this procedure was performed in the decubitus position, because the patient was not able to tolerate lying in the prone position for the procedure. In addition, there was 7.2 cm of subcutaneous fat overlying the posterior ilium. The traditional palpated landmarks for blind marrow biopsies could not be used for this patient.

c) This patient had an attempted blind marrow biopsy, which was also was challenging due the patient size (4.8 cm of subcutaneous fat). Now marrow sample was obtained. On the CT procedure image, the tract in the thin portion of the iliac wing is visualized (arrow), as well as a traumatic hematoma from the procedure (arrowheads). CT-guided marrow biopsy yielded adequate smear and biopsy.

Image includes a caption. Two patients' biopsy images demonstrating reasons CT-guidance is helpful for a marrow biopsy.

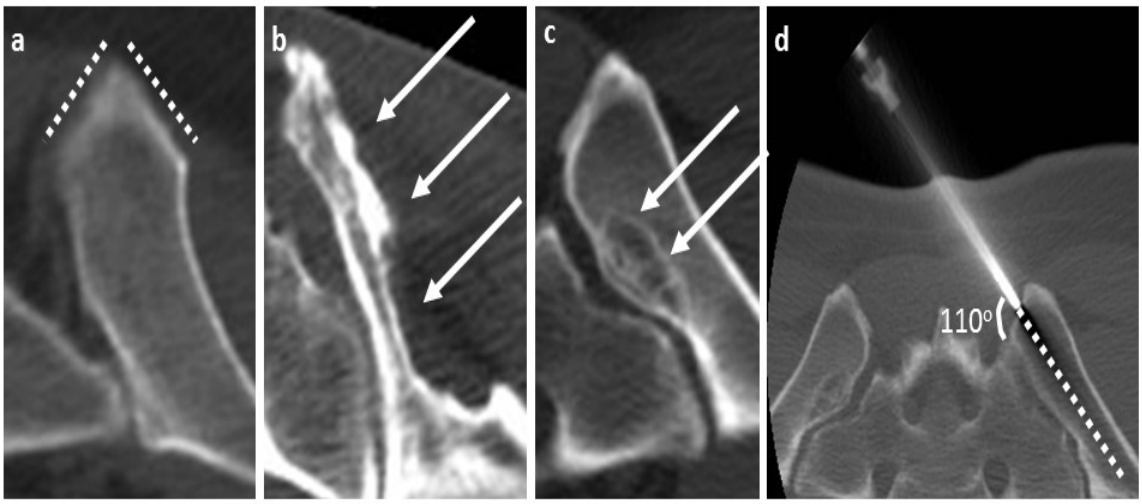

Without direct visualization of the posterior ilium, other unexpected challenges can be encountered, resulting in a suboptimal or inadequate smears and biopsy samples.

a) This posterior ilium has a sharp point, with steep adjacent slanting bone (dashed lines). Steep angles are more difficult for a bone biopsy needle to access, as the needle will easily slide off the edge of the bone.
b) This posterior ilium is a prior bone graft harvest site (arrows); there is little available marrow for a biopsy. The contralateral side was targeted for biopsy.
c) This posterior ilium has a focal bone lesion (arrows), which should be avoided for the biopsy.
d) This posterior ilium has a steep slant extending from medial to lateral. Using CT-guidance allows for planning the approach so that it can both land on the bone at close to a 90 degree angle, which is the best angle for gaining access to the bone. In addition, this trajectory is along the long access of the bone, and therefore there is a long trajectory for both the aspiration and the biopsy. With myelofibrosis, there can be a scarcity of marrow, and a long trajectory (dashed line) makes more marrow available to attempt aspiration.

Image includes a caption. Four patients with four different reasons that make blind arrow biopsies challenging.

Podium #9

ILIAC BONE MARROW BIOPSY AND ASPIRATION WITH FLUOROSOCOPIC GUIDANCE - EXPERIENCE WITH 775 CASES

Jeremiah Long, MD[1]; James Stensby, MD[2]; Travis Hillen, MD[3]; Jack Jennings, MD, PhD[3]; Stephen Herrmann, MD[3]; Elizabeth Wiesner, BA[3]

[1]Mayo Clinic, Phoenix, AZ, USA; [2]University of Missouri, Columbia, MO, USA; [3]Mallinckrodt Institute of Radiology, Saint Louis, MO, USA

(Presented by: Jeremiah Long, MD, Mayo Clinic)

Purpose: To evaluate the efficacy and safety of performing a fluoroscopically guided bone marrow aspiration and biopsy (BMAB) using a drill-powered needle in a large patient population.

Materials and Methods: This retrospective study received institutional review board approval with a waiver of patient informed consent. From August 2012 through December 2016, a total of 775 BMAB procedures were performed at a single institution using fluoroscopic guidance and a drill-powered needle. Clinical diagnosis, patient age, patient gender, biopsy site, biopsy needle gauge, bone marrow aspirate volume, bone marrow core biopsy length, patient platelet count, conscious sedation details, complications and diagnostic adequacy were investigated for each case and summarized.

Results: Samples obtained from the procedures in our series were diagnostic in 93% of cases. The complication rate for our series was 0.3% (2 episodes of hypoxia and 1 episode of supraventricular tachycardia, no fatalities). The patients in this study ranged in age from 16 to 91 years (average age 53 years). In cases where conscious sedation was utilized and details were recorded (738/775), the average sedation time was 21.1 minutes.

Conclusion: The use of fluoroscopic guidance and a drill-powered needle for bone marrow biopsy and aspiration is a safe and efficacious procedure.

Modality % - Radiography / Fluoroscopy:	100
Modality % - CT:	0
Modality % - MRI:	0
Modality % - US:	0
Modality % - Nuclear Medicine:	0

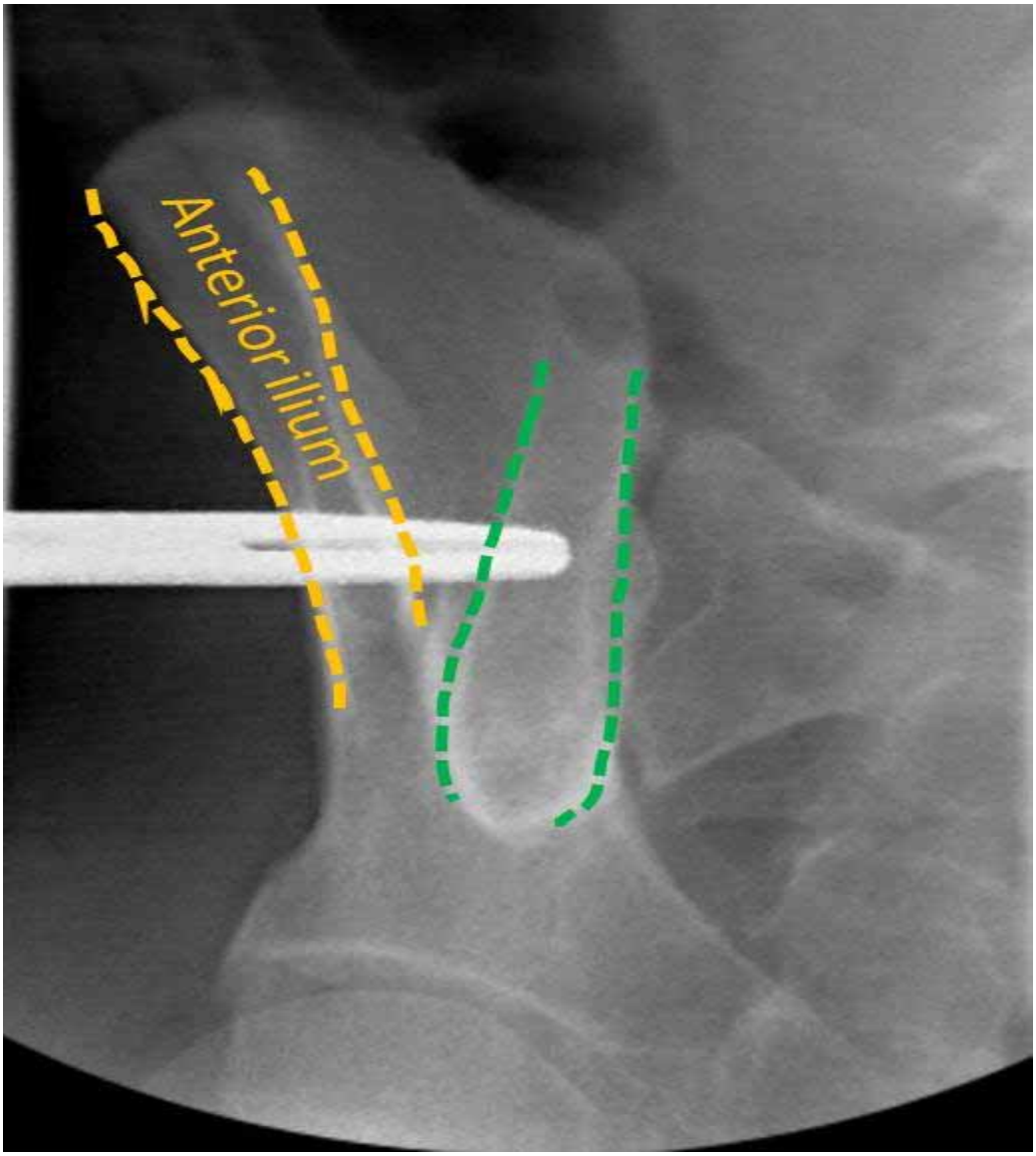

Fluoroscopic image with the anterior (yellow) and posterior (green) ilium demarcated by dotted lines. A clamp identifies the middle third of the posterior ilium.

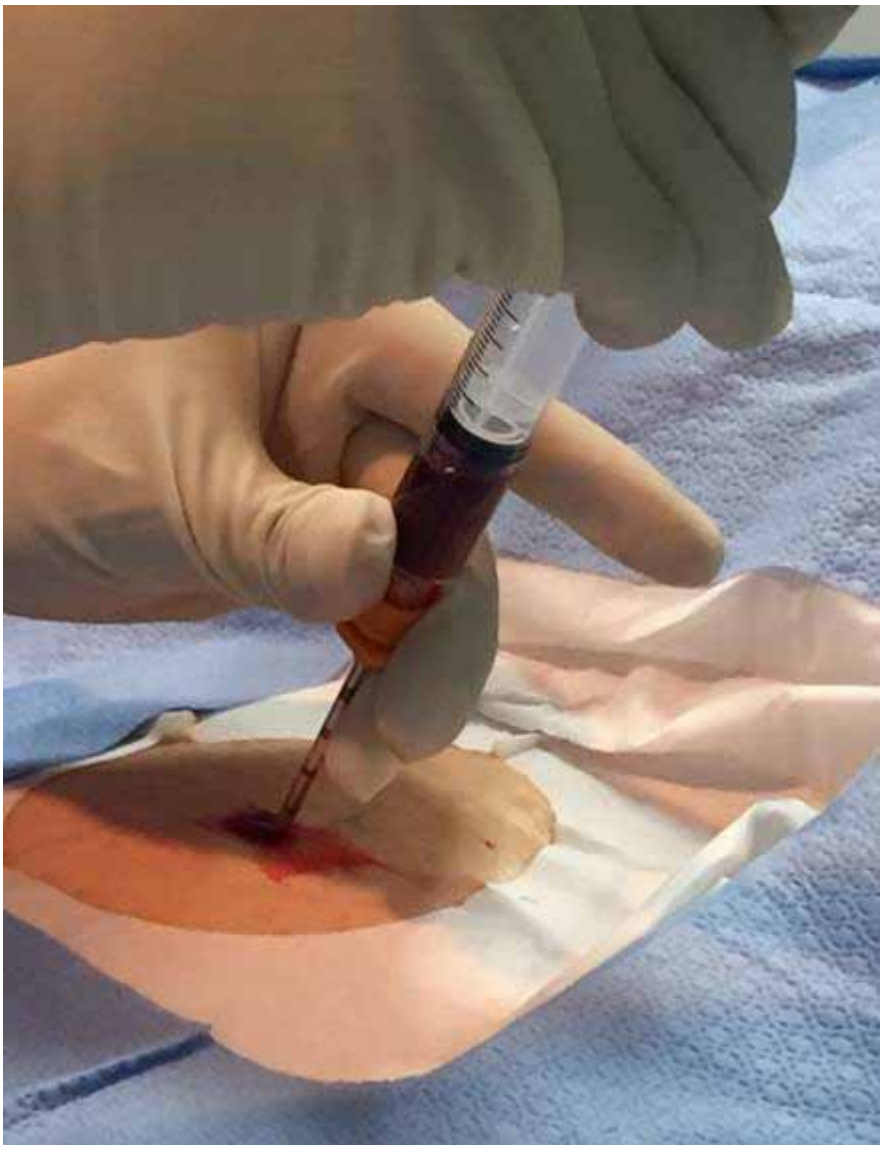

Fluoroscopic image showing the biopsy needle en face with a clamp holding it in position at the middle third of the posterior ilium.

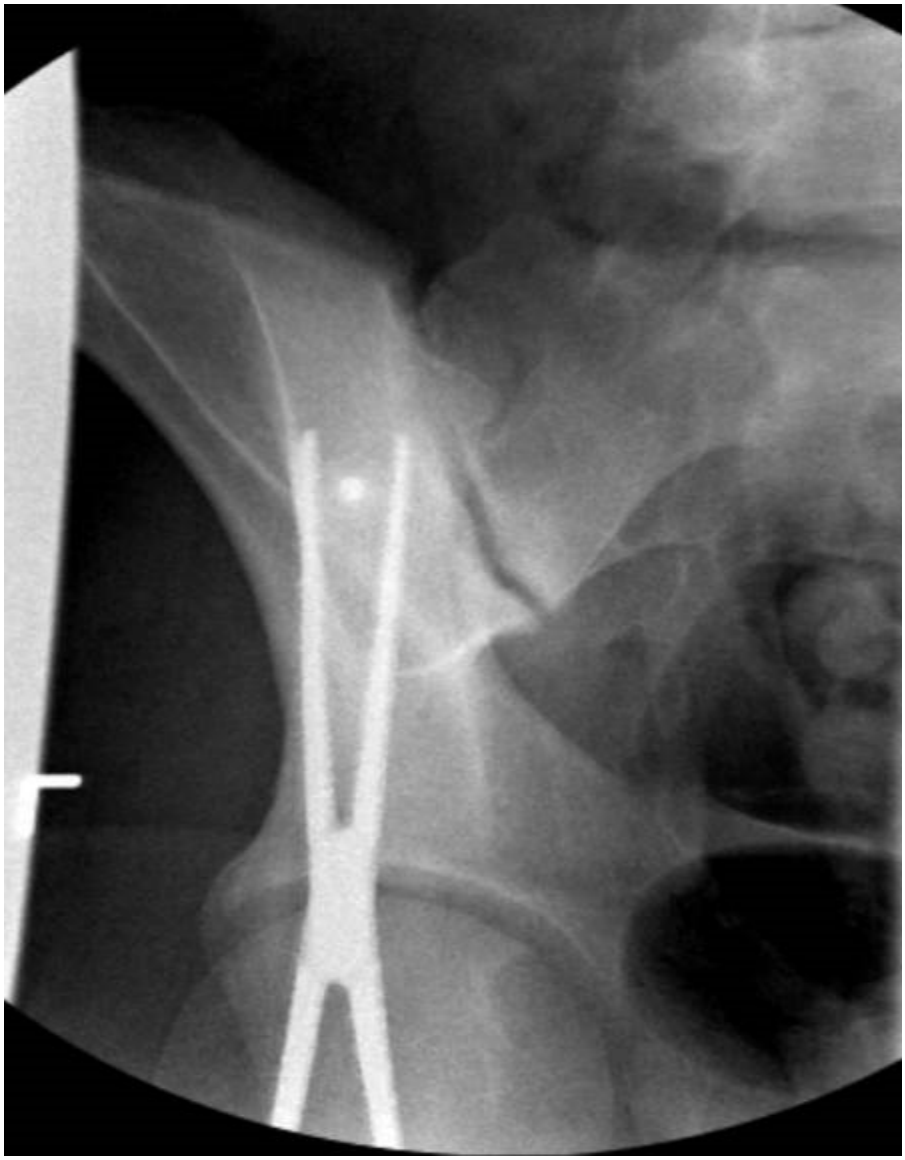

Photo showing aspiration of bone marrow aspirate from the posterior ilium.

Photo showing the drill on the end of the needle during bone core biopsy from the posterior ilium.

MONDAY

Society of Skeletal Radiology

42nd Annual Meeting

March 10-13, 2019

Monday, March 11, 2019

7:00 a.m.–7:55 a.m. **Continental Breakfast**

7:00 a.m.–12:35 p.m. **Registration/Information Desk Open**

7:00 a.m.–12:30 p.m. **Exhibit Hall Open**

7:45 a.m.–8:00 a.m. ESSR Best Paper Award Presentation

LUMBAR SPINE MRI: ARE T1 SAGITTAL IMAGES STILL REQUIRED WHEN USING T2 DIXON SEQUENCES?

Moderators: Laura Bancroft, MD, FACR, Lawrence White, MD FRCPC

8:00 a.m.–10:00 a.m. **UPPER EXTREMITY**

Moderators: Mark Anderson, MD, Naveen Subhas, MD

8:00 a.m. #10 **STABLE VERSUS UNSTABLE OSTEOCHONDRAL LESIONS OF THE ELBOW: PERFORMANCE OF MR IMAGING CRITERIA FOR INSTABILITY**

Jie Nguyen, MD, MS[1]; Andrew Degnan, MD[1]; Theodore Ganley, MD[1]; Christian Barrera, MD[1]; Thor Perrin Hee[1]; Richard Kijowski, MD[2]

[1]Children's Hospital of Philadelphia, Philadelphia, PA, USA; [2]University of Wisconsin Hospital & Clinics, Madison, WI, USA

(Presented by: Jie Nguyen, MD, MS, Children's Hospital of Philadelphia)

8:15 a.m. #11 **THE SMOKE SIGN: A SIGN OF PECTORALIS TENDON HUMERAL INSERTIONAL INJURY ON ROUTINE SHOULDER MRI**

Devin Vaswani, MD[1]; CATHERINE PETCHPRAPA, MD[1]; ELISABETH GARWOOD, MD[2]; MOHAMMAD SAMIM, MD[1]; JENNY BENCARDINO, MD[1]

[1]NYU Medical Center/ Hospital for Joint Diseases Langone Medical Center, New York, NY, USA; [2]University of Massachusetts Memorial Medical Center, Worcester, MA, USA

(Presented by: Devin Vaswani, MD, NYU Medical Center/ Hospital for Joint Diseases Langone Medical Center)

8:30 a.m. #12 **MAGNETIC RESONANCE IMAGING FINDINGS IN THE FAILED SUPERIOR CAPSULAR RECONSTRUCTION**

Harry Greditzer, IV, MD, MS[1]; George Balazs, MD[2]; Susan Lee, MD[1]; Jean Jose, DO[3]; Joshua Dines, MD[1]

[1]Hospital for Special Surgery, New York, NY, USA; [2]Naval Medical Center, portsmouth, VA, USA; [3]University of Miami Miller School of Medicine, miami, FL, USA

(Presented by: Harry Greditzer, IV, MD, MS, Hospital for Special Surgery)

8:45 a.m. #13 **PREVALENCE OF PSEUDOEROSIONS OF THE HAND AND WRIST: ULTRASOUND FINDINGS IN 100 ASYMPTOMATIC VOLUNTEERS**

Anna Falkowski, MD, MHBA[1]; Jon Jacobson, MD[1]; Vivek Kalia, MD, MPH[1]; Angela Atinga, MB BChir FRCR[2]; Girish Gandikota, MBBS FRCS FRCR[1]; Ralf Thiele, MD[3]

[1]University of Michigan Medical Center, Ann Arbor, MI, USA; [2]University of Toronto, Toronto, ON, Canada; [3]The University of Rochester School of Medicine and Dentistry, Rochester, NY, USA

(Presented by: Anna Falkowski, MD, MHBA, University of Michigan Medical Center)

9:00 a.m. #14 **SUPRASPINATUS AND INFRASPINATUS TENDON TEARS: NEW INSIGHTS ON LOCATION FROM RECENT ANATOMIC STUDIES**

Michael Tuite, MD; Brian Chan, MD

University of Wisconsin Hospital & Clinics, Madison, WI, USA

(Presented by: Michael Tuite, MD, University of Wisconsin Hospital & Clinics)

9:15 a.m. #15

LOSS OF REDUCTION IS COMMON AFTER CORACOCLAVICULAR LIGAMENT RECONSTRUCTION
Brian Kennedy, MD; Michael Alaia, MD; Erin Alaia, MD;
NYU Medical Center/ Hospital for Joint Diseases Langone Medical Center, New York, NY, USA
(Presented by: Brian Kennedy, MD, NYU Medical Center/ Hospital for Joint Diseases Langone Medical Center)

9:30 a.m. #16 **POSTERIOR ELBOW DISLOCATION. MRI IMAGING FEATURES AND PATHOPHYSIOLOGIC CONSIDERATIONS**
Michael Zlatkin, MD; Timothy Sanders, MD
Nationalrad, Deerfield Beach, FL, USA
(Presented by: Michael Zlatkin, MD, Nationalrad)

9:45 a.m. #17 **ULTRASOUND-MRI CORRELATION FOR HEALING OF ROTATOR CUFF REPAIRS USING VASCULARITY AND TENDON ELASTICITY: A PILOT STUDY**
Ronald Adler, MD, PhD; Soterios Gyftopoulos, MD; Nicole Nocera, MD
NYU Medical Center/ Hospital for Joint Diseases Langone Medical Center, New York, NY, USA
(Presented by: Ronald Adler, MD, PhD, NYU Medical Center/ Hospital for Joint Diseases Langone Medical Center)

10:00 a.m.–10:05 a.m. **CASE OF THE DAY**
Presenting author: Kaushal Mehta, MD

10:05 a.m.–10:30 a.m. **Break - Visit the Exhibit Hall**

10:30 a.m.–12:30 p.m. **INTERVENTION**
Moderators: MK Jesse, MD, Kenneth Lee, MD

10:30 a.m. #18 **PLATELET-RICH PLASMA FOR TREATMENT OF MODERATE-TO-SEVERE MIDSUBSTANCE ACHILLES TENDINOPATHY: A PILOT RCT WITH CONVENTIONAL AND NOVEL ULTRASOUND IMAGING CORRELATION**
David Gimarc, MD; Paul Michelin, MD; Darryl Thelen, PhD; John Wilson, MD, MS; Kenneth Lee, MD
University of Wisconsin Hospital & Clinics, Madison, WI, USA
(Presented by: David Gimarc, MD, University of Wisconsin Hospital & Clinics)

10:45 a.m. #19 **TO DRILL OR NOT TO DRILL, THAT IS THE QUESION**
Kevin He, MD; John Campbell; Bryan Wolf, MD; Barry Hansford, MD; Brooke Beckett, MD
Oregon Health Sciences University, Portland, OR, USA
(Presented by: Kevin He, MD, Oregon Health Sciences University)

11:00 a.m. #20 **CT-GUIDED BONE BIOPSY IN CHRONIC NON-SPINAL OSTEOMYELITIS: FRUITFUL OR FUTILE?**
Jan Fritz, MD; Ethan Dyer, BS; Janice Wang, BS; Moustafa Abou-Areda, BS; Bao Chau Ly, BS; Laura Fayad, MD
Johns Hopkins University, Baltimore, MD, USA
(Presented by: Jan Fritz, MD, Johns Hopkins University)

11:15 a.m. #21 **DIAGNOSTIC YIELD OF IMAGE-GUIDED SYNOVIAL BIOPSY FOR INTRA-ARTICULAR SYNOVIAL LESIONS**
Jeffrey Belair, MD; Conor McKee, MD; Vishal Desai, MD; Johannes Roedl, MD, PhD; Adam Zoga, MD; William Morrison, MD
Thomas Jefferson University Hospital, Philadelphia, PA, USA
(Presented by: Jeffrey Belair, MD, Thomas Jefferson University Hospital)

11:30 a.m. #22 **SHORT-TERM EFFICACY OF ULTRASOUND-GUIDED RETROCALCANEAL BURSA STEROID INJECTION AND CORRELATION WITH SONOGRAPHIC IMAGING FEATURES**
Robert Uzor; Beverly Thornhill; Dominic Catanese; Eric Walter; Elizabeth Elsinger; Eric Fornari; Shlomit Goldberg-Stein
Albert Einstein College of Medicine Montefiore Medical Center, Bronx, NY, USA
(Presented by: Robert Uzor, Albert Einstein College of Medicine Montefiore Medical Center)

11:45 a.m. #23 **SAFETY AND EFFICACY OF IMAGE GUIDED RADIOFREQUENCY ABLATION OF GENICULAR NERVE FOR PAIN MANAGEMENT IN PATIENTS WITH MODERATE TO SEVERE OSTEOARTHRITIS OF THE KNEE: INITIAL SINGLE INSTITUTION EXPERIENCE**
Felix Gonzalez, MD[1]; Philip Wong, MD[1]; Stephen Cole, MD[1]; Samia Sayyid, MD[1]; Zachary Bercu, MD, RPVI[2]; John Prologo, MD, FSIR[2]; Janice Newsome, MD[2]; Monica Umpierrez, MD[1]; Adam Singer, MD[1]; Nima Kokabi, MD[2]; Nickolas Reimer, MD[3]
[1]Emory University Dept. of Radiology, MSK Division, Atlanta, GA, USA; [2]Emory University Department of Radiology, Interventional Radiology and Image-Guided Medicine division, Atlanta, GA, USA; [3]Emory University School of Medicine, Department of Orthopaedics, Atlanta, GA, USA
(Presented by: Felix Gonzalez, MD, Emory University Dept. of Radiology, MSK Division)

12:00 p.m. #24 **MUSCULOSKELETAL (MSK) SOFT TISSUE LESION CORE NEEDLE BIOPSY: VARIATIONS IN BIOPSY PRACTICE PATTERNS AND IMPLICATIONS REGARDING SPECIMEN ADEQUACY**
Anthony Wheeler, MD; Hillary Garner, MD; Daniel Wessell, MD, PhD; Joseph Bestic, MD; Jeffrey Peterson, MD; Jacob Feldhaus, MD
Mayo Clinic Florida, Jacksonville, FL, USA
(Presented by: Anthony Wheeler, MD, Mayo Clinic Florida)

12:15 p.m. #25 **UTILITY OF REPEAT HIP ASPIRATIONS PERFORMED ON PATIENTS WITH THA**
Michael Fox, MD; Jeffrey Hassebrock, MD; Mark Kransdorf, MD; Jonathan Flug, MD; Jeremiah Long, MD; Adam Schwartz, MD
Mayo Clinic Arizona, Phoenix, AZ, USA
(Presented by: Michael Fox, MD, Mayo Clinic Arizona)

12:30 p.m.–12:35 p.m. **CASE OF THE DAY**
Presenting author: Timothy Ryan, MD

12:35 p.m.--12:45 p.m. REVIEW OF OLA PROCESS

1:00p.m.–3:00p.m. ***Musculoskeletal Ultrasound Hands-On Workshop - Ankle/Foot**

6:00 p.m.–9:30 p.m. **Annual Banquet**

Related ePosters

UPPER EXTREMITY

Poster #13 **REVERSE SHOULDER ARTHROPLASTY; PRE AND POSTOPERATIVE IMAGING AND CURRENT CONCEPTS.**
Michael Davis, MD; Alireza Eajazi, MD; Angel Gomez-Cintron, MD; Michael Tall, MD; Robert Cone, MD
UT Health San Antonio, San Antonio, USA

Poster #14 **TERES MINOR ATROPHY AND ASSOCIATED PATHOLOGY**
Derrick Doolittle, MD; William Aibinder, MD; Joaquin Sanchez-Sotelo, MD, PhD; Doris Wenger, MD
Mayo Clinic, Rochester, MN, USA

Poster #15 **ROTATOR CUFF REPAIR/RECONSTRUCTION FOR 'UNREPAIRABLE' TEARS**
Nicholas Rhodes, MD[1]; Amanda Baillargeon, MD[1]; Christin Tiegs Heiden, MD[1]; Bassem Elhassan, MD[1]; Daniel Wessell, MD[2]
[1]Mayo Clinic, Rochester, MN, USA; [2]Mayo Clinic Florida, Jacksonville, FL, USA

Poster #16 **POST-SURGICAL IMAGING OF ACROMIOCLAVICULAR (AC) JOINT SEPARATIONS**
Kimia Kani[1]; Jack Porrino, MD[2]; Hyojeong Mulcahy, MD[3]; Felix Chew, MD[3]
[1]University of Maryland School of Medicine, Baltimore, MD, USA; [2]Yale University School of Medicine, New Haven, CT, USA; [3]University of Washington / Harborview Medical Center, Seattle, WA, USA

Poster #17 **AN APPROACH TO THE PAINFUL STERNOCLAVICULAR JOINT: DIAGNOSIS AND INTERVENTION**
Gregory Matthews, MD; Maha Torabi, MD; Scott Wuertzer, MD
Wake Forest University School of Medicine, Winston-Salem, NC, USA

Poster #18 **POST-OPERATIVE COMPLICATIONS OF DISTAL BICEPS TENDON REPAIR: AN EDUCATIONAL MULTI-MODALITY IMAGING REVIEW**
ANESH CHAVDA, BSc, MRCP, FRCR; Isabelle Dupuis, MD.CM, FRCPC; Yara Alhajjar; JEFF PIKE, RCPSC; PARHAM DANESHVAR, RCPSC; MARK CRESSWELL, MBBCh, FRCPC; DARRA MURPHY
ST PAUL'S HOSPITAL, VANCOUVER, BC, Canada

Poster #19 **GLENOID BONE STOCK AND ROTATOR CUFF PATHOLOGY.**
Oganes Ashikyan, MD; Mathew Siebert, BS; Majid Chalian, MD
University of Texas Southwestern Medical Center at Dallas, Dallas, TX, USA

Poster #20 **USING THE RAVER VIEW AND ACROMIAL INDEX TO PREDICT ROTATOR CUFF TEARS ON RADIOGRAPHS**
Adam Zoga, MD, MBA[1]; Christopher Aland, MD[2]; Weilong Shi, MD[2]; Vishal Desai, MD[1]; William Morrison, MD[1]
[1]Thomas Jefferson University Hospital, Philadelphia, PA, USA; [2]Rothman Orthopaedics Institute, Philadelphia, PA, USA

Poster #21 **A MULTIMODALITY CENSUS OF CARPAL COALITIONS**
Aleksandr Rozenberg, MD; Alessandra Sax, MD; Jeffrey Belair, MD; Kristen McClure, MD; Johannes Roedl, MD, PhD; William Morrison, MD; Adam Zoga, MD, MBA
Thomas Jefferson University Hospital, Philadelphia, PA, USA

INTERVENTION

Poster #22 **PREOPERATIVE ULTRASOUND GUIDED BOTULINUM TOXIN A INJECTION FOR COMPLEX VENTRAL WALL HERNIA REPAIR: ONE TERTIARY CARE CENTER'S APPROACH**

Christopher Nall, MD; Dana Feraco, DO; Joshua Powell
Beaumont Health System, Royal Oak, MI, USA

Poster #23 **BIOPSY OF SUSPICIOUS OSSEOUS LESIONS IN PATIENTS WITH A KNOWN PRIMARY MALIGNANCY: RATE OF ALTERNATE DIAGNOSIS AND COMPLICATION RATE.**

Alexander Grushky, MD[1]; Christopher Nall, MD[1]; Zakaria Aqel, MD[1]; Alyssa Kirsch, MD[1]; Jonathan Im, MS[2]
[1]Beaumont Health System, Royal Oak, MI, USA; [2]Michigan State University College of Human Medicine, Grand Rapids, MI, USA

Poster #24 **THROW ME A BONE: EFFECT OF A BONE BIOPSY SKILLS WORKSHOP UTILIZING ANATOMICALLY ACCURATE 3D PRINTED MODELS**

Michael Durst, MD; Corey Ho, MD; Dorissa Gursahaney, MD; Amanda Crawford, MD; Melody Carroll, PhD
University of Colorado Denver, Aurora, CO, USA

ESSR Best Paper Award

LUMBAR SPINE MRI: ARE T1 SAGITTAL IMAGES STILL REQUIRED WHEN USING T2 DIXON SEQUENCES?

F. Zanchi[1], R. Richard[2], A. Monier[1], M. Hussami[1], J.-F. Knebel[1], F. Becce[1], P. Omoumi[1]
[1]Lausanne/CH, [2]Vevey/CH

Purpose: To determine whether lumbar spine MRI acquisitions in the sagittal plane can be reduced to a single fast spin-echo (FSE) Dixon T2 sequence, we aimed at showing that Fat Only images (FO) obtained from FSE T2 Dixon sagittal sequences can replace the FSE T1 images.

Methods and Materials: Fifty consecutive lumbar spine MRI examinations performed for lumbar pain and/or lumbosciatalgia were reviewed. Three musculoskeletal radiologists independently and randomly performed readings of two protocols separately: standard protocol (T1 sagittal, in-phase (IP) and water only (WO) images of the T2 Dixon sagittal sequence) and short protocol (FO, IP and WO images of the T2 Dixon sagittal sequence). The following items were assessed: bone marrow abnormalities, juxta-discal and marginal abnormalities (including osteophytes, MODIC changes, fatty infiltration, Schmorl nodules, vertebral fractures), foraminal stenosis, facet joint arthritis, and spondylolysis. Interchangeability of these sequences was tested using a previously published method by comparing the interprotocol (short vs. standard protocols) agreement with the intraprotocol agreement using the standard protocol. We used a ±5% limit to define clinically important difference of excess of disagreement. Interprotocol agreement was also compared using kappa statistics.

Results: Interprotocol agreement was similar to intraprotocol agreement on standard protocol (mean difference: -0.15%, 95%CI=[-0.5%;+0.2%]; ranging across structures/lesions from -1.67%, 95%CI=[-2.09%;-1.24%] for erosions to +0.73%, 95%CI=[0.07%;1.4%] for degenerative juxta-discal abnormalities). Interprotocol kappa values were fair to perfect (mean: 0.743, 95%CI=[0.651;0.835]; ranging from 0.378 for focal vertebral abnormalities to 0.914 for vertebral fractures). Sagittal T1, T2 Dixon FO and WO images of the lumbar spine of a 64 year-old male showing Modic 2 changes adjacent to L4-L5 and L5-S1 discs, and severe L2-L3 discarthrosis. Fatty changes are seen with higher contrast on Dixon T2 FO compared to T1 images.

Conclusion: T2 Dixon FO images can replace T1 sagittal images in lumbar spine MRI, providing an opportunity to reduce acquisitions in the sagittal plane to a single FSE Dixon T2 sequence.

Podium #10

STABLE VERSUS UNSTABLE OSTEOCHONDRAL LESIONS OF THE ELBOW: PERFORMANCE OF MR IMAGING CRITERIA FOR INSTABILITY

Jie Nguyen, MD, MS[1]; Andrew Degnan, MD[1]; Theodore Ganley, MD[1]; Christian Barrera, MD[1]; Thor Perrin Hee[1]; Richard Kijowski, MD[2]
[1]Children's Hospital of Philadelphia, Philadelphia, PA, USA; [2]University of Wisconsin Hospital & Clinics, Madison, WI, USA
(Presented by: Jie Nguyen, MD, MS, Children's Hospital of Philadelphia)

Purpose: To retrospectively compare the performance of previously described magnetic resonance (MR) imaging criteria for the detection of instability in children with osteochondral lesions (OCL) of the elbow with clinical and arthroscopic findings as reference standards.

Materials and Methods: This IRB-approved, HIPAA compliant retrospective study included 45 elbow OCLs with MR studies from 43 children (mean age 13.1 years; range 9-17 years, 27 boys & 16 girls) diagnosed between April 1 2010 and May 31, 2018. Twenty-one lesions were stable, determined using arthroscopy or clinical assessment and 24 lesions were unstable, determined during arthroscopy. MR studies were retrospectively reviewed to determine the presence T2 high signal intensity rim, T2 dark signal intensity rim, surrounding cysts, subchondral disruption, overlying cartilage degeneration, fluid-filled osteochondral defect, and intra-articular fragments. Fisher Exact and Mann Whitney U tests were used.

Results: Demographic characteristics of children with stable and unstable OCLs demonstrated no difference in age (p=0.638) or symptom duration (p=0.646). Fluid-filled osteochondral defects (p=0.004) and the presence of subchondral disruption (p=0.007), overlying cartilage degeneration (p=0.006), and intra-articular fragment (p=0.002) were significantly more common with unstable OCLs. Lesion size (p=0.337) and the presence of T2 high signal intensity rim (p=0.555), T2 dark signal intensity rim (p=1), and surrounding cysts (p=0.236) were not significantly different between stable and unstable OCLs. Although, unstable OCLs were more likely to have larger cysts (up to 7mm) and more cysts (up to 5 cysts) than stable OCLs (up to 5mm and up to 2 cysts, respectively).

Conclusion: Only some of the previously described MR imaging criteria for lesion stability for the knee joint can be applied to predict stability of lesions in the elbow joint. This may be due to the high prevalence of unstable lesions presenting with a displaced fragment at the time of diagnosis.

Modality % - Radiography / Fluoroscopy:	10
Modality % - CT:	0
Modality % - MRI:	89
Modality % - US:	0
Modality % - Nuclear Medicine:	0

MRI from a 12 year-old female gymnast showed an OCL with a T2 fluid-high signal rim (arrow). The patient improved on conservative management, 21 months.

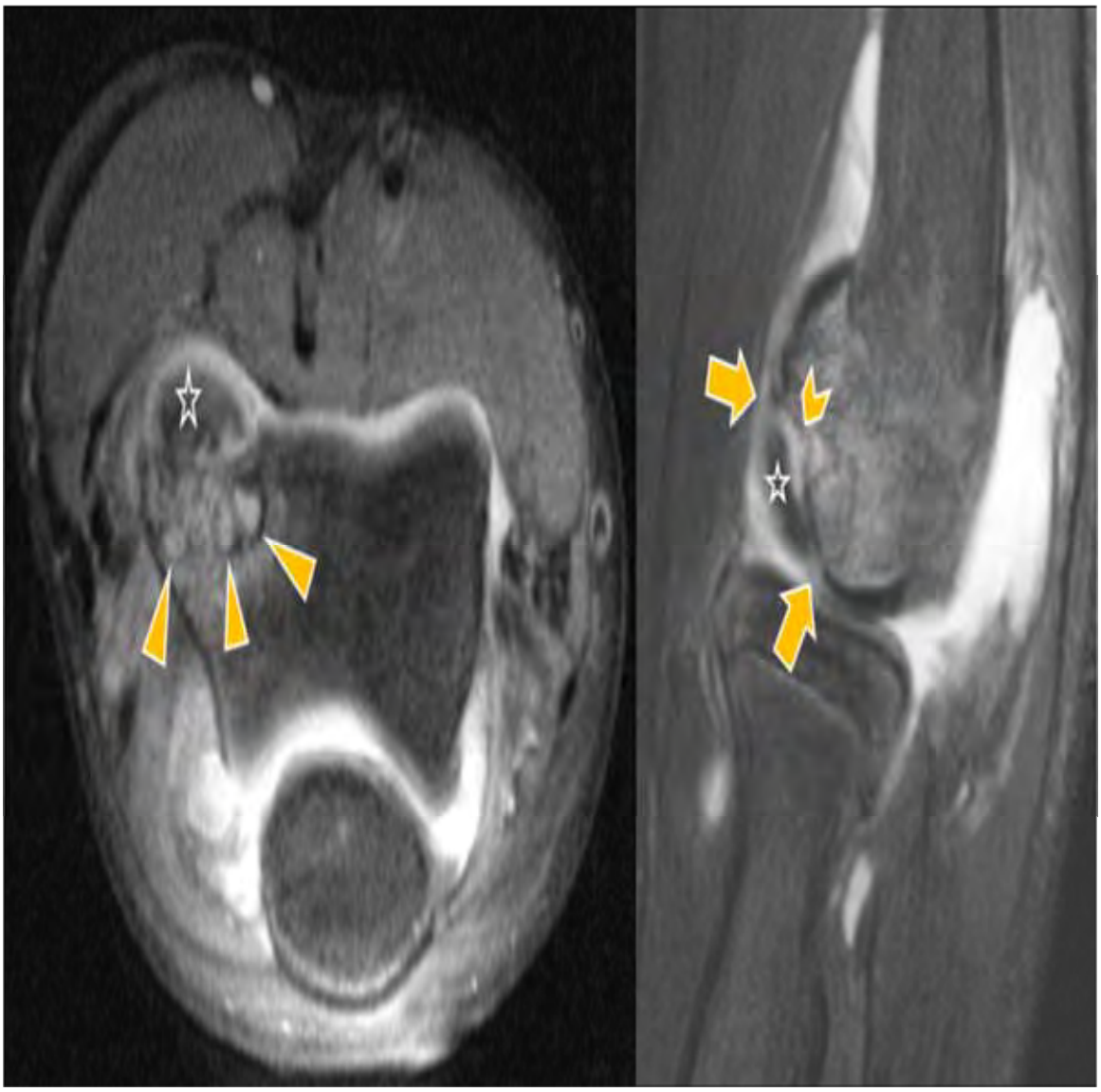

MRI from a 14 year-old male shows an OCL (star) with cysts (arrowheads), T2 high and T2 dark signal rims (chevron), and subchondral disruptions (arrows).

Podium #11

THE SMOKE SIGN: A SIGN OF PECTORALIS TENDON HUMERAL INSERTIONAL INJURY ON ROUTINE SHOULDER MRI

Devin Vaswani, MD[1]; CATHERINE PETCHPRAPA, MD[1]; ELISABETH GARWOOD, MD[2]; MOHAMMAD SAMIM, MD[1]; JENNY BENCARDINO, MD[1]
[1]NYU Medical Center/ Hospital for Joint Diseases Langone Medical Center, New York, NY, USA; [2]University of Massachusetts Memorial Medical Center, Worcester, MA, USA
(Presented by: Devin Vaswani, MD, NYU Medical Center/ Hospital for Joint Diseases Langone Medical Center)

Purpose: Study the diagnostic accuracy of the "smoke sign" on routine shoulder MR examinations for detection of pectoralis tendon humeral insertional injury.

Materials and Methods: IRB approved, HIPAA compliant study. Radiology database queried for MR with reports containing "pectoralis" and "shoulder" from 9/2012 to 7/2018. Patients without prior pectoralis surgery with shoulder and pectoralis MR within 4 months, and shoulder MR positive for pectoralis injury based on report and imaging review that clearly depicted pectoralis injury were included.

Anonymized, randomized shoulder MR reviewed independently by two musculoskeletal fellowship-trained radiologists for "smoke sign" on coronal- and sagittal-oblique sequences. Teaching session provided guidelines for smoke sign (ill-defined edema lateral or anterior to short head biceps/coracobrachialis on coronal- and sagittal-oblique fluid-sensitive images, respectively) before reader review. All MR reviewed by senior author for presence and location of pectoralis injury.

Results: 52 shoulder MR exams total: 33 patients with shoulder and pectoralis MR, 4 patients with shoulder MR and pectoralis imaging on same exam, 15 patients with shoulder MR only.

14/52 exams didn't have pectoralis injury on shoulder or pectoralis MR; "smoke sign" was present in none of these cases.

Remaining 38 patients had pectoralis injuries; 24/38 (humeral avulsion), 4/38 (tendon tear) 8/38 (myotendinous junction), 2/38 (intramuscular injury). Pooled sensitivity, specificity, negative and positive predictive value for "smoke sign" was 86%, 100%, 76% and 100%. When only tendon tears and avulsions were assessed, this rose to 100%, 100%, 100% and 100%. Kappa coefficient was 0.922 for the presence of the sign on coronal oblique 0.876 on sagittal oblique images.

Smoke sign was present in all 8 surgically proven pectoralis injuries.

Conclusion: "Smoke sign" is sensitive and specific for pectoralis humeral insertional injury, especially tendon tears and avulsions. Detection of this sign on routine shoulder MR should prompt careful evaluation of the distal pectoralis tendon and recommendation for dedicated pectoralis imaging.

Modality % - Radiography / Fluoroscopy:	0
Modality % - CT:	0
Modality % - MRI:	100
Modality % - US:	0
Modality % - Nuclear Medicine:	0

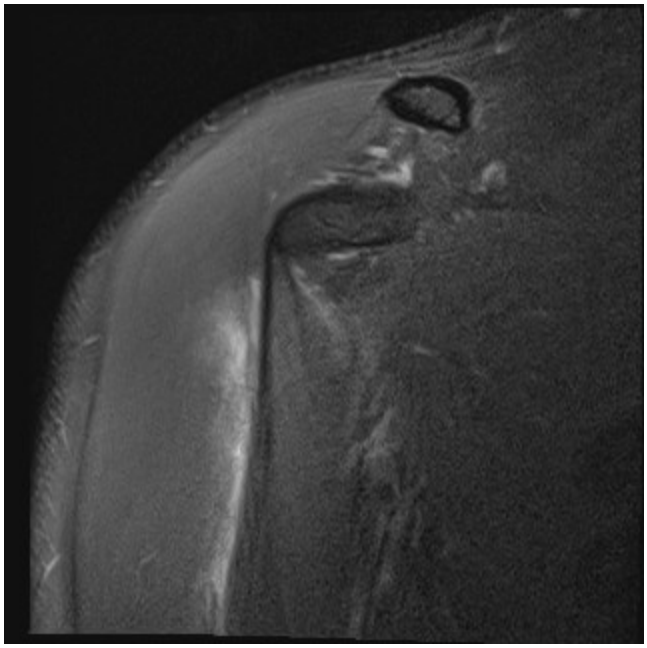

The smoke sign- ill-defined edema lateral to the short head biceps/coracobrachialis on coronal-oblique fluid sensitive sequence.

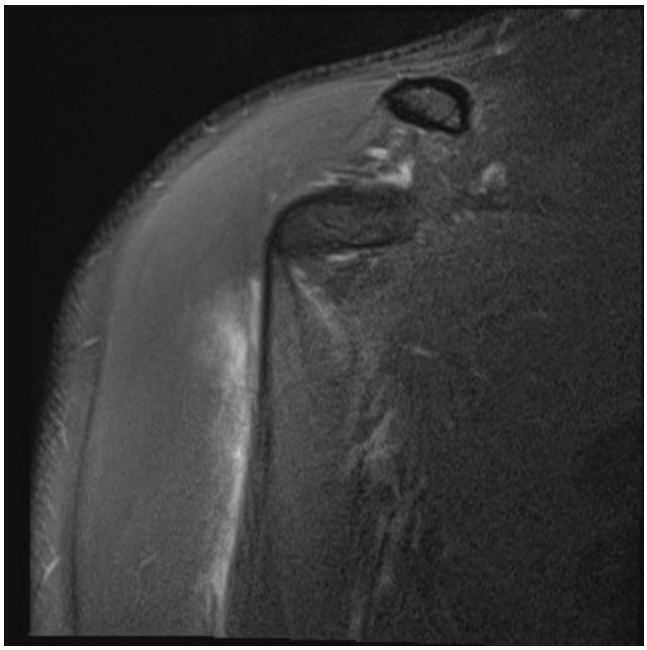

The smoke sign- ill-defined edema anterior to the short head biceps/coracobrachialis on sagittal-oblique fluid sensitive sequence.

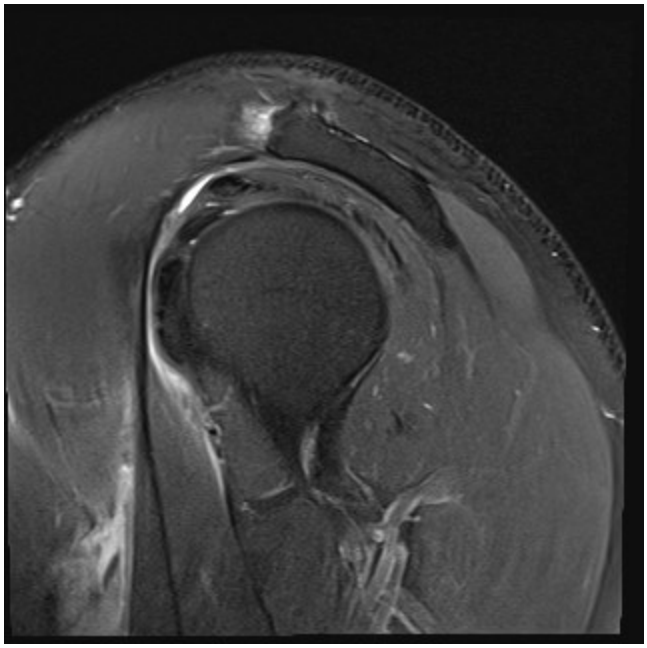

The "smoke sign"- ill-defined edema lateral to the short head biceps/coracobrachialis on coronal-oblique image from routine shoulder MR.

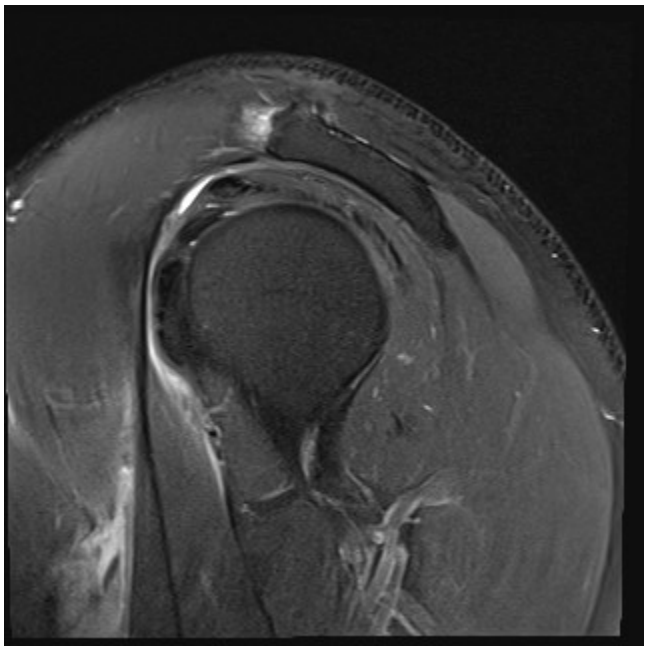

The "smoke sign"- ill-defined edema anterior to the short head biceps/coracobrachialis on sagittal-oblique image from routine shoulder MR.

Podium #12

MAGNETIC RESONANCE IMAGING FINDINGS IN THE FAILED SUPERIOR CAPSULAR RECONSTRUCTION

Harry Greditzer, IV, MD, MS[1]; George Balazs, MD[2]; Susan Lee, MD[1]; Jean Jose, DO[3]; Joshua Dines, MD[1]
[1]Hospital for Special Surgery, New York, NY, USA; [2]Naval Medical Center, portsmouth, VA, USA; [3]University of Miami Miller School of Medicine, miami, FL, USA
(Presented by: Harry Greditzer, IV, MD, MS, Hospital for Special Surgery)

Purpose: Superior capsular reconstruction (SCR) of the shoulder is an increasingly common procedure in the treatment of patients with massive, irreparable rotator cuff tears in the absence of significant osteoarthritis. Post-operatively, the normal appearance of well-functioning grafts on magnetic resonance imaging (MRI) has been well characterized. However, the appearance of failed grafts has only been described in isolated case reports and general review articles. The purpose of this study was to examine the MRI features of all failed SCRs at a single institution over a two-year period.

Materials and Methods: Following Institutional Review Board approval, surgical records at a single tertiary-care facility were queried to identify all patients undergoing SCR from January 2016 through December 2017. Electronic health records were reviewed for patient demographic information, reason for post-operative MRI, and post-operative surgeon assessment.

Results: 74 patients underwent SCR over the study period, of whom 12 received a follow-up MRI post-operatively. One patient was excluded due to missing records; the remaining 11 patients comprise the study cohort. Post-operative MRIs were obtained at mean six months after surgery.
On review of post-operative MRIs, three distinct locations of failure were identified. Four patients (40%) had midsubstance failure of the allograft with all glenoid and humeral head fixation remaining intact. One patient (10%) had complete detachment of the allograft from both glenoid and humeral head fixation. Five patients (50%) had detachment of the allograft from the glenoid.

Conclusion: In this series of ten failed SCRs, the most common mode of failure was loss of fixation on the glenoid, followed closely by midsubstance rupture. We found no instances of isolated fixation failure on the humeral head. This series illustrates the need for careful imaging in patients whose post-operative course suggests clinical failure. These findings also suggest that strengthening glenoid fixation may provide better clinical outcomes as this procedure becomes more common.

Modality % - Radiography / Fluoroscopy: 0
Modality % - CT: 0
Modality % - MRI: 100
Modality % - US: 0
Modality % - Nuclear Medicine: 0

Coronal Proton Density MRI demonstrates a midsubstance rupture of the graft (arrows).

Coronal Inversion Recovery MRI demonstrates complete detachment of the allograft from both glenoid and humeral head fixation and displacement in the subdeltoid bursa (arrows).

Podium #13

Prevalence of pseudoerosions of the hand and wrist: ultrasound findings in 100 asymptomatic volunteers

Anna Falkowski, MD, MHBA[1]; Jon Jacobson, MD[1]; Vivek Kalia, MD, MPH[1]; Angela Atinga, MB BChir FRCR[2]; Girish Gandikota, MBBS FRCS FRCR[1]; Ralf Thiele, MD[3]
[1]University of Michigan Medical Center, Ann Arbor, MI, USA; [2]University of Toronto, Toronto, ON, Canada; [3]The University of Rochester School of Medicine and Dentistry, Rochester, NY, USA
(Presented by: Anna Falkowski, MD, MHBA, University of Michigan Medical Center)

Purpose: Identification of cortical erosions with ultrasound can indicate inflammatory arthritis. While cortical depressions have been described in several metacarpal heads that may simulate an erosion, we have noted similar "pseudoerosions" more frequently than prior descriptions, and with more extensive involvement of the wrist. Thus, our purpose is to evaluate the frequency and location of these pseudoerosions in asymptomatic volunteers.

Materials and Methods: After IRB approval and obtaining informed consent,100 subjects without hand or wrist symptoms were examined bilaterally with ultrasound. Dorsal metacarpal heads, lunate, triquetrum, and distal ulna were examined. Cortical depressions were characterized with regard to location (central, marginal, both), morphology (irregularity, ring-down artifact), and dimensions (length and depth) by two fellow-trained musculoskeletal radiologists in consensus.

Results: 100 patients were evaluated (52 male, 48 female; mean age of 47±16 years). Metacarpal (MC) heads showed a central pseudoerosion in various frequencies (MC1: 21.5%; MC2: 92%; MC3: 85.5%; MC4: 59.5%; MC5: 81%). Only one marginal erosion was present at a MC5 and a marginal plus central at a MC2. Pseudoerosions were present at the lunate (82%), triquetrum (84%), and distal ulna (20%), and were multiple (lunate: 40%; triquetrum: 27%, ulna 5%). Ring-down artifact (30.25-49.7%) was present more than cortical irregularity (12.6-27.9%) of the pseudoerosions. Mean pseudoerosion length and depth of MC was 3 mm (range: 0.6-9 mm) and 0.7 mm (range: 0.2-8), respectively. Wrist dimensions for pseudoerosions varied slightly for the lunate (length: 2.1; depth: 0.8), triquetrum (length: 1.7; depth: 1.0), and ulna (length: 1.7; depth: 1.1) with a range of 0.3 – 6 mm in length and 0.3 – 5 mm in depth.

Conclusion: Central pseudoerosions are a typical finding of metacarpal heads, lunate, triquetrum, and distal ulna in asymptomatic patients and should not be misinterpreted as inflammatory arthritis.

Modality % - Radiography / Fluoroscopy:	0
Modality % - CT:	0
Modality % - MRI:	0
Modality % - US:	100
Modality % - Nuclear Medicine:	0

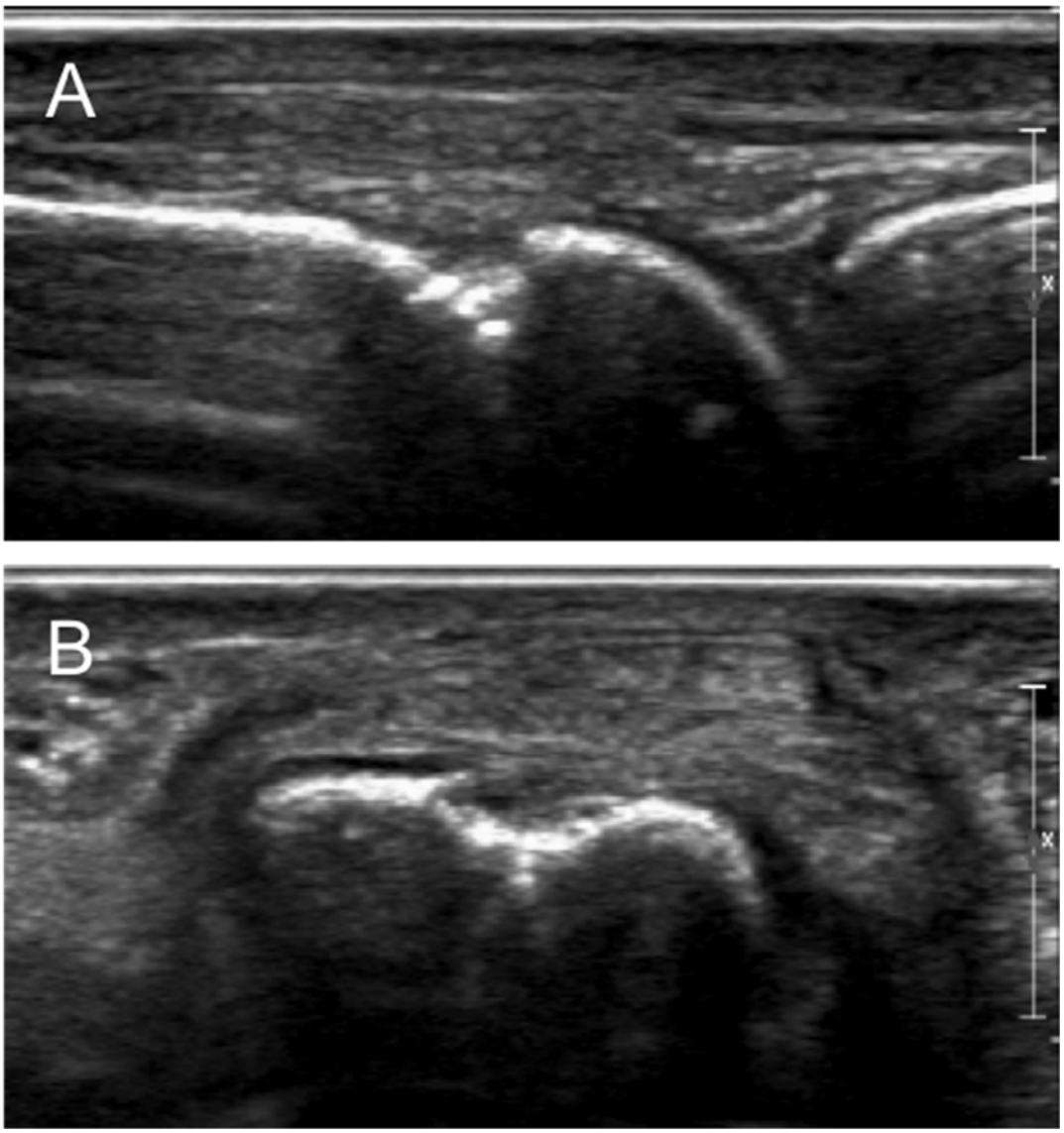

Sagittal (A) and axial (B) ultrasound of a 47-year old asymptomatic male shows a central irregular pseudoerosion with ring-down artifact at the 3rd metacarpal head.

Podium #14

SUPRASPINATUS AND INFRASPINATUS TENDON TEARS: NEW INSIGHTS ON LOCATION FROM RECENT ANATOMIC STUDIES

Michael Tuite, MD; Brian Chan, MD
University of Wisconsin Hospital & Clinics, Madison, WI, USA
(Presented by: Michael Tuite, MD, University of Wisconsin Hospital & Clinics)

Purpose: Use recent anatomic descriptions of supraspinatus (SST) and infraspinatus (IST) tendons to determine which is more commonly torn.

Materials and Methods: We reviewed operative reports of 100 consecutive patients with shoulder MRs followed by arthroscopy within 1 year with $\leq$ 2cm tear at surgery. There were 52 full thickness-, 32 articular partial-, 8 bursal-, and 8 with articular and bursal tears. We measured the greatest AP and Med-Lat dimensions. The junction between the superior and middle facets was identified by its inflection in the greater tuberosity cortex; we measured the AP distance of the margins relative to this junction, and Med-Lat distance to the medial greater tuberosity. A scale drawing of the SST and IST modeled on recent papers was created and an oval representation of each tear was overlayed to determine tendons involved. Tears were remeasured 6 months later by the lead author, and by a senior radiology resident, for intra- and interobserver variability.

Results: The most common location for a tear was 8-10mm anterior to the junction between the facets, and 2mm medial to the medial edge of the tuberosity. The center of the tear was in the SST in 75 tears, in the IST in 26, in the SST-IST overlap in 5, and at the junction of SST and IST in 2. The SST only was involved in 37 tears, and the IST only in 10. Both the SST and IST were torn in 61; the tear involved $\leq$1mm of 1 of 2 tendons in 8, and between 1-2mm in 13. Intraobserver correlation coefficient was 0.90; interobserver coefficient was 0.66

Conclusion: 74% of tears are centered in the SST or the SST/IST overlap. Of tears centered in the SST, 73% involved 0-2mm of the IST.

Modality % - Radiography / Fluoroscopy:	0
Modality % - CT:	0
Modality % - MRI:	100
Modality % - US:	0
Modality % - Nuclear Medicine:	0

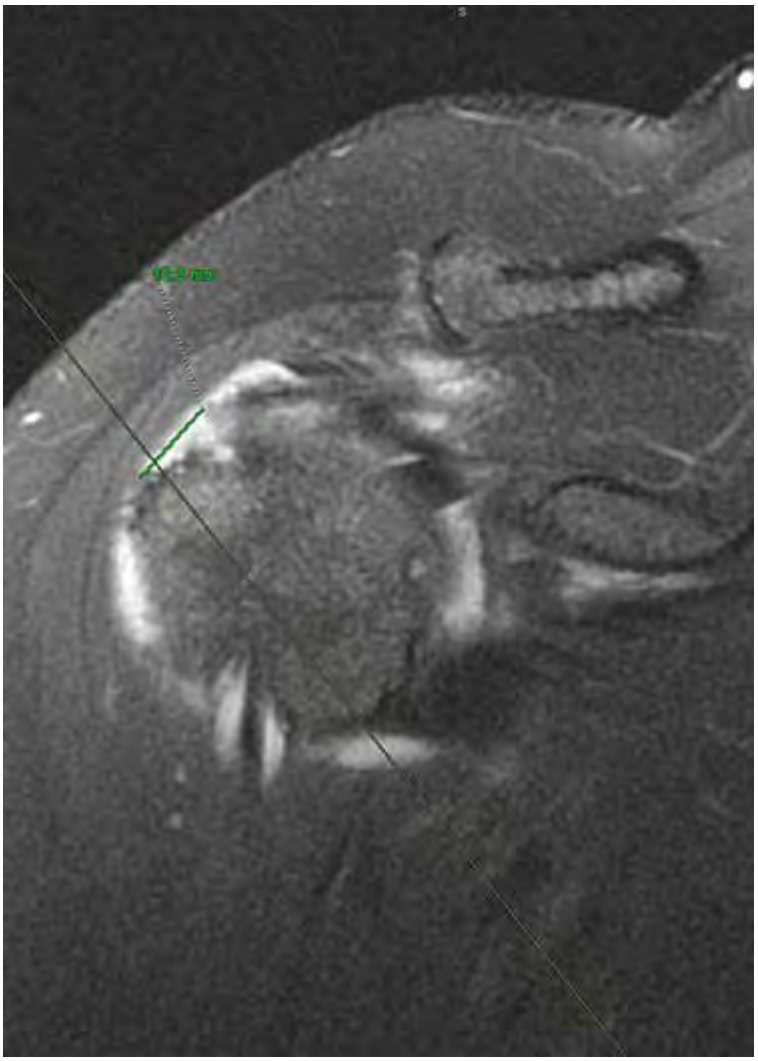

ObCor FS T2 image shows full-thickness tear measuring 10mm on this image. The localizer line is for an angled sagittal image through the greater tuberosity

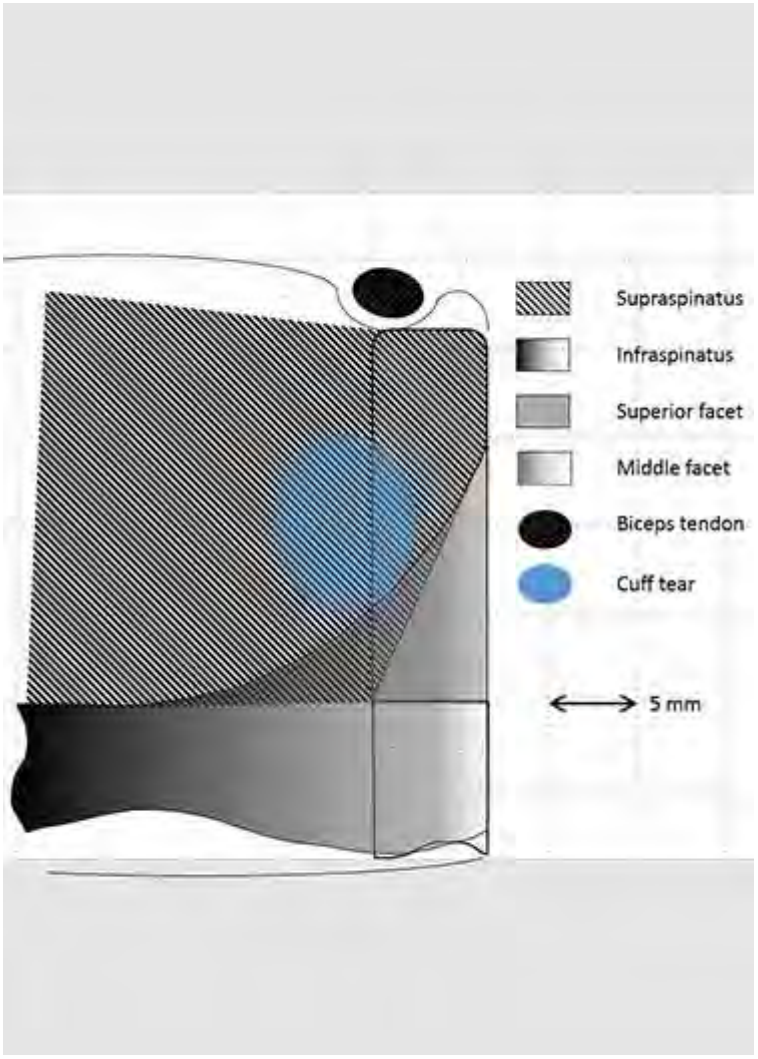

Angled sagittal FS T2 shows the junction between the superior and middle facets (arrow). This was used to determine the AP position of the tear.

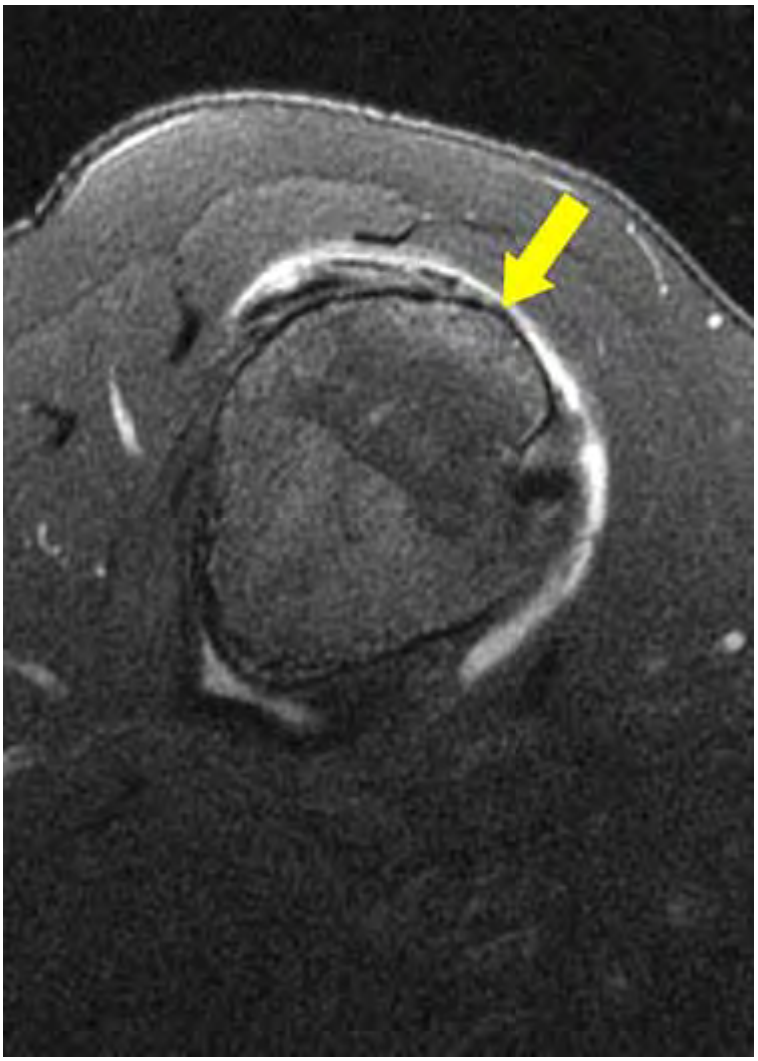

Drawing of the lateral SST and IST and their insertions on the greater tuberosity. Blue oval represents a tear centered in, and involving only SST

Podium #15

Loss of Reduction is Common After Coracoclavicular Ligament Reconstruction

Brian Kennedy, MD; Michael Alaia, MD; Erin Alaia, MD
NYU Medical Center/ Hospital for Joint Diseases Langone Medical Center, New York, NY, USA
(Presented by: Brian Kennedy, MD, NYU Medical Center/ Hospital for Joint Diseases Langone Medical Center)

Purpose: Soft tissue reconstruction of the coracoclavicular ligament is an increasingly common treatment approach for significant acromioclavicular joint separation injury. We have anecdotally noted loss of acromioclavicular joint reduction, coracoclavicular interval widening, distal clavicular osteolysis, and widening of osseous tunnels on follow-up radiographic exams. Our purpose is to report radiographic features and complications following coracoclavicular soft tissue reconstruction.

Materials and Methods: Retrospective query of our imaging database identified 55 cases of coracoclavicular ligament reconstruction. Cases with at least one month of follow-up and available operative report were reviewed with attention to : 1. alignment of the acromioclavicualar joint, 2. coracoclavicular interval widening, 3. radiographic features of distal clavicular osteolysis, and 4. widening of the reconstruction tunnel.

Results: 32 patients with post-operative imaging following coracoclavicular ligament reconstruction (23 male, 9 females; average age 43, age range 24-64, imaged 1 to 34 months following surgery, average 9.5 months) were included. Loss of acromioclavicular joint reduction was the most common imaging finding at follow-up (n = 25, 78%), with 88% of cases seen within 6 months of surgery. 19 (76%) patients with loss of acromioclavicular reduction progressed to coracoclavicular interval widening. Distal clavicular osteolysis was seen in 21 patients (66%), with 90% of cases seen within 6 months of surgery. Reconstruction tunnels widened on average 2 mm (range 0 – 4 mm). Revision surgery was required in 5 patients (16%), with 80% of revisions occurring more than a year following surgery.

Conclusion: Loss of acromioclavicular joint reduction, distal clavicular osteolysis, and tunnel widening are frequently demonstrated after coracoclavicular ligament reconstruction. Radiologists should be aware of the frequently observed imaging findings following coracoclavicular reconstruction. Attention to early loss of reduction or distal clavicular may guide treatment approach and impact patient outcomes.

Modality % - Radiography / Fluoroscopy:	90
Modality % - CT:	5
Modality % - MRI:	5
Modality % - US:	0
Modality % - Nuclear Medicine:	0

Figure 1. 64 year-old female status post coracoclavicular reconstruction for Grade 5 acromioclavicular joint separation injury. Radiographic image obtained immediately following surgery (A) demonstrates near normal acromioclavicular alignment. Three month(B) post-operative radiograph shows subtle loss of acromioclavicular reduction and findings of distal clavicular osteolysis (arrowheads), with erosion of the distal clavicle. Radiographs one year post surgery (C) demonstrate new widening of the acromioclavicular joint (white bracket), due to both loss of reduction and distal clavicular osteolysis, and new mild widening of the coracoclavicular interval (black bracket). There is also new heterotopic ossification (white arrowheads).

Figure 1 - Progressive distal clavicular osteolysis, loss of acromioclavicular joint reduction, and widening of the coracoclavicular interval

Figure 2. 35 year old male status post coracoclavicular reconstruction for Grade 3 acromioclavicular joint separation injury. Immediate post-operative radiograph (A) demonstrates clavicular reconstruction tunnels (brackets), with slight loss of reduction at the acromioclavicular joint, and erosion of the distal clavicle, suggesting osteolysis (arrowheads). 18 month follow-up (B) demonstrating interval tunnel widening (brackets), with new fracture (arrow) through the medial tunnel, presumably due to stress riser effect, with persistent mild loss of acromioclavicular reduction and signs of clavicular osteolysis (arrowheads).

Image 2 - Fracture through one of the reconstruction tunnels, likely due to stress riser effect

Podium #16

POSTERIOR ELBOW DISLOCATION. MRI IMAGING FEATURES AND PATHOPHYSIOLOGIC CONSIDERATIONS

Michael Zlatkin, MD; Timothy Sanders, MD
Nationalrad, Deerfield Beach, FL, USA
(Presented by: Michael Zlatkin, MD, Nationalrad)

Purpose: To examine soft tissue and osseous injuries visualized on magnetic resonance (MRI) imaging after posterior elbow dislocation, and to correlate these injury patterns with pathophysiologic mechanisms.

Materials and Methods: Retrospective review of 16 patients with posterior elbow dislocation, obtained searching the institutional computer database spanning a 60-month period.

Results: Soft tissue injuries: Six patients (37.5%) had complete disruption of the lateral and medial collateral ligament complexes. Two patients (12.5%) had disruptions of the lateral ligament complex, along with partial disruption of the medial collateral ligament (MCL). These two groups conform to Stage 3 *posterolateral rotatory dislocation (PLRD)*. Six patients (37.5%) had complete MCL complex disruption associated with partial disruption of the lateral ligament complex consistent with a less commonly described *posteromedial rotatory dislocation pattern ((PMRD)*. The remaining 12.5% of patients had partial disruptions of both the MCL and LCL ligament complex. Injuries of the common extensor and common flexor tendons accompanied the ligament tears. Grade 1 or 2 strain of the brachialis muscle was identified in all patients.
Bone injuries:Eleven (68.8%) patients had fractures or osteochondral injuries involving one or more sites, either the coronoid process 31.3% (n=5), radial head 25% (n=4), capitellum 18.8% (n=3), and/or trochlea 6.3% (n=1).

Conclusion: MR imaging demonstrates the soft tissue and osseous injury patterns after posterior elbow dislocation. The *posterolateral rotatory dislocation* pattern, with sequential ligament disruption from lateral-to-medial, does not occur in all patients. The pattern of ligament disruption in our series, supports the notion that in a subset of patients, the injury pattern appears to progress from medial to lateral, indicating a *posteromedial rotatory dislocation pattern*. Recognition of patterns of injury may have implications on patient management.

Modality % - Radiography / Fluoroscopy:	0
Modality % - CT:	0
Modality % - MRI:	100
Modality % - US:	0
Modality % - Nuclear Medicine:	0

Spectrum of ligamentous injury associated with the posterior lateral pattern of dislocation.

Ligamentous injury associated with a posterior medial pattern of dislocation. Tthere is high grade injury medially (closed arrows) and low grade injury laterally (open arrow).

Podium #17

ULTRASOUND-MRI CORRELATION FOR HEALING OF ROTATOR CUFF REPAIRS USING VASCULARITY AND TENDON ELASTICITY: A PILOT STUDY

Ronald Adler, MD, PhD; Soterios Gyftopoulos, MD; Nicole Nocera, MD
NYU Medical Center/ Hospital for Joint Diseases Langone Medical Center, New York, NY, USA
(Presented by: Ronald Adler, MD, PhD, NYU Medical Center/ Hospital for Joint Diseases Langone Medical Center)

Purpose: To better understand alterations in repaired supraspinatus tendons using a multimodality approach including MRI, assessment of tendon vascularity by power Doppler (PD), and tendon mechanical properties using shear wave elastography (SWE). To investigate whether SWE and PD can provide quantitative assessment of tendon healing following rotator cuff repair.

Materials and Methods: This HIPAA compliant prospective study was approved by the institutional review board with informed consent. Between 9/2013 and 6/2016, twelve patients (7 males, 5 females; mean age 61 years) with unilateral full-thickness supraspinatus tendon tears underwent MRI and ultrasound pre-operatively, 3-months and 6-months post-surgery. The supraspinatus tendon MRI signal intensity, PD and SWE properties were measured. Repaired and asymptomatic shoulders were compared over time within and between modalities.

Results: No significant association was seen between mean SWE and MRI signal intensity (non-insertional portion -0.25, p=0.467, insertional portion -0.18, p=0.593), or between PD and MRI signal intensity (non-insertional portion -0.19, p=0.599, insertional portion 0.22, p=0.533) within the supraspinatus tendon.

MRI signal intensity and PD within the supraspinatus tendon, both increased and then decreased postoperatively. Shear wave velocities increased throughout the postoperative period in the tendon footprint, while increasing and then decreasing in the distal tendon.

Conclusion: MRI and ultrasound parameters did not achieve statistically significant correlation; however, their respective trend behavior suggests that a temporal relationship exists between modalities. We postulate that a more detailed multiparametric imaging approach and/or comparison with a more selective MR measure, such as T2* values, may be required to evaluate rotator cuff repair.

Modality % - Radiography / Fluoroscopy:	0
Modality % - CT:	0
Modality % - MRI:	40
Modality % - US:	60
Modality % - Nuclear Medicine:	0

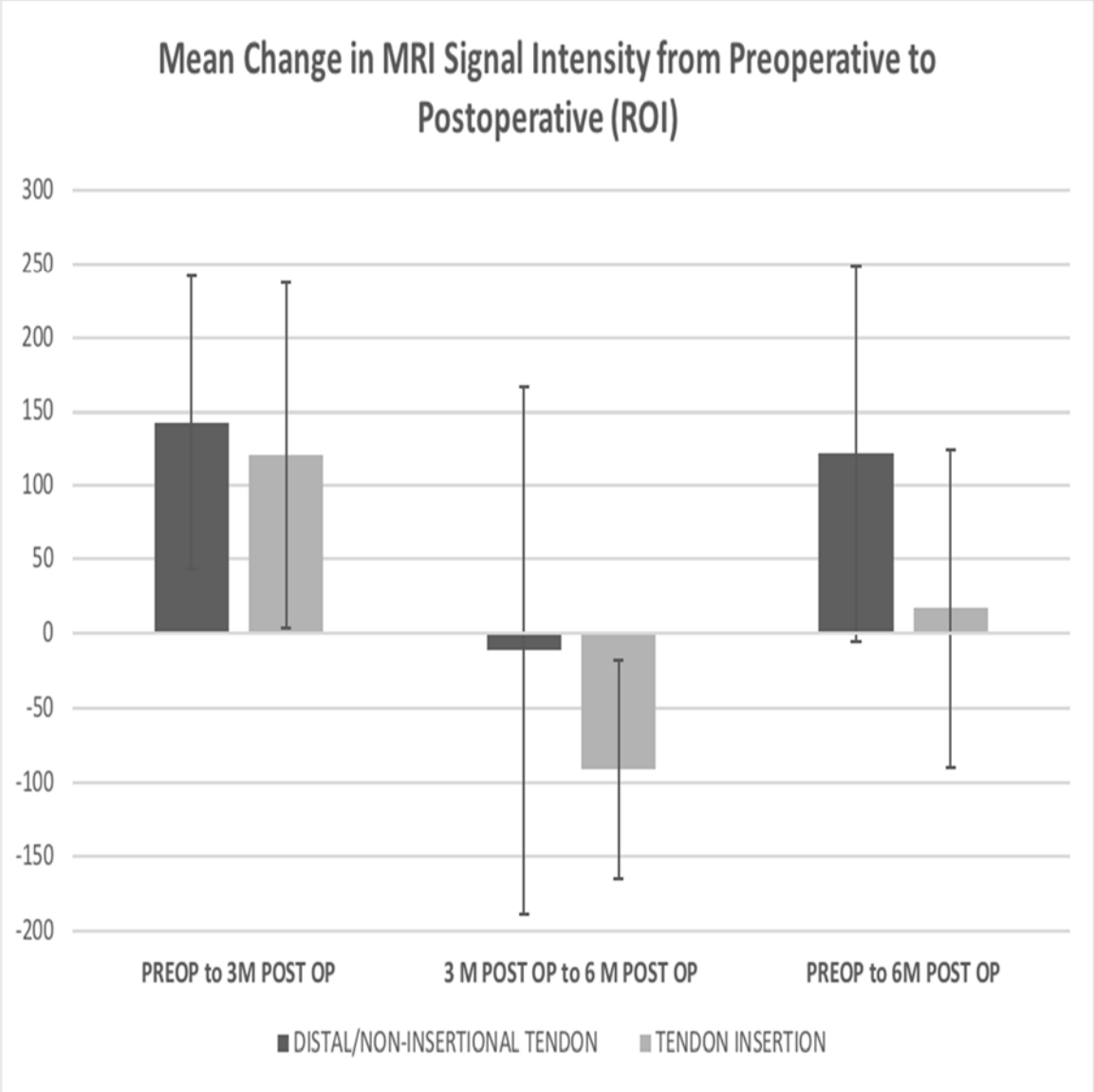

Mean change in supraspinatus tendon MRI signal intensity from preoperative to postoperative time points, shows a trend of increasing and then decreasing intensity.

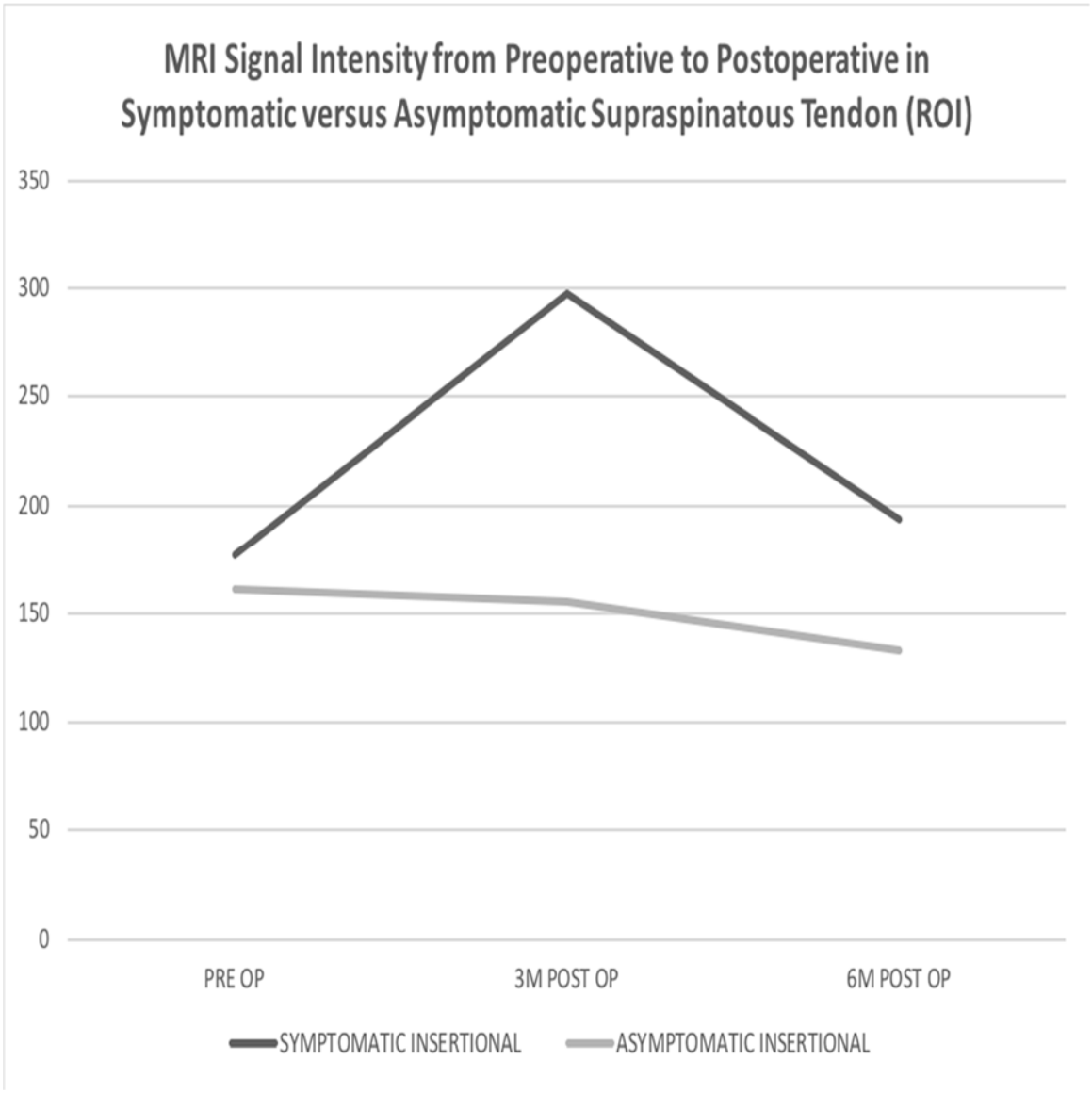

Mean change in shear wave velocities (m/s) from the preoperative to postoperative time points, shows a trend of increasing SWE in the insertional tendon.

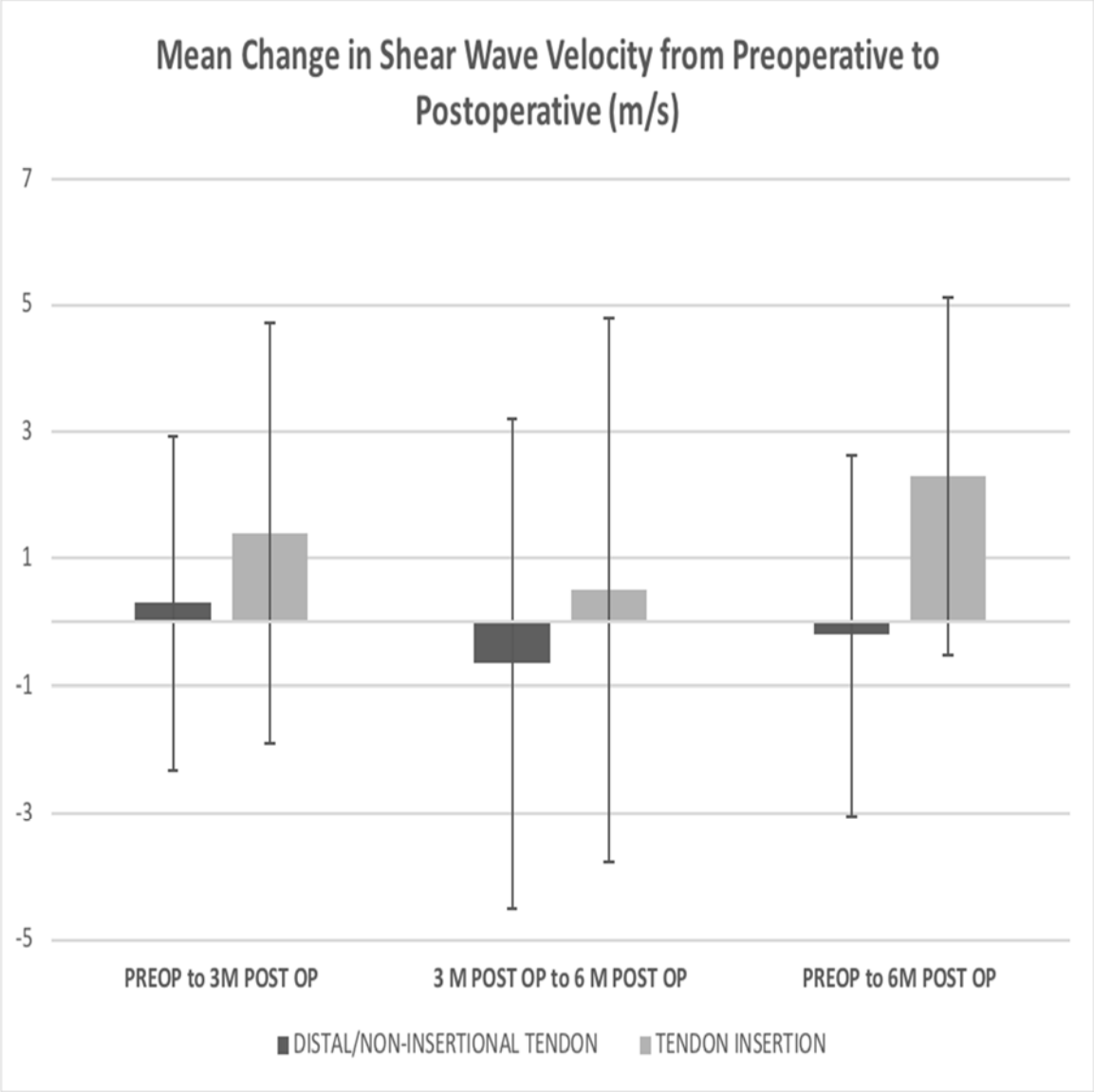

Mean supraspinatus tendon MRI signal intensity in symptomatic versus asymptomatic shoulders, shows an apparent difference in trend behavior between the operated and non-operated sides.

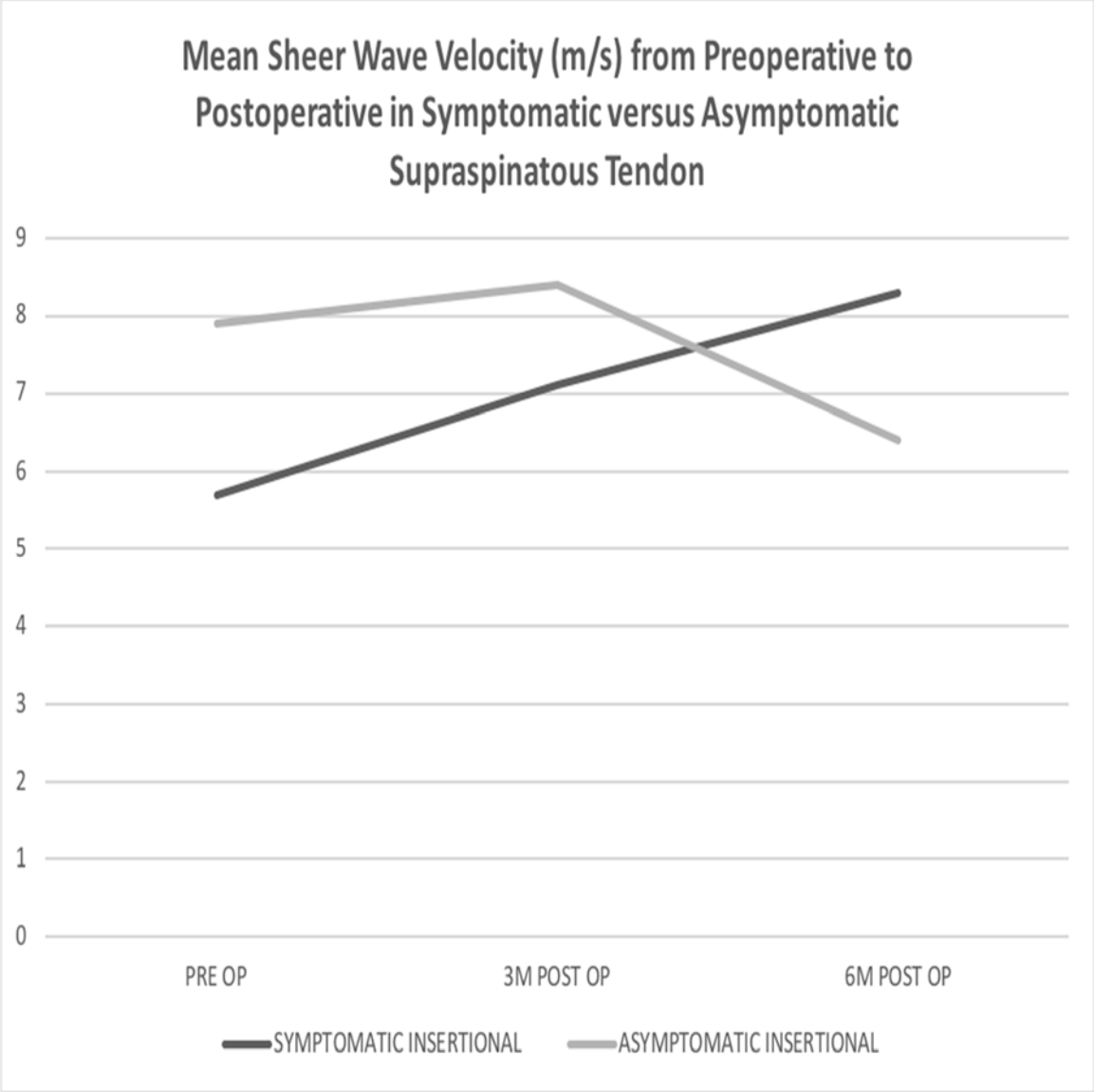

Mean shear wave velocities in symptomatic versus asymptomatic shoulders. Trend of increasing SWV in the operated shoulder likely due to stiffening of the insertional fibers.

Podium #18

PLATELET-RICH PLASMA FOR TREATMENT OF MODERATE-TO-SEVERE MIDSUBSTANCE ACHILLES TENDINOPATHY: A PILOT RCT WITH CONVENTIONAL AND NOVEL ULTRASOUND IMAGING CORRELATION

David Gimarc, MD; Paul Michelin, MD; Darryl Thelen, PhD; John Wilson, MD, MS; Kenneth Lee, MD
University of Wisconsin Hospital & Clinics, Madison, WI, USA
(Presented by: David Gimarc, MD, University of Wisconsin Hospital & Clinics)

Purpose: To investigate the efficacy of PRP for the treatment of midsubstance Achilles tendinopathy (AT) and to correlate clinical outcomes to conventional ultrasound and novel quantitative shear wave elastography.
Materials and Methods: 20 subjects were recruited from April 2014 to November 2017 with moderate-to-severe midsubstance AT and randomized into two groups. Inclusion criteria: 1) age 18-65 yo, 2) pain > 6 months and VAS pain >5, 3) failure of eccentric exercise protocol, and 5) failure of conservative treatments. Exclusion criteria: 1) steroid injection within 6 weeks, 2) past surgery or systemic diseases. Group 1 (PRP) received a single injection of PRP at week 0. Group 2 (control) did not receive an intervention and continued to perform eccentric exercise. Pain and function were evaluated using the validated VISA-A clinical outcome questionnaire (primary outcome) and VAS pain levels at 0, 12 and 24 weeks. Disease modification was assessed by conventional US (tendon thickness, echotexture, hyperemia) and shear wave speed elastography (SWS) at week 0, 12 and 24 weeks. Linear mixed model and ANOVA tests applied with $p<0.05$ significance.
Results: 20 subjects (7 women and 13 men), mean age 54.7 years (range 38-65 yo) recruited. Baseline characteristics showed no statistical difference between groups (Table 1). PRP group VAS scores were 6.9, 1.4, and 1.3 and VISA-A scores were 46.7, 60.4, and 83.3 at 0, 12, and 24 weeks, respectively. Control group VAS scores were 7.2, 7.4, and 6.2 and VISA-A scores were 40.4, 39.2, and 51.5 at 0, 12, and 24 weeks, respectively. Baseline SWS for normal and abnormal tendons averaged 10.99 m/sec and 9.81 m/sec, respectively. No significant difference found in tendon thickness, echotexture or vascularity over time.
Conclusion: PRP is an effective treatment alternative for chronic moderate-to-severe midsubstance Achilles tendinopathy. Imaging outcome measures may not be a reliable biomarker for tendon healing.

Modality % - Radiography / Fluoroscopy:	0
Modality % - CT:	0
Modality % - MRI:	0
Modality % - US:	100
Modality % - Nuclear Medicine:	0

Table 1 - Comparison of Cohort Demographics			
	PRP (Treatment) Group	Control Group	P-value
No. of participants	10	10	-
Average Age (years)	56.4	53.0	0.321
No. of males (%)	8 (80%)	5 (50%)	0.180
VAS Score	6.80	7.10	0.616
VISA-A Score	47.00	43.70	0.708
Achilles Tendon Thickness (mm)	11.00	9.40	0.078
Shear Wave Speed (cm/sec)	10.09	9.98	0.886

Table 1: Comparison of Baseline Cohort Demographics

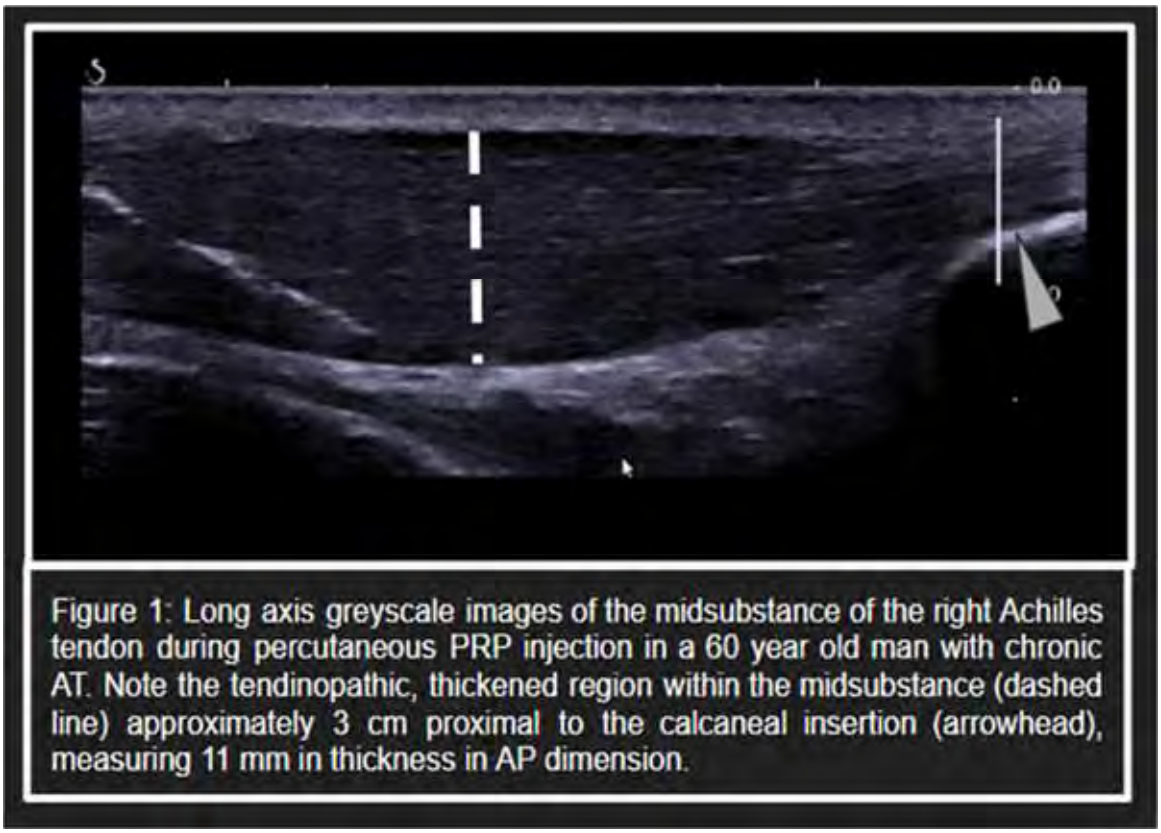

Figure 1: Long axis greyscale images of the midsubstance of the right Achilles tendon during percutaneous PRP injection in a 60 year old man with chronic AT. Note the tendinopathic, thickened region within the midsubstance (dashed line) approximately 3 cm proximal to the calcaneal insertion (arrowhead), measuring 11 mm in thickness in AP dimension.

Image 1: Grayscale long axis image of the midsubstance Achilles tendon during PRP injection.

Podium #19

To Drill or not to Drill, That is the Quesion

Kevin He, MD; John Campbell; Bryan Wolf, MD; Barry Hansford, MD; Brooke Beckett, MD
Oregon Health Sciences University, Portland, OR, USA
(Presented by: Kevin He, MD, Oregon Health Sciences University)

Purpose: At our institution, requests for extraspinal bone biopsies for suspected osteomyelitis are relatively common. Over the past several years, we have observed that the culture yield for such biopsies is frustratingly low. Hence, the objective of our study was to evaluate the yield and treatment impact of CT-guided extraspinal bone biopsies performed for infection over a 10 year period.

Materials and Methods: An IRB-approved retrospective review of CT-guided bone biopsies between 2008 and 2018 was performed. Of 855 biopsies, 35 were performed for suspected osteomyelitis; all spine biopsies were excluded from the study. Biopsies were performed with CT guidance utilizing a 12 or 14G AprioMed Bonopty system. A chart review was performed to ascertain the following for each procedure: pathology results, culture results, open biopsy results when applicable, and clinical course prior to and after biopsy, including antibiotic therapy.

Results: Out of 35 cases, 17 (49%) were positive on pathology for osteomyelitis, 5 (14%) yielded positive cultures, and 4 (11%) demonstrated positive open biopsy cultures after initial negative CT biopsy cultures. There were 5 cases of starting or changing to targeted antiobiotic therapy after positive CT biopsy cultures, 5 cases of starting or continuing antibiotics after positive CT biopsy pathology but negative cultures, and 2 cases of cessation of antiobiotic therapy after negative CT biopsy pathology and cultures, totalling 12 cases (34%) in which treatment was appropriately affected. 6 cases of starting antibiotic therapy despite negative CT biopsy pathology and cultures and 6 cases of not initiating antibiotic therapy despite positive CT biopsy pathology showing chronic osteomyelitis but negative cultures were also observed.

Conclusion: The culture yield for CT-guided extraspinal bone biopsies is extremely low and, at our institution, the majority of biopsies did not change clinical management.

Modality % - Radiography / Fluoroscopy:	33
Modality % - CT:	33
Modality % - MRI:	29
Modality % - US:	0
Modality % - Nuclear Medicine:	0

17 month old male presenting with 5 weeks of limping. Radiograph shows a lucent lesion in the right femoral metaphysis abutting the physis.

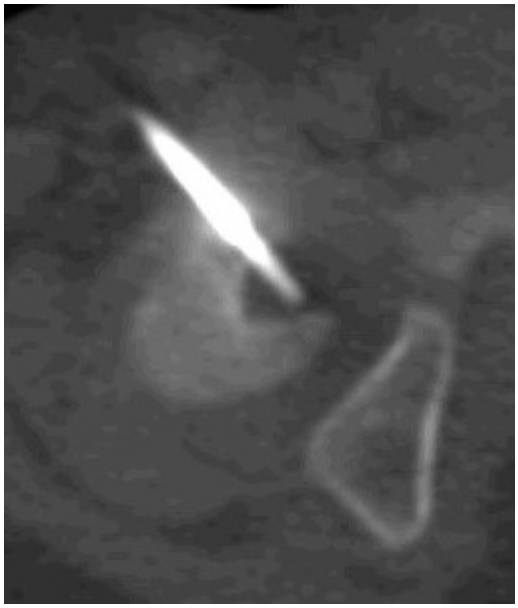

Contrast enhanced MRI demonstrates a rim-enhancing fluid collection in the right femoral metaphysis extending across the physis and involving the cartilaginous femoral head.

CT guided biopsy of the lesion was requested to evaluate for Brodie's abscess. Pathology showed acute on chronic osteomyelitis. Cultures were negative.

The patient received empiric Ancef/Cefazolin to cover MSSA. 2 years later, there is decreased size and conspicuity of the lesion.

Podium #20

CT-GUIDED BONE BIOPSY IN CHRONIC NON-SPINAL OSTEOMYELITIS: FRUITFUL OR FUTILE?

Jan Fritz, MD; Ethan Dyer, BS; Janice Wang, BS; Moustafa Abou-Areda, BS; Bao Chau Ly, BS; Laura Fayad, MD
Johns Hopkins University, Baltimore, MD, USA
(Presented by: Jan Fritz, MD, Johns Hopkins University)

Purpose: To determine the frequency of CT-guided bone biopsy resulting in the identification of a causative pathogen and tailoring of antibiotic treatment in patients with chronic non-spinal osteomyelitis.

Materials and Methods: Following internal review board approval, we identified 181 patients (mean age, 52 years; age range, 20-93 years) with chronic osteomyelitis, who underwent successful non-spinal CT-guided bone biopsy and subsequent microbiological examination. Biopsies were performed in the foot (65/181, 36%), pelvis (75/181, 41%), and other locations (41/181, 23%). The outcome variables included a) diagnostic yield, defined as the identification of a pathogen through microbiological analysis, b) resulting changes of antibiotic treatment, and c) microbiological results from wound cultures. Descriptive statistics were applied. P-values less than 0.05 were considered statistically significant.

Results: The diagnostic yield of CT-guided bone biopsies was 18%, meaning that in 33 of 181 biopsy cases microbiological analysis identified a pathogen conclusively. In 16/75 (21%) pelvis cases and 9/65 (14%) foot and ankle cases, the microbiological analysis was conclusive for a causative pathogen. 18/33 (55%) conclusive cases also had wound cultures performed, of which 14 (42%) had the same organisms identified in both the wound and bone biopsy specimen cultures. In the 33 cases with conclusive microbiological analysis, the isolated pathogen resulted in adaption of the antibiotic treatment in 31/33 (94%).

Conclusion: CT-guided bone biopsy in patients with chronic non-spinal osteomyelitis may result in the identification of a causative pathogen in only 18% of cases and adaptation of antibiotic treatment in only 17% of cases. Taking into consideration the 42% concordance rate of bone and wound cultures, the diagnostic yield of CT-guided biopsy may decrease to 10%. Our study results indicate a limited role of CT-guided bone biopsy in the management of patients with chronic non-spinal osteomyelitis.

Modality % - Radiography / Fluoroscopy:	0
Modality % - CT:	100
Modality % - MRI:	0
Modality % - US:	0
Modality % - Nuclear Medicine:	0

Podium #21

Diagnostic yield of image-guided synovial biopsy for intra-articular synovial lesions

Jeffrey Belair, MD; Conor McKee, MD; Vishal Desai, MD; Johannes Roedl, MD, PhD; Adam Zoga, MD; William Morrison, MD
Thomas Jefferson University Hospital, Philadelphia, PA, USA
(Presented by: Jeffrey Belair, MD, Thomas Jefferson University Hospital)

Purpose: A variety of benign and neoplastic lesions can affect the synovium, the most common including pigmented villonodular synovitis (PVNS) and synovial chondromatosis. Recent treatment advances have opened the door for potential medical therapies for PVNS, which could decrease or eliminate the need for surgery in some cases. Accurate characterization of synovial lesions is thus required prior to treatment.

Materials and Methods: Institutional IRB approval was obtained. 52 synovial biopsies performed under ultrasound (US) or computed tomography (CT) guidance at our institution for intra articular synovial lesions were identified using a comprehensive database search. Cases were reviewed for pathology, location, biopsy approach, preprocedure imaging, and postprocedure complications.

Results: 52 image guided synovial biopsies were performed, 34 using CT guidance and 18 using US guidance. Five different anatomic locations were biopsied (hip, knee, shoulder, elbow and TMJ). Synovial tissue was obtained in 87% of cases (45/52) and the final diagnosis was established in 81% of cases (42/52). CT-guided biopsies had positive yield in 86% of cases (29/34) and established the final diagnosis in 78% (27/34) of cases. US-guided biopsies had positive yield in 89% (16/18) and established the final diagnosis in 83% (15/18). Post-surgical pathology was obtained in 28 of the cases and image-guided biopsy concordance was 100% (28/28). There were no reported complications. Anecdotally, we found that intra-articular injection of iodinated contrast prior to CT-guided biopsy may be useful for accurately identifying the target lesion.

Conclusion: Image-guided synovial biopsy is a safe procedure with a high diagnostic yield. The final diagnosis can be established in the majority of cases.

Modality % - Radiography / Fluoroscopy:	0
Modality % - CT:	33.3
Modality % - MRI:	33.3
Modality % - US:	33.3
Modality % - Nuclear Medicine:	0

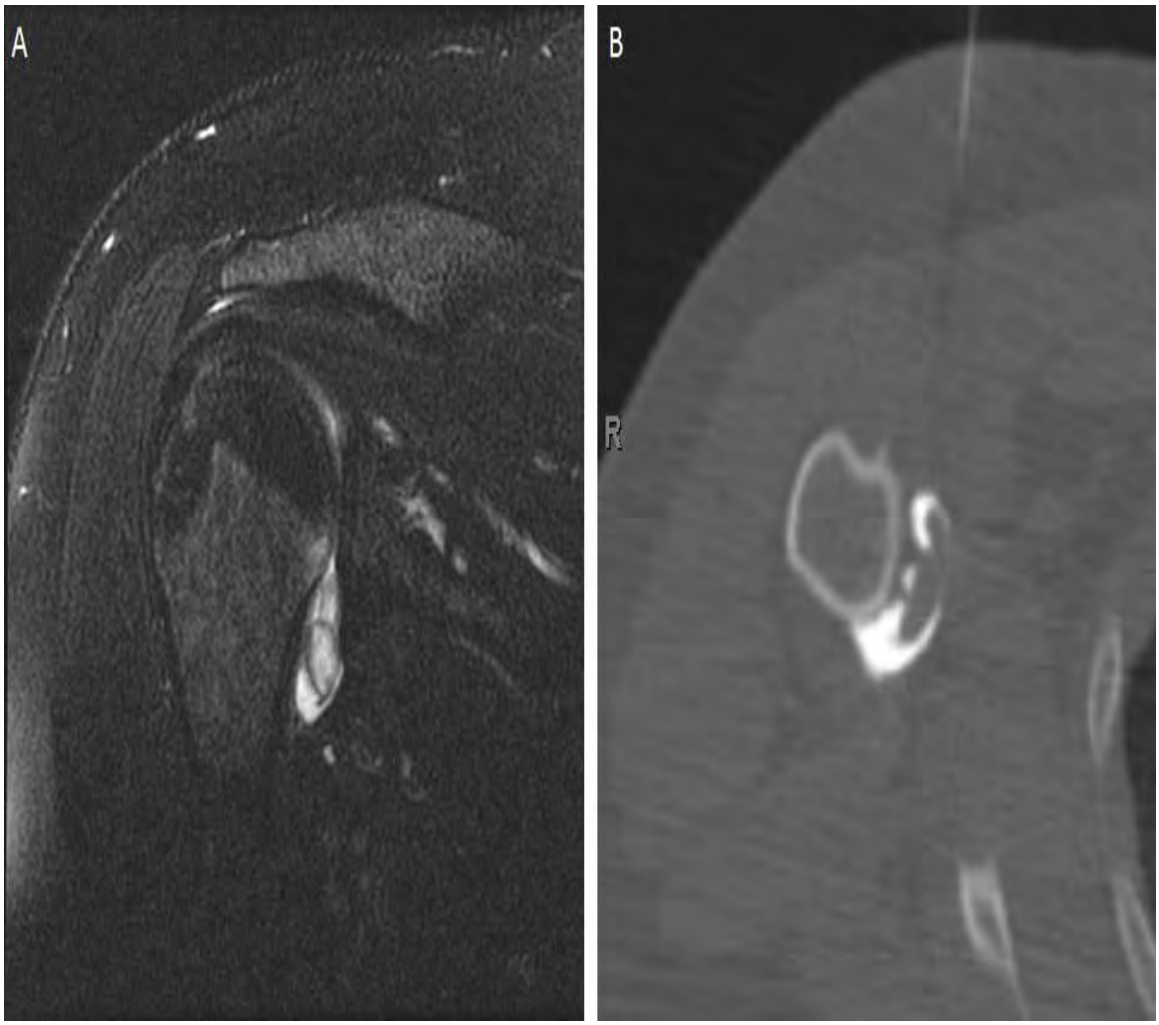

A. Coronal STIR image of the right shoulder demonstrating masslike synovial proliferation in the axillary recess. B. CT-guided biopsy image following intra-articular instillation of contrast.

Podium #22

SHORT-TERM EFFICACY OF ULTRASOUND-GUIDED RETROCALCANEAL BURSA STEROID INJECTION AND CORRELATION WITH SONOGRAPHIC IMAGING FEATURES

Robert Uzor; Beverly Thornhill; Dominic Catanese; Eric Walter; Elizabeth Elsinger; Eric Fornari; Shlomit Goldberg-Stein
Albert Einstein College of Medicine Montefiore Medical Center, Bronx, NY, USA
(Presented by: Robert Uzor, Albert Einstein College of Medicine Montefiore Medical Center)

Purpose: Posterior heel pain due to retrocalcaneal bursitis and/or insertional Achilles tendinopathy is commonly treated with sonographically-guided steroid injection, but the efficacy of this treatment is not well understood. The purpose of this study was to evaluate the clinical effectiveness of ultrasound-guided corticosteroid injection into the retrocalcaneal bursa as a treatment for posterior heel pain and to correlate the pre-injection heel sonographic findings with injection outcome.

Materials and Methods: After IRB approval, consecutive sonographically-guided retrocalcaneal bursa injections (2015-2018) were retrospectively reviewed. Pre-injection heel ultrasound features (presence of Achilles tendinopathy, retrocalcaneal bursitis, bursal or tendon Doppler flow) and pre-and post-injection patient VAS pain scores (scale 0-10) were recorded. Response to treatment was classified as excellent (reduced by 7-10 points), good (reduced by 4-6 points), fair (reduced by 1-3 points), or none. The Fisher exact test was used to evaluate for associations between each ultrasound finding and injection outcome.

Results: 27 injections were performed (22 females, 5 males; mean 55.2 years, range 35-68 years; 13 left heel, 14 right heel), with 100% technical success and no complications. Insertional Achilles tendon pathology and retrocalcaneal bursitis was sonographically present in 24 of 27 cases (89%) and 17 of 27 (63%), respectively. Median pre-procedure and post-procedure (within 1-4 weeks) pain scores were 10 (IQR 8, 10) and 3 (IQR 0, 5), respectively. Statistically significant decrease in pain score was observed following injection, with good or excellent response (> 4-point reduction in pain score) present in 70% of patients, and mean change of 5.18 (95% CI 3.81, 6.56; $p<0.00001$). No significant correlation was identified between change in pain score and sonographic variables.

Conclusion: Sonographically-guided retrocalcaneal bursal steroid injection is an effective technique yielding statistically significant short-term decrease in pain score, with a mean change of 5.18 ($p<0.00001$).

Modality % - Radiography / Fluoroscopy:	0
Modality % - CT:	0
Modality % - MRI:	0
Modality % - US:	100
Modality % - Nuclear Medicine:	0

Long-axis grayscale ultrasound image of the Achilles tendon insertion demonstrates fusiform enlargement of the distal Achilles tendon and sonographic retrocalcaneal bursitis with >3mm bursal distension.

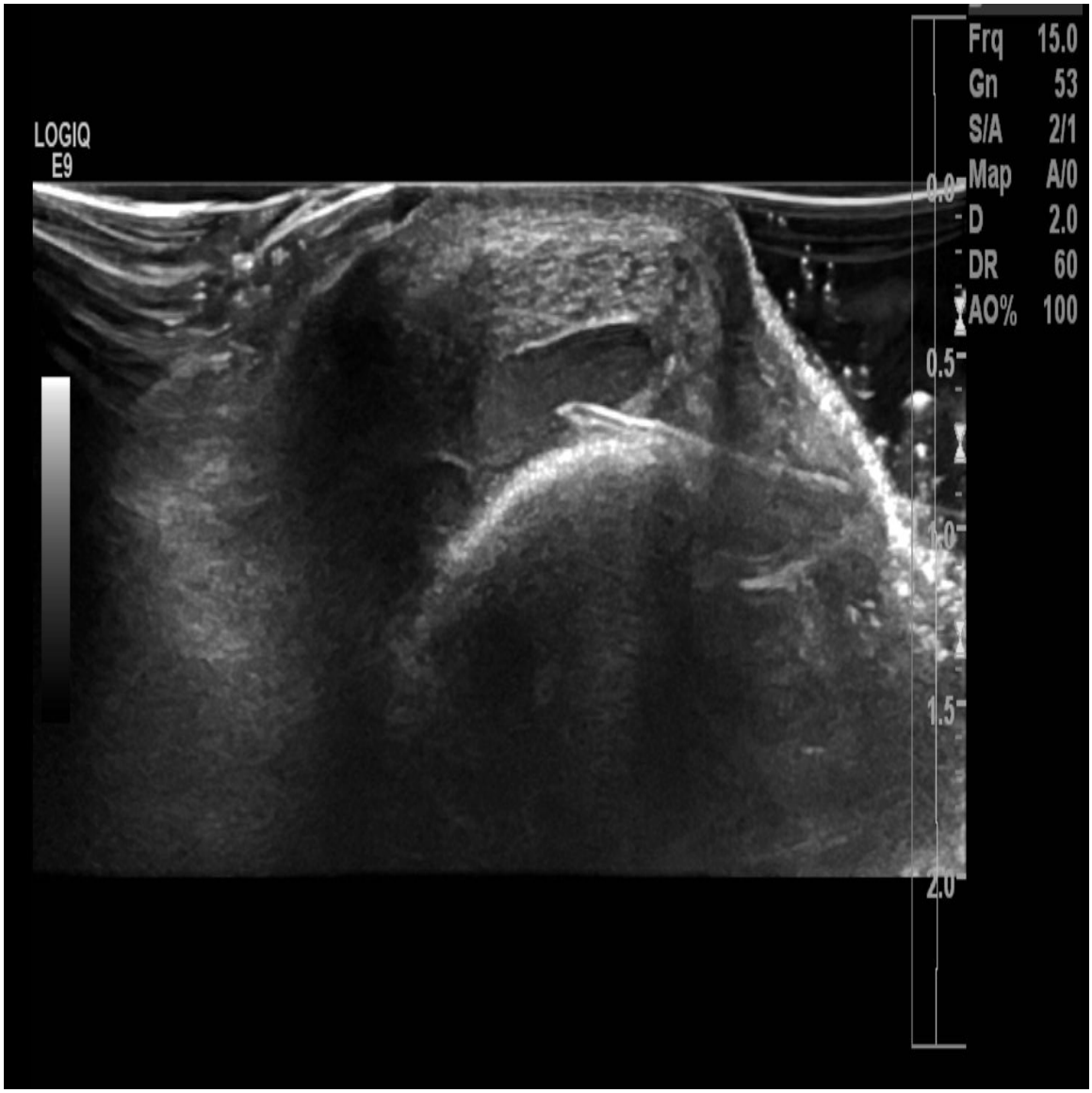

Long-axis Doppler Ultrasound image of the Achilles tendon insertion demonstrates hypoechoic fusiform tendon enlargement and hyperemia, indicating tendinosis.

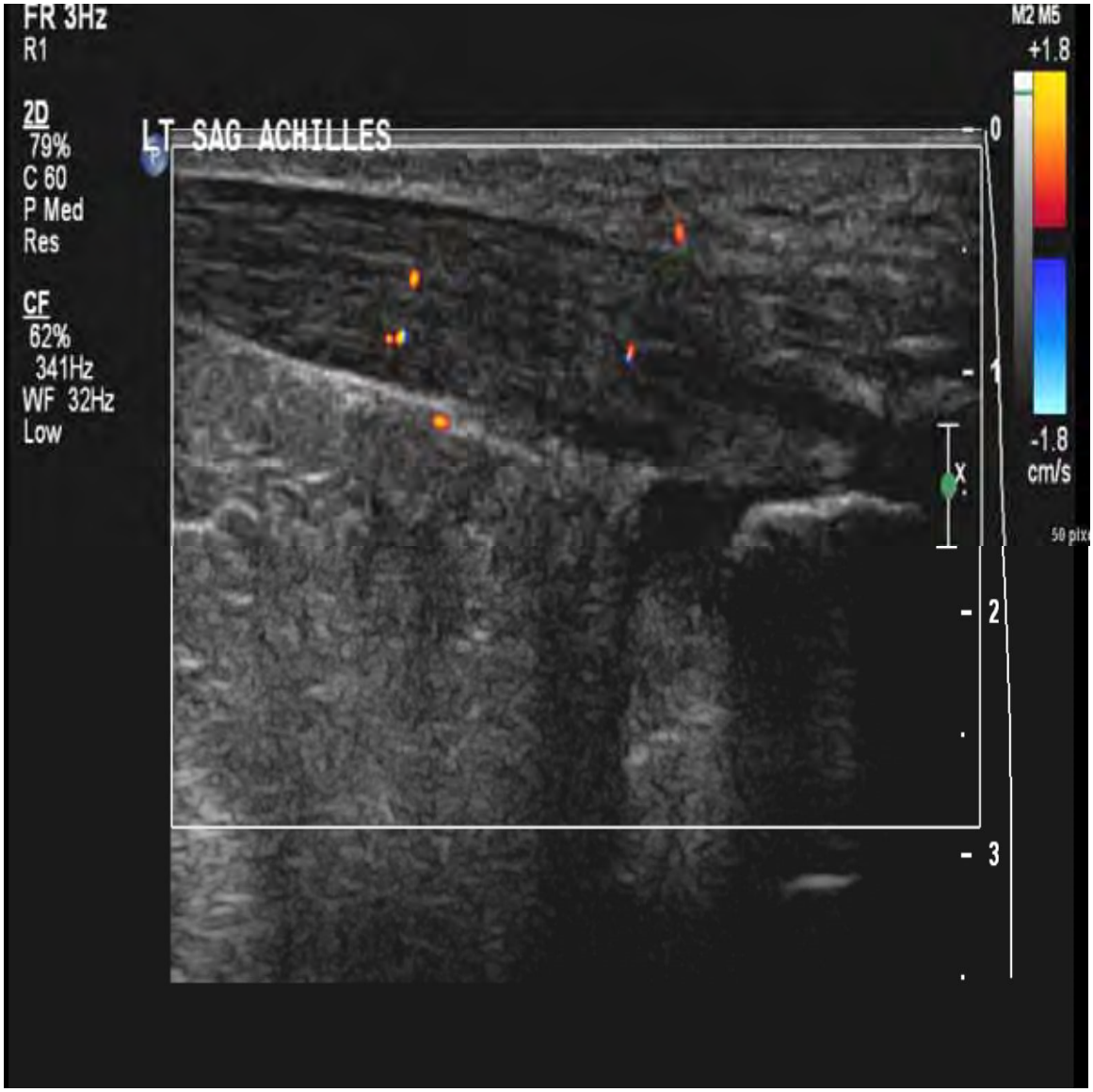

Short axis grayscale ultrasound image demonstrates needle-tip in the retrocalcaneal bursa, with bursal distension following steroid injection.

Podium #23

Safety and Efficacy of Image Guided Radiofrequency Ablation of Genicular Nerve for Pain Management in Patients with Moderate to Severe Osteoarthritis of the Knee: initial single institution experience

Felix Gonzalez, MD[1]; Philip Wong, MD[1]; Stephen Cole, MD[1]; Samia Sayyid, MD[1]; Zachary Bercu, MD, RPVI[2]; John Prologo, MD, FSIR[2]; Janice Newsome, MD[2]; Monica Umpierrez, MD[1]; Adam Singer, MD[1]; Nima Kokabi, MD[2]; Nickolas Reimer, MD[3]
[1]Emory University Dept. of Radiology, MSK Division, Atlanta, GA, USA; [2]Emory University Department of Radiology, Interventional Radiology and Image-Guided Medicine division, Atlanta, GA, USA; [3]Emory University School of Medicine, Department of Orthopaedics, Atlanta, GA, USA
(Presented by: Felix Gonzalez, MD, Emory University Dept. of Radiology, MSK Division)

Purpose: To assess the safety-efficacy of RFA for treatment of moderate-severe knee arthritis pain.
Materials and Methods: 8-patients refractory to conservative treatments underwent genicular nerve RFAs. Anesthetic blocks were followed by RFA 1-2 weeks afterwards. Treatment efficacy was evaluated using the WOMAC index before and at 3 months.
Results: A total of ten knees were treated in 8 patients. The average age of the patients was 70.9 years. Mean follow-up time was 3.5 months. No procedure related complication was identified. The mean total WOMAC score (out of 100) improved significantly from baseline score of 47 to 65.9 at 3 months post treatment (p=0.019). Subanalysis of the overall symptoms component of the WOMAC questionnaire demonstrated significant decrease in mean overall symptoms score from 11.4 to 7.3 (p=0.046). Mean stiffness score decreased from 6.2 to 3.5 (p=0.003) and mean pain score decreased from 22.5 to 13.3 (p=0.026). There was also significant improvement in the functional daily living limitations with mean baseline score of 30.2 and 3 month post therapy score of 20.3 (p=0.037).

Conclusion: Imaged-guided radiofrequency ablation of genicular nerves is a safe treatment option resulting in significant improvement in osteoarthritic index, motility and quality of life in patients with moderate to severe knee OA refractory to conservation treatments

Modality % - Radiography / Fluoroscopy:	80
Modality % - CT:	0
Modality % - MRI:	0
Modality % - US:	20
Modality % - Nuclear Medicine:	0

Podium #24

MUSCULOSKELETAL (MSK) SOFT TISSUE LESION CORE NEEDLE BIOPSY: VARIATIONS IN BIOPSY PRACTICE PATTERNS AND IMPLICATIONS REGARDING SPECIMEN ADEQUACY

Anthony Wheeler, MD; Hillary Garner, MD; Daniel Wessell, MD, PhD; Joseph Bestic, MD; Jeffrey Peterson, MD; Jacob Feldhaus, MD
Mayo Clinic Florida, Jacksonville, FL, USA
(Presented by: Anthony Wheeler, MD, Mayo Clinic Florida)

Purpose: To investigate variations in MSK soft tissue biopsy practice patterns in an effort to determine if a best practice exists in regard to obtaining adequate specimens for pathologic diagnosis.

Materials and Methods: A 17 question Survey Monkey® questionnaire was created to poll SSR members performing MSK soft tissue core biopsies. Demographic questions and questions pertaining to biopsy technique (e.g. needle type, needle gauge, number of passes, specimen length, and verification method of specimen adequacy) were posed. The email survey was distributed to the SSR membership on March 22, 2018, with a completion reminder sent on May 7, 2018. A statistical analysis of collected survey data was performed. A Pearson Chi Square test was used to compare proportional differences of completed biopsy techniques questions and specimen adequacy questions. A multiple comparison Bonferroni adjustment was applied where p-values < 0.007 were statistically significant. All tests were two sided.

Results: 147 of 1454 (10.1%) of members responded to the survey. Of those responding, 85 (57.8%) described their practice as academic, 49 (33.3%) as private practice and 13 (8.8%) as hybrid. The majority (87.1%) perform needle core biopsy and/or FNA of soft tissue lesions. The majority (94.9%) were MSK fellowship trained. There were no statistically significant associations between needle size or type, number of samples obtained (see Figure 1), or in-room verification of specimen adequacy (see Figure 2) with the percentage of time final pathology specimens were deemed non-diagnostic/inadequate (p>0.067 for all analyses).

Conclusion: There is considerable variation in MSK soft tissue tumor biopsy technique among SSR members. However, no statistically significant correlation between the various biopsy techniques and the probability of a non-diagnostic specimen was found.

Modality % - Radiography / Fluoroscopy: 5
Modality % - CT: 20
Modality % - MRI: 0
Modality % - US: 75
Modality % - Nuclear Medicine: 0

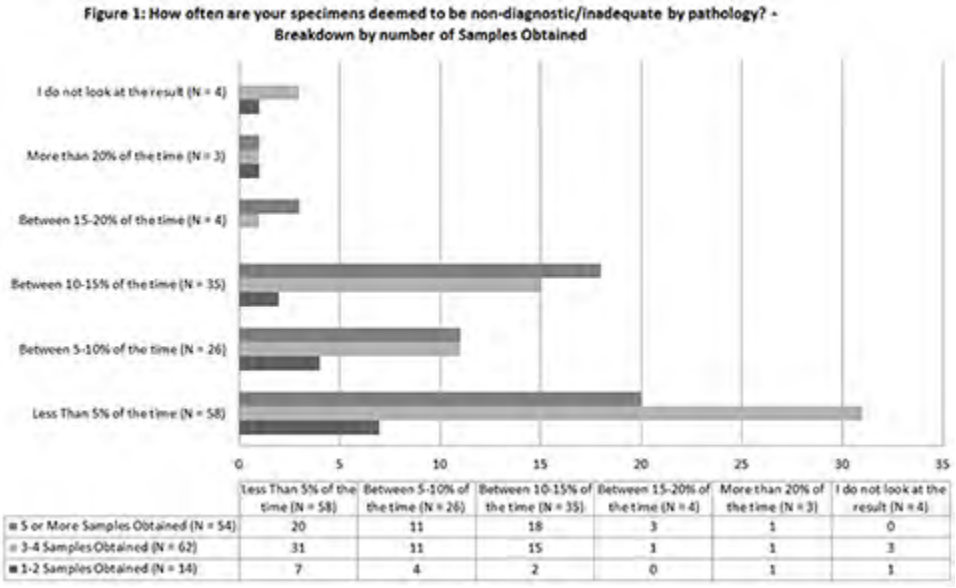

Figure 1. Percentage of Non-Diagnostic Specimens versus Number of Samples Obtained

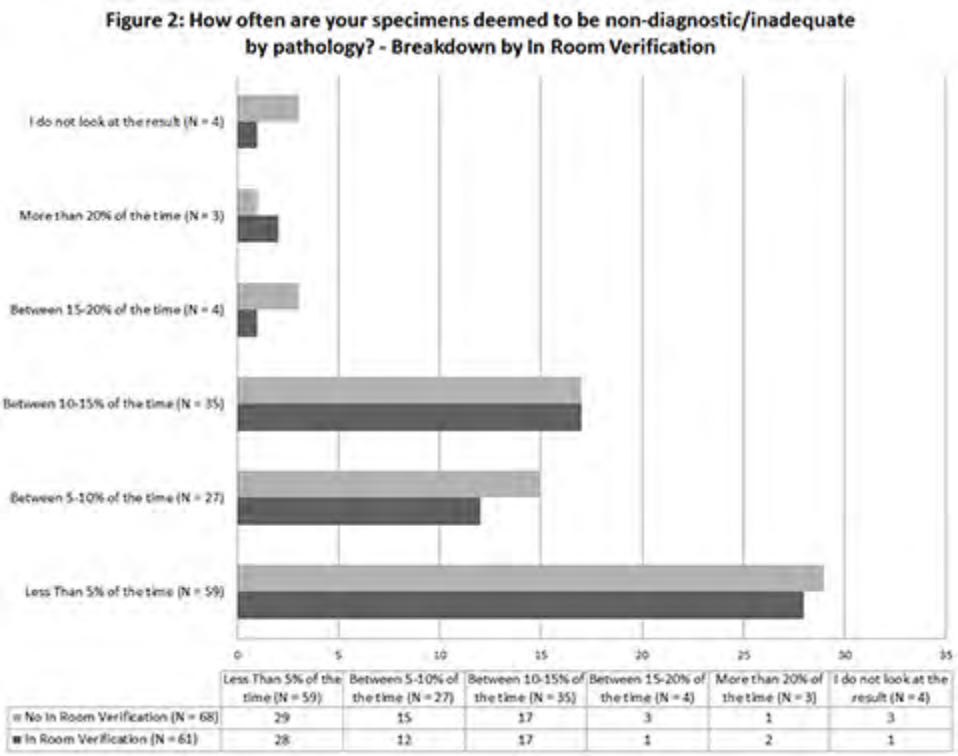

Figure 1. Percentage of Non-Diagnostic Specimens versus In-Room Verification or No In-Room Verification

Podium #25

UTILITY OF REPEAT HIP ASPIRATIONS PERFORMED ON PATIENTS WITH THA

Michael Fox, MD; Jeffrey Hassebrock, MD; Mark Kransdorf, MD; Jonathan Flug, MD; Jeremiah Long, MD; Adam Schwartz, MD
Mayo Clinic Arizona, Phoenix, AZ, USA
(Presented by: Michael Fox, MD, Mayo Clinic Arizona)

Purpose: Evaluate the utility of a repeat hip aspiration performed within 15 days of the first aspiration in patients with total hip arthroplasty (THA).

Materials and Methods: All hip aspirations performed over a 10 year period (2007-2017) at a single institution were retrospectively reviewed. Data recorded included patient age, gender, laterality, interval between aspirations, volume of fluid returned, whether a "joint lavage" was performed, cell count, culture, and fluoro time. Differences between the first and second aspiration that were studied included: Volume returned, Culture result, and Total synovial WBC count.

Results: 27 patients (17F:10M; mean age 66.3) had 31 "pairs" of aspirations on 29 hips (15R:14 L). The mean/median number of days between 1st and 2nd aspirations was 8.1/8.0 days respectively. The mean/median volume (mL) returned was 9.9/2.0. Mean/median volume change between 1st and 2nd aspirations was 5.6/0.0. No fluid was returned in 13% (4/31) of the first attempts; however, all 4 had fluid on the second attempt (mean 3 mL/median 2mL). In the 16 instances when <2 mL of fluid was returned on the 1st aspiration, the 2nd aspiration yielded <1 mL in 19% (3/16); 1-1.9 mL in 31% (5/16), and 2+mL in 50% (8/16) of the cases, respectively. In 54% (7/13) of the 2nd aspirations that returned >1mL, either a positive culture or a synovial WBC of >10,000 was revealed. Mean and median fluoroscopic time was 0.6 and 0.5 minutes.

Conclusion: In 81% (13/16) of THA patients with an initial aspiration of <2mL, a repeat aspiration returned 1+ml of fluid. In over 50% of those 13 patients, a positive culture result or an elevated synovial WBC was evident. When no fluid was returned on the first attempt, at least 1 mL of fluid was returned on repeat aspiration in all cases.

Modality % - Radiography / Fluoroscopy:	100
Modality % - CT:	0
Modality % - MRI:	0
Modality % - US:	0
Modality % - Nuclear Medicine:	0

TUESDAY

Society of Skeletal Radiology

42nd Annual Meeting

March 10-13, 2019

Tuesday, March 12, 2019

7:00 a.m.–7:55 a.m. **Continental Breakfast**

7:00 a.m.–12:35 p.m. **Registration/Information Desk Open**

7:00 a.m.–12:30 p.m. **Exhibit Hall Open**

8:00 a.m.–10:00 a.m. **HIP / PELVIS**

Moderators: Robert Boutin, MD, Jennifer Demertzis, MD

8:00 a.m. #26 **AIIS AND SUBSPINOUS IMPINGEMENT ON MRI: WHEN TWO BECOME ONE**
Terence Farrell, MD; Adam Zoga, MD; Vishal Desai, MD; William Morrison, MD; Johannes Roedl, MD, PhD
Thomas Jefferson University Hospital, Philadelphia, PA, USA
(Presented by: Terence Farrell, MD, Thomas Jefferson University Hospital)

8:15 a.m. #27 **SONOGRAPHIC EVALUATION OF THE LATERAL FEMORAL CUTANEOUS NERVE IN MERALGIA PARESTHETICA**
Andrew Erie, MD; Gavin McKenzie, MD; John Skinner, MD; Christin Tiegs Heiden, MD; Naveen Murthy, MD; Ross Puffer, MD; Robert Spinner, MD; Katrina Glazebrook, M.B.,Ch.B.
Mayo Clinic, Rochester, MN, USA
(Presented by: Andrew Erie, MD, Mayo Clinic)

8:30 a.m. #28 **THERAPEUTIC ARTHROGRAM OF THE HIP FOR ADHESIVE CAPSULITIS: AN INNOVATIVE TREATMENT PROCEDURE THAT REDUCES CAPSULAR STIFFNESS AND INCREASES MUSCLE ACTIVATION**
Anthony Mascia, MD
Humber River Hospital, University of Toronto, Toronto, ON, Canada
(Presented by: Anthony Mascia, MD, Humber River Hospital, University of Toronto)

8:45 a.m. #29 **VALUE OF RESPONSE TO ANESTHETIC INJECTION DURING HIP MR ARTHROGRAPHY TO DIFFERENTIATE BETWEEN INTRA- AND EXTRA-ARTICULAR PATHOLOGY**
Miriam Bredella, MD[1]; Adam Zoga, MD[2]; Joao Terneira Vicentini, MD[1]; Scott Martin, MD[1]; Arvin Kheterpal, MD[1]
[1]Mass General Hospital, Boston, MA, USA; [2]Thomas Jefferson University Hospital, Philadelphia, PA, USA
(Presented by: Miriam Bredella, MD, Mass General Hospital)

9:00 a.m. #30 **ABDUCTOR PATHOLOGY IN ISCHIOFEMORAL IMPINGEMENT (IFI)**
Miriam Bredella, MD; Arvin Kheterpal, MD; Joel Harvey, Mr; Jad Husseini, MD; Scott Martin, MD; Martin Torriani, MD
Mass General Hospital, Boston, MA, USA
(Presented by: Miriam Bredella, MD, Mass General Hospital)

9:15 a.m. #31 **MR APPEARANCE OF ELONGATED GLUTEUS MEDIUS TENDON FOLLOWING TOTAL HIP ARTHROPLASTY**
Dean Busby, MD; Joshua Polster, MD
Cleveland Clinic, Cleveland, OH, USA
(Presented by: Dean Busby, MD, Cleveland Clinic)

9:30 a.m. #32 **CLINICAL USE OF COMPRESSED SENSING-ACCELERATED SEMAC MRI FOR DIAGNOSING PERIPROSTHETIC ABNORMALITIES IN PATIENTS WITH PAINFUL HIP AND KNEE ARTHROPLASTIES: WHAT ARE WE MISSING?**
Jan Fritz, MD[1]; Ali Rashidi, MD[1]; Reto Sutter, MD[2]; Benjamin Fritz, MD[2]
[1]Johns Hopkins University, Baltimore, MD, USA; [2]Balgrist University Hospital, Zurich, Switzerland
(Presented by: Jan Fritz, MD, Johns Hopkins University)

9:45 a.m. #33 **COMPARISON BETWEEN RADIOGRAPHY AND MAGNETIC RESONANCE IMAGING FOR THE DETECTION OF SACROILIITIS IN THE INITIAL DIAGNOSIS OF AXIAL SPONDYLOARTHRITIS: A COST-EFFECTIVENESS STUDY**
Natalia Gorelik, MD[1]; Farah Tamizuddin[2]; Tatiane Rodrigues, MD[1]; Luis Beltran, MD[3]; Fardina Malik, MD[4]; Soumya Reddy, MD[4]; Naveen Subhas, MD, MPH[5]; Soterios Gyftopoulos, MD, MS[1]
[1]NYU Medical Center/ Hospital for Joint Diseases Langone Medical Center, New York, NY, USA; [2]New York University School of Medicine, New York, NY, USA; [3]Brigham and Women''s Hospital, Harvard Medical School, Boston, MA, USA; [4]NYU School of Medicine, New York, NY, USA; [5]Cleveland Clinic, Cleveland, OH, USA
(Presented by: Natalia Gorelik, MD, NYU Medical Center/ Hospital for Joint Diseases Langone Medical Center)

10:00 a.m.–10:05 a.m. **CASE OF THE DAY**
Presenting author: Troy Storey, MD

10:05 a.m.–10:30 a.m. **Break - Visit the Exhibit Hall**

10:30 a.m.–12:30 p.m. **SPINE**
Moderators: David Rubin, MD, Connie Chang, MD

10:30 a.m. #34 **MINDING THE GAP: VERTEBRAL BODY FRACTURE CLEFTS AND WHAT THEY MEAN FOR POST-VERTEBROPLASTY OUTCOMES**
MK Jesse, MD
University of Colorado Denver, Aurora, CO, USA
(Presented by: MK Jesse, MD, University of Colorado Denver)

10:45 a.m. #35 **VARIABILITY IN PERCUTANEOUS PROCEDURES FOR VERTEBRAL OSTEOMYELITIS AMONG RADIOLOGISTS**
Claus Simpfendorfer, MD; Hakan Ilaslan, MD
Cleveland Clinic, Cleveland, OH, USA
(Presented by: Claus Simpfendorfer, MD, Cleveland Clinic)

11:00 a.m. #36 **THE ROLE OF SARCOPENIA IN CLINICAL VERTEBRAL AUGMENTATION OUTCOMES**
Amanda Crawford, MD; Michael Durst, MD; Corey Ho, MD; MK Jesse, MD; Debayan Bhaumik, MD
University of Colorado Denver, Aurora, CO, USA
(Presented by: Amanda Crawford, MD, University of Colorado Denver)

11:15 a.m. #37 **IS SPINAL MRI VALUABLE IN ADDITION TO MRI OF THE SACROILIAC JOINTS IN THE DIAGNOSIS OF SPONDYLOARTHRITIS?**
STUBBS EUAN, MBChB; Rebello Ryan, MD; Raj Carmona, MD; George Ioannidis; Harish Srini, MD
McMaster University, Hamilton, ON, Canada
(Presented by: STUBBS EUAN, MBChB, McMaster University)

11:30 a.m. #38 **THE ROLE OF PARASPINAL EDEMA IN CLINICAL VERTEBRAL AUGMENTATION OUTCOMES**
Michael Durst, MD; MK Jesse, MD; Amanda Crawford, MD; Corey Ho, MD; Debayan Bhaumik, MD
University of Colorado Denver, Denver, CO, USA
(Presented by: Michael Durst, MD, University of Colorado Denver)

11:45 a.m. #39 **TRANSPEDICULAR-TRANSDISCAL CEMENT AUGMENTATION TECHNIQUE FOR TREATMENT OF PROXIMAL JUNCTIONAL FAILURE OF SPINAL FUSION**
Corey Ho, MD; MK Jesse, MD
University of Colorado Denver, Aurora, CO, USA
(Presented by: Corey Ho, MD, University of Colorado Denver)

12:00 p.m. #40 **MIDLINE INTERLAMINAR LUMBAR EPIDURAL INJECTIONS: INSTITUTIONAL EXPERIENCE SAFELY UTILIZING DEPO-MEDROL®.**
Daniel Carr, MD; Damon Spitz, MD; Tal Rencus, MD; John Falardeau, MD; Sam Madoff, MD; Manisha Raythatha, MD
New England Baptist Hosp. Tufts University School of Med, Boston, MA, USA
(Presented by: Daniel Carr, MD, New England Baptist Hosp. Tufts University School of Med)

12:15 p.m. #41 **FLUOROSCOPICALLY-GUIDED LUMBAR SPINE INTERLAMINAR AND TRANSFORAMINAL INJECTIONS: INCIDENCE AND LOCATION OF INADVERTENT INTRAVASCULAR INJECTION**
Connie Chang, MD; Jad Husseini, MD
Mass General Hospital, Boston, MA, USA
(Presented by: Connie Chang, MD, Mass General Hospital)

12:30 p.m.–12:35 p.m. **CASE OF THE DAY**
Presenting author: Rupert Stanborough, MD

1:00 p.m.–6:00 p.m. **SSR Annual Golf Outing**

Related ePosters

HIP / PELVIS

Poster #25 **ACCURACY OF PREOPERATIVE MRI AND MRA FOR THE ASSESSMENT OF ACETABULAR LABRAL SIZE IN PATIENTS WITH FEMOROACETABULAR IMPINGEMENT (FAI)**
Richard Marshall, MD; Daniel Kaplan, MD; Christopher Burke, MD; Soterios Gyftopoulos, MD; Jonathan Vigdorchik, MD; Robert Meislin, MD; Thomas Youm, MD; Mohammad Samim, MD
NYU Medical Center/ Hospital for Joint Diseases Langone Medical Center, New York, NY, USA

Poster #26 **SACROILIAC JOINT INFECTIONS IN CHILDREN: MR IMAGING FEATURES**
Sara Cohen, MD; David Biko, MD; Christian Barrera, MD; Suraj Serai, PhD; Jie Nguyen, MD
Children's Hospital of Philadelphia, Philadelphia, PA, USA

Poster #27 **WITHDRAWN**

Podium #26

AIIS AND SUBSPINOUS IMPINGEMENT ON MRI: WHEN TWO BECOME ONE

Terence Farrell, MD; Adam Zoga, MD; Vishal Desai, MD; William Morrison, MD; Johannes Roedl, MD, PhD
Thomas Jefferson University Hospital, Philadelphia, PA, USA
(Presented by: Terence Farrell, MD, Thomas Jefferson University Hospital)

Purpose: The morphology of the anterior inferior iliac spine (AIIS) and subspinous region are increasingly being identified as important components in the spectrum of extra-articular hip impingement (EA-HI). The purpose of this study in progress is to detail the normal spectrum of morphology and imaging appearance of the AIIS and subspinous region on MRI, demonstrate variant morphology and pathology of these regions associated with EA-HI, highlight the distinct nature of these two entities with MRI patterns and discuss appropriate imaging protocols in the evaluation of EA-HI.

Materials and Methods: A retrospective MRI report database was searched for "subspinous", "AIIS impingement", "rectus femoris tendinosis" and "bursitis" with "anterior". An MRI indication database was searched for "subspinous", "AIIS" and "extra-articular" with the term "impingement". Identified MRIs were reviewed by two MSK rads in consensus for AIIS anatomy, sub-spinous space size, rectus femoris origin pathology, bursitis, soft tissue edema and acetabular labrum tear. Exclusion criteria included fracture, osteoarthritis and active core injury.

Results: 30 subject group MRIs were reviewed along with 10 control group studies. There was great variability in the sub-spinous space, but the distance was smaller in the setting of soft tissue edema anterior to the hip capsule. Rectus femoris tendinosis varied from tendinous enlargement to peritendinous edema, but was isolated to the subject group. Anterior labrum tears were present in both groups without statistically significant difference. A constellation of AIIS prominence, rectus femoris tendinosis and pericapsular soft tissue edema was exclusive to the subject group.

Conclusion: AIIS impingement and subspinous impingement are separate entities in closely apposed regions which frequently coexist as causes of EA-HI. The clinical presentation may be analagous to CAM/pincer type femoroacetabular impingement and a high index of suspicion and knowledge of normal AIIS and subspinous anatomy, variant morphology and pathology is crucial to accurately diagnose and treat EA-HI.

Modality % - Radiography / Fluoroscopy:	10
Modality % - CT:	10
Modality % - MRI:	80
Modality % - US:	0
Modality % - Nuclear Medicine:	0

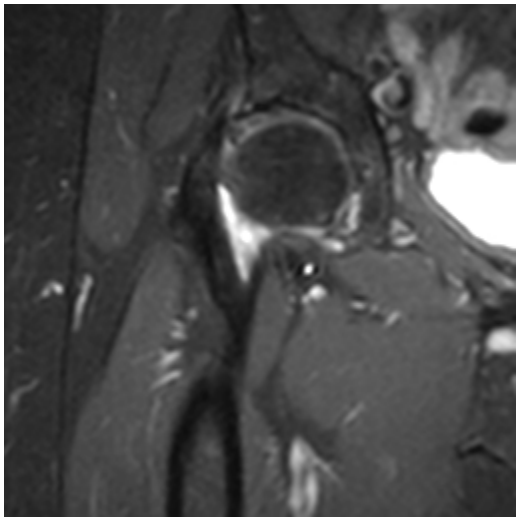

Coronal STIR image from a noncontrast hip MRI shows enlargement of the rectus femoris, precapsular soft tissue edema, and osseous prominence of the AIIS.

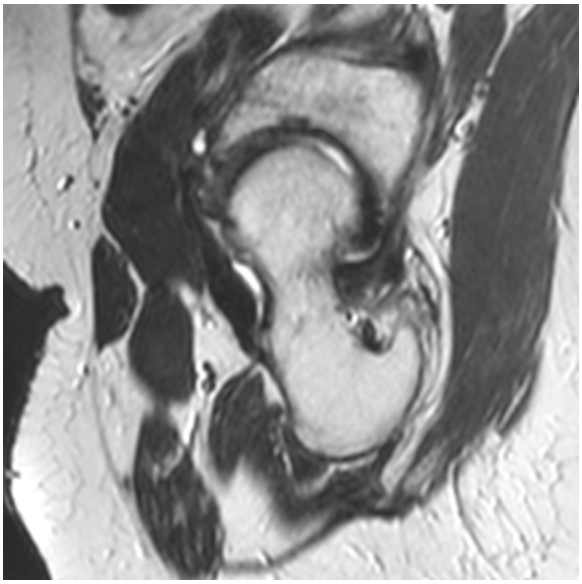

Axial oblique PD FSE image of the hip shows a narrow subspinous interval, soft tissue edema and maceration of the anterior labrum.

Podium #27

SONOGRAPHIC EVALUATION OF THE LATERAL FEMORAL CUTANEOUS NERVE IN MERALGIA PARESTHETICA

Andrew Erie, MD; Gavin McKenzie, MD; John Skinner, MD; Christin Tiegs Heiden, MD; Naveen Murthy, MD; Ross Puffer, MD; Robert Spinner, MD; Katrina Glazebrook, M.B.,Ch.B.
Mayo Clinic, Rochester, MN, USA
(Presented by: Andrew Erie, MD, Mayo Clinic)

Purpose: Identify sonographic abnormalities of the lateral femoral cutaneous nerve (LFCN) in meralgia paresthetica (MP).
Materials and Methods: IRB approved, retrospective chart review was performed on 51 ultrasound reports of the LFCN in patients with clinically suspected MP. Ultrasounds were considered positive for MP if the ultrasound report suggested the diagnosis. A control group included 20 ultrasounds of the LFCN in lower extremities without symptoms of MP.
Results: Of the 51 ultrasounds in clinically suspected MP, 36 (70%) cases had positive findings suggestive of MP, 10 (20%) cases were negative, and in 5 (10%) cases the LFCN was not seen. Sonographic findings in the 36 positive cases included nerve enlargement in all cases (mean area of 0.1 cm^2 +/- 0.01 cm^2 compared to 0.03 cm^2 +/- 0.01 cm^2 in the negative cases and normal controls; $p < 0.01$), nerve hypoechogenicity (30 of 36 cases, 83%), and/or focal injury including neuroma or neuroma-in-continuity (8 of 36 cases, 22%). Sixteen ultrasounds that were positive for MP had MRI imaging of the LFCN, with 4 of the 16 (25%) MRI reports describing a concordant abnormality of the LFCN (nerve enlargement or T2 hyperintensity). The remaining 12 (75%) MRI reports did not describe a LFCN abnormality, however, in retrospect 5 of these cases had subtle MR abnormalities. Twenty-six of the 36 (72%) patients with positive ultrasounds had an US-guided nerve block (local anesthetic +/- corticosteroid) of the LFCN, with 25 of 26 (96%) patients reporting immediate symptom improvement. Eighteen of the 36 (50%) patients with positive ultrasounds underwent neurectomy or neurolysis of the LFCN, with symptom improvement in all cases.
Conclusion: Ultrasound is a useful modality in assessing the LFCN in clinically suspected meralgia paresthetica and is more sensitive for abnormalities than MRI. US-guided nerve block of the LFCN can help further confirm the diagnosis, especially in patients considering surgery.

Modality % - Radiography / Fluoroscopy:	0
Modality % - CT:	0
Modality % - MRI:	30
Modality % - US:	70
Modality % - Nuclear Medicine:	0

A. Normal LFCN with hyperechoic nerve fascicles (measures 0.04 cm^2) B/C. LFCN in MP demonstrates focal hypoechoic enlargement (0.07 cm^2) consistent with neuroma-in-continuity

Podium #28

THERAPEUTIC ARTHROGRAM OF THE HIP FOR ADHESIVE CAPSULITIS: AN INNOVATIVE TREATMENT PROCEDURE THAT REDUCES CAPSULAR STIFFNESS AND INCREASES MUSCLE ACTIVATION

Anthony Mascia, MD
Humber River Hospital, University of Toronto, Toronto, ON, Canada
(Presented by: Anthony Mascia, MD, Humber River Hospital, University of Toronto)

Purpose: Adhesive capsulitis (AC) is characterized by local joint pain and progressive stiffness, often described as 'frozen shoulder'. AC of the hip (ACH) exhibits similar distinguishing features and clinical presentation. Controversy exists surrounding ACH management, ranging from benign neglect to surgical intervention. Intermediate options are needed for those failing conservative care or reluctant toward surgery. We describe an innovative technique, therapeutic arthrogram (TA), which is a minimally-invasive, radiological intervention involving imaging-guided, intra-articular instillation of fluid and air to release capsular. Chronic capsule contracture influences intra-articular pressure (IAP), which may inhibit surrounding musculature. Releasing adhesions and pressure are hypothesized to reduce stiffness and improve muscle activation.

Materials and Methods: Seven patients (3M/4F) with ACH participated, with an average age, height and body mass of 38.9 ± 11.5 years, 177.4 ± 7.6 cm and 86.0 ± 18.4 kg, respectively. Pain scores (VAS), passive range of motion (pROM) and electromyography (EMG) while performing hip rehabilitation exercises were collected before and after TA procedure. Under fluoroscopic-guidance, a 22-gauge spinal needle was inserted into the hip joint and connected to a pressure sensor. Once needle position was confirmed, sterile saline and air was instilled until capsular disruption occurred. IAP was measured throughout the TA and maximum joint volume recorded.

Results: All patients had confirmed ACH and reduced hip capsular volumes. The procedure was well tolerated with no complications. During TA, IAP values increased linearly, then exponentially up to the maximum capsular volume, which diminished following rupture. Following the TA, increases in pROM were observed, with no significant changes in VAS. Hip EMG increased significantly following the TA procedure.

Conclusion: The TA procedure appears to be a promising, minimally-invasive treatment option for ACH. Our results suggest that joint capsular disruption of adhesions/fibrosis by TA contribute to immediate benefits of reduced capsular stiffness, increased pROM, restoration of IAP and increased muscle activation.

Modality % - Radiography / Fluoroscopy:	100
Modality % - CT:	0
Modality % - MRI:	0
Modality % - US:	0
Modality % - Nuclear Medicine:	0

Podium #29

VALUE OF RESPONSE TO ANESTHETIC INJECTION DURING HIP MR ARTHROGRAPHY TO DIFFERENTIATE BETWEEN INTRA- AND EXTRA-ARTICULAR PATHOLOGY

Miriam Bredella, MD[1]; Adam Zoga, MD[2]; Joao Terneira Vicentini, MD[1]; Scott Martin, MD[1]; Arvin Kheterpal, MD[1]
[1]Mass General Hospital, Boston, MA, USA; [2]Thomas Jefferson University Hospital, Philadelphia, PA, USA
(Presented by: Miriam Bredella, MD, Mass General Hospital)

Purpose: To determine the value of anesthetic injection during hip MR arthrography (anesthetic MRA) to differentiate between intra- and extra-articular pathology in patients with hip pain.

Materials and Methods: Our retrospective study was IRB-approved and HIPAA-compliant. Sixty-two consecutive patients (38 F, 24 M, 38±13 years) who were referred for MRA were studied. All patients underwent a focused hip examination including active and passive flexion, internal and external rotation immediately prior to injection and pain was recorded on a numeric scale. MRA was performed following fluoroscopically-guided intraarticular injection of 10–12 ml of a mixture of 0.1 ml gadolinium and 10 ml normal saline, 5 ml Isovue-M200 and 5 ml Ropivacaine. Following the injection, the hip examination was repeated and the pain response was recorded. MRA was performed per clinical protocol and reviewed by two musculoskeletal radiologists blinded to the pain response. Clinical records, including physical therapy notes and operative reports were reviewed for verification of intra- and extra-articular pathology as the source of hip pain (gold standard). The positive (PPV) and negative predictive value (NPP) of anesthetic MRA to detect intra- and extra-articular pathology were calculated.

Results: Based on the gold standard, the source of pain was intra-articular in 36 patients and extra-articular in 26 patients. On MRI, 28 patients had only intra-articular and 9 patients only extra-articular pathology, while 25 patients had both intra- and extra-articular pathology. Twenty-nine patients had pain relief and 33 patients had no pain relief after anesthetic injection. PPV of anesthetic MRA to detect intra-articular pathology was 83% and NPV was 64%.

Conclusion: Anesthetic MRA can be used as an adjunct to define the origin of hip pain. A positive response suggests intra-articular pathology which can be helpful to localize the source of pain in equivocal cases where both intra-and extra-articular pathology is evident on MRI.

Modality % - Radiography / Fluoroscopy:	50
Modality % - CT:	0
Modality % - MRI:	50
Modality % - US:	0
Modality % - Nuclear Medicine:	0

Podium #30

ABDUCTOR PATHOLOGY IN ISCHIOFEMORAL IMPINGEMENT (IFI)

Miriam Bredella, MD; Arvin Kheterpal, MD; Joel Harvey, Mr; Jad Husseini, MD; Scott Martin, MD; Martin Torriani, MD
Mass General Hospital, Boston, MA, USA
(Presented by: Miriam Bredella, MD, Mass General Hospital)

Purpose: Ischiofemoral impingement (IFI) is associated with abnormalities of the quadratus femoris muscle and narrowing of the ischiofemoral (IF) and quadratus femoris (QF) spaces. The hip abductors play important roles in pelvic stability. We hypothesized that abductor insufficiency might be a contributing factor to the development of IFI. The purpose of our study was to assess hip abductor pathology in patients with IFI.

Materials and Methods: The study was IRB approved and HIPAA compliant. The study group comprised 140 patients with IFI (mean age: 56±13 y, 130 f, 10 m) and 140 age and gender-matched controls without IFI. Two MSK radiologists performed measurements of IF and QF distances, assessed quadratus femoris muscle for edema and atrophy, and the integrity of the tensor fascia lata, gluteus medius and minimus tendons. IFI and control groups were compared with a two-tailed t-test or chi-squared test.

Results: As expected, patients with IFI had decreased IF and QF distances ($p<0.0001$) compared to controls. All patients with IFI had abnormalities of the quadratus femoris muscle, whereas the QF muscle was normal in controls ($p<0.0001$). Patients with IFI had a higher prevalence of gluteal medius and minmus partial and full-thickness tears compared to controls ($p=0.007$). There were no tears of the tensor fascia lata in either group. When stratified by age, abductor pathology was only associated with IFI in patients ≥45 years ($p=0.001$), while there was no difference in prevalence of abductor tears in patients with IFI <45 years ($p=0.8$) compared to controls.

Conclusion: Abductor insufficiency might play a role in the pathophysiology of IFI in elderly patients. This emphasizes the need of abductor strengthening or repair in the treatment of IFI.

Modality % - Radiography / Fluoroscopy:	0
Modality % - CT:	0
Modality % - MRI:	100
Modality % - US:	0
Modality % - Nuclear Medicine:	0

Podium #31

MR appearance of Elongated Gluteus medius tendon following total hip arthroplasty

Dean Busby, MD; Joshua Polster, MD
Cleveland Clinic, Cleveland, OH, USA
(Presented by: Dean Busby, MD, Cleveland Clinic)

Purpose: To evaluate the MR appearance of the gluteus medius tendon following total hip arthroplasty performed by different surgical techniques.

Materials and Methods: Retrospective records review of MRIs of the pelvis and hips performed following total hip arthroplasty. Review of medical records indicated surgical approach and physical exam findings around the time of imaging. Cases were divided into 2 groups based on whether the surgery was performed by a posterolateral approach or a straight lateral approach. All cases were reviewed in consensus by one attending musculoskeletal radiologist and one MSK fellow to identify cases in which the gluteus medius tendon appeared elongated on coronal images. Original radiology reports were also evaluated.

Results: There were a total of 47 patients with 50 hip arthroplasties. 25 hips had arthroplasty via a straight lateral approach and 25 had a posterolateral surgical approach. 19/25 (76%) of the cases with straight lateral approach had the appearance of an elongated gluteus medius tendon and 3/12 (12%) in the posterolateral approach group had this finding. 4/17 (23%) of the cases with elongated tendons in the straight lateral approach group were described as tears of the tendon in their original reports. There was no indication of tendon dysfunction in follow-up clinical notes.

Conclusion: The appearance of gluteus medius tendon elongation on coronal MR images following total hip arthroplasty is much more common following a straight lateral surgical approach and likely reflects localized muscle injury from surgery rather than a clinically relevant tendon abnormality.

Modality % - Radiography / Fluoroscopy:	0
Modality % - CT:	0
Modality % - MRI:	100
Modality % - US:	0
Modality % - Nuclear Medicine:	0

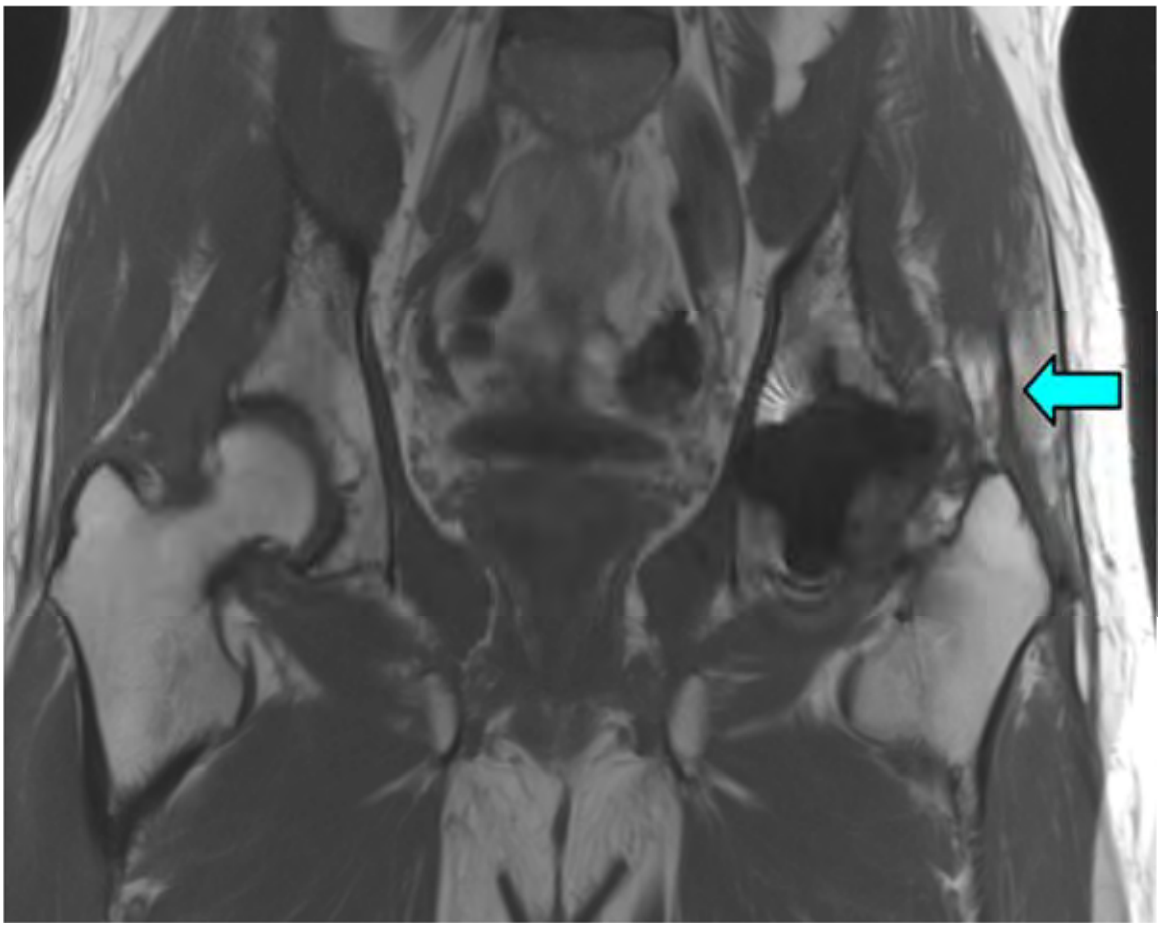

Long appearance of the gluteus medius tendon on the left (arrow) following hip arthroplasty

Podium #32

CLINICAL USE OF COMPRESSED SENSING-ACCELERATED SEMAC MRI FOR DIAGNOSING PERIPROSTHETIC ABNORMALITIES IN PATIENTS WITH PAINFUL HIP AND KNEE ARTHROPLASTIES: WHAT ARE WE MISSING?

Jan Fritz, MD[1]; Ali Rashidi, MD[1]; Reto Sutter, MD[2]; Benjamin Fritz, MD[2]
[1]Johns Hopkins University, Baltimore, MD, USA; [2]Balgrist University Hospital, Zurich, Switzerland
(Presented by: Jan Fritz, MD, Johns Hopkins University)

Purpose: When compared to parallel imaging (PI), compressed-sensing (CS) allows for 50-60% faster acquisition of slice-encoding-for-metal-artifact-correction (SEMAC). CS-SEMAC produces similar image quality in subjects with well-functioning arthroplasty implants; however, there is limited data on diagnosing abnormalities in patients. Therefore, we compared the performance of standard 3-fold-accelerated PI-SEMAC and investigational 8-fold-accelerated CS-SEMAC MRI for diagnosing periprosthetic abnormalities in patients with painful total hip and knee arthroplasty implants.

Materials and Methods: Our study was IRB-approved and all patients gave written informed consent. Between 2014 and 2017, we prospectively recruited 60 patients with pain and dysfunction after hip (14 women, 16 men; age, 68(44–87) years) and knee (10 women, 20 men; age, 62(28–91) years) arthroplasty. Each patient underwent 1.5-Tesla MRI, including coronal (hip) and sagittal (knee) PI-accelerated (factor=3, 22-min) and CS-accelerated (factor=8, 10-min) PD-weighted and STIR SEMAC with 19 spectral encoding steps. Paired PD-weighted and STIR dataset were separated, image annotations were removed and randomly reassigned. Two MSK attendings evaluated the global image quality and six periprosthetic abnormalities. Wilcoxon test, Kendall W agreement, and substitutability testing were applied. P-values < 0.05 indicated statistical significance.

Results: Image quality of hip and knee studies were overall good with slight non-significant (p=0.12/0.37) dominance of PI-SEMAC over CS-SEMAC. Reader agreements were moderate to very good (W range, 0.51-0.85). Inter-method agreement was overall good (W, 0.67/0.40). For each joint, substitution analysis demonstrated that the faster CS-SEMAC could replace the slower PI-SEMAC technique (p-value range, 0.38-0.90) in diagnosing the six abnormalities, including periprosthetic osteolysis, synovitis, bone marrow edema, fractures, tendon tears, and extra-capsular collections.

Conclusion: In patients with painful hip and knee arthroplasty implants, PI-SEMAC and CS-SEMAC techniques produce similar image quality. The faster acquired CS-SEMAC can substitute the slower PI-SEMAC technique for diagnosing a wide spectrum of periprosthetic abnormalities, thereby realizing single SEMAC sequences with 19 spectral encoding steps in 4-5 min acquisition time.

Modality % - Radiography / Fluoroscopy:	0
Modality % - CT:	0
Modality % - MRI:	100
Modality % - US:	0
Modality % - Nuclear Medicine:	0

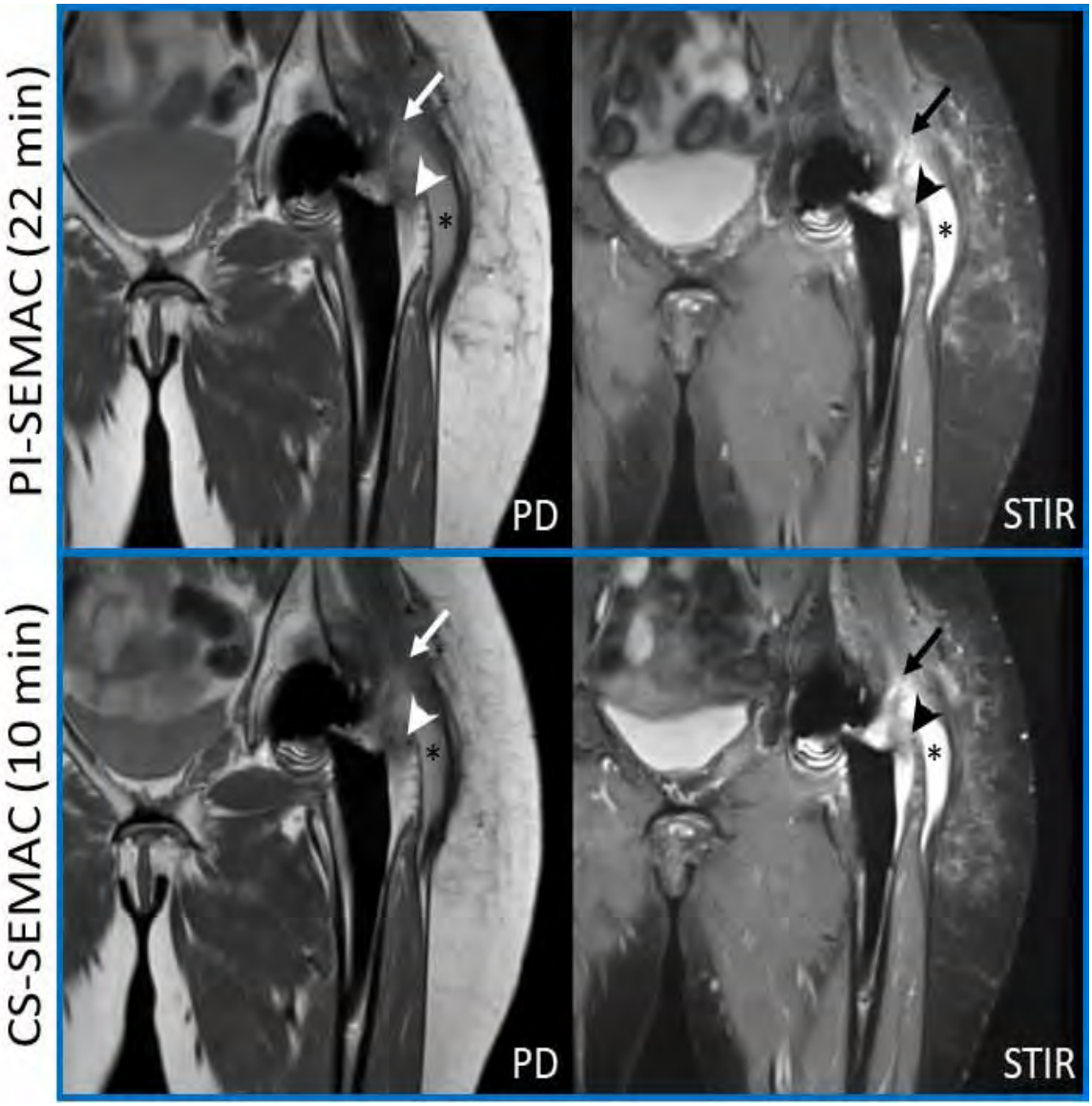

Coronal left hip MRI using 3-fold parallel imaging-(PI)-accelerated SEMAC and 8-fold compressed sensing-(CS)-accelerated SEMAC show osteolysis (arrowheads), bursal fluid (asterisks), and retracted abductor tear (arrows).

Podium #33

COMPARISON BETWEEN RADIOGRAPHY AND MAGNETIC RESONANCE IMAGING FOR THE DETECTION OF SACROILIITIS IN THE INITIAL DIAGNOSIS OF AXIAL SPONDYLOARTHRITIS: A COST-EFFECTIVENESS STUDY

Natalia Gorelik, MD[1]; Farah Tamizuddin[2]; Tatiane Rodrigues, MD[1]; Luis Beltran, MD[3]; Fardina Malik, MD[4]; Soumya Reddy, MD[4]; Naveen Subhas, MD, MPH[5]; Soterios Gyftopoulos, MD, MS[1]
[1]NYU Medical Center/ Hospital for Joint Diseases Langone Medical Center, New York, NY, USA; [2]New York University School of Medicine, New York, NY, USA; [3]Brigham and Women''s Hospital, Harvard Medical School, Boston, MA, USA; [4]NYU School of Medicine, New York, NY, USA; [5]Cleveland Clinic, Cleveland, OH, USA
(Presented by: Natalia Gorelik, MD, NYU Medical Center/ Hospital for Joint Diseases Langone Medical Center)

Purpose: The purpose of this study was to determine the cost-effectiveness of radiograph and MRI based imaging strategies for the initial diagnosis of sacroiliitis in a population with suspected axial spondyloarthritis.
Materials and Methods: A decision analytic model from the health care system perspective for patients with inflammatory back pain suggestive of axial spondyloarthritis was used to evaluate the incremental cost-effectiveness of 3 imaging strategies for the sacroiliac joints during a 3-year horizon: radiography, MRI, and radiography followed by MRI. Comprehensive literature search and expert opinion provided input data on cost, probability, and utility estimates. The primary effectiveness outcome was quality-adjusted life-years (QALYs), with a willingness-to-pay threshold set to $100,000/QALY gained (2018 U.S. dollars). Costs and health benefits were discounted at 3%.
Results: Radiography was the dominant strategy, as it was the least costly ($64,782) and most effective (2.43 QALYs) option over a 3-year course. MRI-based and radiograph/MRI-based strategies were not found to be cost-effective imaging options for this patient population. One-way sensitivity analysis demonstrated that radiography was favored over the other two imaging strategies over a wide range of reasonable costs and probabilities.
Conclusion: Radiography is the most cost-effective imaging strategy for the initial diagnosis of sacroiliitis in patients with inflammatory back pain suspicious for axial spondyloarthritis.

Modality % - Radiography / Fluoroscopy:	50
Modality % - CT:	0
Modality % - MRI:	50
Modality % - US:	0
Modality % - Nuclear Medicine:	0

Podium #34

MINDING THE GAP: VERTEBRAL BODY FRACTURE CLEFTS AND WHAT THEY MEAN FOR POST-VERTEBROPLASTY OUTCOMES

MK Jesse, MD
University of Colorado Denver, Aurora, CO, USA
(Presented by: MK Jesse, MD, University of Colorado Denver)

Purpose: Percutaneous vertebroplasty/kyphoplasty has been documented as a safe and effective treatment for vertebral body fractures. Cement nonunion is a documented cause of failed vertebral cement fixation. We focus on how pre-procedural fracture cleft morphology and procedural cement filling may be associated with the development of non-union and furthermore how this may affect patient outcomes.

Materials and Methods: Retrospective review of 296 patients (172 women, 124 men) who underwent vertebroplasty/kyphoplasty for compression fractures. Variables included pre-procedure CT/MRI cleft presence and morphology, pain improvement, underlying pathology, fracture level, morphology of cement fill, and post-procedure non-union. Statistical analysis was performed utilizing ordinal logistic regression, logistic regression, Fisher's exact, and conditional t-tests of proportions, with significance level set to 0.05.

Results: Majority of patients with nonunion cement fill (75%) demonstrated large cleft morphology. The presence of a fracture cleft resulted in an 4.981 odds ratio of non-union and odds of cleft presence is 5.195 times higher for non-union (95% CI: 1.636, 20.157). There was a significant association between nonunion cement fill and cleft-only fill ($p<0.0001$). Patients with secondary osteoporosis had 2.831 higher odds of cleft (95% CI: 1.119, 7.299). Odds of cleft presence was 1.029 times higher for each one year increase in age (95% CI: 1.119, 7.299). The presence of a vertebral cleft did not significantly alter pain relief outcomes.

Conclusion: Because risk of cement non-union increases with increasing age, secondary osteoporosis, size of the fracture clefts, and cleft-only cement fill, we should pay special attention when these variables are present to adjust our procedure protocol and expectation. The presence of a cleft should not deter the decision to proceed with vertebroplasty/kyphoplasty, as pain relief was not significantly altered; however added attention to increasing trabecular fill during the procedure is warranted to decrease the risk of non-union.

Modality % - Radiography / Fluoroscopy:	33
Modality % - CT:	33
Modality % - MRI:	33
Modality % - US:	0
Modality % - Nuclear Medicine:	0

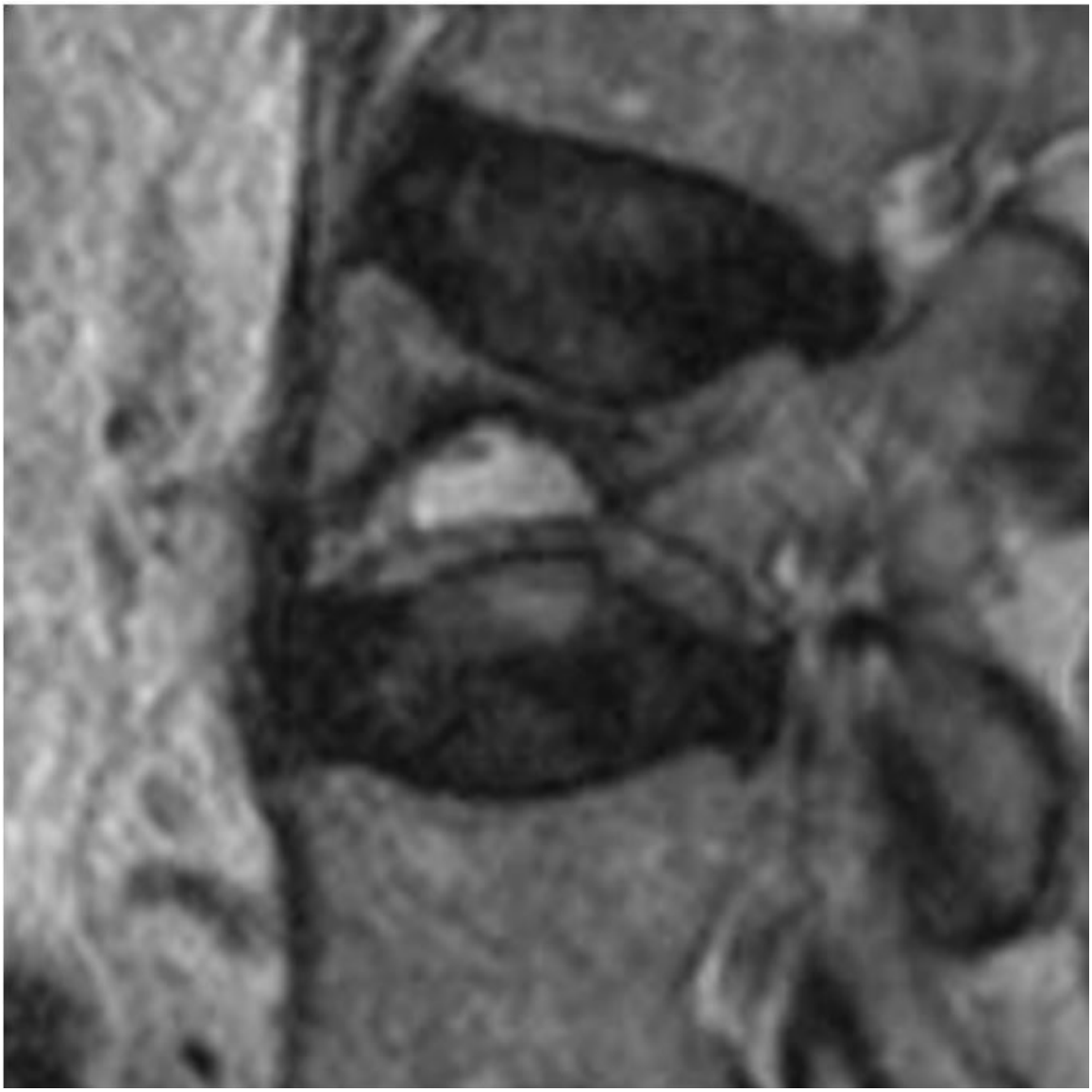

T2 MR image depicts ovoid intervening fluid signal within a large L2 fracture cleft.

Fluid sensitive MR demonstrates a T2 hypointense cement bolus with near circumferential T2 hyperintense fluid rim in keeping with non-union.

Podium #35

VARIABILITY IN PERCUTANEOUS PROCEDURES FOR VERTEBRAL OSTEOMYELITIS AMONG RADIOLOGISTS

Claus Simpfendorfer, MD; Hakan Ilaslan, MD
Cleveland Clinic, Cleveland, OH, USA
(Presented by: Claus Simpfendorfer, MD, Cleveland Clinic)

Purpose: To poll those radiologists who perform spine biopsies in regards to their decision-making and biopsy technique in attempt to identify and highlight the variability and inconsistencies between practices and individual radiologists.
Materials and Methods: Survey of SSR members who perform spinal procedures.
Results: A total of 88 SSR members responded to the survey. Of the respondents, 45 (51%) worked in an academic/university setting, 35 (40%) were private practice and 8 (9%) in a hybrid practice. The majority of respondents, 68%, were unaware of the 2015 Infectious Diseases Society of America (IDSA) guidelines for the diagnosis and treatment of vertebral osteomyelitis. CT was the preferred modality for image guidance used by 73%. Core biopsy or combination of core biopsy/FNA was performed by 86%, with a combination of the disc and endplate targeted for biopsy by 70%. Pathology specimen sent routinely by 75% of respondents and two or more samples obtained by 73%. Antibiotics are not routinely held by the majority of respondents, 65%, despite recommendation to hold antibiotics in IDSA guidelines. Most respondents will not perform biopsies of the cervical spine or aspirate epidural collections, 75% and 71% respectively. Only 11% of respondents will perform a therapeutic drainage or lavage of a lumbar epidural abscess for persistent bacteremia. Those respondents working in an academic setting were more likely to be aware of the IDSA guidelines and more likely to perform a biopsy in the cervical spine.
Conclusion: There is significant variation among radiologists prior to and during diagnostic biopsies for vertebral osteomyelitis despite the Infectious Diseases Society of America guidelines for the managemtn of vertebral osteomyelitis published in 2015. Additionally, the majority of radiologist will not biopsy the cervical spine in suspected cases of vertebral osteomyelitis or perform a therapeutic aspiration/lavage of a lumbar epidural abscess.

Modality % - Radiography / Fluoroscopy:	20
Modality % - CT:	80
Modality % - MRI:	0
Modality % - US:	0
Modality % - Nuclear Medicine:	0

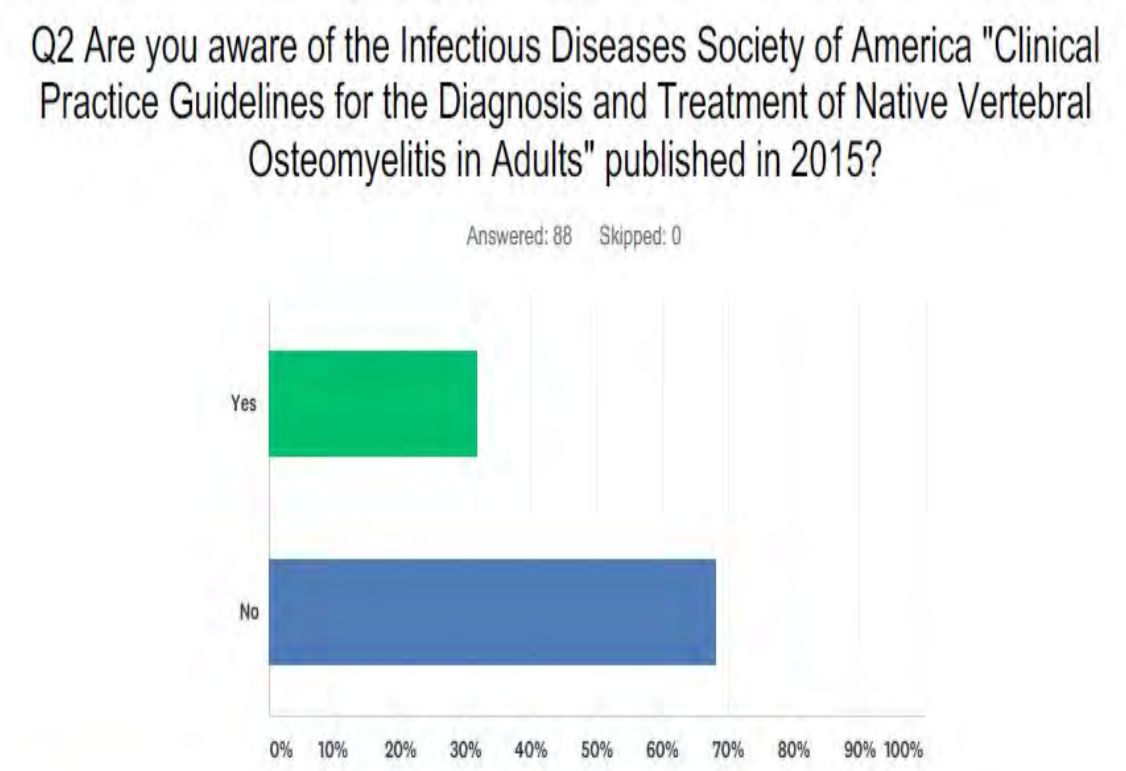

ANSWER CHOICES	RESPONSES	
Yes	31.82%	28
No	68.18%	60
TOTAL		88

Graph demonstrating the number of respondents aware of the Infectious Diseases Society of America (IDSA) guidelines for the diagnosis and treatment of vertebral osteomyelitis.

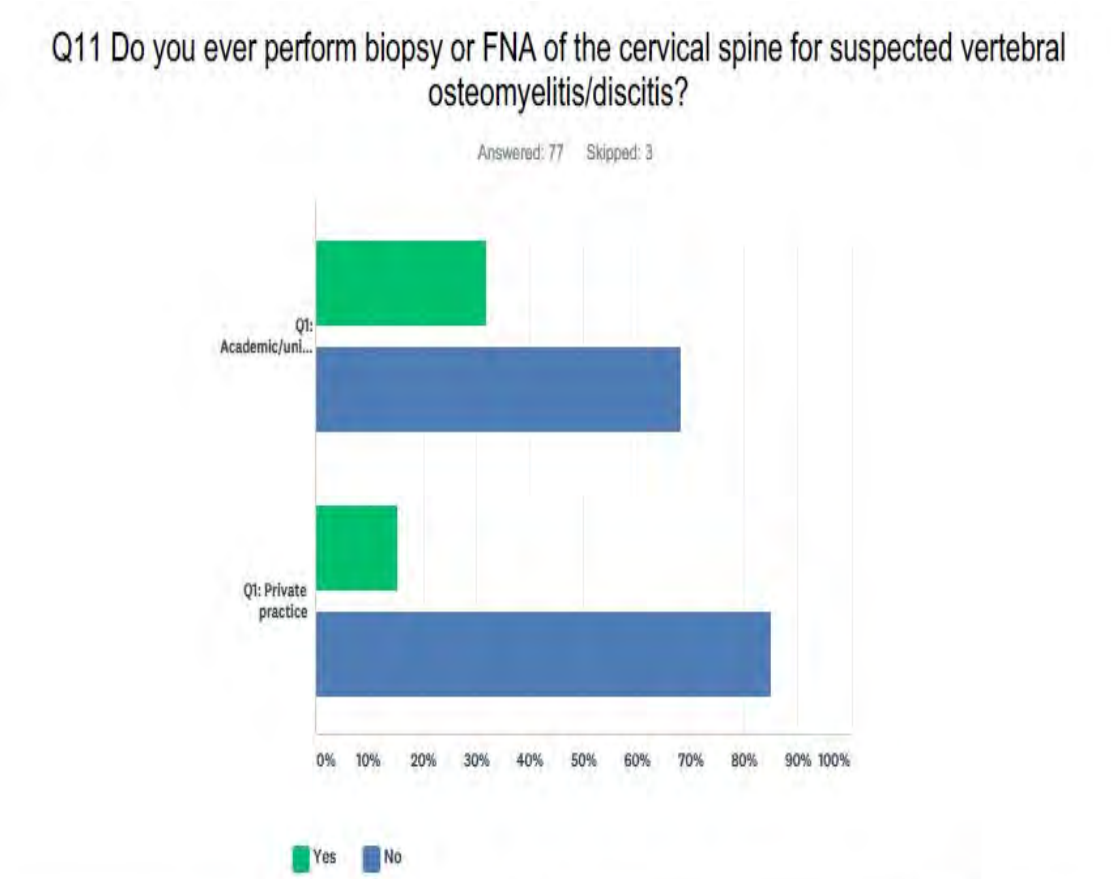

	YES	NO	TOTAL
Q1: Academic/university	31.82% 14	68.18% 30	57.14% 44
Q1: Private practice	15.15% 5	84.85% 28	42.86% 33
Total Respondents	19	58	77

Graph comparing the performance of cervical spine biopsies for vertebral osteomyelitis between radiologists working in an Academic/University setting versus private practice.

Podium #36

THE ROLE OF SARCOPENIA IN CLINICAL VERTEBRAL AUGMENTATION OUTCOMES

Amanda Crawford, MD; Michael Durst, MD; Corey Ho, MD; MK Jesse, MD; Debayan Bhaumik, MD
University of Colorado Denver, Aurora, CO, USA
(Presented by: Amanda Crawford, MD, University of Colorado Denver)

Purpose: Age related muscle deterioration (sarcopenia) has been implicated in detrimental changes in spinal biomechanics. With the high prevalence of vertebral body fractures in the elderly, it is important to investigate the role of sarcopenia as it relates to vertebral augmentation outcomes. The purpose of our study is to investigate this association.

Materials and Methods: With IRB approval, this study retrospectively reviews patients who underwent kyphoplasty or vertebroplasty at our institution from 2008 until 2017 for the treatment of thoracic or lumbar vertebral body fractures.

Analysis included assessment of sarcopenia by calculating the total psoas area (TPA) based on CT imaging. This was measured using the cross-sectional area of the psoas muscles at the level of L4. Other variables included: the rate of adjacent level fractures, the difference between pre-procedural and post-procedure pain scores, and the prescription of post-procedural pain medication and muscle relaxants.

Results: Initial exploratory analysis with a sample of 40 patients suggests there is a positive correlation between low pre-procedural sarcopenia values and the rate at which patients suffer an adjacent level fracture following kyphoplasty. Initial evaluation also suggests more reliable improvement in pain scores for patients with TPA in the immediate post-procedural period. Power and statistics to follow with the addition of ~230 more patients to our data set.

Conclusion: Predicting clinical outcomes in the treatment of thoracic and lumbar spinal fractures with vertebral augmention is an important part of treating our growing elderly population. Recognizing patients susceptible to adjacent level fracture not only improves our clinical management but may also influence the need for prophylactic fixation of adjacent levels. Improved prediction of expected pain may also assist in referral to other medical subspecialties including physical therapy and pain management.

Modality % - Radiography / Fluoroscopy:	0
Modality % - CT:	100
Modality % - MRI:	0
Modality % - US:	0
Modality % - Nuclear Medicine:	0

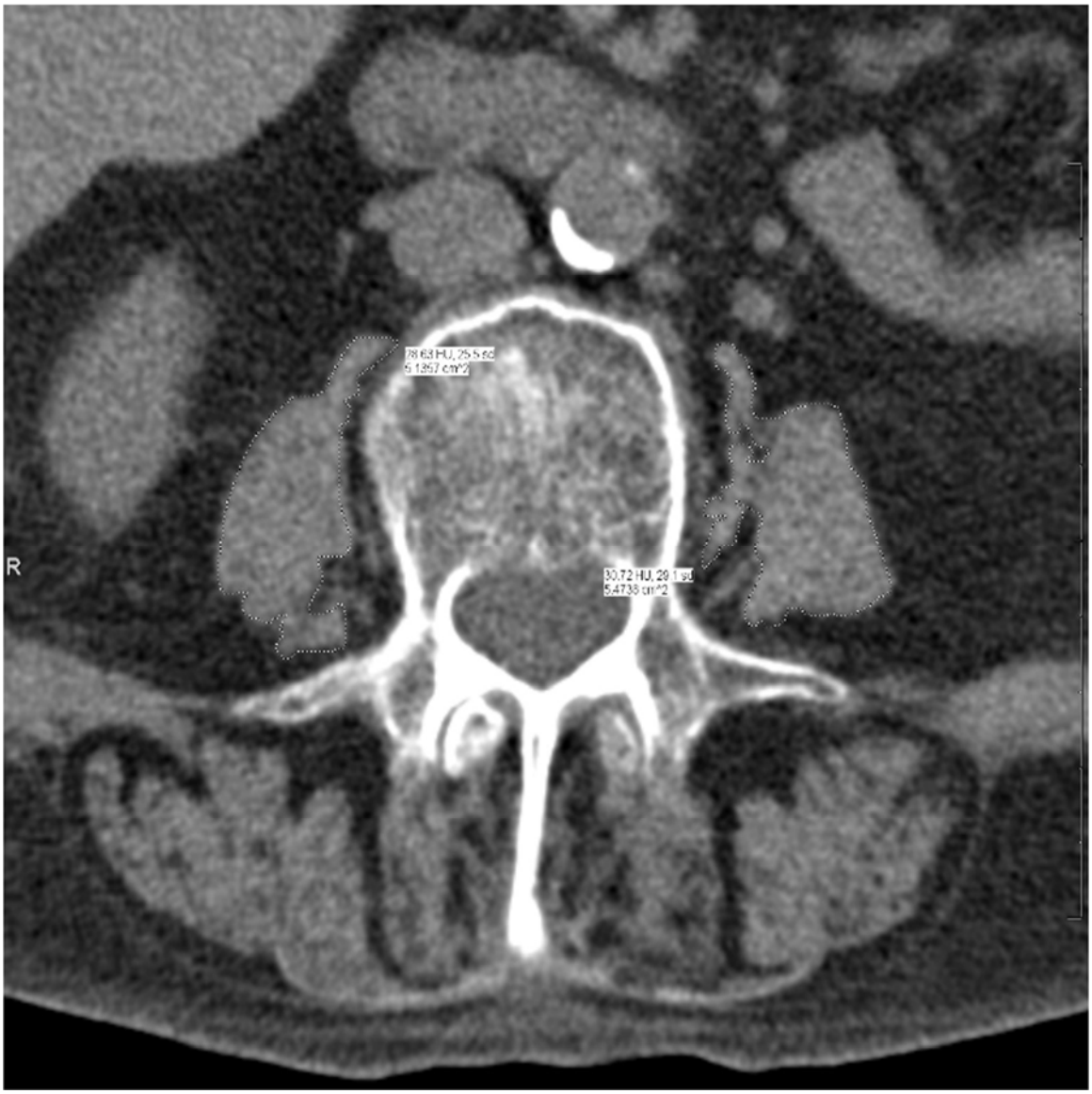

Measurement of sarcopenia using total psoas area (TPA) at the level of L4.

Podium #37

IS SPINAL MRI VALUABLE IN ADDITION TO MRI OF THE SACROILIAC JOINTS IN THE DIAGNOSIS OF SPONDYLOARTHRITIS?

STUBBS EUAN, MBChB; Rebello Ryan, MD; Raj Carmona, MD; George Ioannidis; Harish Srini, MD
McMaster University, Hamilton, ON, Canada
(Presented by: STUBBS EUAN, MBChB, McMaster University)

Purpose: To determine if MRI of the entire spine offers additive value to MRI of the sacroiliac joints in the imaging evaluation of patients referred with suspected spondyloarthritis.

Materials and Methods:

Retrospective study of 119 consecutive patients, over a 24 week period referred by rheumatologists for MRI evaluation for spondyloarthritis (SpA). All patients underwent MRI of the entire spine and sacroiliac joints. MRI examinations were separated into 'spine' and 'sacroiliac joint' components and were evaluated separately and as a combined set 2 months apart . Two staff radiologist readers were asked to answer the question 'Does the patient have spondyloarthritis?' and record their level of certainty in the diagnosis on a 5-point Likert scale. Differences in reader certainty in the diagnosis of SPA for spine, sacroiliac joints and combined evaluations were calculated using McNemar's test. Using final diagnosis by the rheumatologists as the gold standard, sensitivities and specificities for the diagnosis of SPA on MRI for each read, and absolute differences in sensitivity and specificity between evaluations were calculated.

Results:

The addition of MRI of the spine to MRI of the SIJs did not significantly improve radiologist certainty for the diagnosis of SpA (147/268 for combined read compared with 163/268 for SIJ read- p value of 0.07). Sensitivity and specificity for the diagnosis of SpA from combined read versus SIJ read demonstrated no absolute difference (p 0.07 to 1.0 and p 0.17-0.79 respectively).

Conclusion: MRI of the SIJs alone may be as effective as the combination of MRI SIJs and Spine in the diagnosis of SpA. MRI of the spine provided no significant benefit in reader certainty or diagnostic accuracy for the diagnosis of SpA.

Modality % - Radiography / Fluoroscopy:	0
Modality % - CT:	0
Modality % - MRI:	100
Modality % - US:	0
Modality % - Nuclear Medicine:	0

Podium #38

THE ROLE OF PARASPINAL EDEMA IN CLINICAL VERTEBRAL AUGMENTATION OUTCOMES

Michael Durst, MD; MK Jesse, MD; Amanda Crawford, MD; Corey Ho, MD; Debayan Bhaumik, MD
University of Colorado Denver, Denver, CO, USA
(Presented by: Michael Durst, MD, University of Colorado Denver)

Purpose: With high prevalence of vertebral body fractures in a growing elderly population, it is important to investigate preoperative factors affecting surgical outcomes of vertebral augmentation. The presence and degree of severity of paraspinal edema varies on preoperative MRIs obtained in surgical candidates for spinal fracture fixation. The purpose of our study is to investigate associations between pre-procedural paraspinal edema and reported pain scores in the post-procedural period.

Materials and Methods: With IRB approval, this study retrospectively reviews patients who underwent kyphoplasty or vertebroplasty at our institution from 2008 until 2017 for the treatment of thoracolumbar vertebral body fractures.

Paraspinal edema on MRI was scored by a musculoskeletal radiologist. Each patient was assigned an edema score from "0-3" based on an internally set standard. Variables included the patients' pain scores, obtained pre-procedure, immediately post-procedure, at post-procedural day 1, and in the following weeks (when available).

Results: Initial exploratory analysis suggests positive correlation between pre-procedural paraspinal edema and higher pre-procedural pain scores. Regardless of edema, patients report similar immediate post-procedural pain scores. On post-procedural day 1, the cohort with more paraspinous edema demonstrated a rebound increase in pain higher than their lower edema counterparts; while those with lower edema scores continued to improve. Pre-procedural, immediate post-procedural, and post-procedural day 1 scores averaged 7.1/10, 4.0/10, and 3.7/10 respectively in the lower edema group, while higher edema groups reported an average of 8.6/10, 3.8/10, and 6.4/10, respectively. Power and statistics to follow with addition of ~230 patients to our data set.

Conclusion: Predicting clinical outcomes in the treatment of thoracic and lumbar spinal fractures with vertebral augmentation is an important part of treating our growing elderly population. Improved diagnostic radiologic detection of factors predicting pain and peri-procedural course will improve our clinical management and help set realistic expectations for our patients.

Modality % - Radiography / Fluoroscopy:	0
Modality % - CT:	0
Modality % - MRI:	100
Modality % - US:	0
Modality % - Nuclear Medicine:	0

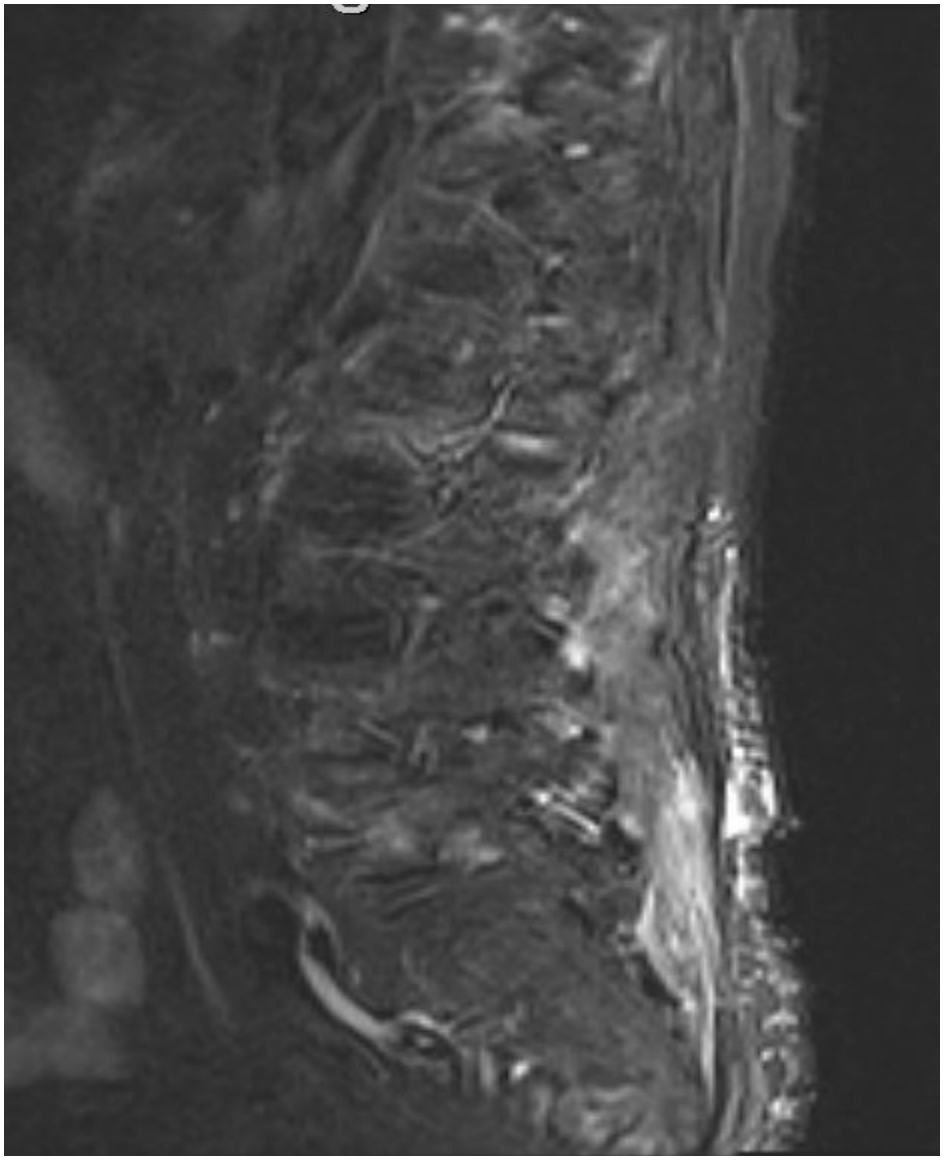

Example of paraspinal muscular edema in the setting of L4 and L5 vertebral body fractures.

Podium #39

TRANSPEDICULAR-TRANSDISCAL CEMENT AUGMENTATION TECHNIQUE FOR TREATMENT OF PROXIMAL JUNCTIONAL FAILURE OF SPINAL FUSION

Corey Ho, MD; MK Jesse, MD
University of Colorado Denver, Aurora, CO, USA
(Presented by: Corey Ho, MD, University of Colorado Denver)

Purpose: Spinal deformity often requires long instrumented fusion constructs for treatment. However, complications occur, including development of fracture and kyphosis at the junctional level between the fused and mobile spine. Proximal junction kyphosis (PJK), defined as a Cobb angle change >10-degrees from pre-operative measurement, has an incidence as high as 40%. Symptomatic PJK often requires revision surgery and hardware extension. Vertebral cement augmentation (VCA) can be performed prophylactically to prevent proximal junctional level failure but is not always performed. We report a single center experience using a novel percutaneous transdiscal technique to stabilize the proximal instrumentation and adjacent level in an attempt to treat hardware failure and avoid revision surgery.
Materials and Methods: Retrospective review of VCA was performed with selection of cases using transpedicular-transdiscal fluoroscopic technique to treat symptomatic proximal junctional failure. Worsening sagittal imbalance as well as fractures of the upper instrumented and proximal non-instrumented vertebrae were present. VCA of the proximal instrumented and adjacent level was performed using a percutaneous transdiscal approach. Pre-and post-procedure pain levels and sagittal balance measurements were obtained.
Results: 6 patients (2 women, 4 men), with average age of 71 years (range 58-82), underwent transpedicular-transdiscal VCA varying from the T3-T11 levels. Average pre-procedural pain was 7.2 out of 10 (range 0-10) with average pre-procedural sagittal imbalance of 9.1 cm (range 6.4-11.5). Average post-procedural pain level was 2.7 out of 10 (range 0-6) with average post-procedural sagittal imbalance of 7.7 cm (range 5.4-13.0). None of the patients experienced an increase in pain. All but one patient demonstrated a decrease in sagittal imbalance following the procedure. Revision surgery was not required for any case with average follow-up time of 14.6 months (range 8-21).

Conclusion: VCA can be performed utilizing transpedicular-transdiscal approach to treat proximal junctional level failure to provide stabilization, pain relief, and possible avoidance of revision surgery.

Modality % - Radiography / Fluoroscopy:	100
Modality % - CT:	0
Modality % - MRI:	0
Modality % - US:	0
Modality % - Nuclear Medicine:	0

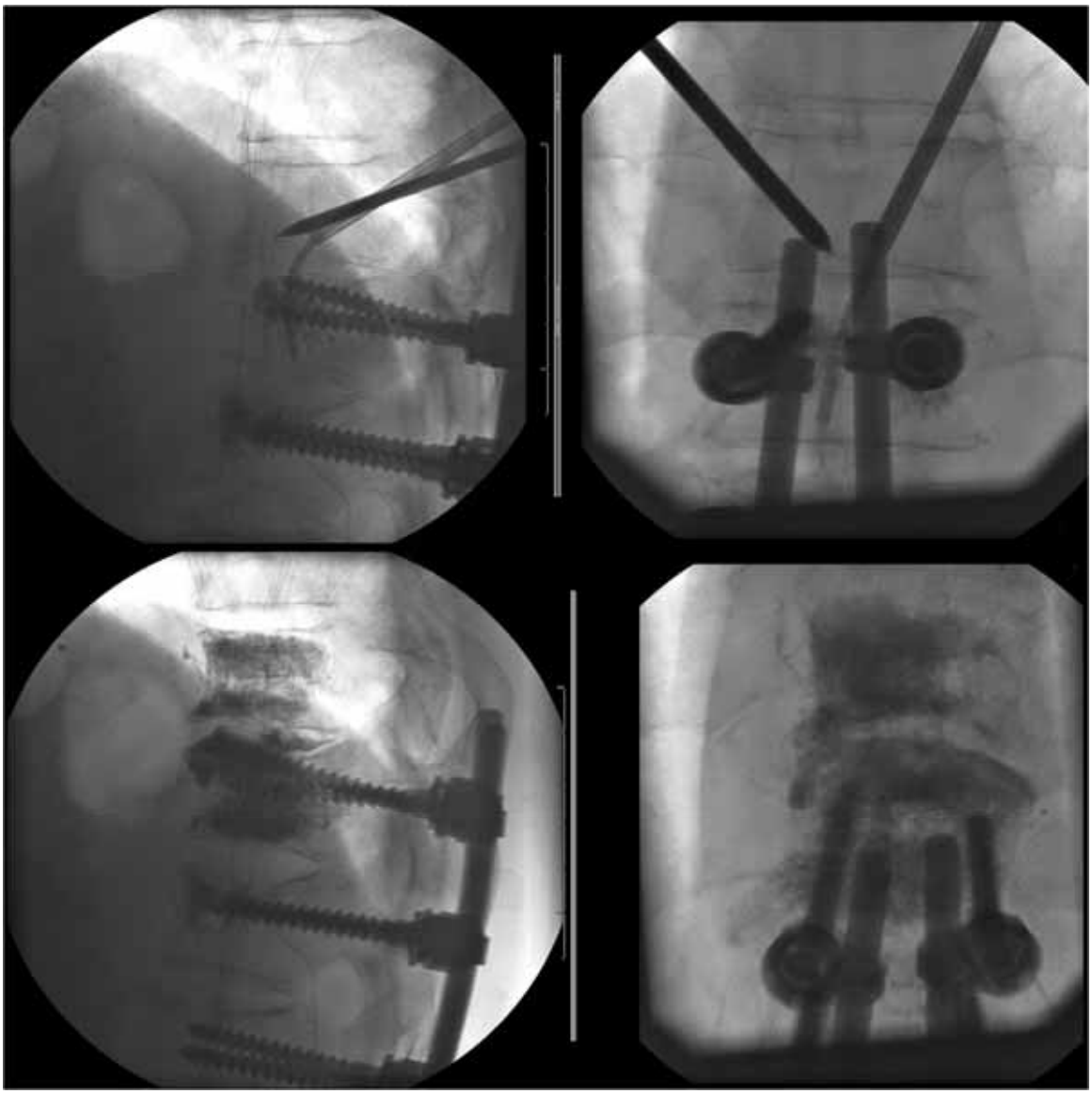

Fluoroscopic spot images demonstrate transpedicular-transdiscal approach with subsequent vertebral cement augmentation of the proximal instrumented and adjacent level.

Podium #40

MIDLINE INTERLAMINAR LUMBAR EPIDURAL INJECTIONS: INSTITUTIONAL EXPERIENCE SAFELY UTILIZING DEPO-MEDROL®.

Daniel Carr, MD; Damon Spitz, MD; Tal Rencus, MD; John Falardeau, MD; Sam Madoff, MD; Manisha Raythatha, MD
New England Baptist Hosp. Tufts University School of Med, Boston, MA, USA
(Presented by: Daniel Carr, MD, New England Baptist Hosp. Tufts University School of Med)

Purpose: Epidural steroid injection is a common procedure for treatment of low back pain with radiculopathy. Depo-Medrol® (Pfizer, methylprednisolone acetate), one formulation of particulate steroid, has come under scrutiny in the press, questioning its safety[1]. Although catastrophic complications[2] have been associated with paraspinal injection of particulate steroid, our data shows the formulation is safe when used via the midline interlaminar approach for lumbar epidural injections. We report our experience with this approach using Depo-Medrol® with the aim of evaluating its safety.

Materials and Methods: We retrospectively reviewed fluoroscopically guided interlaminar epidural lumbar spine injections at our institution. In just the last 10 years, 13,955 fluoroscopically guided, interlaminar lumber epidural injections with Depo-Medrol® were performed. Fluoroscopic images, reports, and patient records were reviewed for any significant related complications.

Results: Over 10 years, 13,955 patients underwent fluoroscopically guided interlaminar epidural steroid injection with Depo-Medrol®. No documented significant complications related to particulate steroid administration were identified.

Conclusion: Fluoroscopically guided lumbar spine epidural Depo-Medrol® injection is a safe procedure when utilizing the interlaminar approach.

Modality % - Radiography / Fluoroscopy:	90
Modality % - CT:	5
Modality % - MRI:	5
Modality % - US:	0
Modality % - Nuclear Medicine:	0

Podium #41

Fluoroscopically-guided lumbar spine interlaminar and transforaminal injections: incidence and location of inadvertent intravascular injection

Connie Chang, MD; Jad Husseini, MD
Mass General Hospital, Boston, MA, USA
(Presented by: Connie Chang, MD, Mass General Hospital)

Purpose: To prospectively evaluate the incidence of inadvertent intravascular injection for fluroscopically guided lumbar injections.

Materials and Methods: Our study was IRB-approved and HIPAA-compliant. 77 patients who presented for lumbar injection were prospectively enrolled. All injections were performed with fluoroscopic guidance using a 22 gauge spinal needle by either interlaminar or transforaminal approach. A minimum of 1 mL of iodinated contrast was injected under 15 frame/second live fluoroscopy to evaluate for intravascular flow. Patient demographics, history of surgery at the injected level or an adjacent lumbar level, injection side, site, and approach, and volume of contrast injected when blood vessels became visible were recorded. Chi-square comparison was performed to compare patient surgery and inadvertent intravascular injection.

Results: The patient cohort was 95 ± 14 (16-88) years old with 41 (53%) males and 36 (47%) females. There were 32 (42%) interlaminar and 45 (58%) transforaminal; 38 (52%) left and 39 (48%) right; 2 (3%) L1-L2, 9 (12%) L2-L3; 14 (14%) L3-L4; 26 (34%) L4-L5, 8 (10%) L5-S1, and 8 (10%) S1-S2 injections. For 17 (22%) patients, there had been surgery at the injected or adjacent lumbar level

There were 8 (10%) inadvertent intravascular injections, 1 (13%) interlaminar and 7 (87%) transforaminal. The blood vessels were visualized after 0.3 ± 0.2 (0.1-1) mL contrast was injected (the 1 mL was the interlaminar injection). A higher percentage of patients with inadvertent intravascular injection (6/8, 75%) had surgery at the injected level or an adjacent level, compared with patients without inadvertent intravascular injection (11/69, 16%) (P = 0.0001).

Conclusion: Inadvertent intravascular injection occurred in 10% of our lumbar injection cohort, and may be more common with transforaminal injection and at a level at or adjacent or prior surgery. Injection of adequate contrast volume and knowledge of vascular contrast patterns are important to avoid complications for lumbar injections.

Modality % - Radiography / Fluoroscopy:	100
Modality % - CT:	0
Modality % - MRI:	0
Modality % - US:	0
Modality % - Nuclear Medicine:	0

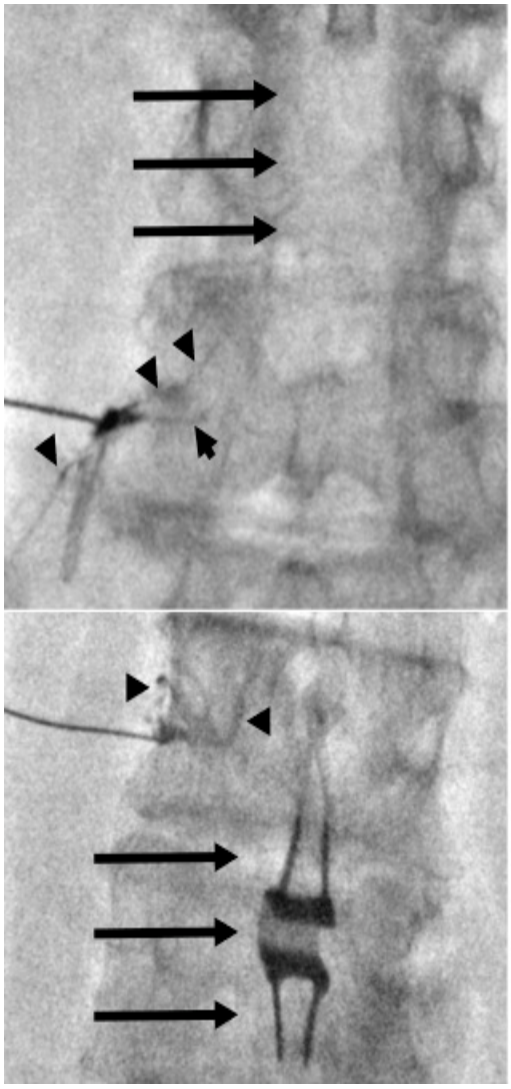

64 year old woman presenting for L5-S1 transforaminal injection. Fluoroscopic image demonstrates inadvertent vascular injection into both central and peripheral blood vessels (arrowheads). There has been laminectomy at the level above (arrows).

67 year old man presenting for L3-L4 transforaminal injection. Fluoroscopic image demonstrates inadvertent vascular injection into both central and peripheral blood vessels (arrowheads). There is an interlaminar stabilization device (arrows) at the same level.

Detailed caption on image. Two transforaminal injections with inadvertent intravascular contrast injection.

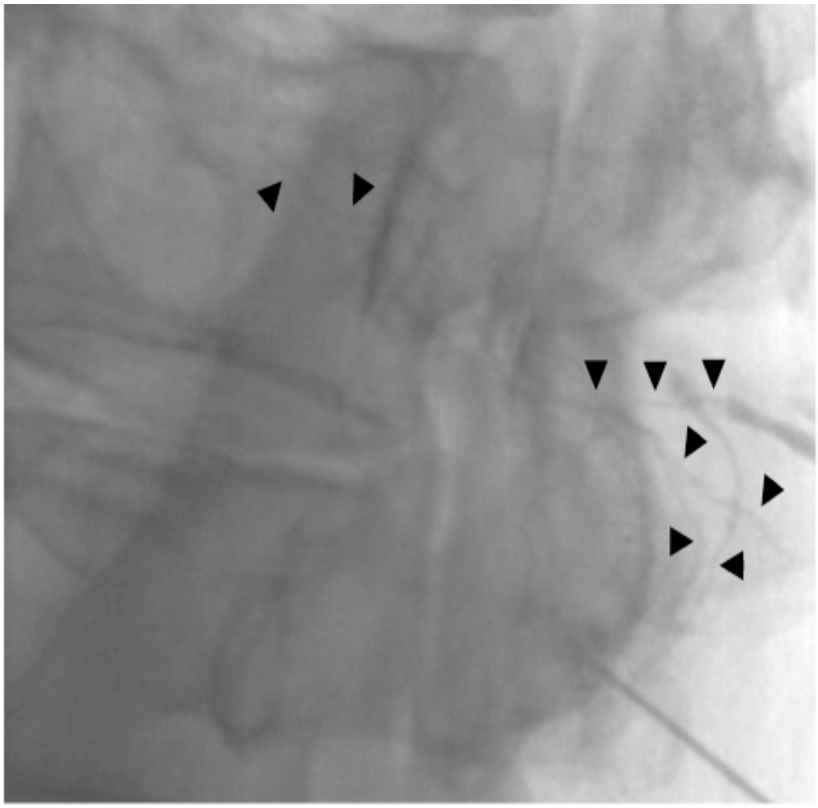

72 year old man presenting for L2-L3 interlaminar injection. Fluoroscopic image demonstrates inadvertent injection into both anterior and posterior blood vessels (arrowheads). There has been laminectomy from L3-S1 (not shown). 1 mL of contrast was injected before these vessels were visualized, compared with an average of 0.3 mL for the other inadvertent intravascular injections. The needle was repositioned multiple times, but the blood vessels could not be avoided and the procedure was aborted.

Detailed caption on image. One interlaminar injection with inadvertent intravascular contrast injection.

WEDNESDAY

Society of Skeletal Radiology

42nd Annual Meeting

March 10-13, 2019

Wednesday, March 13, 2019

7:00 a.m.–7:55 a.m. **Continental Breakfast**

7:00 a.m.–12:30 p.m. **Registration/Information Desk Open**

7:00 a.m.–10:30 a.m. **Exhibit Hall Open**

8:00 a.m.–10:00 a.m. **TUMOR/MARROW**

Moderators: Mark Kransdorf, MD, Doris Wenger, MD

8:00 a.m. #42 **CHARACTERIZATION OF INDETERMINATE LIPOMATOUS TUMORS: WHAT IS THE ADDED VALUE OF ADVANCED MRI SEQUENCES?**
Shivani Ahlawat, MD; Brett Shannon, MD; Adam Levin, MD; Carol Morris, MD; Laura Fayad, MD
Johns Hopkins University, Baltimore, MD, USA
(Presented by: Shivani Ahlawat, MD, Johns Hopkins University)

8:15 a.m. #43 **IMAGING FEATURES OF LIPOMATOUS TUMORS ON 18F-FDG PET/CT**
Francis Baffour, MD; Doris Wenger, MD; Stephen Broski, MD
Mayo Clinic, Rochester, MN, USA
(Presented by: Francis Baffour, MD, Mayo Clinic)

8:30 a.m. #44 **ROUND CELL COMPONENTS OF MYXOID LIPOSARCOMA: CAN WE IDENTIFY THESE CONCERNING AREAS ON IMAGING?**
Mariam Malik, MD[1]; Mark Murphey, MD[1]; Michael Shvarts, MD[1]; Lien Senchak, MD[2]; James Jelinek, MD[3]; Mark Kransdorf, MD[4]
[1]American Institute for Radiologic Pathology, Silver Spring, MD, USA; [2]Walter Reed National Military Medical Center, Bethesda, MD, USA; [3]MedStar Washington Hospital Center, Washington, DC, USA; [4]Mayo Clinic, Phoenix, AZ, USA
(Presented by: Mariam Malik, MD, American Institute for Radiologic Pathology)

8:45 a.m. #45 **ADVANCED MR IMAGING OF BONE MARROW: QUANTIFICATION OF T1-WEIGHTED AND T2-WEIGHTED DIXON SIGNAL ALTERATIONS OF RED MARROW, YELLOW MARROW AND PATHOLOGICAL BENIGN AND MALIGNANT MARROW LESIONS.**
Oganes Ashikyan, MD; Parham Pezeshk, MD; Avneesh Chhabra, MBBS, MD
University of Texas Southwestern Medical Center at Dallas, Dallas, TX, USA
(Presented by: Oganes Ashikyan, MD, University of Texas Southwestern Medical Center at Dallas)

9:00 a.m. #46 **MUSCULOSKELETAL (MSK) UTILIZATION AND PERFORMANCE OF WHOLE-BODY MRI (WBMRI) IN THE ADULT POPULATION**
Jacob Feldhaus, MD; Daniel Wessell, MD, PhD; Hillary Garner, MD; Joseph Bestic, MD; Jeffrey Peterson, MD; Anthony Wheeler, MD
Mayo Clinic Florida, Jacksonville, FL, USA
(Presented by: Jacob Feldhaus, MD, Mayo Clinic Florida)

9:15 a.m. #47 **OSTEOID OSTEOMAS OF THE HIP: A WELL-RECOGNIZED ENTITY WITH A PROCLIVITY FOR MISDIAGNOSIS**
Doris Wenger, MD; Meagan Tibbo, MD; Rafael Sierra, MD; Matthew Houdek, MD; Welch Tim, MD
Mayo Clinic, Rochester, MN, USA
(Presented by: Doris Wenger, MD, Mayo Clinic)

9:30 a.m. #48 **DESMOPLASTIC FIBROBLASTOMA: AN UNCOMMON SOFT TISSUE TUMOR WITH A RELATIVELY CHARACTERISTIC MR IMAGING APPEARANCE**
Maxine Kresse, MD; Mark Kransdorf, MD; Jonathan Flug, MD; Jeremiah Long, MD; Michael Fox, MD
Mayo Clinic, Phoenix, AZ, USA
(Presented by: Maxine Kresse, MD, Mayo Clinic)

9:45 a.m. #49 **RADIOMIC FEATURES EXTRACTED FROM T1 MRI DISTINGUISH MYXOMAS FROM MYXOFIBROSARCOMAS BETTER THAN IMAGE INTENSITY**
Teresa Martin-Carreras, MD; Ronnie Sebro, MD
Hospital of University of Pennsylvania, Philadelphia, PA, USA
(Presented by: Ronnie Sebro, MD, Hospital of University of Pennsylvania)

10:00 a.m.–10:05 a.m. **CASE OF THE DAY**
Presenting author: Kenneth Buckwalter, MD

10:05 a.m.–10:30 a.m. **Break - Visit the Exhibit Hall**

10:30 a.m.–12:30 p.m. **LOWER EXTREMITY**
Moderators: William Morrison, MD, Kate Stevens, MD, BS (hons)

10:30 a.m. #50 **"POSSIBLE" MENISCAL TEARS AT KNEE MRI: REVISITING THE SINGLE-TOUCH RULE**
Lindsay Stratchko, DO; Kenneth Lee, MD; Richard Kijowski, MD
University of Wisconsin Hospital & Clinics, Madison, WI, USA
(Presented by: Lindsay Stratchko, DO, University of Wisconsin Hospital & Clinics)

10:45 a.m. #51 **COMPARING CLINICAL AND SEMI-QUANTITATIVE CARTILAGE GRADING IN PREDICTING OUTCOMES AFTER ARTHROSCOPIC PARTIAL MENISCECTOMY**
Naveen Subhas, MD, MPH[1]; Ceylan Colak, MD[1]; Joshua Polster, MD[1]; Nancy Obuchowski, PhD[1]; Morgan Jones, MD, MPH[1]; Greg Strnad[1]; Soterios Gyftopoulos, MD, MS[2]; Kurt Spindler, MD[1]
[1]Cleveland Clinic, Cleveland, OH, USA; [2]NYU Medical Center/ Hospital for Joint Diseases Langone Medical Center, New York, NY, USA
(Presented by: Naveen Subhas, MD, MPH, Cleveland Clinic)

11:00 a.m. #52 **DOWNSTREAM COSTS ASSOCIATED WITH INCIDENTAL CARTILAGE LESIONS DETECTED ON RADIOGRAPHS**
Paul-Michel Dossous, MD; Tatiane Rodrigues, MD; William Walter, MD; Michelle Lam, BA; Mohammad Samim, MD; Xi Xue, MD; Andrew Rosenkrantz, MD; Soterios Gyftopoulos, MD
NYU Medical Center/ Hospital for Joint Diseases Langone Medical Center, New York, NY, USA
(Presented by: Paul-Michel Dossous, MD, NYU Medical Center/ Hospital for Joint Diseases Langone Medical Center)

11:15 a.m. #53 **CAN PREOPERATIVE MR IMAGING FINDINGS PREDICT EARLY FAILURE FOLLOWING ANTERIOR CRUCIATE LIGAMENT RECONSTRUCTION?**
Jenny Bencardino, MD; Michele Mastio, MD; Alejandra Duarte, MD; Laith Jazrawi, MD; Jose Raya, PhD
NYU Medical Center/ Hospital for Joint Diseases Langone Medical Center, New York, NY, USA
(Presented by: Jenny Bencardino, MD, NYU Medical Center/ Hospital for Joint Diseases Langone Medical Center)

11:30 a.m. #54

RUPTURE OF THE ANTEROLATERAL LIGAMENT IN COMPLETE ACUTE TRAUMATIC ANTERIOR CRUCIATE LIGAMENT TEAR: NEW INSIGHTS INTO ACUTE PIVOT SHIFT TRAUMA TO THE KNEE.

Jenny Bencardino, MD; Michele Mastio, MD; Alejandra Duarte, MD; Laith Jazrawi, MD; Jose Raya, PhD
NYU Medical Center/ Hospital for Joint Diseases Langone Medical Center, New York, NY, USA
(Presented by: Jenny Bencardino, MD, NYU Medical Center/ Hospital for Joint Diseases Langone Medical Center)

11:45 a.m. #55

ULTRASOUND SHEAR WAVE ELASTOGRAPHY (SWE) OF THE TIBIALIS POSTERIOR TENDON (PTT) AND TIBIOSPRING/SPRING LIGAMENTS AT REST AND STRESS IN NORMAL FEET COMPARED TO ASYMPTOMATIC AND SYMPTOMATIC ACQUIRED FLATFOOT DEFORMITY

Mihra Taljanovic, MD, PhD[1]; Wonsuk Kim, MD[2]; Chelsea Caruso, MD[1]; Elizabeth Krupinski, PhD[3]; Andres Nuncio Zuniga, BSN[1]; L. Latt, MD, PhD[1]
[1]University of Arizona HCS - Tucson, Tucson, AZ, USA; [2]Beth Israel Deaconess Medical Center Harvard Med School, Boston, MA, USA; [3]Emory University Dept. of Radiology, MSK Division, Atlanta, GA, USA
(Presented by: Mihra Taljanovic, MD, PhD, University of Arizona HCS - Tucson)

12:00 p.m. #56

REDUCTION OF UNNECESSARY REPEAT KNEE RADIOGRAPHS DURING OSTEOARTHRITIS FOLLOW UP VISITS IN A LARGE TEACHING MEDICAL CENTER.

Oganes Ashikyan, MD; Dustin Buller, BS; Parham Pezeshk, MD; Majid Chalian, MD; Avneesh Chhabra, MD
University of Texas Southwestern Medical Center at Dallas, Dallas, TX, USA
(Presented by: Oganes Ashikyan, MD, University of Texas Southwestern Medical Center at Dallas)

12:15 p.m. #57

LATERAL FEMORAL CONDYLE INSUFFICIENCY FRACTURES: ASSOCIATED MORPHOLOGICAL FINDINGS

Adam Zoga, MD, MDA[1]; Terence Farrell, MD, MRCPI, FFRRCSI, FRCRUK[2]; Kristen McClure, MD[1]; Diane Deely, MD[1]
[1]Thomas Jefferson University Hospital, Philadelphia, PA, USA; [2]Jefferson Radiology Musculoskeletal Radiology Fellowship, Philadelphia, PA, USA
(Presented by: Adam Zoga, MD, MDA, Thomas Jefferson University Hospital)

Related ePosters

TUMOR / MARROW

Poster #28 **B-CELL PERIPHERAL NEUROLYMPHOMATOSIS: MRI AND 18F-FDG PET/CT IMAGING CHARACTERISTICS**
Stephen Broski, MD; Anthony DeVries, MD; Benjamin Howe, MD; Robert Spinner, MD
Mayo Clinic, Rochester, MN, USA

Poster #29 **FRIENDLY FAT MASQUERADING AS AN AGGRESSIVE FOE ON PLAIN RADIOGRAPHY: A CASE SERIES**
Bhumin Patel, MD; Douglas Mintz, MD
Hospital for Special Surgery, New York, NY, USA

Poster #30 **INTRANEURAL LIPOMA: A CASE SERIES**
Christin Tiegs-Heiden, MD; Katarina Glazebrook, MB, ChB; Matthew Frick, MD; Tara Anderson, MD; Robert Spinner, MD; Kimberly Amrami, MD
Mayo Clinic, Rochester, MN, USA

Poster #31 **POPLITEAL LYMPH NODES IN PATIENTS WITH OSTEOSARCOMA: ARE THEY METASTATIC?**
Shivani Ahlawat, MD; Mark Cleary, MD; Laura Fayad, MD
Johns Hopkins University, Baltimore, MD, USA

Poster #32 **SCAPULAR AND PERISCAPULAR LESIONS: WHAT THE RADIOLOGIST NEEDS TO KNOW**
Terence Farrell, MD, MRCPI, FFRRCSI, FRCRUK[1]; Kristen McClure, MD[2]; DIane Deely, MD[2]; Adam Zoga, MD, MBA[2]
[1]Jefferson Radiology Musculoskeletal Radiology Fellowship, Philadelphia, PA, USA; [2]Thomas Jefferson University Hospital, Philadelphia, PA, USA

Poster #33 **IMAGING OF EPITHELIOID SARCOMA WITH PATHOLOGIC CORRELATION**
Mariam Malik, MD[1]; James Jelinek, MD[2]; Mark Kransdorf, MD[3]; Mark Murphey, MD[1]
[1]American Institute for Radiologic Pathology, Silver Spring, MD, USA; [2]MedStar Washington Hospital Center, Washington, DC, USA; [3]Mayo Clinic, Phoenix, AZ, USA

LOWER EXTREMITY

Poster #34 **WITHDRAWN**

Poster #35 **CURRENT CONCEPTS IN FOOT AND ANKLE TRAUMA: IMAGING FEATURES, HARDWARE AND COMPLICATIONS**
Zachary Ashwell, MD, MS; Hyo-Jeong Mulcahy, MD; Felix Chew, MD
University of Washington / Harborview Medical Center, Seattle, WA, USA

Poster #36 **IMAGING EVALUATION OF HEEL PAIN**
Sailaja Yadavalli, MD, PhD; Onowenerhi Omene, MD
Beaumont Health System, Royal Oak, MI, USA

Poster #37 **COMMUNICATION BETWEEN THE NAVICULOCUNEIFORM AND SECOND AND THIRD TARSOMETATARSAL ARTICULATIONS: UNDERAPPRECIATED NORMAL ANATOMY AND HOW IT MAY IMPACT FLUOROSCOPIC GUIDED INJECTIONS**
Barry Hansford, MD[1]; Megan Mills, MD[2]; Sarah Stilwill, MD[2]; Anna McGow, MD[2]; Chris Hanrahan, MD, PhD[2]
[1]Oregon Health Sciences University, Portland, OR, USA; [2]University of Utah Medical Center / SOM, Salt Lake City, UT, USA

Poster #38 **ADDED BENEFIT OF KNEE MRI VERSUS RADIOGRAPHS ALONE IN PATIENTS 60 YEARS AND OLDER**

Michael Fox, MD, MBA, FACR[1]; Jeremiah Long, MD[1]; Mark Kransdorf, MD[1]; Jonathan Flug, MD[1]; Ashtyn Chamberland[2]; Adam Schwartz, MD[1]
[1]Mayo Clinic Arizona, Phoenix, AZ, USA; [2]Grand Canyon University, Phoenix, AZ, USA

Poster #39 **ROUTINE KNEE MRI: HOW COMMON ARE PERIPHERAL NERVE ABNORMALITIES?**

Shivani Ahlawat, MD; Laura Fayad, MD
Johns Hopkins University, Baltimore, MD, USA

Poster #40 **INCIDENCE AND SPECIFICITY OF INTRALESIONAL FAT GLOBULES WITHIN MOREL-LAVALLEE LESIONS ABOUT THE KNEE**

Justin Friske, MD; Stephen Broski, MD
Mayo Clinic, Rochester, MN, USA

Poster #41 **MULTIMODAL IMAGING OF ACUTE TRAUMATIC BONE MARROW LESIONS IN THE KNEE: NEW INSIGHTS WITH HIGH RESOLUTION PERIPHERAL QUANTITATIVE CT**

Richard Walker, MD[1]; Andres Kroker, MS[2]; Mariya Shtil[2]; Sarah Manske, MS, PhD[1]; Nicholas Mohtadi, MD, MS[3]; Steven Boyd, MS, PhD[1]
[1]Department of Radiology, Cumming School of Medicine, University of Calgary, Calgary, AB, Canada; [2]University of Calgary, Calgary, AB, Canada; [3]University of Calgary Sport Medicine Centre, Calgary, AB, Canada

Poster #42 **EFFECT OF PATELLAR INSTABILITY ON EXTENSOR MECHANISM DYSFUNCTION**

Jehan Ghany, MD; Vishal Desai, MD; William Morrison, MD; Johannes Roedl, MD, PhD; Jeffrey Belair, MD; Adam Zoga, MD
Thomas Jefferson University Hospital, Philadelphia, PA, USA

Poster #43 **THE ANTERIORLY DISPLACED ACL STUMP: A FREQUENT FINDING BUT UNCOMMON CAUSE FOR A "LOCKED KNEE"**

Richard Walker, MD[1]; Andres Kroker, MS[2]; Peter Salat, MD[1]; Nicholas Mohtadi, MD, MS[3]
[1]Department of Radiology, Cumming School of Medicine, University of Calgary, Calgary, AB, Canada; [2]University of Calgary, Calgary, AB, Canada; [3]University of Calgary Sport Medicine Centre, Calgary, AB, Canada

Poster #44 **REDUCING UNNECESSARY KNEE MRI IN PATIENTS WITH KNOWN OSTEOARTHRITIS**

Dorian Nobbee, MD
University of Calgary, Calgary, AB, Canada

Podium #42

CHARACTERIZATION OF INDETERMINATE LIPOMATOUS TUMORS: WHAT IS THE ADDED VALUE OF ADVANCED MRI SEQUENCES?

Shivani Ahlawat, MD; Brett Shannon, MD; Adam Levin, MD; Carol Morris, MD; Laura Fayad, MD
Johns Hopkins University, Baltimore, MD, USA
(Presented by: Shivani Ahlawat, MD, Johns Hopkins University)

Purpose: To evaluate the added value of dynamic contrast enhancement(DCE), diffusion weighted imaging(DWI), and chemical shift imaging(CSI) to a routine MRI protocol for the characterization of indeterminate lipomatous tumors.
Materials and Methods: In this HIPAA compliant, IRB approved study, two musculoskeletal radiologists retrospectively reviewed pre-procedure MRI of 32 histologically proven indeterminate lipomatous tumors. MRI included fluid-sensitive, CSI, DWI (b-values 50, 400, 800 s/mm^2), pre- and post-contrast T1-weighted and DCE (7-second time resolution) sequences. MRI studies were reviewed for tumor septations, nodules, early arterial enhancement by DCE, apparent diffusion coefficient (ADC) values of the tumor and largest nodule, and CSI signal-loss on opposed-phase compared with in-phase sequences. Radiologist diagnosis (lipoma, lipoma variant, atypical lipomatous tumors(ALT) or dedifferentiated liposarcomas(DDLPS)) was recorded after review of imaging in 3 sessions: 1) T1/fluid-sensitive sequences, 2) with addition of post-contrast T1, and 3) with addition of DCE, DWI and CSI sequences. Histology was the diagnostic gold standard. Descriptive statistics and diagnostic accuracy were reported.
Results: All tumors without thick septations were lipomas, and 12/13 tumors with nodules >1cm were ALT or DDLPS. For lipomas, variants, ALT, and DDLPS, respectively: early arterial enhancement was present in 0/14(0%), 1/4(25%), 1/5 20%), and 5/6(83%); average tumor ADC values were 0.3, 0.9, 1.2, and 0.9; CSI signal loss >20% was present in 4/13(31%), 3/4(75%), 6/7(86%), and 6/6(100%). The radiologist's interpretation accuracy using pre-contrast, post-contrast, and functional/CSI sequences, respectively, was 6/6(100%), 6/6(100%) and 6/6(100%) for lipomas; 0/2(0%), 0/1(0%), and 0/2(0%) for lipoma variants; 5/15(33%), 5/16(32%), and 5/15(33%) for ALT; and 5/9(56%), 5/9(56%), and 5/9(56%) for DDLPS.
Conclusion: Diagnostic interpretation for indeterminate lipomatous tumors is not changed by the addition of contrast or functional imaging with DCE or DWI, as thick septations and large nodules are important to differentiating low grade (lipoma/variants) from higher grade lesions (ALT/DDLPS). However, DCE has the potential to distinguish DDLPS from ALT.

Modality % - Radiography / Fluoroscopy:	0
Modality % - CT:	0
Modality % - MRI:	100
Modality % - US:	0
Modality % - Nuclear Medicine:	0

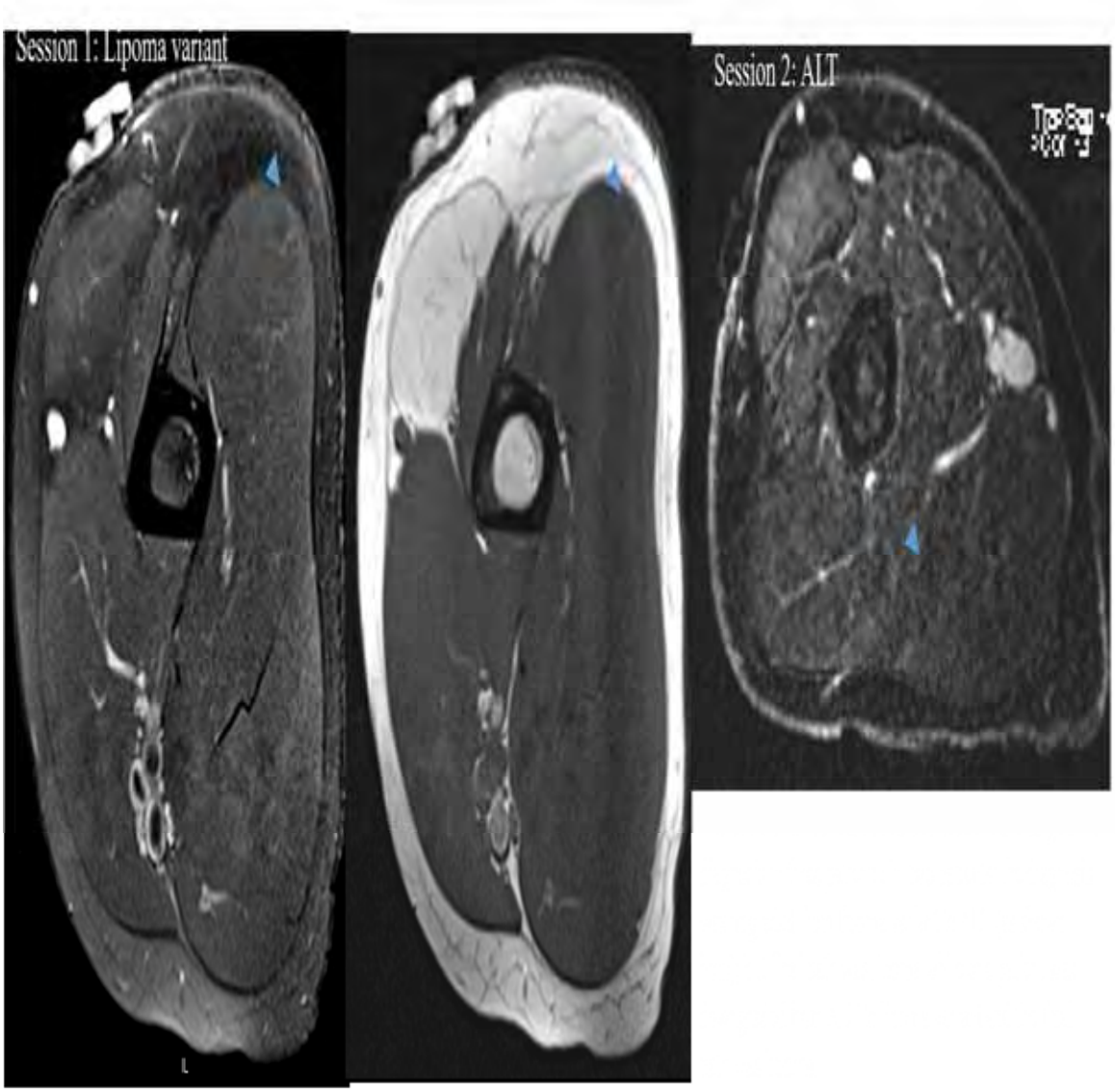

Diagnostic interpretation for indeterminate lipomatous tumors is not changed by the addition of contrast or functional imaging with CSI, DCE or DWI,

Podium #43

IMAGING FEATURES OF LIPOMATOUS TUMORS ON 18F-FDG PET/CT

Francis Baffour, MD; Doris Wenger, MD; Stephen Broski, MD
Mayo Clinic, Rochester, MN, USA
(Presented by: Francis Baffour, MD, Mayo Clinic)

Purpose: To evaluate the ^{18}F-FDG PET/CT characteristics of benign and malignant lipomatous tumors.
Materials and Methods: Patients undergoing ^{18}F-FDG PET/CT from 01/2005 to 03/2018 with pathologically-confirmed lipomatous tumors were retrospectively reviewed. 13 lipomas, 5 hibernomas, 16 well-differentiated liposarcomas (WDL), 16 dedifferentiated liposarcomas (DDL), 15 mxyoid liposarcomas (ML), and 2 pleomorphic liposarcomas (PL) were included, and multiple imaging features were analyzed.
Results: There were 67 patients (44M, 23F; mean age 58.8±13.6 years). Mean SUVmax of lipomas was 0.8 ± 0.2, WDL 2.3 ± 1.2, ML 3.0 ± 1.0, hibernomas 11.9 ± 8.4, PL 13.5 ± 2.9, and DDL 16.3 ± 11.4. SUVmax was not significantly different between lipomas and WDL ($p = 0.52$), lipomas and ML ($p = 0.35$), or WDL and ML ($p = 0.75$). SUVmax was also similar between hibernomas and DDL ($p = 0.16$), hibernomas and PL ($p = 0.76$), and DDL and PL ($p = 0.53$). Overall, SUVmax was not significantly different between benign (3.9 ± 6.5) and malignant (7.6 ±9.2) tumors, $p = 0.13$, but high-grade liposarcomas were more hypermetabolic than low grade liposarcomas (SUVmax 12.8 ± 10.8 vs. 2.5 ±1.2, $p = 0.0001$). Hibernomas and WDL had similar CT attenuation (-60.9 ± 21.0 vs. -49.3 ±37.9 HU, $p=0.31$), but hibernomas had higher SUVmax (11.9 ± 8.4 vs. 2.3 ± 1.2, $p = 0.0033$). 10/13 (76.9%) lipomas were superficially located, while 47/54 (87.0%) of other subtypes were deep ($p < 0.0001$). DDL were significantly larger than hibernomas ($p = 0.026$) and lipomas ($p = 0.005$); otherwise there were no significant volume differences.
Conclusion: There is no significant difference in metabolic activity between benign and malignant lipomatous tumors, but FDG PET/CT can differentiate between high and low-grade liposarcomas. In some cases, a combination of metabolic activity and CT morphology can distinguish between lipomatous tumor subtypes.

Modality % - Radiography / Fluoroscopy:	0
Modality % - CT:	50
Modality % - MRI:	0
Modality % - US:	0
Modality % - Nuclear Medicine:	50

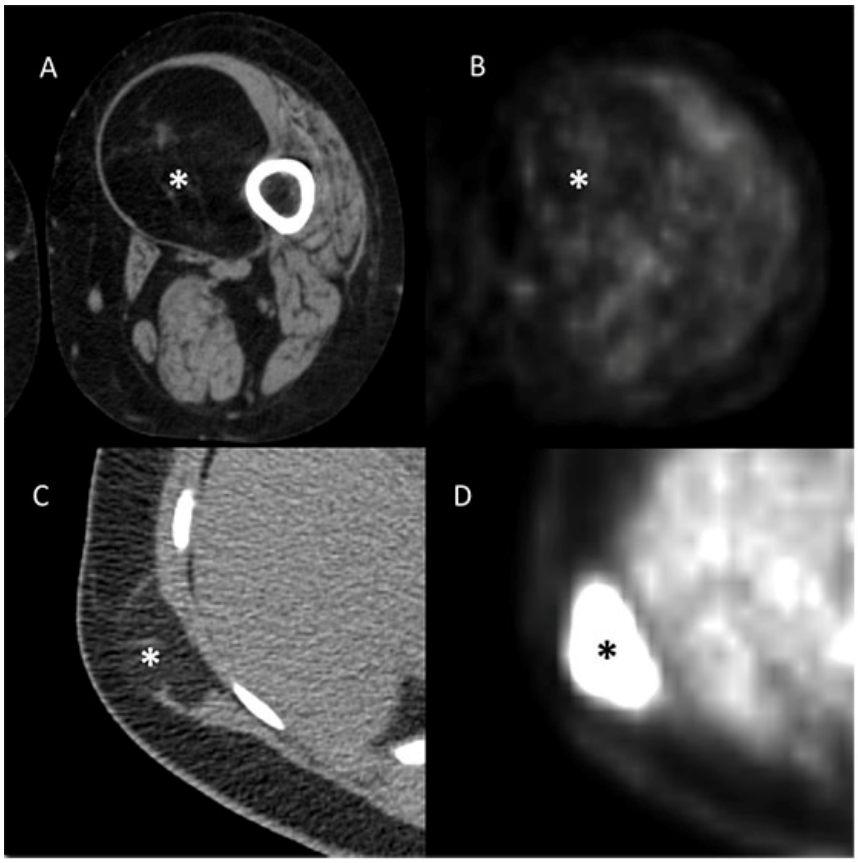

Axial PET/CT images of a WDLS (A,B) and hibernoma (C, D) showing overlapping CT appearance, but sharply contrasting metabolic activity, allowing differentiation between these tumors.

Podium #44

ROUND CELL COMPONENTS OF MYXOID LIPOSARCOMA: CAN WE IDENTIFY THESE CONCERNING AREAS ON IMAGING?

Mariam Malik, MD[1]; Mark Murphey, MD[1]; Michael Shvarts, MD[1]; Lien Senchak, MD[2]; James Jelinek, MD[3]; Mark Kransdorf, MD[4]
[1]American Institute for Radiologic Pathology, Silver Spring, MD, USA; [2]Walter Reed National Military Medical Center, Bethesda, MD, USA; [3]MedStar Washington Hospital Center, Washington, DC, USA; [4]Mayo Clinic, Phoenix, AZ, USA
(Presented by: Mariam Malik, MD, American Institute for Radiologic Pathology)

Purpose: To determine whether pathologically confirmed round cell components of myxoid liposarcoma representing higher grade regions can be detected on imaging.
Materials and Methods: We retrospectively reviewed 22 pathologically confirmed cases of myxoid liposarcoma with round cell components. Studies were reviewed by three musculoskeletal radiologists with agreement by consensus and included radiographs (n=11), CT (n=9), and MRI (n=20). Evaluation included patient history, demographics, lesion size, location, character of intralesional fat, and intrinsic characteristics on CT and MRI. Higher grade round cell components were seen as foci of higher attenuation or mildly high T1 or low T2 signal or focal enhancement.
Results: Average patient age was 51 years, with male predominance (59%). Symptoms included swelling, enlarging mass (100%), and pain (9%). Most commonly tumors were Intermuscular (59%), found in the thigh (75%). The average lesion measured 7.8 x 8.7 x 14.6 cm. Radiographs demonstrate soft tissue mass or fullness (91%). On CT, all tumors were well defined, containing fat (89%), although less than 10% fat by volume (100%). On MRI, all tumors were well defined and the majority were heterogeneously hypo- or isointense to muscle (88%) on T1 weighted imaging. Tumors demonstrated heterogeneously high or intermediate (83%) T2 signal. Hemorrhage was identified in 12%, and fat in 70% of tumors (70%), most commonly less than 10% of neoplasm volume (92%). Areas suggesting round cell components were seen on CT in 11% of cases and MR in 55% of cases.
Conclusion: A significant round cell component within myxoid liposarcoma, representing high grade foci, may commonly be identified on MR (55%). These are seen as foci of increased T1 or decreased T2 signal, or diffuse focal enhancement relative to the myxoid regions of the lesion. These components are important to detect and target at biopsy as they are associated with worsened prognosis and may alter therapy.

Modality % - Radiography / Fluoroscopy:	20
Modality % - CT:	10
Modality % - MRI:	70
Modality % - US:	0
Modality % - Nuclear Medicine:	0

Lateral radiograph of the leg demonstrates nonspecific fullness in the calf.

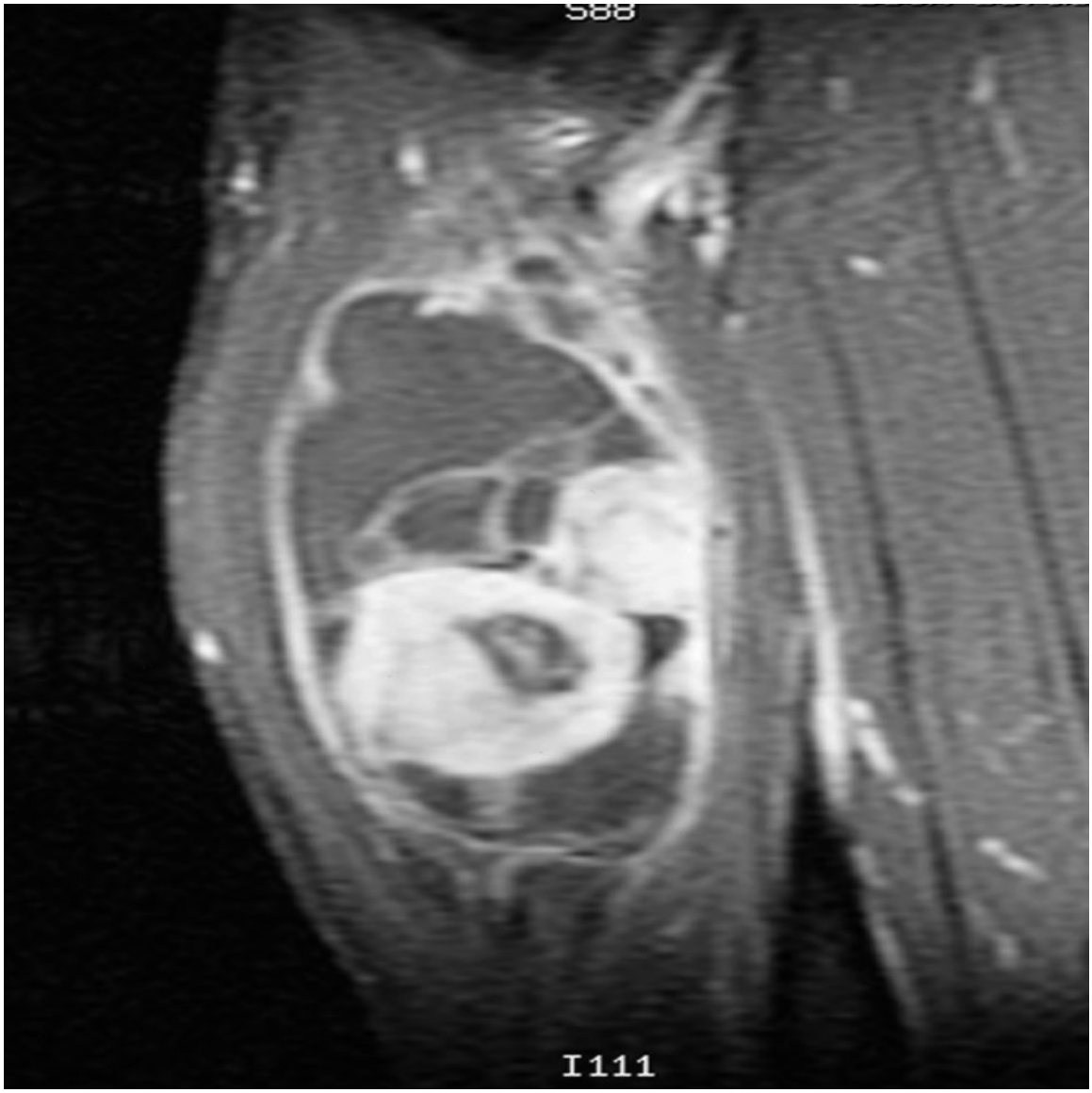

Post contrast T1 weighted image demonstrates diffuse focal enhancement within the mass.

Podium #45

ADVANCED MR IMAGING OF BONE MARROW: QUANTIFICATION OF T1-WEIGHTED AND T2-WEIGHTED DIXON SIGNAL ALTERATIONS OF RED MARROW, YELLOW MARROW AND PATHOLOGICAL BENIGN AND MALIGNANT MARROW LESIONS.

Oganes Ashikyan, MD; Parham Pezeshk, MD; Avneesh Chhabra, MBBS, MD
University of Texas Southwestern Medical Center at Dallas, Dallas, TX, USA
(Presented by: Oganes Ashikyan, MD, University of Texas Southwestern Medical Center at Dallas)

Purpose: T2-weighted (W) Dixon imaging is being frequently used in musculoskeletal MRI. Despite the advantages of T2W Dixon in producing both fat- and fat-suppressed contrasts, the changes in signal intensity of yellow marrow, red marrow, benign and malignant lesions have not been characterized and it is not known whether the T2W Dixon imaging performs like T1W chemical shift imaging (current gold standard) in separating reactive marrow from lesions.

Materials and Methods: Patient demographics and final diagnoses were recorded (77 controls, 64 lesions—33 benign, 31 malignant). For controls, fixed 2 cm^2 ROI were drawn by two readers independently at L5 vertebra, bilateral ilium and femurs on in-phase and out-of-phase T1W and T2W Dixon images. For lesions, best fit ROI were drawn. Fat fractions on T2W Dixon images were calculated and compared. Inter-reader analysis was performed and decision model was generated.

Results: Yellow marrow exhibited significantly lower fat fraction loss as compared to red marrow on T1W and T2W Dixon imaging at all locations ($p < 0.0001$) except at L5 on T2W Dixon ($p = 0.206$). Both benign and malignant lesions showed lower fat fractions as compared to both yellow ($p = 0.0087$, $p < 0.0001$) and red marrow ($p = 0.0004$, $p < 0.0001$) on T2W Dixon imaging. Malignant lesions showed lower fat fraction as compared to the benign lesions on T2W Dixon imaging ($p = 0.0005$). Signal intensity loss on red and yellow marrow were lower on T1W Dixon as compared to T2W Dixon (0.49-0.64, 0.27-0.31 vs 0.70-0.74, 0.48-0.71). Inter-reader agreements were excellent (0.91-0.97).

Conclusion: T2W Dixon imaging signal intensity changes can sufficiently differentiate between yellow marrow, red marrow, benign and malignant bone marrow lesions. Along with its ability to provide four comprehensive maps—in-phase, out-of-phase, water and fat only images—T2W Dixon imaging can be an important singular imaging modality in bone marrow characterization and bony lesion identification.

Modality % - Radiography / Fluoroscopy:	0
Modality % - CT:	0
Modality % - MRI:	100
Modality % - US:	0
Modality % - Nuclear Medicine:	0

A

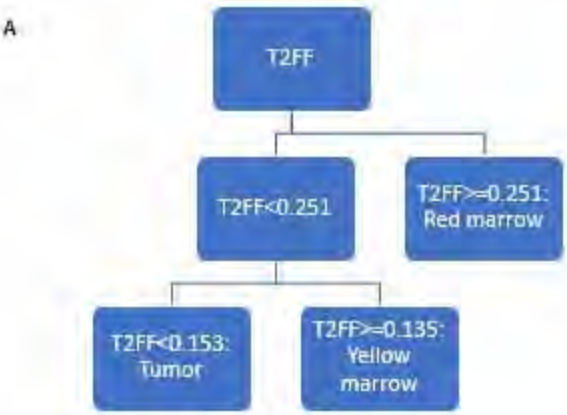

B

Confusion Matrices					
	Actual	Predicted			Error Rate
		R	Tumor	Y	
Model Based	R	214	0	12	0.0531
	Tumor	4	24	5	0.2727
	Y	62	0	52	0.5439
Cross Validation	R	214	2	10	0.0531
	Tumor	4	20	9	0.3939
	Y	70	2	42	0.6316

Figure 1. A) Decision tree model predicting red marrow, yellow marrow or tumor, B) Confusion matrix describing decision tree performance.

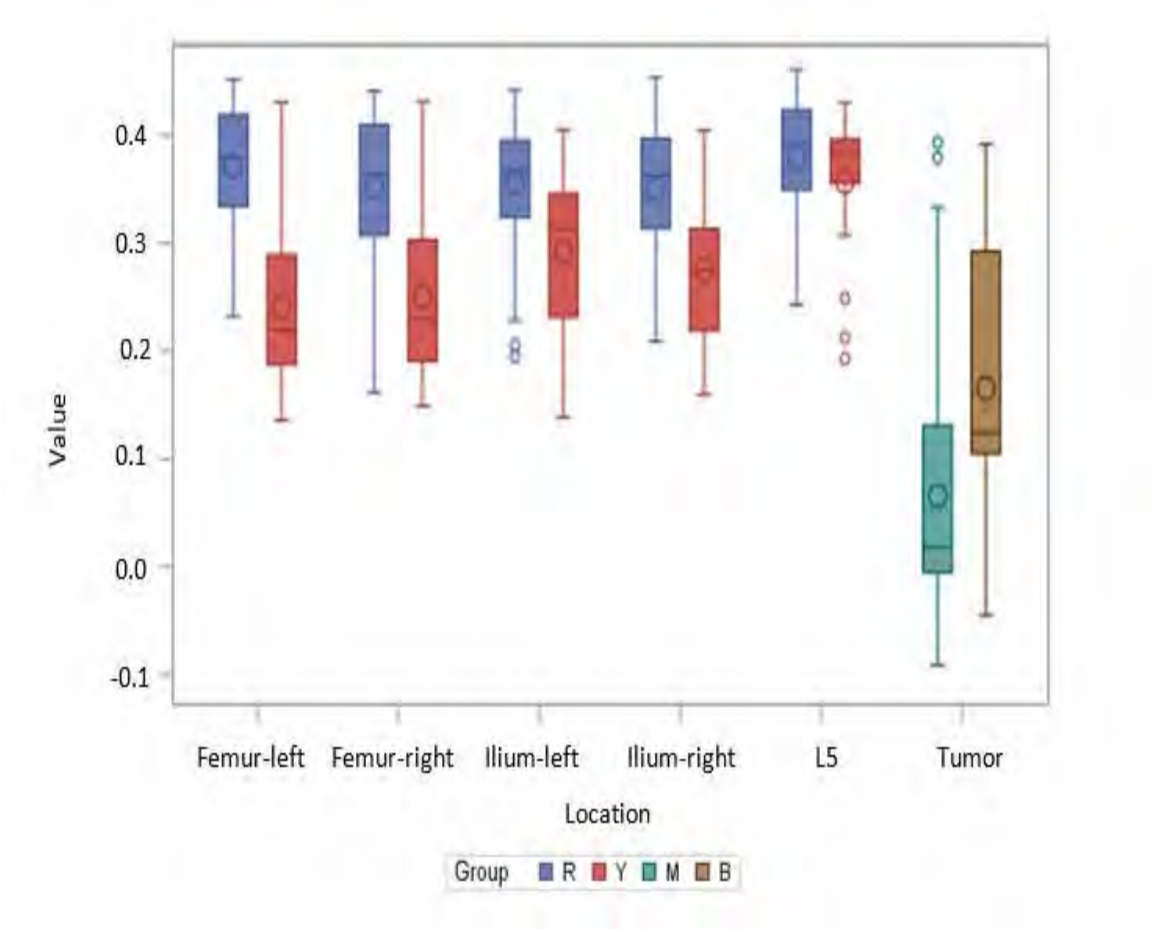

Figure 2. T2W FF of red marrow, yellow marrow, benign tumor and malignant tumor.

Podium #46

MUSCULOSKELETAL (MSK) UTILIZATION AND PERFORMANCE OF WHOLE-BODY MRI (WBMRI) IN THE ADULT POPULATION

Jacob Feldhaus, MD; Daniel Wessell, MD, PhD; Hillary Garner, MD; Joseph Bestic, MD; Jeffrey Peterson, MD; Anthony Wheeler, MD
Mayo Clinic Florida, Jacksonville, FL, USA
(Presented by: Jacob Feldhaus, MD, Mayo Clinic Florida)

Purpose: To evaluate MSK practice patterns of WBMRI in the adult population across multiple institutions in an effort to better understand current clinical practice utilization and understand the need for best practice and/or dedicated WBMRI Current Procedural Terminology (CPT) code development.

Materials and Methods: A 12-question survey was created in Survey Monkey®. The survey was distributed to the SSR membership by email on September 19, 2018. The survey included demographic questions and questions regarding the use of whole body MRI in the adult population, such as specific scanning parameters, indications for WBMRI, and details related to billing/coding.

Results: 89 of 1454 (6%) SSR members responded to the survey. 29% of physicians completing the survey stated that they routinely performed WBMRI. The most common indication for performing WBMRI at these institutions was multiple myeloma (82%) followed by tumor staging (30%), assessing response to therapy (30%), and evaluation of cancer predisposing syndromes (30%). The most commonly utilized MRI sequences were coronal short tau inversion recovery (STIR) (82%) and coronal T1 without fat saturation (74%). No other single sequence was performed by greater than 40% of respondents. No preference was shown for either 1.5-T or 3-T magnetic field strengths. There was variability for billing code utilization with 24% of respondents using the bone marrow MRI code and 18% the unlisted MRI procedure code (24% did not know).

Conclusion: WBMRI is currently being utilized at a significant minority of institutions for evaluation of metastatic disease and various systemic disease processes in adult patients. There is considerable variation in usage, imaging technique, and billing code selection among radiology practices based on our survey results. Therefore, further investigation regarding WBMRI best practice and dedicated CPT code development may be warranted.

Modality % - Radiography / Fluoroscopy:	0
Modality % - CT:	0
Modality % - MRI:	100
Modality % - US:	0
Modality % - Nuclear Medicine:	0

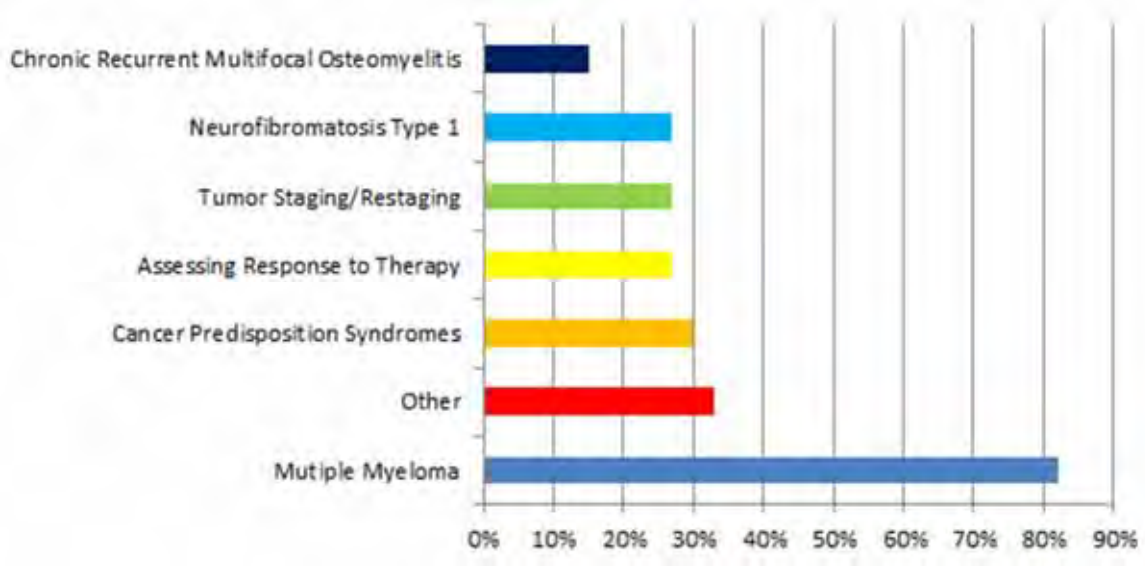

Indications for performing WBMRI

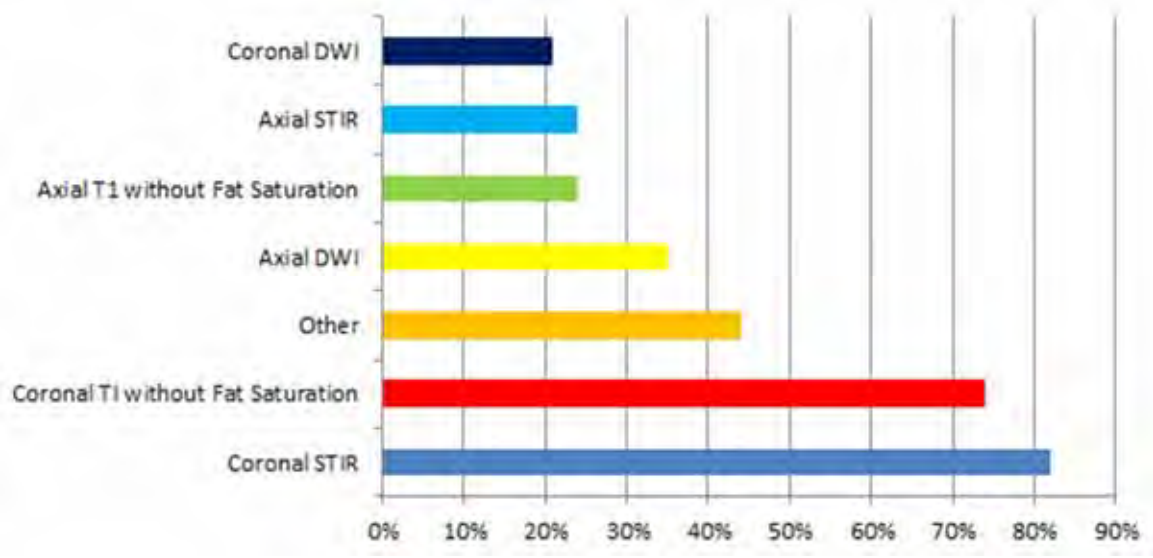

MR sequences typically performed for WBMRI

Podium #47

OSTEOID OSTEOMAS OF THE HIP: A WELL-RECOGNIZED ENTITY WITH A PROCLIVITY FOR MISDIAGNOSIS

Doris Wenger, MD; Meagan Tibbo, MD; Rafael Sierra, MD; Matthew Houdek, MD; Welch Tim, MD
Mayo Clinic, Rochester, MN, USA
(Presented by: Doris Wenger, MD, Mayo Clinic)

Purpose: Despite their small size and well-documented clinical and radiographic features, the diagnosis of osteoid osteomas about the hip can be challenging with potential for delayed or inaccurate diagnosis. Presenting symptoms and imaging features can mimic FAI, stress fracture and tumor. The goals of our study were to 1) assess the most common misdiagnoses and treatments, 2) define the mean delay in diagnosis, 3) describe the imaging features and 4) provide tips for avoiding diagnostic imaging pitfalls.

Materials and Methods: We identified 26 patients (27 tumors) with OO of the femoral neck (n=25) and acetabulum (n=2) referred for ablation between 1998 and 2017. There were 14M/12FM; mean age 19 years. 26 of 27 patients were referred after initial evaluation and/or treatment elsewhere. Imaging studies included radiographs (n= 24), CT (n=27) and MRI (n=22).

Results: The most common initial diagnoses were stress fracture (n = 8), FAI (n = 4), malignant tumor or infection (n = 4). 3 patients were initially diagnosed as having OO. Prior interventions included ORIF for femoral neck stress fracture (n = 2), hip arthroscopy and PAO (n = 1), synovectomy (n = 1), and attempted RFA (n = 1). Mean time from symptom onset to diagnosis of OO was 15 months (range, 0.4 – 84). All MRI exams showed bone marrow edema (BME) in the femur (n=20) or acetabulum (n=2), which was attributed to other pathology for 20 of 22 MRI exams. The OO was evident on all CT exams and in retrospect on 14 of 22 MRIs.

Conclusion: 75% of OO were initially misdiagnosed in our series. This led to delay in diagnosis for the majority and unnecessary intervention in 15%. Consideration of OO in the differential diagnosis of hip pain in young patients and familiarity with the imaging features is essential for making an accurate and timely diagnosis.

Modality % - Radiography / Fluoroscopy:	10
Modality % - CT:	30
Modality % - MRI:	60
Modality % - US:	0
Modality % - Nuclear Medicine:	0

AP radiograph of right hip of 19-year-old female with right hip pain initially misdiagnosed with a femoral neck stress fracture.

Coronal T2 fat suppressed MRI of the right hip shows increased T2 signal in the femoral neck.

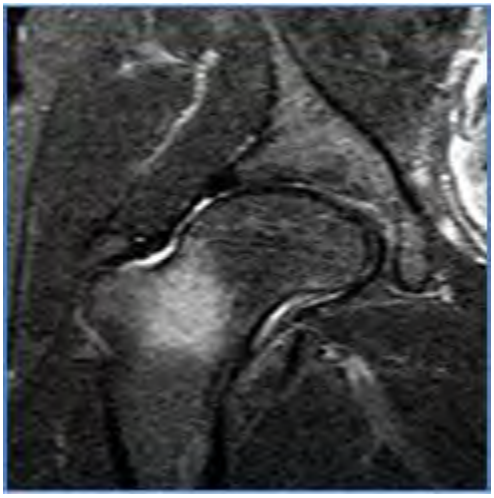

Sagittal CT images illustrates a small intracortical lytic lesion classic for an osteoid osteoma.

Podium #48

DESMOPLASTIC FIBROBLASTOMA: AN UNCOMMON SOFT TISSUE TUMOR WITH A RELATIVELY CHARACTERISTIC MR IMAGING APPEARANCE

Maxine Kresse, MD; Mark Kransdorf, MD; Jonathan Flug, MD; Jeremiah Long, MD; Michael Fox, MD
Mayo Clinic, Phoenix, AZ, USA
(Presented by: Maxine Kresse, MD, Mayo Clinic)

Purpose: We describe the MR, CT, US and radiographic imaging features of desmoplastic fibroblastoma.

Materials and Methods: We retrospectively reviewed the imaging features of 20 pathologically confirmed cases identified in our institutional pathology database.

Results: The 20 patients consisted of 12 woman (60%) and 8 men (40%) ranging from 20 to 96 years of age (average 59 years, 5 months). Lesions were relatively small ranging from 1 to 11 cm (average 4.4 cm) and most commonly ovoid and/or lobulated in shape. History was available in 19 cases identifying a slowly growing mass in 11cases (58%), two becoming painful over time, with the remaining 8 cases (42%) being incidental findings. Most lesions were deep (85%) with only 3 (15%) being superficial. Deep lesions were most often intermuscular (9; 53%), followed by intramuscular (5: 29%) and juxta-articular (3: 18%.). MR imaging was available for 18 cases (15 with/without contrast), CT in 10 case, ultrasound in 12, radiographs in 11, and PET/CT in one. Lesion margins were well-defined in all cases typically demonstrating varying amount of very low (dark) and intermediate signal, similar to that of tendon and skeletal muscle respectively. On fluid sensitive sequences, lesions showed greater heterogeneity with generally more prominent decreased (dark) signal and variable intermediate signal similar to and greater than that of skeletal muscle. Contrast enhancement was characteristically peripheral and septal with varying areas of homogeneous enhancement (Fig.1). Nonconrast CT showed attenuation similar to that of skeletal muscle in all cases except one which was mildly heterogeneous. Ultrasound typically showed a mixed echogenic mass while radiographs were negative or demonstrated a nonmineralized mass with one case showing osseous remodeling.

Conclusion: The MR imaging features of desmoplastic fibroma are most characteristic demonstrating a relatively small, well-defined mass, with low and intermediate signal with the low signal intensity becoming more pronounced with increased T2-weighting.

Modality % - Radiography / Fluoroscopy:	5
Modality % - CT:	15
Modality % - MRI:	75
Modality % - US:	5
Modality % - Nuclear Medicine:	0

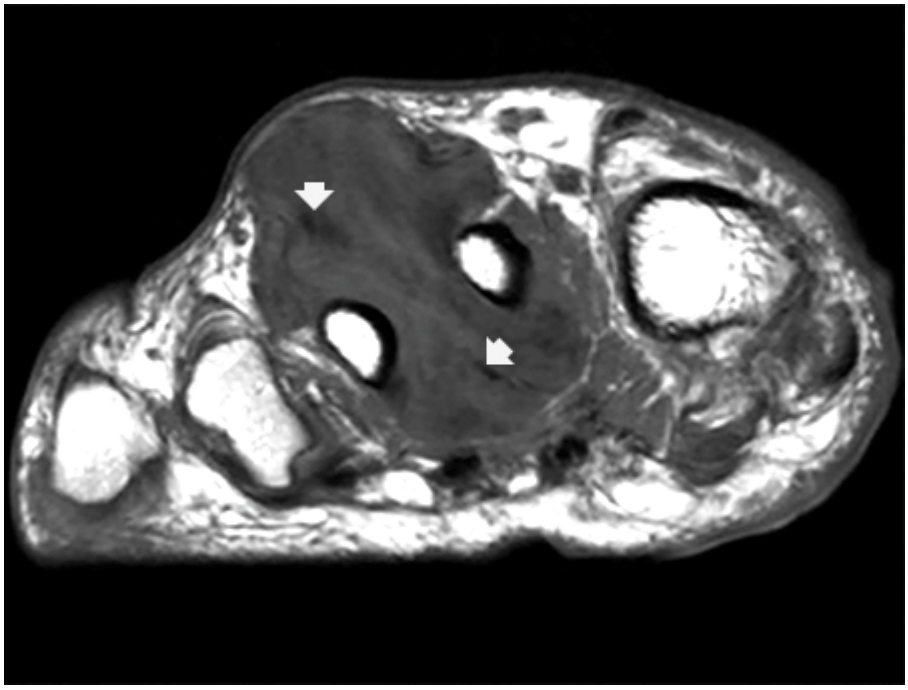

T1-weighted MR image MR imaging shows a lobulated mass with intermediate signal intensity and band-like areas of decreased signal (arrows).

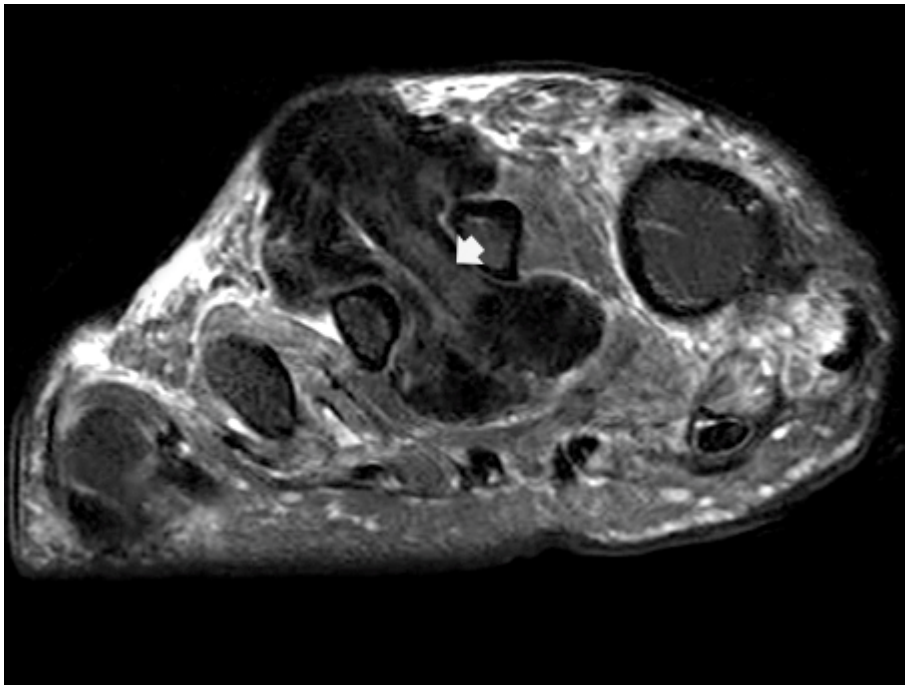

Corresponding fluid sensitive image shows showed greater heterogeneity with generally more prominent decreased (dark) signal and intermediate signal similar to that of skeletal (arrow).

Podium #49

RADIOMIC FEATURES EXTRACTED FROM T1 MRI DISTINGUISH MYXOMAS FROM MYXOFIBROSARCOMAS BETTER THAN IMAGE INTENSITY

Teresa Martin-Carreras, MD; Ronnie Sebro, MD
Hospital of University of Pennsylvania, Philadelphia, PA, USA
(Presented by: Ronnie Sebro, MD, Hospital of University of Pennsylvania)

Purpose: Myxoid tumors pose great diagnostic challenges for radiologists. Myxomas are benign pauci-cellular, bland myxoid tumors which do not metastasize, but can recur. Myxofibrosarcomas are malignant myxoid tumors that are histologically heterogenous and have the propensity to metastasize. We hypothesized that T1 MRI could help distinguish myxomas from myxofibrosarcomas. We evaluated the performance of image intensity information, tumor volume, and radiomic features extracted from T1 MRI to distinguish myxomas from myxofibrosarcomas.
Materials and Methods: T1 MRI dataset of 56 patients, consisting of 29 patients with myxoma and 27 patients with myxofibrosarcomas was analyzed. We identified a solid tumor region, and a reference region to normalize image intensity values across subjects. A total of 89 radiomic features were also extracted from the dataset. Random forests based classifiers were built upon the radiomic features for distinguishing myxoma from myxofibrosarcomas. Performance of the classifiers built upon radiomic features was compared with those built using image intensity and volume features. The number of trees and the minimum leaf size of the random forests classifiers were set to 500 and 3, respectively. The classifiers were validated using a leave-one-out cross-validation. Classification accuracy, sensitivity, specificity, and area under the receiver operating characteristic curve (AUC) were used to evaluate the classification performance.
Results: Myxoma tumors had lower normalized T1 signal intensity values than myxofibrosaromas (p=0.006) and AUC was 0.713. The classification model built upon radiomic features obtained an AUC of 0.885 (accuracy=0.839, sensitivity=0.852, specificity=0.828), and outperformed the classification models built upon image intensity and tumor volume features (AUC=0.838). The classifier built upon the image intensity values had worse classification performance than the classifier built upon the radiomic features (p=0.039, DeLong test).
Conclusion: The results that radiomic features could provide more discriminative information for distinguishing myxoma from myxofibrosarcoma tumors compared to volume-based measures and T1 image intensity values.

Modality % - Radiography / Fluoroscopy:	0
Modality % - CT:	0
Modality % - MRI:	100
Modality % - US:	0
Modality % - Nuclear Medicine:	0

Podium #50

"POSSIBLE" MENISCAL TEARS AT KNEE MRI: REVISITING THE SINGLE-TOUCH RULE

Lindsay Stratchko, DO; Kenneth Lee, MD; Richard Kijowski, MD
University of Wisconsin Hospital & Clinics, Madison, WI, USA
(Presented by: Lindsay Stratchko, DO, University of Wisconsin Hospital & Clinics)

Purpose: To determine the positive predictive (PPV) value of a "possible" meniscus tear according to the single-touch rule using arthroscopy as the reference standard.

Materials and Methods: A retrospective review was performed to identify all knee MRI exams with reports containing the terms "possible" or "probable meniscus tear" from March 2006 to August 2018. Patients with a history of prior meniscus surgery, meniscal root abnormality, absence of knee arthroscopy, or knee arthroscopy performed more than four months after the MRI exam were excluded. Two musculoskeletal radiologists independently reviewed all MRI exams blinded to the arthroscopy findings. Only cases with agreement of both radiologists for a "possible" meniscus tear, defined as signal abnormality extending to an articular surface on only a single image slice, were included in the analysis. PPVs were calculated using arthroscopy as the reference standard based on demographics, history of knee injury, presence of anterior cruciate ligament (ACL) injury, scanner type, location of meniscus tear, and presence of radiographic knee osteoarthritis (OA) and were compared using Fischer's exact tests.

Results: 136 MRI exams met the inclusion criteria and had a "possible" meniscus tear according to the single-touch rule confirmed independently by two radiologists (Figure 1). The overall PPV of a "possible" meniscus tear was 33.9% with PPVs for the medial and lateral meniscus of 29.8% and 36.7% respectively. The PPVs for subjects with age of 40 years and younger and age older than 40 years were 27.5% and 40.3% respectively. The PPV for subjects with and without ACL injury were 40.0% and 30.2% respectively. The PPV for subjects with and without knee OA was 40.8% and 32.5% respectively. However, the differences failed to reach statistical significance (Figure 2).

Conclusion: The PPV of a "possible" meniscus tear according to the single-touch rule was only 33.9%.

Modality % - Radiography / Fluoroscopy:	10
Modality % - CT:	0
Modality % - MRI:	90
Modality % - US:	0
Modality % - Nuclear Medicine:	0

Figure 1: (A) Example of a "possible" meniscal tear involving the posterior horn of the lateral meniscus as demonstrated by linear high signal extending to the superior articular surface on a single sagittal proton density-weighted fast spin-echo image slice. (B) Subsequent arthroscopic image confirmed the presence of small superior surface tear of the posterior horn.

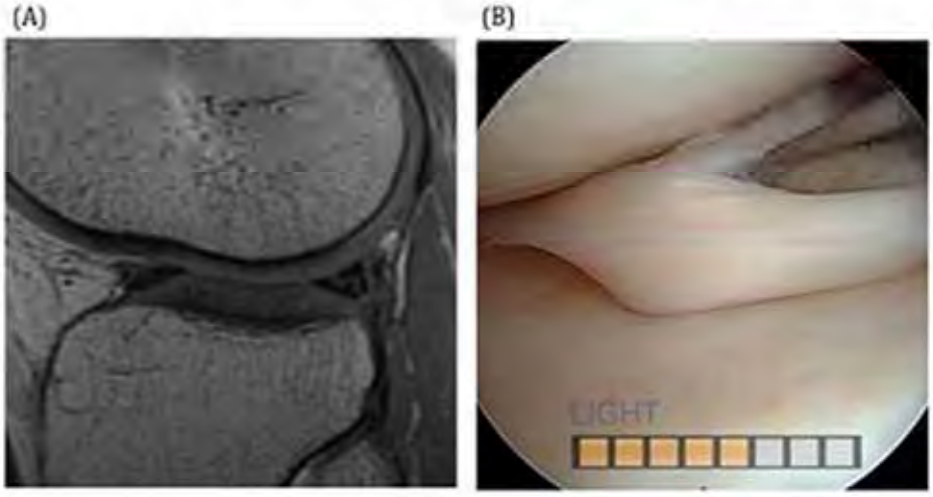

Figure 1: Example of "possible" meniscal tear with arthroscopic confirmation.

Figure 2: PPV of "possible" meniscus tear based on demographics, history of knee injury, presence of ACL injury, scanner type, location of meniscus tear, and presence of knee OA.

Criteria	Number of Exams	PPV	P-Value
Male	70	32.9%	P=0.86
Female	66	34.8%	
Age ≤ 40 years	69	27.5%	P=0.14
Age > 40 years	67	40.3%	
History of Knee Trauma	64	32.8%	P=0.86
Absence of Knee Trauma	72	34.7%	
Presence of ACL Injury	50	40.0%	P=0.26
Absence of ACL Injury	86	30.2%	
1.5 T Scanner	89	32.6%	P=0.71
3.0 T Scanner	47	36.2%	
Medial Meniscus	57	29.5%	P=0.46
Lateral Meniscus	79	36.7%	
Anterior Horn/Body Junction	20	35.0%	
Body	32	34.4%	P=0.84
Body/Posterior Horn Junction	22	36.3%	
Posterior Horn	62	32.3%	
Presence of Knee OA	49	40.8%	P=0.35
Absence of Knee OA	77	32.5%	

Figure 2: PPV of "possible" meniscal tears.

Podium #51

COMPARING CLINICAL AND SEMI-QUANTITATIVE CARTILAGE GRADING IN PREDICTING OUTCOMES AFTER ARTHROSCOPIC PARTIAL MENISCECTOMY

Naveen Subhas, MD, MPH[1]; Ceylan Colak, MD[1]; Joshua Polster, MD[1]; Nancy Obuchowski, PhD[1]; Morgan Jones, MD, MPH[1]; Greg Strnad[1]; Soterios Gyftopoulos, MD, MS[2]; Kurt Spindler, MD[1]
[1]Cleveland Clinic, Cleveland, OH, USA; [2]NYU Medical Center/ Hospital for Joint Diseases Langone Medical Center, New York, NY, USA
(Presented by: Naveen Subhas, MD, MPH, Cleveland Clinic)

Purpose: Preoperative cartilage loss is a predictor of poor outcomes after arthroscopic partial meniscectomy (APM). Previous studies have used time-intensive MRI grading systems, such as MOAKS (MRI OsteoArthritis Knee Score), which are not amenable for routine clinical use. This study's purpose was to test whether cartilage loss graded using MOAKS provides better prediction of outcomes than a simpler clinically used grading system.
Materials and Methods: 80 cases were selected meeting the following criteria: 1. Preoperative knee MRI performed within 6 months of APM surgery 2. Outcomes measured at the time of surgery and 1 year after surgery. Surgical failure was defined as a less than 10 point improvement in the Knee Osteoarthritis Pain Score ($KOOS_{pain}$). Cases were independently evaluated by 2 musculoskeletal (MSK) radiologists and 1 radiology fellow using MOAKS and a modified Outerbridge grading system used clinically. Accuracy of each system in discriminating success and failure was estimated using area under the ROC (AUC) with 95% confidence intervals (CI).
Results: 78 patients (38 females) with mean age of 56.6 years (range of 45-77) were studied. 32 patients (41%) were surgical failures. At least Grade 2 (< 50% cartilage thickness loss) ranged from 8% (lateral tibial plateau) to 26% (medial femoral condyle) of the observations. AUC values of the clinical grading system (range 0.585 – 0.625) were very similar to MOAKS (range 0.553 to 0.667) for all cartilage surfaces and non-inferior to MOAKS in the medial femoral condyle (p = 0.015) and trochlea (p =0.031). The lateral femoral condyle was the only surface where MOAKS (0.667) was significantly higher than the clinical grading system (0.614).
Conclusion: Cartilage loss graded using MOAKS and a simpler clinically used system have similar ability in predicting outcomes after APM. This suggests that it is feasible to use routine clinical grading of cartilage to develop models to predict outcomes after APM.

Modality % - Radiography / Fluoroscopy:	0
Modality % - CT:	0
Modality % - MRI:	100
Modality % - US:	0
Modality % - Nuclear Medicine:	0

Cartilage Surface	MOAKS	Clinical	Non-Inferiority
	[95% CI]	[95% CI]	[95% CI for diff]
Medial femoral cartilage	0.579	0.585	P=0.015
	[0.442, 0.716]	[0.463, 0.707]	[-0.089, 0.102]
Medial Tibial Plateau Cartilage	0.638	0.597	P=0.171
	[0.514, 0.762]	[0.483, 0.712]	[-0.163, 0.082]
Lateral Femoral Condyle Cartilage	0.667	0.614	P=0.138
	[0.578, 0.755]	[0.528, 0.700]	[-0.128, -0.001]
Lateral Tibial Plateau Cartilage	0.596	0.59	P=0.085
	[0.480, 0.712]	[0.480, 0.700]	[-0.141, 0.128]
Trochlea Cartilage	0.553	0.625	P=0.031
	[0.431, 0.675]	[0.507, 0.744]	[-0.109, 0.254]
Patella Cartilage	0.64	0.607	P=0.195
	[0.544, 0.747]	[0.509, 0.705]	[-0.179, 0.101]

Table 1: AUC Values of MOAKS and Clinical Grading Systems

Podium #52

DOWNSTREAM COSTS ASSOCIATED WITH INCIDENTAL CARTILAGE LESIONS DETECTED ON RADIOGRAPHS

Paul-Michel Dossous, MD; Tatiane Rodrigues, MD; William Walter, MD; Michelle Lam, BA; Mohammad Samim, MD; Xi Xue, MD; Andrew Rosenkrantz, MD; Soterios Gyftopoulos, MD
NYU Medical Center/ Hospital for Joint Diseases Langone Medical Center, New York, NY, USA
(Presented by: Paul-Michel Dossous, MD, NYU Medical Center/ Hospital for Joint Diseases Langone Medical Center)

Purpose: To explore variation in downstream costs associated with cartilage lesions incidentally detected on radiographs.

Materials and Methods: The cohort was composed of 120 patients with incidental, not previously diagnosed, cartilage lesions seen on appendicular plain radiographs. The population was divided into three subgroups based on the interpreting radiologist's description: enchondroma, low-grade cartilage lesion, and chondrosarcoma. Downstream events (follow-up imaging, office visits, biopsy, tumor resection) associated with the lesions were identified from the electronic medical record. American College of Radiology (ACR) Appropriateness Criteria were used to classify radiologists' recommendations. National Medicare rates were used to estimate costs of downstream events. Average cost per lesion was stratified, and cost ratios were computed among subgroups.

Results: Average downstream cost per lesion was $75.56. Costs were 4.6 times greater in patients under the age of 65 than over. Costs were 13.2 and 13.7 times higher when radiologists characterized lesions as chondrosarcoma versus low-grade cartilage lesion and enchondroma, respectively. There was no statistically significant difference in costs between the subgroups when accounting for size and location of lesions. Compared to when follow-up imaging was neither recommended nor obtained, costs rose from $0 to $26.03 per patient when follow-up imaging was recommended and obtained, and $62.21 per patient when follow-up imaging was obtained despite not being recommended. Costs rose from $0 to $14.83 per patient when radiologists' recommendations for follow-up were adherent to the ACR guidelines for management of incidental bone lesions. Costs were 2.3 times greater when ordering physicians overmanaged compared with radiologists' recommendations. No malignancy was pathologically proven in the cohort.

Conclusion: Costs for incidental cartilage lesions vary. Size and location of lesions do not have a significant effect on downstream costs; however, radiologists' characterization and recommendation have an impact. Therefore, it is imperative that radiologists accurately characterize such lesions and recommendations reflect the best value for patient care.

Modality % - Radiography / Fluoroscopy:	100
Modality % - CT:	0
Modality % - MRI:	0
Modality % - US:	0
Modality % - Nuclear Medicine:	0

Podium #53

CAN PREOPERATIVE MR IMAGING FINDINGS PREDICT EARLY FAILURE FOLLOWING ANTERIOR CRUCIATE LIGAMENT RECONSTRUCTION?

Jenny Bencardino, MD; Michele Mastio, MD; Alejandra Duarte, MD; Laith Jazrawi, MD; Jose Raya, PhD
NYU Medical Center/ Hospital for Joint Diseases Langone Medical Center, New York, NY, USA
(Presented by: Jenny Bencardino, MD, NYU Medical Center/ Hospital for Joint Diseases Langone Medical Center)

Purpose: The aim of this study is to identify markers of early failure of anterior cruciate ligament graft reconstruction (ACLR) based on preoperative MR imaging.
Materials and Methods: We identified 26 patients with early ACLR graft failure (<2 years) who underwent revision between 2011-2015 in a retrospective review of our database. Exclusion criteria included graft choice other than autografts (n=4) and non available preoperative MRI (n=3). Nineteen patients with early ACLR failure were included in the study group. The control group consisted of 38 subjects who underwent ACLR with a minimum of 2 years of clinical follow up and no evidence of graft failure matched by age, sex, BMI and graft type. Preoperative MRI obtained within 8 weeks (range 1-8) following initial trauma were reviewed blinded to the ACLR failure by an experienced (20 years) musculoskeletal radiologist for intra and periarticular lesions including: anterolateral ligament (ALL) injuries (stretch, partial, complete), medial meniscus tear (MM), lateral meniscus tear (LM) tear, posteromedial corner injury (PMC), posterolateral corner injury (PLC) injury, medial collateral ligament tear (MCL), and lateral collateral ligament tear (LCL). Logistic regression analysis was performed.
Results: Mean time to ACLR failure was 14 months (range, 1-24 months). Mean follow up of those in the control group was 38 months (range, 2561). Medial meniscus (MM) tear was the best predictor of early ACLR failure (Accuracy=66.7%, p=0.08) followed by the lateral meniscus (p=0.13). MM was a significant predictor of ACLR failure (p=0.02) with odds ratio (OR) 4.2 and 95% confidence interval (CI) [1.19 14.9]. All other variables were not associated with ACLR failure (p>0.20).
Conclusion: MM tears were the best predictor of early failure of ACLR. Thus, preserving the integrity of the MM during ACLR procedure may be crucial in minimizing the risk for early ACLR failure.

Modality % - Radiography / Fluoroscopy:	0
Modality % - CT:	0
Modality % - MRI:	100
Modality % - US:	0
Modality % - Nuclear Medicine:	0

Podium #54

RUPTURE OF THE ANTEROLATERAL LIGAMENT IN COMPLETE ACUTE TRAUMATIC ANTERIOR CRUCIATE LIGAMENT TEAR: NEW INSIGHTS INTO ACUTE PIVOT SHIFT TRAUMA TO THE KNEE.

Jenny Bencardino, MD; Michele Mastio, MD; Alejandra Duarte, MD; Laith Jazrawi, MD; Jose Raya, PhD
NYU Medical Center/ Hospital for Joint Diseases Langone Medical Center, New York, NY, USA
(Presented by: Jenny Bencardino, MD, NYU Medical Center/ Hospital for Joint Diseases Langone Medical Center)

Purpose: To evaluate the prevalence and association of anterolateral ligament (ALL) rupture with other meniscal and ligamentous injuries of the knee in patients with complete acute traumatic anterior cruciate ligament (ACL) tear.
Materials and Methods: Based on retrospective review of our orthopedic surgery database, 57 patients M45:F12, mean age 21 (range:13-34) with acute post traumatic ACL rupture who underwent ACLR seen between 2011 and 2015 were enrolled in this cohort. Preoperative MR examinations was performed by an experienced (20 years) MSK radiologist assessing these variables: anterolateral ligament (ALL) rupture, MM tear, LM tear tear, posteromedial corner injury (PMC), posterolateral corner injury (PLC) injury, MCL tear, and lateral collateral ligament tear (LCL). Odds ratios and their 95% confidence interval were used to assess the associations of ALL with other injuries in the knee. To rule out confounding factors we used the Cochran Mantel Haenszel method in an analysis stratified by gender and BMI (normal, overweight).
Results: Most commonly reported lesions were of the MM 63%, and PLC 64%. ALL partial or complete tears and Segond avulsion fracture were reported in 28 patients (49%). Anterolateral
lesions were associated with a 10 fold decreased risk of MM tear (odds ratio [OR] = 0.10, 95% [CI]=[0.028, 0.38]) and a 4.6 fold increased risk of LCL tear (OR=4.68, 95% CI=[1.28 17.1]). Neither gender nor BMI were confounding for the associations of ALL with MM and LCL tears. No other statistically significant associations between ALL rupture and LM, PMC, PLC and MCL injury were found.
Conclusion: Failure of the ALL during acute traumatic ACL rupture is often associated with tear of the LCL. This may have a protective effect over the MM due to potential “capsular release” ewith increased mobility of the MM and decreased risk of clipping/tearing between the approximating medial compartment surfaces during pivot shift trauma.

Modality % - Radiography / Fluoroscopy:	0
Modality % - CT:	0
Modality % - MRI:	100
Modality % - US:	0
Modality % - Nuclear Medicine:	0

Podium #55

ULTRASOUND SHEAR WAVE ELASTOGRAPHY (SWE) OF THE TIBIALIS POSTERIOR TENDON (PTT) AND TIBIOSPRING/SPRING LIGAMENTS AT REST AND STRESS IN NORMAL FEET COMPARED TO ASYMPTOMATIC AND SYMPTOMATIC ACQUIRED FLATFOOT DEFORMITY

Mihra Taljanovic, MD, PhD[1]; Wonsuk Kim, MD[2]; Chelsea Caruso, MD[1]; Elizabeth Krupinski, PhD[3]; Andres Nuncio Zuniga, BSN[1]; L. Latt, MD, PhD[1]
[1]University of Arizona HCS - Tucson, Tucson, AZ, USA; [2]Beth Israel Deaconess Medical Center Harvard Med School, Boston, MA, USA; [3]Emory University Dept. of Radiology, MSK Division, Atlanta, GA, USA
(Presented by: Mihra Taljanovic, MD, PhD, University of Arizona HCS - Tucson)

Purpose: The PTT and spring ligament stabilize the medial longitudinal foot arch and are affected in adult acquired flatfoot deformity (AAFD). This study measured ultrasound (US) shear wave velocities (SWV) of the PTT and tibiospring/spring ligaments in individuals with a normal arch and in those with asymptomatic and symptomatic AAFD to assess differences in SWE velocity values.

Materials and Methods: Two observers performed SWE of the PTT in the long and short axes in two anatomic locations and along the tibiospring/spring ligaments at rest in 8 normal feet, 5 asymptomatic and 7 symptomatic flatfeet. The second observer repeated measurements in the PTT long axis in the upper location and in tibiospring/spring at stress. The study was performed on a Siemens S3000 unit with a 9-MHz linear transducer. Each measurement was repeated three times. The values at rest and stress at each location were compared with paired t-tests. ANOVAs were used to test SWV differences at rest and stress between the three groups.

Results: There was high interreader agreement (ICC = 0.9134, 95% CI = 0.8769 – 0.9391), thus scores from both readers were averaged. There was a significant difference ($F = 31.51$, $p < 0.0001$), with post hoc Protected Least Squares Difference test showing lower SWV of the short PPT axes compared to long. Lower SWVs were found in the PTT and ligaments in the symptomatic flatfeet, compared with normal in each location. Higher SWVs were found along the PTT in the lower long axis location in the asymptomatic flatfeet compared with other two groups. None reached significance although SWV in the spring ligament and PTT lower long axis at rest approached significance. There was a significant difference for PTT upper long axis at stress.

Conclusion: SWE may be a useful adjunct in evaluation and management of patients with AAFD.

Modality % - Radiography / Fluoroscopy:	1
Modality % - CT:	0
Modality % - MRI:	0
Modality % - US:	100
Modality % - Nuclear Medicine:	0

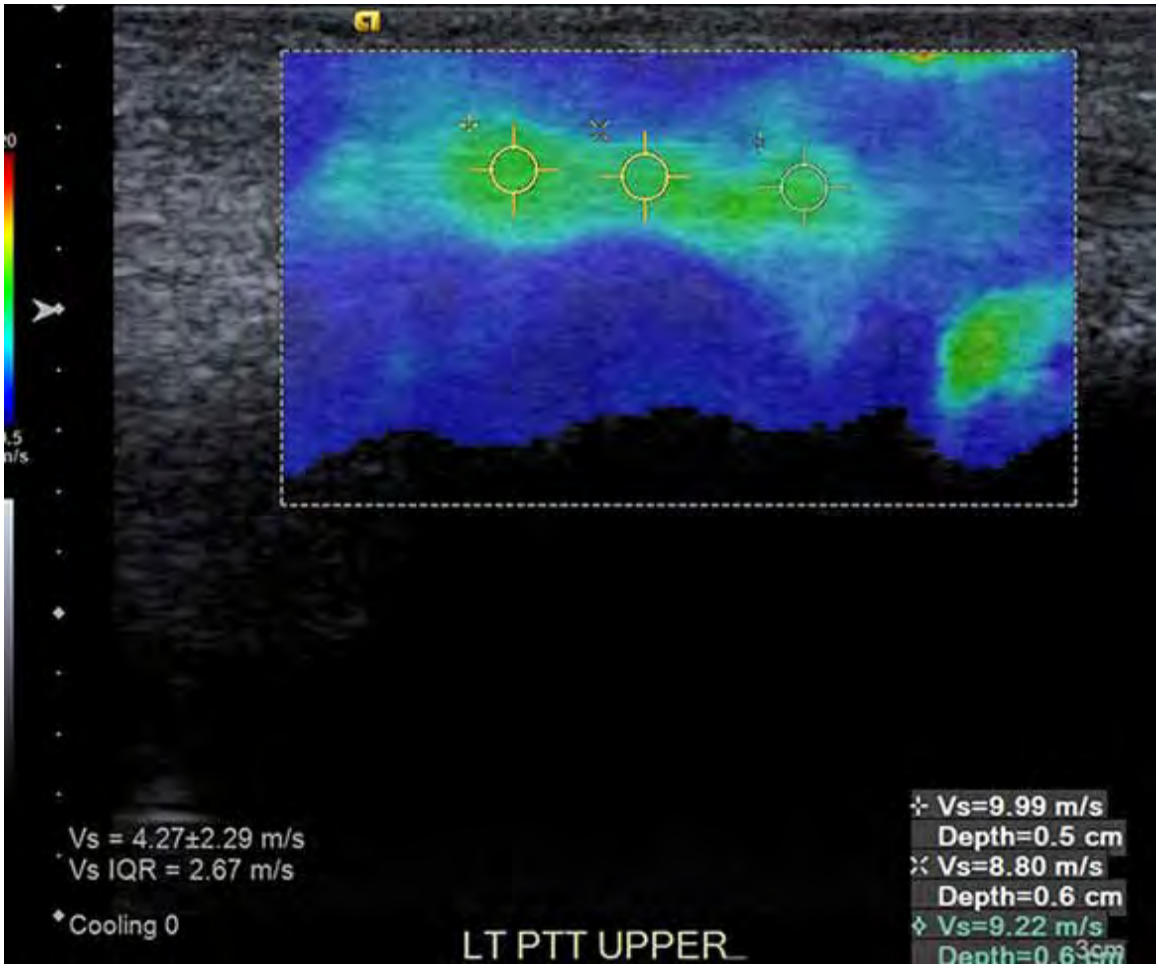

PTT upper long axis at rest

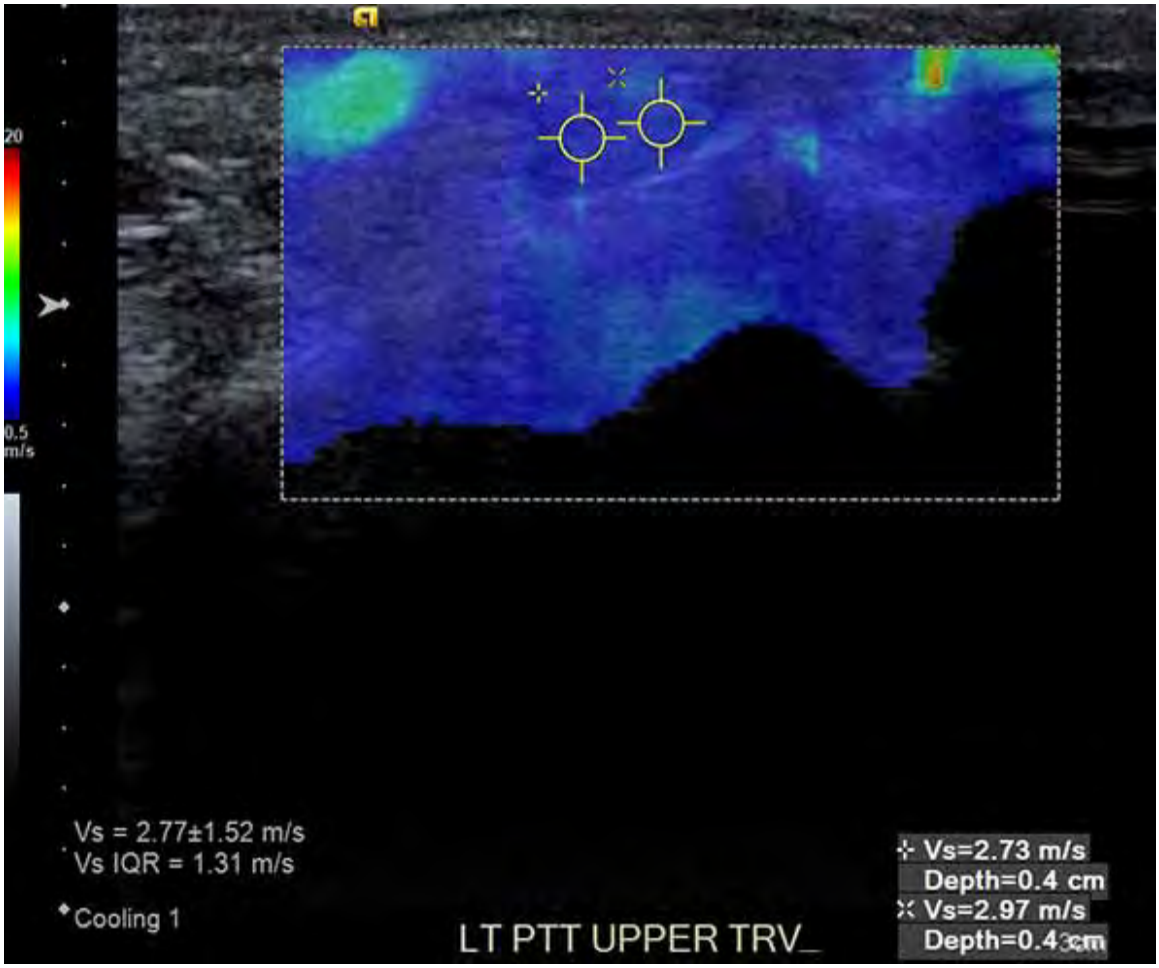

PTT upper short axis at rest

Podium #56

REDUCTION OF UNNECESSARY REPEAT KNEE RADIOGRAPHS DURING OSTEOARTHRITIS FOLLOW UP VISITS IN A LARGE TEACHING MEDICAL CENTER.

Oganes Ashikyan, MD; Dustin Buller, BS; Parham Pezeshk, MD; Majid Chalian, MD; Avneesh Chhabra, MD
University of Texas Southwestern Medical Center at Dallas, Dallas, TX, USA
(Presented by: Oganes Ashikyan, MD, University of Texas Southwestern Medical Center at Dallas)

Purpose: The purpose of our project was to determine the baseline frequency of unnecessary knee radiographs obtained for evaluation of severe osteoarthritis. We also determined whether clinician education can reduce the frequency of unnecessary radiographs.

Materials and Methods: Radiology reports of knee radiographs were searched in our database filtered for presence of word "severe" anywhere within the report. The resulting database was further filtered based on presence of any of the following terms: "degenerative", "osteoarthritis", "DJD", "joint space", "compartment", and "narrowing." Consecutive 500 reports and corresponding medical records were reviewed to confirm presence of severe osteoarthritis and presence or absence of repeat radiograph. The indication for repeat radiograph was determined. Repeat radiographs were counted as "non-indicated" when provided history and review of corresponding clinic visit note revealed no new symptoms or new suspected injuries. Educational PowerPoint presentation was distributed to all faculty, fellows, and residents in orthopedic and family practice departments via email in May 2018. The radiology reports database was again searched for knee radiographs obtained from June 2018 to August 2018. Rate of repeat radiographs was again calculated.

Results: Initial search returned 1517 reports. Further filtering of the reports returned 1227 reports. There were 112 repeat radiographs (22.4%) within 6 months in a subsample of manually reviewed 500 radiograph reports. 77 (69%) knee radiographs of 112 were classified as "not indicated." Repeat search of radiology reports after the educational intervention was performed after the initial three months follow up period. Only two repeat radiographs were found in the follow up sample. One of this was not indicated. The second was obtained to evaluate new injury. (Longer follow up data will become available prior to the meeting and results based on additional data will be presented.)

Conclusion: Simple clinician educational intervention results in significant reduction of number of unnecessary repeat knee radiographs.

Modality % - Radiography / Fluoroscopy:	100
Modality % - CT:	0
Modality % - MRI:	0
Modality % - US:	0
Modality % - Nuclear Medicine:	0

Podium #57

LATERAL FEMORAL CONDYLE INSUFFICIENCY FRACTURES: ASSOCIATED MORPHOLOGICAL FINDINGS

Adam Zoga, MD, MDA[1]; Terence Farrell, MD, MRCPI, FFRRCSI, FRCRUK[2]; Kristen McClure, MD[1]; Diane Deely, MD[1]
[1]Thomas Jefferson University Hospital, Philadelphia, PA, USA; [2]Jefferson Radiology Musculoskeletal Radiology Fellowship, Philadelphia, PA, USA
(Presented by: Adam Zoga, MD, MDA, Thomas Jefferson University Hospital)

Purpose: Medial femoral condyle insufficiency fractures (MFCIF) are strongly associated with medical meniscal tears and medial compartment high-grade chondrosis. We hypothesise that lateral femoral condyle insufficiency fractures (LFCIF) are less frequently associated with meniscal tears and high-grade chondrosis in the lateral compartment. The purpose of this study is to evaluate the MRI characteristics of LFCIF and their associated morphological findings.

Materials and Methods: A retrospective review of consecutive patients with LFCIF was performed after excluding post-traumatic fractures and other pathological subchondral fractures (e.g. underlying bone lesions). Data collection is in progress and at the time of submission 59 consecutive patients with LFCIF were included (age range 17-86 years, median 57 years). Morphological findings including lesion size and location, presence of bone marrow and soft tissue edema, chondrosis grade and associated meniscal pathology were classified by two board-certified musculoskeletal radiologists and a fellow.

Results: 32 male (54.2%) and 27 female (45.8%) patients were included. Central weight bearing (49.2%, 29/59) and posterior (47.5%, 28/59) locations for LFCIF were most prevalent. The majority of patients had an associated meniscal tear/s (55.9%, 33/59) with medial meniscus tears (42.4%, 25/59) more prevalent than lateral meniscus tears (27.1%, 16/59). High grade chondrosis (grade 3/4) was present in 62.7% (37/59) of patients. Overlying lateral compartment high grade chondrosis was present in 27.1% of patients (16/59) with patellofemoral (42.4%, 25/59) and medial (35.6%, 21/59) compartment high grade chondrosis more prevalent. Bone marrow edema was present in all cases (59/59) and soft tissue edema was present in 83.1% (49/59). Anecdotally 4 subjects with LFCIF previously had a MFCIF at MRI.

Conclusion: LFCIF are less strongly associated with meniscal tears and high grade chondrosis than MFCIF, and unlike MFCIF, more commonly involve the unfractured (medial) compartment than the fractured (lateral) compartment. Patients with LFCIF are in a similar demographic subset to those with MFCIF.

Modality % - Radiography / Fluoroscopy:	0
Modality % - CT:	0
Modality % - MRI:	2
Modality % - US:	0
Modality % - Nuclear Medicine:	0

Coronal STIR MRI of the knee demonstrating a lateral femoral condyle insufficiency fracture.

Sagittal proton density MRI of the knee demonstrating a lateral femoral condyle insuffciency fracture with intact lateral meniscus and overlying lateral femoral condyle cartilage.

ePOSTERS

Society of Skeletal Radiology

42nd Annual Meeting

March 10-13, 2019

ePoster* Complete Listing

**As these sessions are not moderated, ePosters are not CME accredited*

Location: Exhibit Hall

Sunday, March 10, 2019 .....7:00 a.m. – 4:30 p.m.

Monday, March 11, 2019.....7:00 a.m. – 12:30 p.m.

Tuesday, March 12, 2019.....7:00 a.m. – 12:30 p.m.

Wednesday, March 13, 2019 .....7:00 a.m. – 10:30 a.m.

ePoster Complete Listing

**As these sessions are not moderated, ePosters are not CME accredited*

BEST PRACTICE & EMERGING TRENDS

Poster #1 **CARTILAGE ICING AND CHONDROCALCINOSIS IN THE DIFFERENTIATION BETWEEN GOUT AND PSEUDOGOUT ON RADIOGRAPHS**
Anna Falkowski, MD, MHBA; Jon Jacobson, MD
University of Michigan Medical Center, Ann Arbor, MI, USA

Poster #2 **MUSCULOSKELETAL MANIFESTATIONS OF DIABETES MELLITUS: A REVIEW FOR THE PRACTICING RADIOLOGIST AND RADIOLOGIST IN TRAINING, WITH EMPHASIS ON CLINICAL PRESENTATION, PATHOGENESIS, AND IMAGING APPEARANCE.**
Alexander Grushky, MD[1]; David Marcantonio, MD[1]; Jonathan Im, MS[2]
[1]Beaumont Health System, Royal Oak, MI, USA; [2]Michigan State Univeristy College of Human Medicine, Grand Rapids, MI, USA

Poster #3 **PERIPROSTHETIC JOINT INFECTIONS**
Kimia Kani, MD[1]; Jack Porrino, MD[2]; Hyojeong Mulchay, MD[3]; Felix Chew, MD[3]
[1]University of Maryland School of Medicine, Baltimore, MD, USA; [2]Yale University School of Medicine, New Haven, CT, USA; [3]University of Washington / Harborview Medical Center, Seattle, WA, USA

Poster #4 **EXTERNAL FIXATORS: LOOKING BEYOND THE HARDWARE MAZE**
Kimia Kani, MD[1]; Jack Porrino, MD[2]; Hyojeong Mulcahy, MD[3]; Felix Chew, MD[3]
[1]University of Maryland School of Medicine, Baltimore, MD, USA; [2]Yale University School of Medicine, New Haven, CT, USA; [3]University of Washington / Harborview Medical Center, Seattle, WA, USA

Poster #5 **GUN VIOLENCE AND RADIOLOGY UTILIZATION AT A MAJOR CITY ACADEMIC CENTER**
William Morrison, MD; Ankit Gandhi, MD; Corbin Pomeranz, MD; Lauren Brown, MD; Kimberly Klinger, MD; Adam Zoga, MD; Johannes Roedl, MD; Jeffrey Belair, MD; Suzanne Long, MD
Thomas Jefferson University Hospital, Philadelphia, PA, USA

Poster #6 **DON'T MISS THE BULL'S-EYE: MRI APPEARANCE OF LYME DISEASE ARTHRITIS**
Sean Cleary, MD; Johnny Monu, MBBS, MD; Gregory Dieudonne, MD; Scott Schiffman, MD
The University of Rochester School of Medicine and Dentistry, Rochester, NY, USA

Poster #7 **MUSCULOSKELETAL MANIFESTATIONS OF SCLERODERMA ON MRI AND ULTRASOUND**
Emily Casaletto, BS; Ogonna Nwawka, MD; Alissa Burge, MD
Hospital for Special Surgery, New York, NY, USA

TECHNOLOGIES & TECHNIQUES

Poster #8 **HYBRID 18F-FDG PET/MR IN THE EVALUATION OF PEDAL OSTEOMYELITIS**
Margaret Kincaid, MD[1]; Stephen Broski, MD[1]; Drake McArthur, MD[2]; Erik Weiss, MD[3]
[1]Mayo Clinic, Rochester, MN, USA; [2]Tulane University Health Sciences Center, New Orleans, LA, USA; [3]Phoenix VA Medical Center, Phoenix, AZ, USA

Poster #9 **ULTRASOUND IMAGING OF NERVES IN THE NECK: CORRELATION TO MRI, ELECTRODIAGNOSTIC AND CLINICAL FINDINGS**
Ogonna Nwawka, MD; Emily Casaletto, BS
Hospital for Special Surgery, New York, NY, USA

Poster #10 **COMPRESSED SENSING MAGNETIC RESONANCE IMAGING (CS-MRI) OF THE KNEE: ASSESSMENT OF QUALITY, INTER-READER AGREEMENT, AND TIME SAVINGS**
George Matcuk, Jr., MD; Jordan Gross, MD; Brandon Fields, BA, BM; Steven Cen, PhD
KECK School of Medicine of USC, Los Angeles, CA, USA

Poster #11 **NEXT-GENERATION 5-MIN KNEE MRI WITH COMBINED SIMULTANEOUS MULTI-SLICE AND PARALLEL IMAGING ACCELERATION**
Jan Fritz, MD; Ali Rashidi, MD; Miho Tanaka, MD; Filippo Del Grande, MD
Johns Hopkins University, Baltimore, MD, USA

Poster #12 **PERIPHERAL NERVE IMAGING: A REVIEW OF ANATOMY, IMAGING TECHNIQUES, AND IMPORTANT PATHOLOGY**
Ryan Joyce, MD; Sarah Stilwill, MD; Richard Leake, MD; Megan Mills, MD; Patrick Kobes, DO; Hailey Allen, MD
University of Utah Medical Center / SOM, Salt Lake City, UT, USA

UPPER EXTREMITY

Poster #13 **REVERSE SHOULDER ARTHROPLASTY; PRE AND POSTOPERATIVE IMAGING AND CURRENT CONCEPTS.**
Michael Davis, MD; Alireza Eajazi, MD; Angel Gomez-Cintron, MD; Michael Tall, MD; Robert Cone, MD
UT Health San Antonio, San Antonio, USA

Poster #14 **TERES MINOR ATROPHY AND ASSOCIATED PATHOLOGY**
Derrick Doolittle, MD; William Aibinder, MD; Joaquin Sanchez-Sotelo, MD, PhD; Doris Wenger, MD
Mayo Clinic, Rochester, MN, USA

Poster #15 **ROTATOR CUFF REPAIR/RECONSTRUCTION FOR 'UNREPAIRABLE' TEARS**
Nicholas Rhodes, MD[1]; Amanda Baillargeon, MD[1]; Christin Tiegs Heiden, MD[1]; Bassem Elhassan, MD[1]; Daniel Wessell, MD[2]
[1]Mayo Clinic, Rochester, MN, USA; [2]Mayo Clinic Florida, Jacksonville, FL, USA

Poster #16 **POST-SURGICAL IMAGING OF ACROMIOCLAVICULAR (AC) JOINT SEPARATIONS**
Kimia Kani[1]; Jack Porrino, MD[2]; Hyojeong Mulcahy, MD[3]; Felix Chew, MD[3]
[1]University of Maryland School of Medicine, Baltimore, MD, USA; [2]Yale University School of Medicine, New Haven, CT, USA; [3]University of Washington / Harborview Medical Center, Seattle, WA, USA

Poster #17 **AN APPROACH TO THE PAINFUL STERNOCLAVICULAR JOINT: DIAGNOSIS AND INTERVENTION**
Gregory Matthews, MD; Maha Torabi, MD; Scott Wuertzer, MD
Wake Forest University School of Medicine, Winston-Salem, NC, USA

Poster #18 **POST-OPERATIVE COMPLICATIONS OF DISTAL BICEPS TENDON REPAIR: AN EDUCATIONAL MULTI-MODALITY IMAGING REVIEW**
ANESH CHAVDA, BSc, MRCP, FRCR; Isabelle Dupuis, MD.CM, FRCPC; Yara Alhajjar; JEFF PIKE, RCPSC; PARHAM DANESHVAR, RCPSC; MARK CRESSWELL, MBBCh, FRCPC; DARRA MURPHY
ST PAUL'S HOSPITAL, VANCOUVER, BC, Canada

Poster #19 **GLENOID BONE STOCK AND ROTATOR CUFF PATHOLOGY.**
Oganes Ashikyan, MD; Mathew Siebert, BS; Majid Chalian, MD
University of Texas Southwestern Medical Center at Dallas, Dallas, TX, USA

Poster #20 **USING THE RAVER VIEW AND ACROMIAL INDEX TO PREDICT ROTATOR CUFF TEARS ON RADIOGRAPHS**

Adam Zoga, MD, MBA[1]; Christopher Aland, MD[2]; Weilong Shi, MD[2]; Vishal Desai, MD[1]; William Morrison, MD[1]
[1]Thomas Jefferson University Hospital, Philadelphia, PA, USA; [2]Rothman Orthopaedics Institute, Philadelphia, PA, USA

Poster #21 **A MULTIMODALITY CENSUS OF CARPAL COALITIONS**

Aleksandr Rozenberg, MD; Alessandra Sax, MD; Jeffrey Belair, MD; Kristen McClure, MD; Johannes Roedl, MD, PhD; William Morrison, MD; Adam Zoga, MD, MBA
Thomas Jefferson University Hospital, Philadelphia, PA, USA

INTERVENTION

Poster #22 **PREOPERATIVE ULTRASOUND GUIDED BOTULINUM TOXIN A INJECTION FOR COMPLEX VENTRAL WALL HERNIA REPAIR: ONE TERTIARY CARE CENTER'S APPROACH**

Christopher Nall, MD; Dana Feraco, DO; Joshua Powell
Beaumont Health System, Royal Oak, MI, USA

Poster #23 **BIOPSY OF SUSPICIOUS OSSEOUS LESIONS IN PATIENTS WITH A KNOWN PRIMARY MALIGNANCY: RATE OF ALTERNATE DIAGNOSIS AND COMPLICATION RATE.**

Alexander Grushky, MD[1]; Christopher Nall, MD[1]; Zakaria Aqel, MD[1]; Alyssa Kirsch, MD[1]; Jonathan Im, MS[2]
[1]Beaumont Health System, Royal Oak, MI, USA; [2]Michigan State University College of Human Medicine, Grand Rapids, MI, USA

Poster #24 **THROW ME A BONE: EFFECT OF A BONE BIOPSY SKILLS WORKSHOP UTILIZING ANATOMICALLY ACCURATE 3D PRINTED MODELS**

Michael Durst, MD; Corey Ho, MD; Dorissa Gursahaney, MD; Amanda Crawford, MD; Melody Carroll, PhD
University of Colorado Denver, Aurora, CO, USA

HIP / PELVIS

Poster #25 **ACCURACY OF PREOPERATIVE MRI AND MRA FOR THE ASSESSMENT OF ACETABULAR LABRAL SIZE IN PATIENTS WITH FEMOROACETABULAR IMPINGEMENT (FAI)**

Richard Marshall, MD; Daniel Kaplan, MD; Christopher Burke, MD; Soterios Gyftopoulos, MD; Jonathan Vigdorchik, MD; Robert Meislin, MD; Thomas Youm, MD; Mohammad Samim, MD
NYU Medical Center/ Hospital for Joint Diseases Langone Medical Center, New York, NY, USA

Poster #26 **SACROILIAC JOINT INFECTIONS IN CHILDREN: MR IMAGING FEATURES**

Sara Cohen, MD; David Biko, MD; Christian Barrera, MD; Suraj Serai, PhD; Jie Nguyen, MD
Children's Hospital of Philadelphia, Philadelphia, PA, USA

Poster #27 **WITHDRAWN**

TUMOR / MARROW

Poster #28 **B-CELL PERIPHERAL NEUROLYMPHOMATOSIS: MRI AND 18F-FDG PET/CT IMAGING CHARACTERISTICS**

Stephen Broski, MD; Anthony DeVries, MD; Benjamin Howe, MD; Robert Spinner, MD
Mayo Clinic, Rochester, MN, USA

Poster #29 **FRIENDLY FAT MASQUERADING AS AN AGGRESSIVE FOE ON PLAIN RADIOGRAPHY: A CASE SERIES**

Bhumin Patel, MD; Douglas Mintz, MD
Hospital for Special Surgery, New York, NY, USA

Poster #30 **INTRANEURAL LIPOMA: A CASE SERIES**
Christin Tiegs-Heiden, MD; Katarina Glazebrook, MB, ChB; Matthew Frick, MD; Tara Anderson, MD; Robert Spinner, MD; Kimberly Amrami, MD
Mayo Clinic, Rochester, MN, USA

Poster #31 **POPLITEAL LYMPH NODES IN PATIENTS WITH OSTEOSARCOMA: ARE THEY METASTATIC?**
Shivani Ahlawat, MD; Mark Cleary, MD; Laura Fayad, MD
Johns Hopkins University, Baltimore, MD, USA

Poster #32 **SCAPULAR AND PERISCAPULAR LESIONS: WHAT THE RADIOLOGIST NEEDS TO KNOW**
Terence Farrell, MD, MRCPI, FFRRCSI, FRCRUK[1]; Kristen McClure, MD[2]; DIane Deely, MD[2]; Adam Zoga, MD, MBA[2]
[1]Jefferson Radiology Musculoskeletal Radiology Fellowship, Philadelphia, PA, USA; [2]Thomas Jefferson University Hospital, Philadelphia, PA, USA

Poster #33 **IMAGING OF EPITHELIOID SARCOMA WITH PATHOLOGIC CORRELATION**
Mariam Malik, MD[1]; James Jelinek, MD[2]; Mark Kransdorf, MD[3]; Mark Murphey, MD[1]
[1]American Institute for Radiologic Pathology, Silver Spring, MD, USA; [2]MedStar Washington Hospital Center, Washington, DC, USA; [3]Mayo Clinic, Phoenix, AZ, USA

LOWER EXTREMITY

Poster #34 **WITHDRAWN**

Poster #35 **CURRENT CONCEPTS IN FOOT AND ANKLE TRAUMA: IMAGING FEATURES, HARDWARE AND COMPLICATIONS**
Zachary Ashwell, MD, MS; Hyo-Jeong Mulcahy, MD; Felix Chew, MD
University of Washington / Harborview Medical Center, Seattle, WA, USA

Poster #36 **IMAGING EVALUATION OF HEEL PAIN**
Sailaja Yadavalli, MD, PhD; Onowenerhi Omene, MD
Beaumont Health System, Royal Oak, MI, USA

Poster #37 **COMMUNICATION BETWEEN THE NAVICULOCUNEIFORM AND SECOND AND THIRD TARSOMETATARSAL ARTICULATIONS: UNDERAPPRECIATED NORMAL ANATOMY AND HOW IT MAY IMPACT FLUOROSCOPIC GUIDED INJECTIONS**
Barry Hansford, MD[1]; Megan Mills, MD[2]; Sarah Stilwill, MD[2]; Anna McGow, MD[2]; Chris Hanrahan, MD, PhD[2]
[1]Oregon Health Sciences University, Portland, OR, USA; [2]University of Utah Medical Center / SOM, Salt Lake City, UT, USA

Poster #38 **ADDED BENEFIT OF KNEE MRI VERSUS RADIOGRAPHS ALONE IN PATIENTS 60 YEARS AND OLDER**
Michael Fox, MD, MBA, FACR[1]; Jeremiah Long, MD[1]; Mark Kransdorf, MD[1]; Jonathan Flug, MD[1]; Ashtyn Chamberland[2]; Adam Schwartz, MD[1]
[1]Mayo Clinic Arizona, Phoenix, AZ, USA; [2]Grand Canyon University, Phoenix, AZ, USA

Poster #39 **ROUTINE KNEE MRI: HOW COMMON ARE PERIPHERAL NERVE ABNORMALITIES?**
Shivani Ahlawat, MD; Laura Fayad, MD
Johns Hopkins University, Baltimore, MD, USA

Poster #40 **INCIDENCE AND SPECIFICITY OF INTRALESIONAL FAT GLOBULES WITHIN MOREL-LAVALLEE LESIONS ABOUT THE KNEE**
Justin Friske, MD; Stephen Broski, MD
Mayo Clinic, Rochester, MN, USA

Poster #41 **MULTIMODAL IMAGING OF ACUTE TRAUMATIC BONE MARROW LESIONS IN THE KNEE: NEW INSIGHTS WITH HIGH RESOLUTION PERIPHERAL QUANTITATIVE CT**

Richard Walker, MD[1]; Andres Kroker, MS[2]; Mariya Shtil[2]; Sarah Manske, MS, PhD[1]; Nicholas Mohtadi, MD, MS[3]; Steven Boyd, MS, PhD[1]
[1]Department of Radiology, Cumming School of Medicine, University of Calgary, Calgary, AB, Canada; [2]University of Calgary, Calgary, AB, Canada; [3]University of Calgary Sport Medicine Centre, Calgary, AB, Canada

Poster #42 **EFFECT OF PATELLAR INSTABILITY ON EXTENSOR MECHANISM DYSFUNCTION**

Jehan Ghany, MD; Vishal Desai, MD; William Morrison, MD; Johannes Roedl, MD, PhD; Jeffrey Belair, MD; Adam Zoga, MD
Thomas Jefferson University Hospital, Philadelphia, PA, USA

Poster #43 **THE ANTERIORLY DISPLACED ACL STUMP: A FREQUENT FINDING BUT UNCOMMON CAUSE FOR A "LOCKED KNEE"**

Richard Walker, MD[1]; Andres Kroker, MS[2]; Peter Salat, MD[1]; Nicholas Mohtadi, MD, MS[3]
[1]Department of Radiology, Cumming School of Medicine, University of Calgary, Calgary, AB, Canada; [2]University of Calgary, Calgary, AB, Canada; [3]University of Calgary Sport Medicine Centre, Calgary, AB, Canada

Poster #44 **REDUCING UNNECESSARY KNEE MRI IN PATIENTS WITH KNOWN OSTEOARTHRITIS**

Dorian Nobbee, MD
University of Calgary, Calgary, AB, Canada

Poster #1

Cartilage Icing and Chondrocalcinosis in the Differentiation Between Gout and Pseudogout on Radiographs

Anna Falkowski, MD, MHBA; Jon Jacobson, MD
University of Michigan Medical Center, Ann Arbor, MI, USA
(Presented by: Anna Falkowski, MD, MHBA, University of Michigan Medical Center)

Purpose: The double-contour-sign or icing is a well-known ultrasound finding helping to differentiate gout from pseudogout (CPPD). Additionally, chondrocalcinosis is often described with pseudogout and also gout. The purpose of the study is to determine if cartilage icing and distribution of chondrocalcinosis on radiographs can differentiate between gout and pseudogout.

Materials and Methods: IRB approval was given and informed consent was waived for the retrospective study. Electronic medical records from >2.3 million patients were searched for key words (e.g. “gout”, “pseudogout”, “CPPD”, “joint aspiration”, and their combinations). Only aspiration-proven cases of gout or CPPD were included. Exclusion criteria were negation of these terms, postoperative cases, and cases with no available imaging. Radiographs were analyzed in consensus by two fellowship-trained musculoskeletal radiologists in randomized order, blinded to the patients’ diagnosis. Images were evaluated regarding presence or absence of icing-calcifications and chondrocalcinosis each for meniscus and hyaline cartilage separately for medial, lateral, anterior, and posterior compartment on knee radiographs. Presence of effusion was evaluated. Descriptive statistics, sensitivity, specificity, positive and negative predictive value were used for data evaluation.

Results: 55 patients were evaluated (34 male, 25 female; mean age 66±13 years) with 36 having an aspiration-proven diagnosis of pseudogout and 19 of gout. Cartilage icing was more common in pseudogout (3-36%) than gout (0-21%). Chondrocalcinosis had a positive predictive value of 89-100% to distinguish pseudogout from gout (100% at the lateral compartment), with only one gout patient (5%) showing chondrocalcinosis. 94.5% of patients had a joint effusion (100% pseudogout and 80% gout).

Conclusion: While cartilage icing is not helpful in differentiating gout from pseudogout, finding of chondrocalcinosis especially laterally involving hyaline cartilage and meniscus showed 100% positive predictive value in differentiating pseudogout from gout. Joint effusion without trauma should raise awareness for possible crystal deposition disease.

Modality % - Radiography / Fluoroscopy:	100
Modality % - CT:	0
Modality % - MRI:	0
Modality % - US:	0
Modality % - Nuclear Medicine:	0

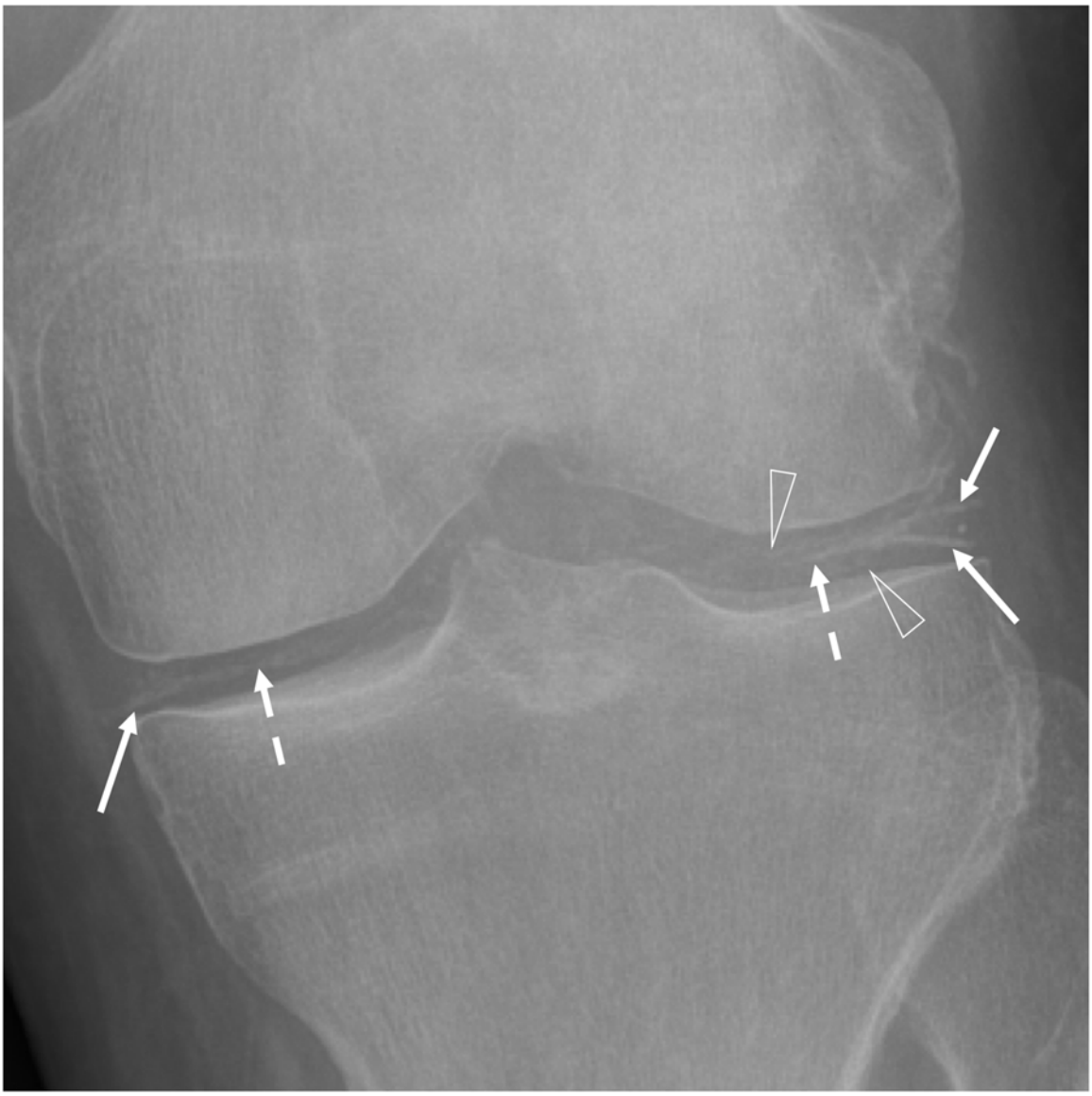

Cartilage icing at menisci (arrows) and hyaline cartilage (dashed arrows). Chondrocalcinosis with diffuse calcifications within hyaline cartilage (open arrowheads), especially lateral. Joint aspiration revealed CPPD.

Poster #2

MUSCULOSKELETAL MANIFESTATIONS OF DIABETES MELLITUS: A REVIEW FOR THE PRACTICING RADIOLOGIST AND RADIOLOGIST IN TRAINING, WITH EMPHASIS ON CLINICAL PRESENTATION, PATHOGENESIS, AND IMAGING APPEARANCE.

Alexander Grushky, MD[1]; David Marcantonio, MD[1]; Jonathan Im, MS[2]
[1]Beaumont Health System, Royal Oak, MI, USA; [2]Michigan State Univeristy College of Human Medicine, Grand Rapids, MI, USA
(Presented by: Alexander Grushky, MD, Beaumont Health System)

Purpose: To review and highlight the musculoskeletal manifestations of diabetes mellitus (DM), including osteomyelitis, neuropathic arthropathy, diabetic myonecrosis, and dialysis-associated spondyloarthropathy. The imaging appearance of these various entities will be highlighted at commonly encountered locations, including the spine, thigh, and foot. This exhibit also will provide a useful and relevant review of the clinical presentation and pathogenesis of the various DM-related entities. Emphasis will be placed on features that may help distinguish these entities from other similar appearing processes, with the goal of avoiding unnecessary patient imaging, intervention, and morbidity.
Materials and Methods: This exhibit will review the clinical presentation and multi-modality imaging appearance of DM-related musculoskeletal pathology using a practical case-based approach, with the goal of educating the practicing radiologist and radiologist in training to facilitate early and accurate recognition of these conditions.
Results: Diabetes mellitus is one of the most common chronic disease processes in the body and has a wide range of musculoskeletal manifestations which must be recognized by the practicing radiologist and radiologist in training. This exhibit will provide education regarding common diabetes mellitus related musculoskeletal pathologic conditions, sites of occurrence, and multimodality imaging appearance.
Conclusion: Diabetes mellitus involves the musculoskeletal system through a variety of pathologic entities which require accurate and prompt diagnosis to avoid severe, and potentially fatal, complications. Given the prevalence of diabetes mellitus in the general population, an increased understanding of the DM-related musculoskeletal pathology spectrum will help the practicing radiologist and radiologist in training recognize these entities and provide swift diagnosis allowing adequate and appropriate treatment.

Modality % - Radiography / Fluoroscopy:	10
Modality % - CT:	45
Modality % - MRI:	45
Modality % - US:	0
Modality % - Nuclear Medicine:	0

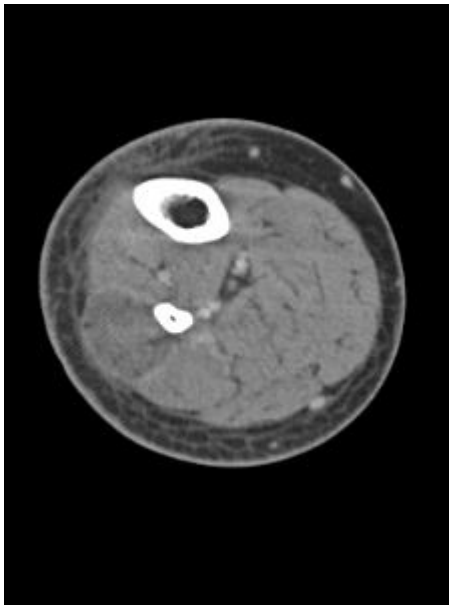

Enlargement and relative hypodensity of the peroneal muscles with bulging of the fascia superficial to the musculature and deep to the subcutaneous tissues.

Poster #3

PERIPROSTHETIC JOINT INFECTIONS

Kimia Kani, MD[1]; Jack Porrino, MD[2]; Hyojeong Mulchay, MD[3]; Felix Chew, MD[3]
[1]University of Maryland School of Medicine, Baltimore, MD, USA; [2]Yale University School of Medicine, New Haven, CT, USA;
[3]University of Washington / Harborview Medical Center, Seattle, WA, USA
(Presented by: Kimia Kani, MD, University of Maryland School of Medicine)

Purpose: Background information/purpose:

Periprosthetic infections are a frequent cause of implant failure occurring in approximately 5% of cases. Periprosthetic infections are more common in open relative to closed fracture fixations and in revision versus primary arthroplasties.

Materials and Methods: Educational goals:

1. Define and classify periprosthetic infections
2. Recognize the imaging spectrum of implant infection on different imaging modalities
3. Recognize the expected appearance and complications of the various surgical modalities used to treat periprosthetic infections on imaging

Results: Key issues:

1. Definition of periprosthetic infection with emphasis on the Musculoskeletal Infection Society (MSIS) criteria
2. Epidemiology, pathogenesis, and classification of orthopedic implant infections
3. Imaging findings of implant infection and differential diagnosis
4. Operative techniques for management of periprosthetic infections, including polyethylene exchange with component retention, replacement arthroplasty (1 or more commonly 2 stage), resection arthroplasty, arthrodesis and amputation
5. Expected appearance and complications of the above techniques on imaging
6. Imaging appearance of antibiotic impregnated spacers with emphasis on the different types of articulating spacers

Conclusion: Periprosthetic infections are a frequent cause of implant failure. Recognizing the imaging spectrum of implant infection on different imaging modalities along with the expected appearance and complications of the various surgical modalities used to treat periprosthetic infections is necessary for accurate interpretation of images.

Modality % - Radiography / Fluoroscopy:	80
Modality % - CT:	10
Modality % - MRI:	10
Modality % - US:	0
Modality % - Nuclear Medicine:	0

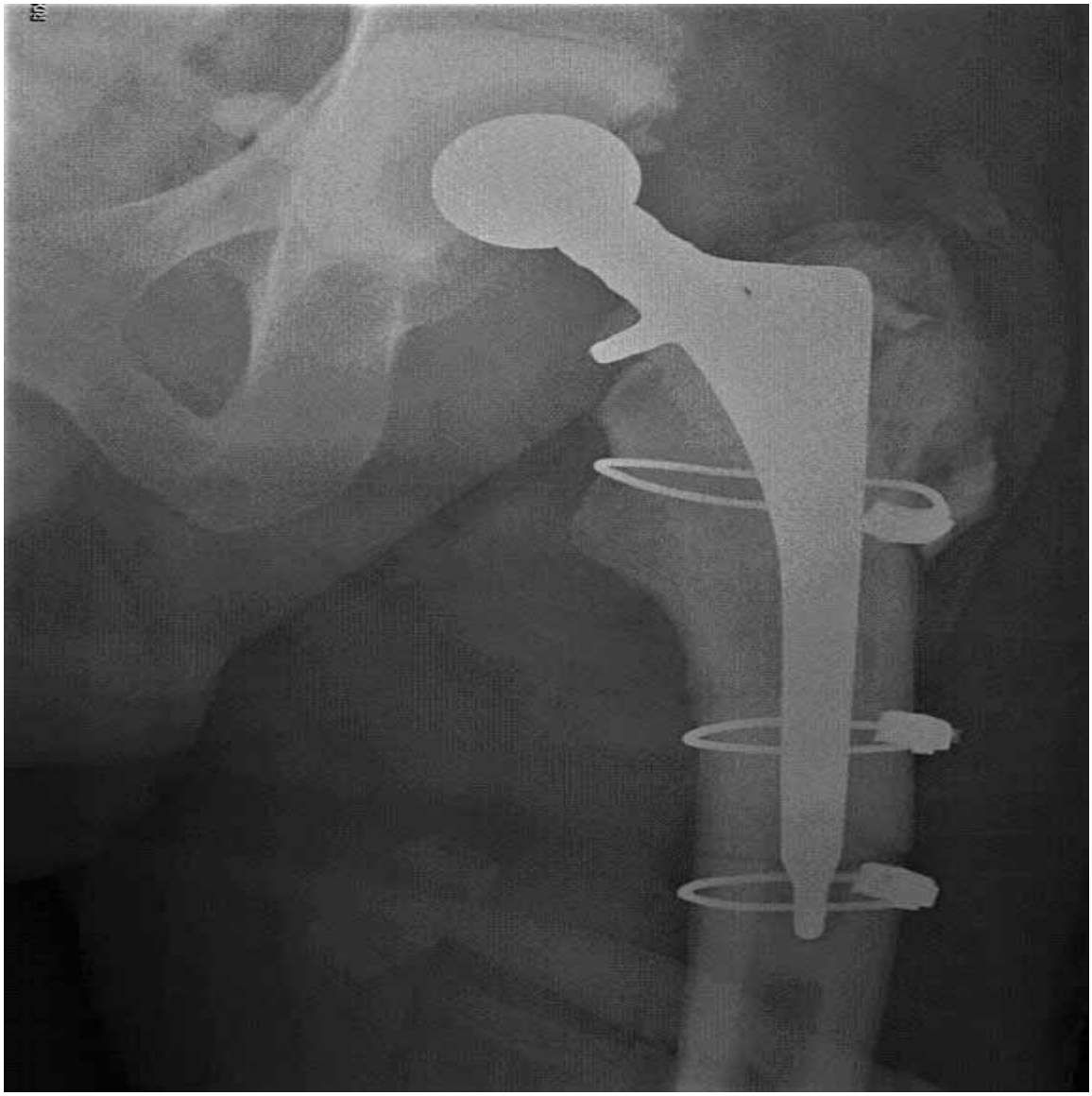

Temporary PROSTALAC (prosthesis with antibiotic-loaded acrylic cement) total hip arthroplasty for infected total hip arthroplasty

Failed prosthetic hip and knee infections status post multiple revisions for infection. Fracture of the femoral spacer and abscess (arrow) at level of knee stump

Poster #4

EXTERNAL FIXATORS: LOOKING BEYOND THE HARDWARE MAZE

Kimia Kani, MD[1]; Jack Porrino, MD[2]; Hyojeong Mulcahy, MD[3]; Felix Chew, MD[3]
[1]University of Maryland School of Medicine, Baltimore, MD, USA; [2]Yale University School of Medicine, New Haven, CT, USA;
[3]University of Washington / Harborview Medical Center, Seattle, WA, USA
(Presented by: Kimia Kani, MD, University of Maryland School of Medicine)

Purpose: Background information:

External fixators have multiple orthopedics applications. Appropriate use along with early recognition and correction of complications of these constructs can lead to excellent results.

Materials and Methods: Educational goals:

1. Describe indications, biomechanics and biology of external fixators
2. Define frame types and components
3. Recognize the techniques of bone transport
4. Accurately evaluate external fixator frames and their complications on imaging

Results: Key issues:

1. Indications: Damage control external fixation and reconstructive orthopedics
2. Frame types: Dynamic versus static fixators; Monolateral, circular or hybrid fixators
3. Frame components: Pins, transfixion wires, longitudinal bars, circular rings
4. Biomechanics and biology of compression osteosynthesis and distraction osteogenesis
5. Bone transport: Technique and imaging evaluation
6. Imaging assessment of fracture and distraction sites prior to frame removal: What to look for
7. Imaging evaluation of external fixator complications

Conclusion: Familiarity with the biomechanics, designs, frame components, and complications of external fixators is necessary for accurate image interpretation.

Modality % - Radiography / Fluoroscopy:	80
Modality % - CT:	10
Modality % - MRI:	10
Modality % - US:	0
Modality % - Nuclear Medicine:	0

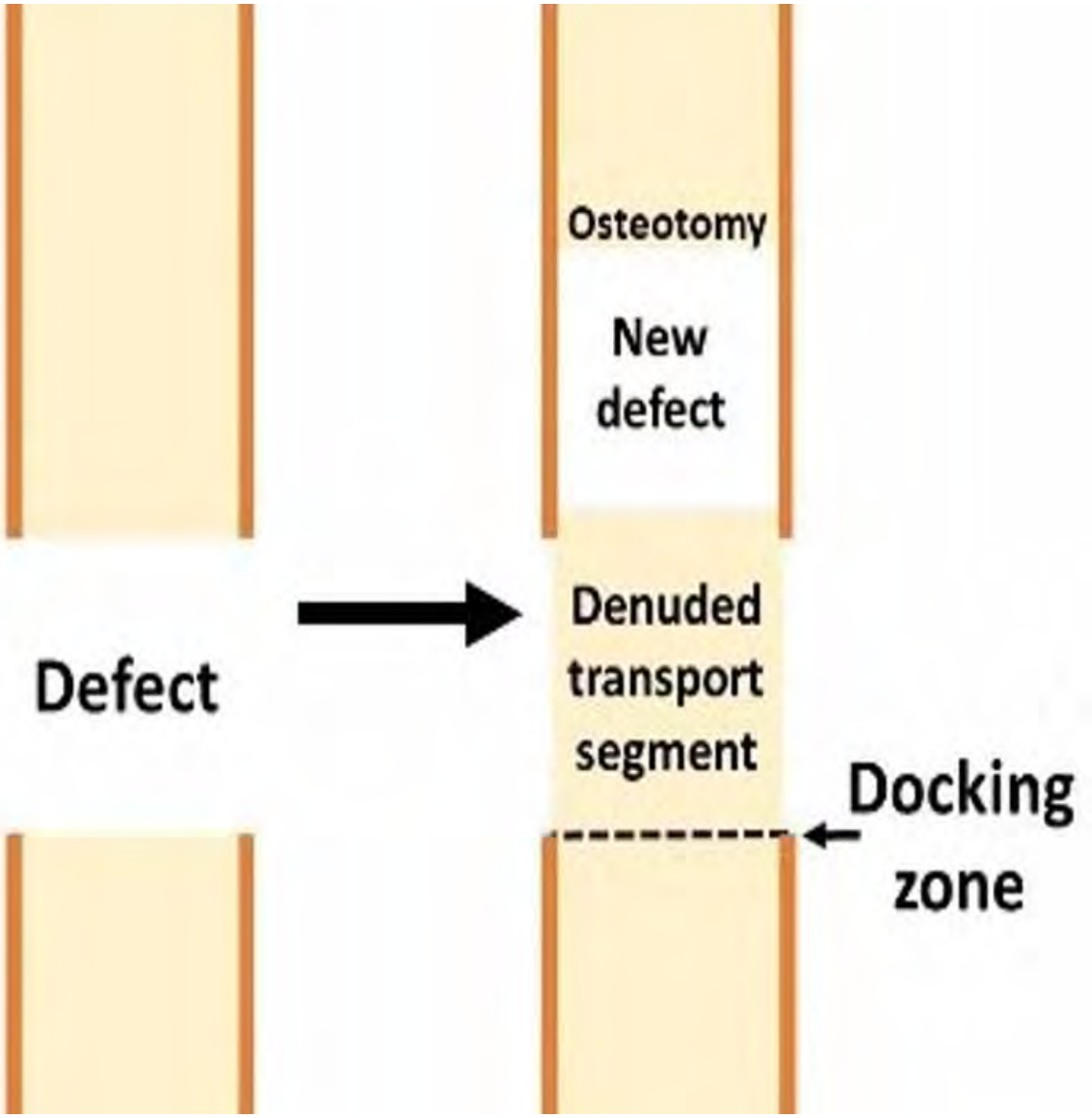

Simple illustration of bone transport

Double bone transport using the Ilizarov circular fixator

Poster #5

GUN VIOLENCE AND RADIOLOGY UTILIZATION AT A MAJOR CITY ACADEMIC CENTER

William Morrison, MD; Ankit Gandhi, MD; Corbin Pomeranz, MD; Lauren Brown, MD; Kimberly Klinger, MD; Adam Zoga, MD; Johannes Roedl, MD; Jeffrey Belair, MD; Suzanne Long, MD
Thomas Jefferson University Hospital, Philadelphia, PA, USA
(Presented by: William Morrison, MD, Thomas Jefferson University Hospital)

Purpose: National health databases lack substantial information related to gun violence. We sought to assess the demographics, injury patterns, and radiology utilization in patients with gunshot injuries at our institution.

Materials and Methods: A retrospective analysis was performed by searching our radiology reports database for gunshot wound (GSW)-related imaging exams from January 2016 to April 2018. Keywords 'gunshot wound', 'GSW', 'bullet', 'shrapnel', 'buckshot', and 'pellet' were included. Studies without acute or remote history of GSW and without evidence of retained shrapnel were excluded. Data were classified into acute and remote gun-related injury. Radiologic exam modality, injury location, patient age and sex were recorded.

Results:

Over the study period 960 patients with gunshot wound underwent 1869 imaging exams. The average patient age for the acute gunshot injury category is 31 (SD 13). Men account for 93% of acute and 89% of remote GSW injuries. Most common modalities used, regardless of injury chronicity, are radiographs (acute N=257, remote N=941) and computed tomography (acute N=146, remote N=407). A total of 432 imaging studies were performed for acute GSW-related trauma on 120 patients, yielding approximately 4 studies per patient. A total of 1437 studies performed on 840 patients show sequelae of remote gunshot injury with the majority demonstrating retained bullets/shrapnel. The most common site of injury is the musculoskeletal system (N=579), followed by the chest (N=577) and the abdomen (N=374).

Conclusion: Healthcare cost, morbidity, and mortality related to gun violence can only be assessed after attaining a more complete understanding of demographics, injury patterns, hospitalization and radiology utilization. By characterizing these fundamental aspects of gunshot injuries, we hope our study contributes to defining gun violence as a public health issue. Data collection is ongoing and future plans include collaborating with regional trauma centers, categorizing injuries using ICD-10 codes to analyze hospitalization costs, impact on healthcare and determining patient outcome.

Modality % - Radiography / Fluoroscopy:	70
Modality % - CT:	28
Modality % - MRI:	2
Modality % - US:	0
Modality % - Nuclear Medicine:	0

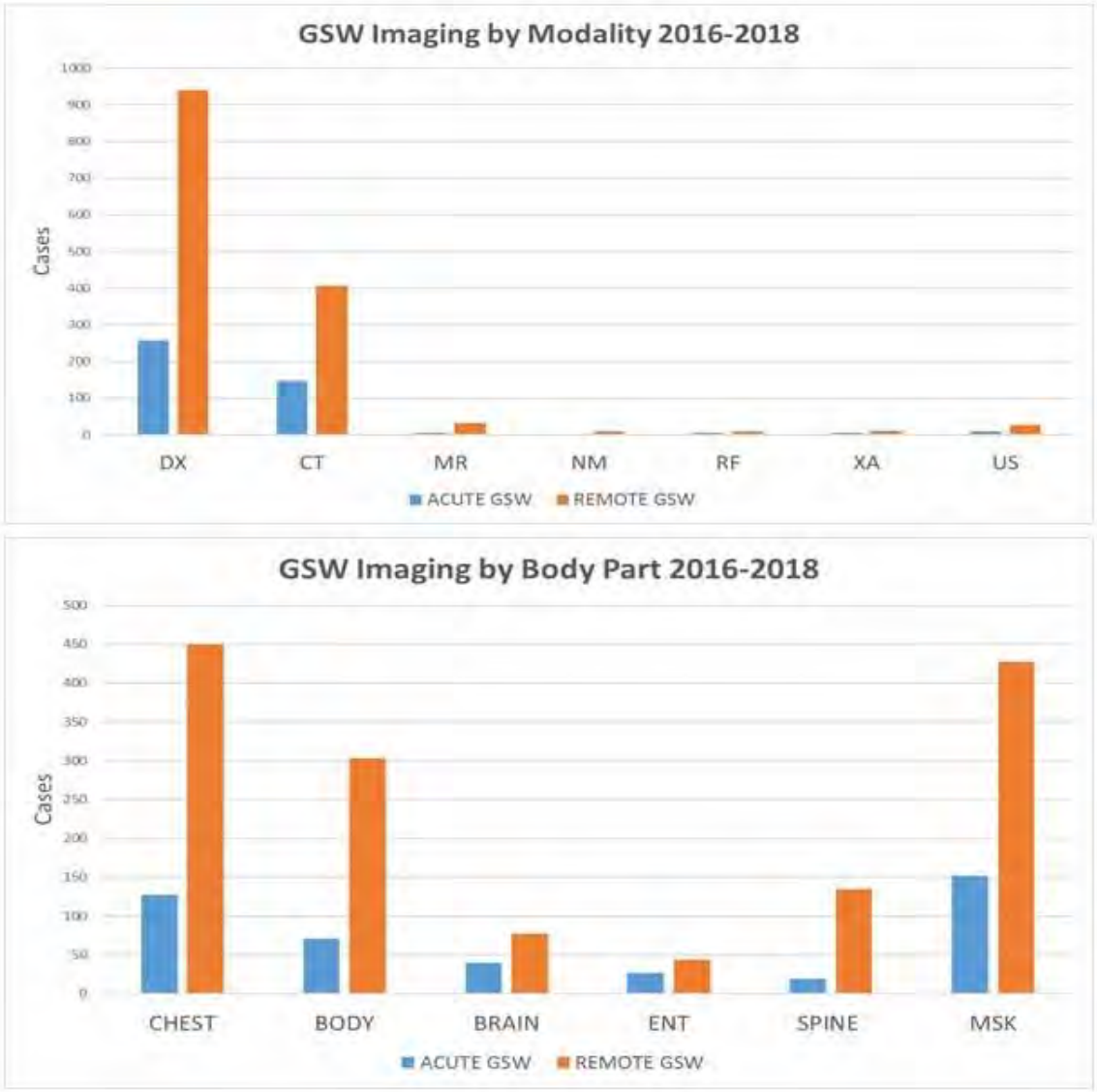

Fig. 1. Radiology utilization in patients with acute or prior gunshot wound

Poster #6

DON'T MISS THE BULL'S-EYE: MRI APPEARANCE OF LYME DISEASE ARTHRITIS

Sean Cleary, MD; Johnny Monu, MBBS, MD; Gregory Dieudonne, MD; Scott Schiffman, MD
The University of Rochester School of Medicine and Dentistry, Rochester, NY, USA
(Presented by: Sean Cleary, MD, The University of Rochester School of Medicine and Dentistry)

Purpose: Lyme disease is a relatively common clinical entity with an estimated annual incidence of 300,000 in the US. The manifestations of Lyme disease in the musculoskeletal system are rarely described in the radiology literature. Some patient's don't present with the classic Bull's-eye rash (erythema migrans) and instead come to medical attention with nonspecific myalgias and arthralgias as a late stage manifestation. This presentation reviews the imaging findings associated with Lyme disease arthritis especially focused on MRI. The epidemiology and clinical manifestations will also be discussed so as to arouse a proper suspicion and a confident diagnosis by the practicing radiologist in an appropriate setting.

Materials and Methods: A retrospective review of the radiology and pathology databases was performed to evaluate for patients with a diagnosis of Lyme disease arthritis. Patients were included with positive serology for Lyme disease (positive Lyme C6 Peptide Antibody) or synovectomy with pathologic findings of Lyme disease.

Results: 6 patients (4 females and 2 males) aged between 16-68 years who have had MR imaging with laboratory proven Lyme disease were identified. Extensive diffuse synovitis appeared as a common feature. Adenopathy and pericapsular soft tissue edema were also encountered. All our patients presented with arthralgias which were initially ascribed to other etiologies. The imaging features overlapped with inflammatory and infectious etiologies of arthritis with imaging examples most strikingly appearing similar to rheumatoid arthritis, reactive arthritis and PVNS.

Conclusion: Knowledge of the imaging appearance of Lyme disease arthritis especially extensive diffuse synovitis, pericapsular edema and adenopathy may help aid in diagnosing Lyme disease arthritis in the appropriate clinical setting.

Modality % - Radiography / Fluoroscopy:	10
Modality % - CT:	0
Modality % - MRI:	90
Modality % - US:	0
Modality % - Nuclear Medicine:	0

Fat saturated coronal T1-W image from an MR arthrogram of the right hip demonstrates marked synovial thickening (intra-articular foci hypointense to muscle).

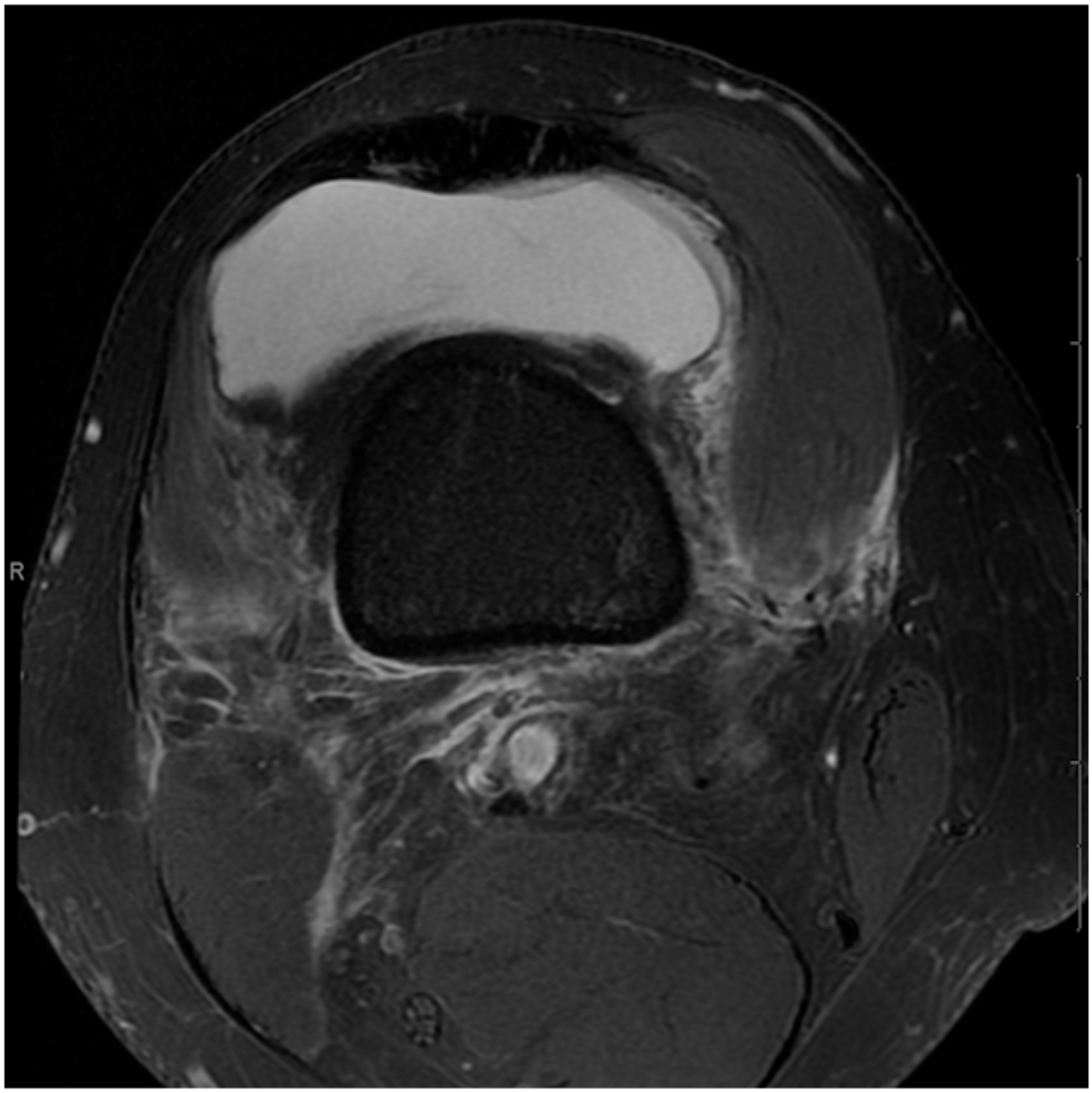

Fat saturated axial T2-W image of the right knee demonstrating a large joint effusion with synovitis and adjacent edematous changes in the quadriceps.

Poster #7

MUSCULOSKELETAL MANIFESTATIONS OF SCLERODERMA ON MRI AND ULTRASOUND

Emily Casaletto, BS; Ogonna Nwawka, MD; Alissa Burge, MD
Hospital for Special Surgery, New York, NY, USA
(Presented by: Emily Casaletto, BS, Hospital for Special Surgery)

Purpose: To show the breadth of musculoskeletal abnormalities that can be detected using MRI and US in patients with scleroderma.

Materials and Methods: Between January 1, 2003 and September 19, 2018, a search of the radiology imaging system was performed to identify the patients with scleroderma that had undergone MRI and US imaging of the wrist and hand. A retrospective review of the patients' medical records, including medical imaging, reports, and clinician notes, was performed. MRI and US reports were reviewed for indications of synovitis, tenosynovitis, erosions, hyperemia, pulley or skin thickening, skin ulceration, vascular abnormalities, and bursitis.

Results: A total of 27 MRI exams and 29 US exams were conducted of the wrist and hand of the HSS scleroderma patient population over the last 15 years. Six MRI exams reported 10 cases of synovitis, most commonly at the radioulnar joint (2 exams) and pisotriquetral joint (2 exams). Sixteen US exams reported 33 cases of synovitis, most commonly at the metacarpophalangeal joint (13 exams), carpal joint (10 exams), and interphalangeal joint (7 exams). Seven MRI exams reported 10 cases of tenosynovitis, which was present at the flexor muscles in 4 exams and at the extensor muscles in 6 exams. Eleven US exams reported 12 cases of tenosynovitis, which was present at the flexor muscle in 8 exams and the extensor muscle in 4 exams. Both MRI and US exams reported osseous erosions, skin ulceration and skin thickening. Only MRI characterized vascular abnormalities, and bursitis. Pulley thickening was only reported on US. US also characterized synovial hyperemia.

Conclusion: This is a descriptive report on the musculoskeletal manifestations that may be visualized in scleroderma patients using MRI and US. Information from these imaging modalities may be useful in monitoring scleroderma symptoms and disease course over time. Future studies should correlate musculoskeletal imaging abnormalities with scleroderma disease severity.

Modality % - Radiography / Fluoroscopy:	0
Modality % - CT:	0
Modality % - MRI:	50
Modality % - US:	50
Modality % - Nuclear Medicine:	0

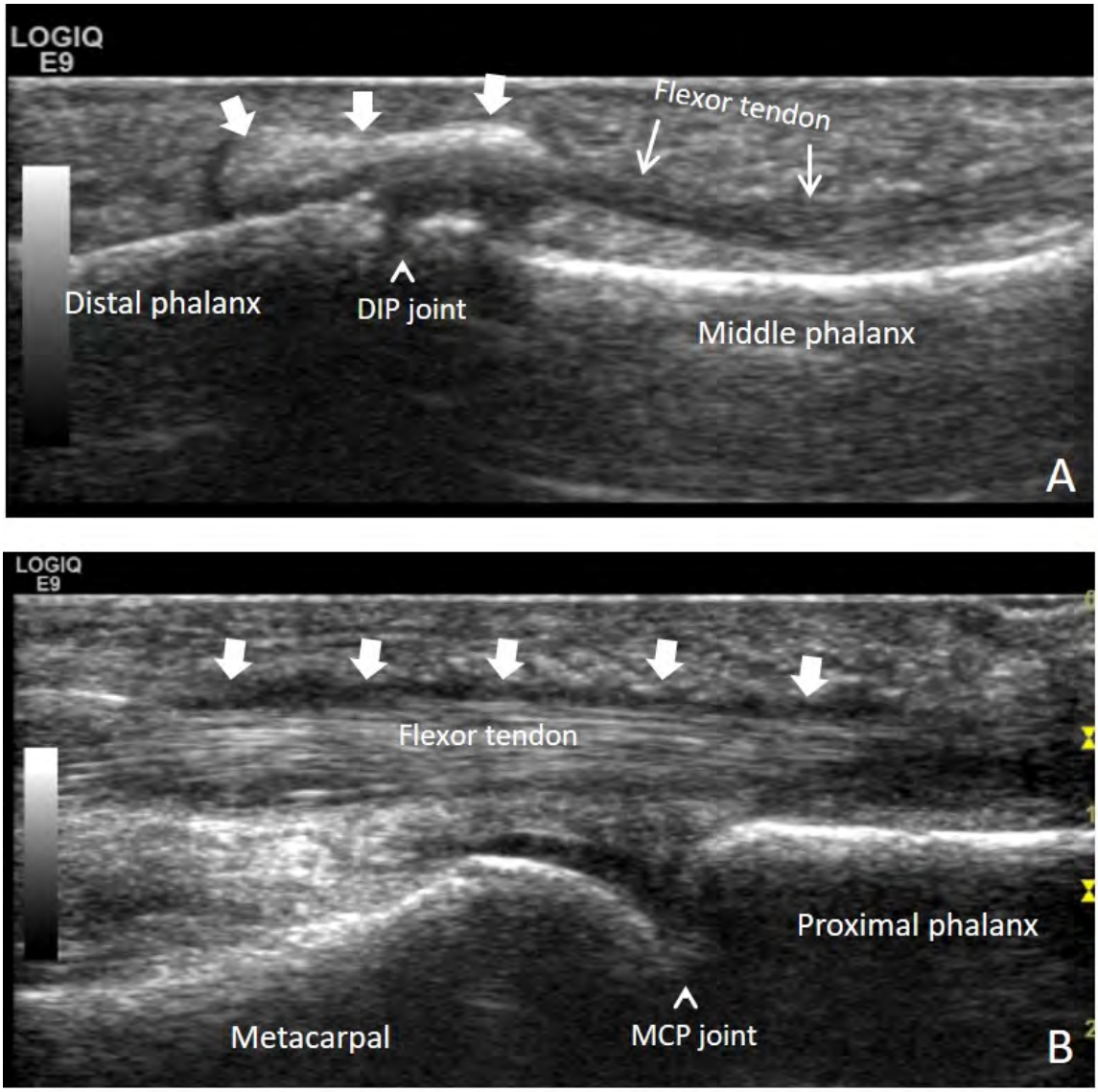

Tendinopathy on ultrasound in scleroderma. A) Mineralization (block arrows) along a finger flexor tendon. B) Tendon sheath thickening (block arrows) along a finger flexor tendon.

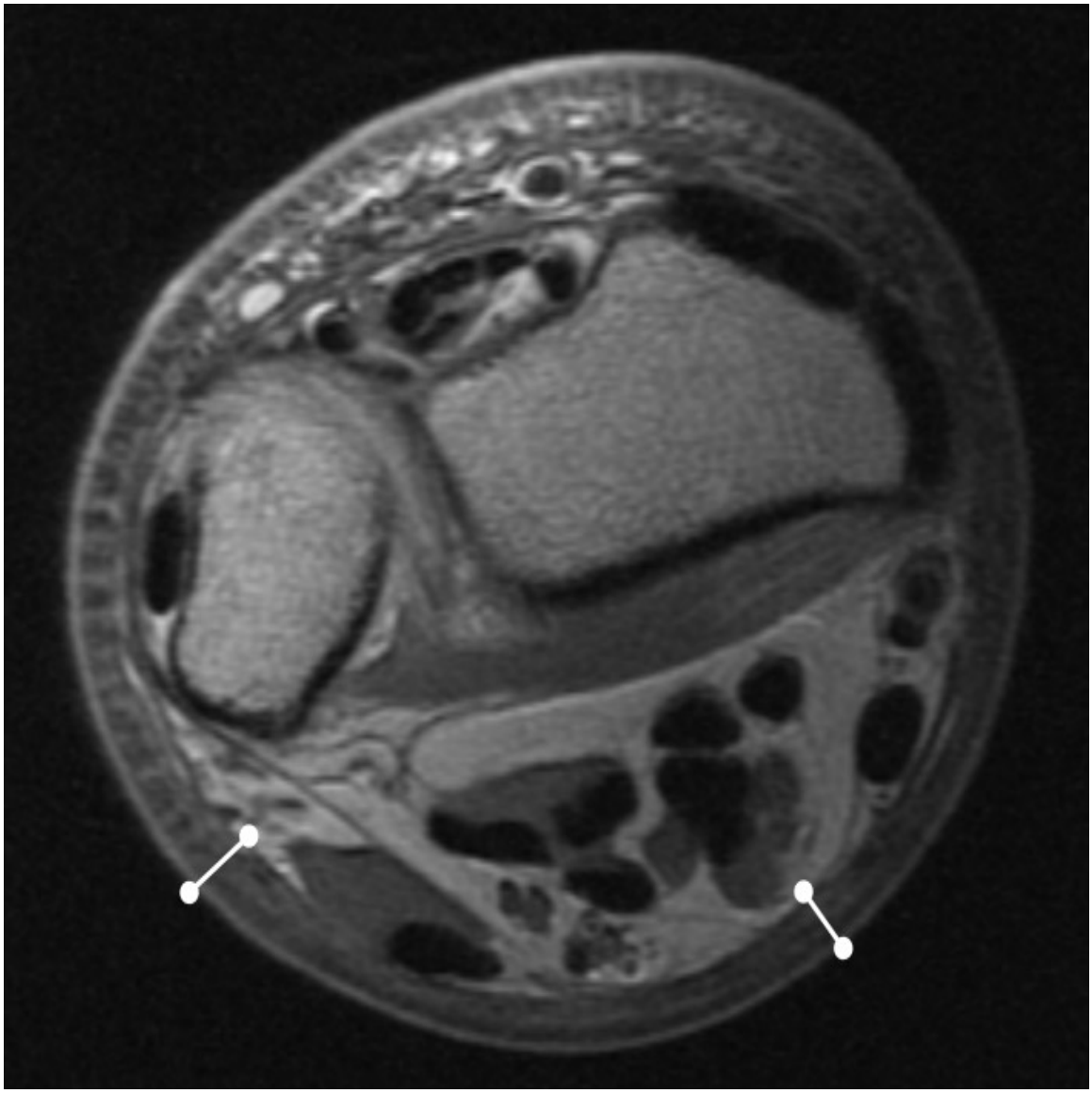

Skin thickening in scleroderma on MRI. Axial PD image in demonstrates marked circumferential skin thickening (calipers) at the wrist.

Poster #8

HYBRID 18F-FDG PET/MR IN THE EVALUATION OF PEDAL OSTEOMYELITIS

Margaret Kincaid, MD[1]; Stephen Broski, MD[1]; Drake McArthur, MD[2]; Erik Weiss, MD[3]
[1]Mayo Clinic, Rochester, MN, USA; [2]Tulane University Health Sciences Center, New Orleans, LA, USA; [3]Phoenix VA Medical Center, Phoenix, AZ, USA
(Presented by: Margaret Kincaid, MD, Mayo Clinic)

Purpose: To evaluate the accuracy of hybrid ^{18}F-FDG PET/MR in the detection of pedal osteomyelitis.

Materials and Methods: A retrospective review was performed in patients who received an ^{18}F-FDG PET/MRI for suspected pedal osteomyelitis between 1/1/16 and 3/31/18. Patients with a corresponding bone biopsy within six weeks of PET/MR were selected for further review. 77 cases met these inclusion criteria. PET, MR and fusion images were analyzed. MR positivity was defined as confluent, marrow-replacing T1 hypointense signal in bone. PET positivity was defined as FDG uptake in bone above background marrow. SUVmax for normal bone was determined from an ROI drawn in the posterior calcaneus or distal tibia.

Results: 74 cases were biopsy-positive for osteomyelitis. The three biopsy-negative cases were negative by both PET and MR. 63/74 biopsy-positive cases were positive by PET and MR. Eight biopsy-proven cases were MR-negative, but PET-positive and demonstrated edema on T2-weighted images. One biopsy-proven case demonstrated pronounced confluent T1 hypointense signal but was PET-negative, favored to reflect osteomyelitis with gangrene. Two additional cases were biopsy-positive, MR (T1) and PET negative, but exhibited bone marrow edema. There were no cases that appeared positive by imaging with a negative biopsy result. In cases that subjectively appeared PET-positive, the mean SUVmax for affected bone was 3.8+/-2.1 (range 0.9-11.2) and mean SUVmax of background normal bone was 0.2+/-0.1. 18 PET-positive/biopsy-proven exams had an SUVmax < 2.5.

Conclusion: In the detection of pedal osteomyelitis, the accuracy of hybrid PET/MR (97%) proved superior to MR (87%) alone. The large range of SUV values corresponding to biopsy-proven osteomyelitis suggests that SUVmax thresholds commonly employed in oncologic PET/CT are insensitive for pedal osteomyelitis. Further, the results indicate that qualitatively increased FDG activity above background marrow activity may be sufficient for diagnosing osteomyelitis in the correct clinical setting.

Modality % - Radiography / Fluoroscopy:	0
Modality % - CT:	0
Modality % - MRI:	50
Modality % - US:	0
Modality % - Nuclear Medicine:	50

Poster #9

ULTRASOUND IMAGING OF NERVES IN THE NECK: CORRELATION TO MRI, ELECTRODIAGNOSTIC AND CLINICAL FINDINGS

Ogonna Nwawka, MD; Emily Casaletto, BS
Hospital for Special Surgery, New York, NY, USA
(Presented by: Ogonna Nwawka, MD, Hospital for Special Surgery)

Purpose: To assess the diagnostic performance of ultrasound (US) and magnetic resonance imaging (MRI) for imaging nerves in the neck.

Materials and Methods: Between January 1, 2016 and September 19, 2018, a search of the radiology imaging system was performed to identify patients that had undergone US of the long thoracic, phrenic, spinal accessory, or suprascapular nerve. A retrospective review of the patients' medical records was performed, including medical imaging and reports, electrodiagnostic (EDX) reports, and clinician notes. The diagnosis to the relevant nerve made with US, MRI, and clinical examination was recorded. MRI and clinical diagnoses were compared with US diagnoses for agreement. Any limitations encountered during imaging were also recorded.

Results: Within the search period, 56 patients presented at our institution for evaluation of the long thoracic, phrenic, spinal accessory, or suprascapular nerve. Five patients underwent US examination that commented on two or more nerves, resulting in 61 total cases in the present study. The target nerve was successfully visualized using US in 53 of the 61 total US cases (87%). When the target nerve was visualized by US, there was agreement between US and clinical diagnosis on the presence of an abnormality in 50 cases (91%). MRI evaluation was performed in 57 of the 61 US cases and MRI successfully visualized the target nerve in 47 (82%) of these cases. When the target nerve was visualized by both modalities, there was agreement between US and MRI on the presence of an abnormality in 41 cases (93%).

Conclusion: This retrospective review demonstrated that both US and MRI are highly successful in imaging nerves in the neck, and demonstrate excellent agreement with clinical and EDX findings.

Modality % - Radiography / Fluoroscopy:	0
Modality % - CT:	0
Modality % - MRI:	50
Modality % - US:	50
Modality % - Nuclear Medicine:	0

Photograph depicts the spinal accessory nerve (SAN) course in the posterior triangle (dashed line). The US transducer can be placed here to detect the SAN.

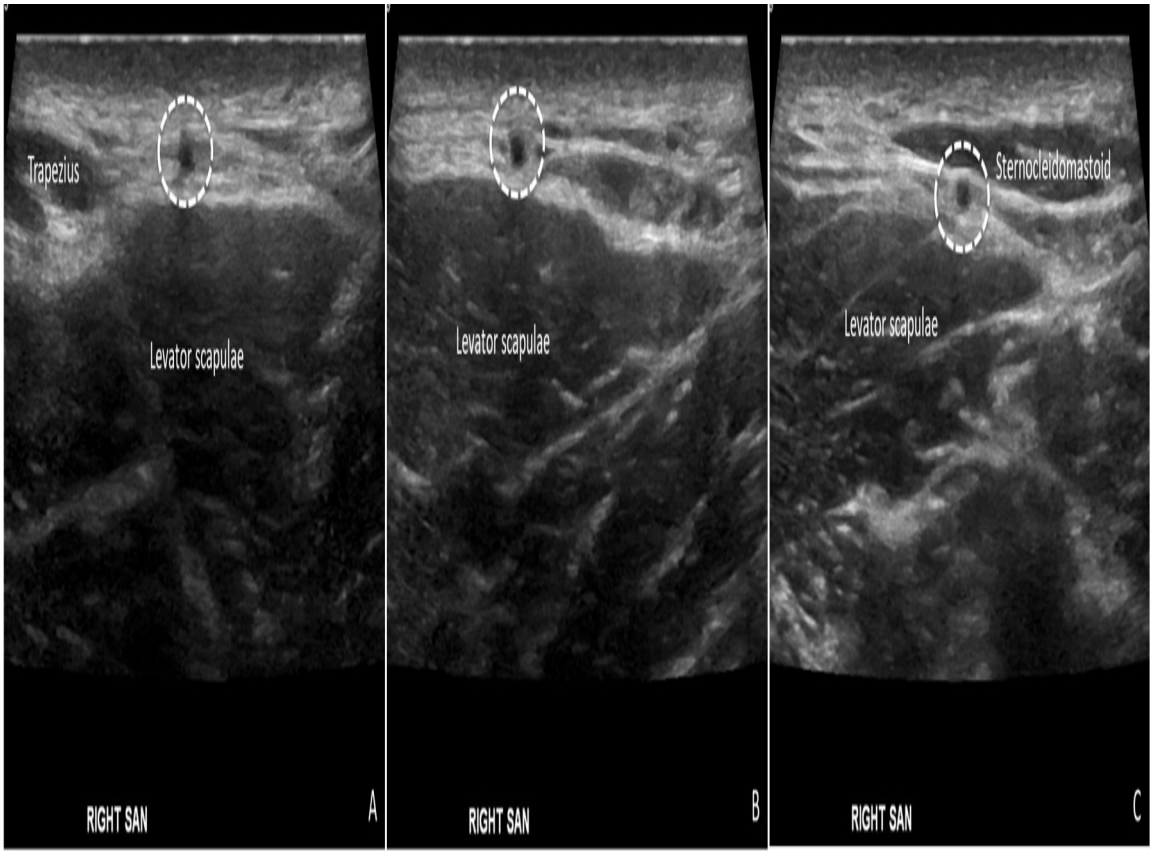

Transverse (A-C) US images demonstrate the spinal accessory nerve (circle) from the trapezius muscle (A), over the levator scapulae muscle (B), to the sternocleidomastoid muscle.

Poster #10

Compressed Sensing Magnetic Resonance Imaging (CS-MRI) of the Knee: Assessment of Quality, Inter-reader Agreement, and Time Savings

George Matcuk, Jr., MD; Jordan Gross, MD; Brandon Fields, BA, BM; Steven Cen, PhD
KECK School of Medicine of USC, Los Angeles, CA, USA
(Presented by: George Matcuk, Jr., MD, KECK School of Medicine of USC)

Purpose: To compare 3 Tesla (3T) compressed sensing (CS) magnetic resonance imaging (MRI) of different pulse sequences with various acceleration factors to standard fast spin echo (FSE) sequences in terms of time, quality, and inter-reader agreement.

Materials and Methods: 10 clinical patients scheduled for knee 3T MRI examinations (Canon Vantage Titan) were prospectively enrolled into the study. In addition to the routine clinical FSE MRI sequences, additional compressed sensing axial proton density (PD) fat saturation (FS), coronal T1 and sagittal T2 FS sequences were obtained with acceleration factors of 2.0, 2.4, 2.7, and 3.0 for each sequence. These images were then anonymized and randomized and reviewed by two musculoskeletal radiologists. Each sequence in the set was qualitatively ranked and then qualitatively scored for blurring, artifact, low contrast detection, noise pattern, signal-to-noise ratio, and overall quality.

Results: Although the routine sequence had a higher mean qualitative ranking compared to the CS-MRI sequences, all were scored as good or very good for each of the quality categories. Inter-reader agreement for the qualitative ranking was poor, but fair for blurring, moderate for artifacts, and good for all other quality score categories.

Conclusion: The CS-MRI sequences demonstrated excellent overall quality compared to routine FSE sequences with overall good inter-reader agreement. The time savings from using CS-MRI sequence as part of a knee 3T MRI protocol could be used to increase patient throughput, obtain higher resolution images, or add additional sequences such as T2 mapping without affecting diagnostic quality.

Modality % - Radiography / Fluoroscopy:	0
Modality % - CT:	0
Modality % - MRI:	100
Modality % - US:	0
Modality % - Nuclear Medicine:	0

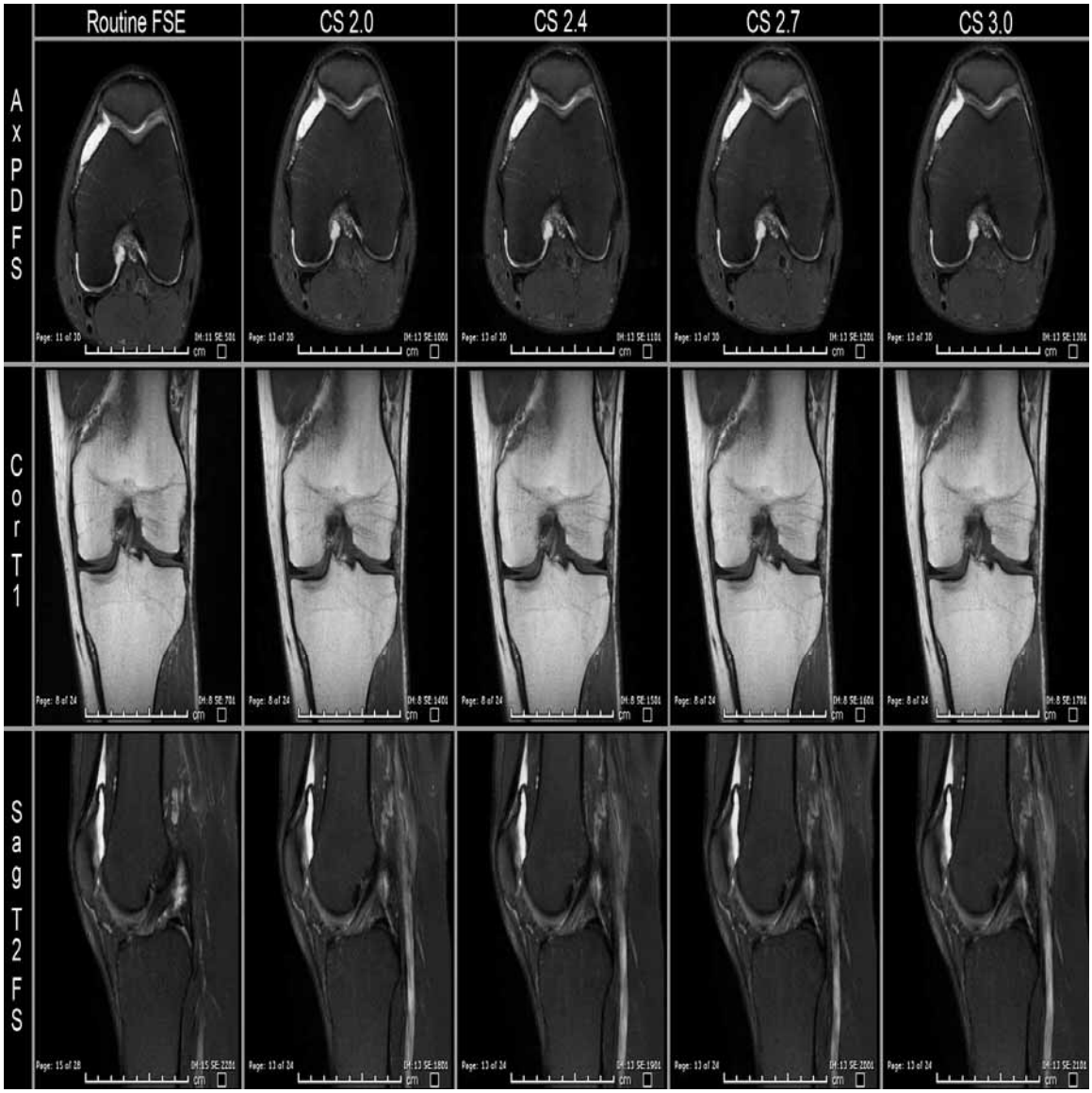

Fig. 1 Sample image of routine fast spine echo (FSE) and each compressed-sensing (CS) MRI sequence and acceleration factor is presented for each sequence

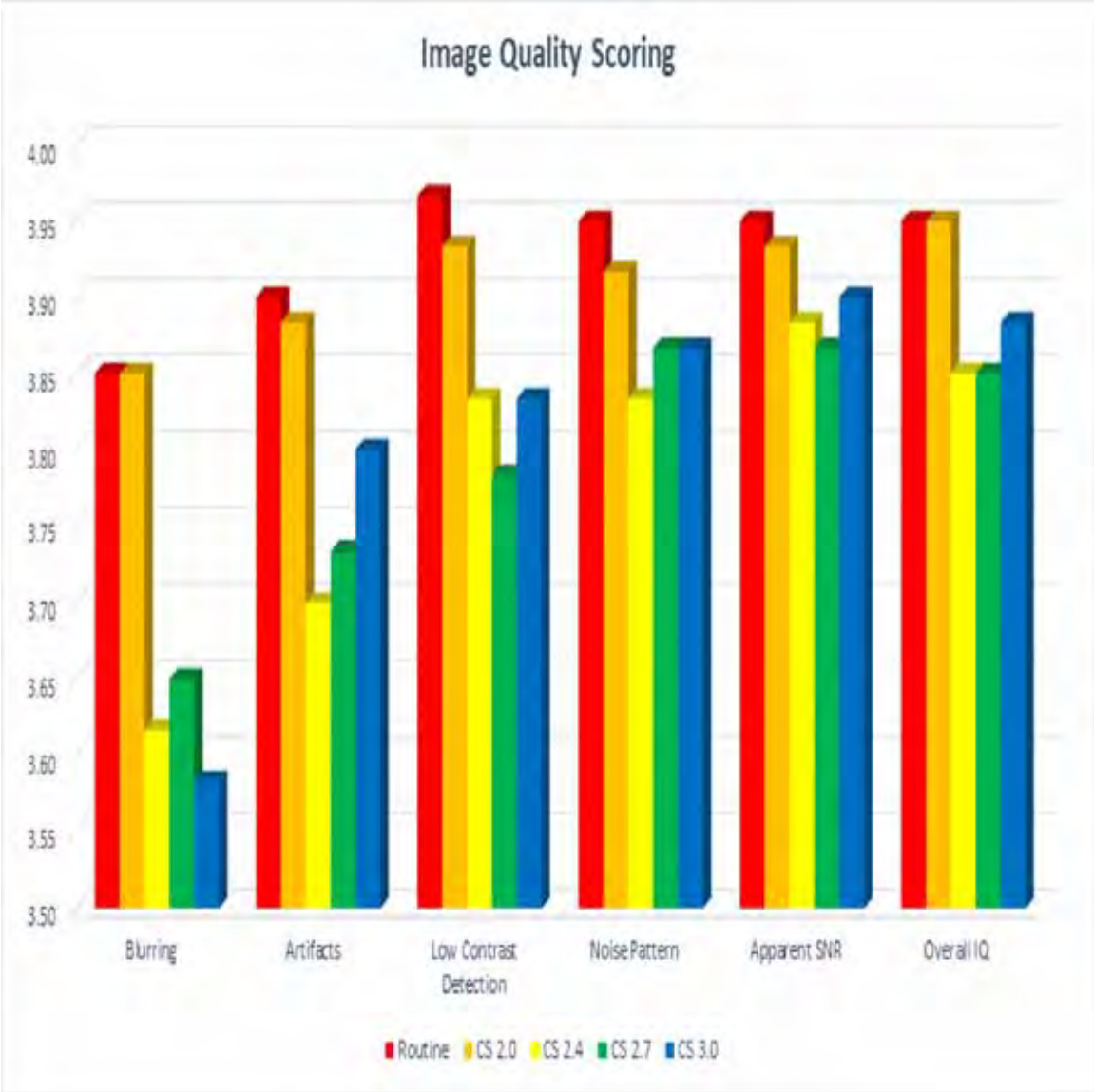

Fig. 2 Overall image quality scores for each category (x-axis labels) for the routine FSE sequences versus each CS-MRI sequence acceleration factor

Poster #11

NEXT-GENERATION 5-MIN KNEE MRI WITH COMBINED SIMULTANEOUS MULTI-SLICE AND PARALLEL IMAGING ACCELERATION

Jan Fritz, MD; Ali Rashidi, MD; Miho Tanaka, MD; Filippo Del Grande, MD
Johns Hopkins University, Baltimore, MD, USA
(Presented by: Jan Fritz, MD, Johns Hopkins University)

Purpose: 2-fold parallel imaging (PI) acceleration can realize 5-min 2D FSE MRI of the knee, but the associated signal loss may require compromises in image quality and anatomical coverage. In contrast, 2-fold simultaneous multi-slice (SMS) acceleration is near signal neutral. Advances in pulse sequence design now allow for the combined use of PI and SMS enabling 4-fold-accelerated 2D FSE, which can achieve fast MRI with higher image quality and improved coverage. We compared traditional 2-fold PI- and novel 4-fold SMS-PI-accelerated 2D FSE MRI of the knee for the detection of internal derangement.

Materials and Methods: Following IRB approval and informed consent, 25 symptomatic patients [12 women, 13 men; age 44 (18-64) years] prospectively underwent 1.5T MRI of the knee, including a 2-fold PI-accelerated 5-min 2D FSE MRI protocol, and a 4-fold SMS-PI-accelerated 5-min 2D FSE MRI protocol with higher spatial resolution, higher anatomic coverage, smaller inter-slicer gaps, improved suppression of vascular flow artifacts, and stronger and more homogenous fat suppression. Both protocols included sagittal PD, sagittal PDFS, coronal T1, coronal T2FS, axial PDFS sequences. Two MSK radiologists independently assessed image contrast, noise, artifacts, structural visibility, and abnormalities. Non-parametric comparison, kappa agreement, and interchangeability tests were applied.

Results: The inter-reader reliability (kappa=0.681) was good. 5-min SMS-PI MRI of the knee had better image contrast ($p<0.001$), less noise, ($p<0.001$), better structural visibility ($p<0.001$), and no flow or aliasing artifacts ($p=0.657$). There was unidirectional interchangeability in favor of SMS-PI MRI for the diagnosis of meniscal tears and cartilage defects, and bidirectional interchangeability for anterior cruciate and collateral ligament tears, tendon tears, bone marrow edema pattern, and fractures.

Conclusion: Combined, 4-fold-accelerated SMS-PI 2D FSE enables artifact-free 5-min MRI of the knee with higher image quality, better visibility of anatomic structures, and possibly better detectability of cartilage defects and meniscal tears than 2-fold PI-accelerated 5-min 2D FSE MRI of the knee.

Modality % - Radiography / Fluoroscopy:	0
Modality % - CT:	0
Modality % - MRI:	100
Modality % - US:	0
Modality % - Nuclear Medicine:	0

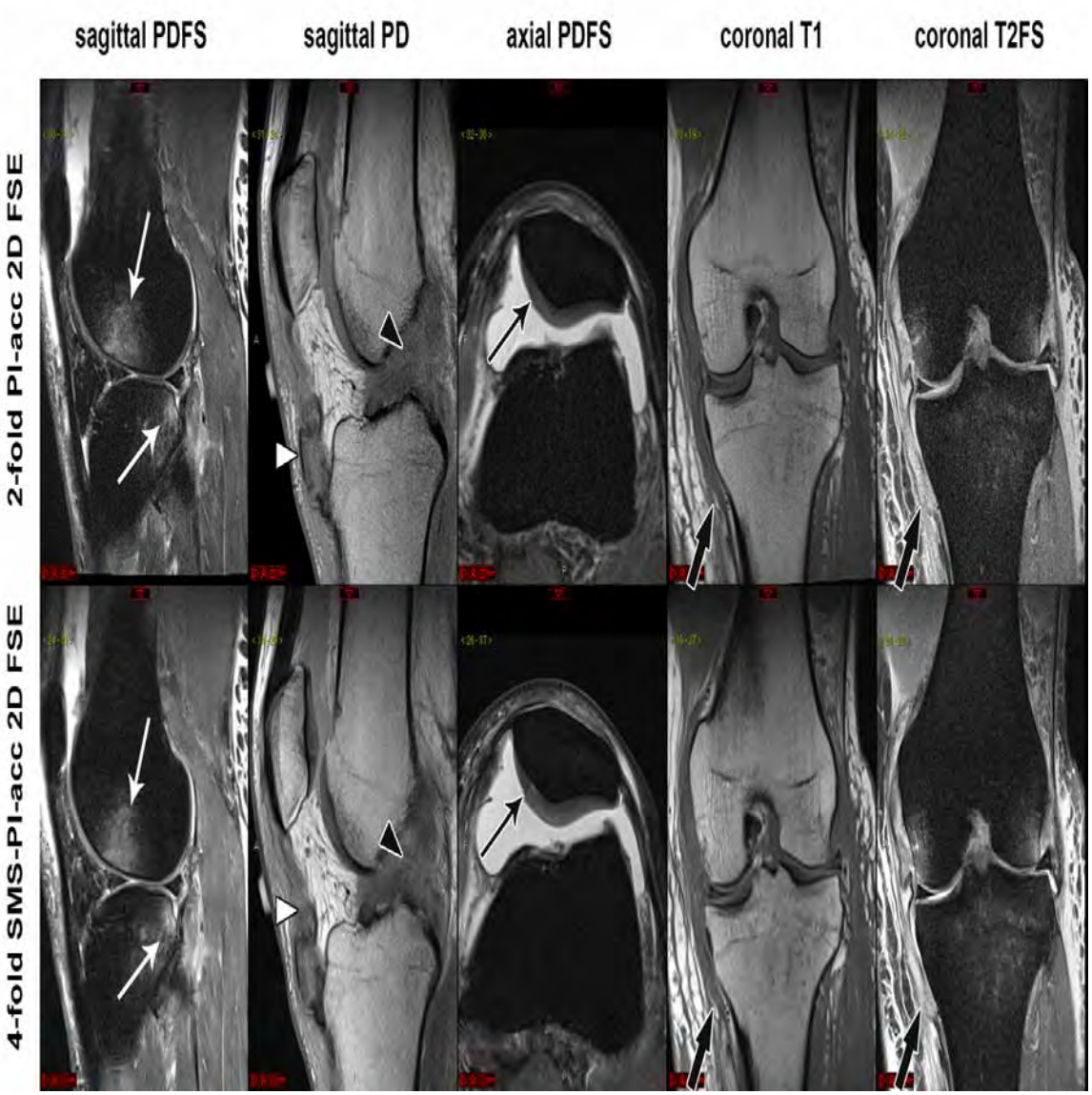

5-min protocols show pivot-shift contusions (white arrows), patella tendon tear (white arrowheads), ACL-tear (black arrowheads), cartilage defect (black narrow arrow), and MCL-tear (black wide arrows).

Poster #12

PERIPHERAL NERVE IMAGING: A REVIEW OF ANATOMY, IMAGING TECHNIQUES, AND IMPORTANT PATHOLOGY

Ryan Joyce, MD; Sarah Stilwill, MD; Richard Leake, MD; Megan Mills, MD; Patrick Kobes, DO; Hailey Allen, MD
University of Utah Medical Center / SOM, Salt Lake City, UT, USA
(Presented by: Ryan Joyce, MD, University of Utah Medical Center / SOM)

Purpose: To prepare radiology trainees and aid the practicing radiologist in the imaging evaluation of peripheral nerves.

Materials and Methods: Educational Goals:

The learner will be presented with a structured approach to the evaluation of peripheral nerves utilizing both MRI and ultrasound. Upon completion of the exhibit, the learner should be proficient in recognizing important peripheral nerve pathology and forming a succinct and relevant differential diagnosis for abnormal findings.

Results: Outline:

A. Normal and abnormal appearance of peripheral nerves on both MRI and ultrasound
B. Sample MRI protocol and systematic search pattern for peripheral neurography
C. Technical considerations in the sonographic evaluation of peripheral nerves
D. Review of important peripheral nerve anatomy, with attention to the most commonly imaged sites
E. Case based review of pathology affecting peripheral nerves, including features of each entity with both direct and indirect imaging findings.
    a. Entrapment
    b. Trauma
    c. Tumor and Tumor-Like Conditions
    d. Infectious and Inflammatory Pathology

Conclusion: The evaluation and treatment of patients who present with symptoms of peripheral nerve pathology is complex and requires a team-based, comprehensive approach. As imaging is a key component to accurately identifying, localizing, and characterizing nerve abnormalities, a radiologist proficient in multimodal nerve imaging can significantly contribute to the care of these patients and can help direct their management.

Modality % - Radiography / Fluoroscopy:	20
Modality % - CT:	0
Modality % - MRI:	40
Modality % - US:	40
Modality % - Nuclear Medicine:	0

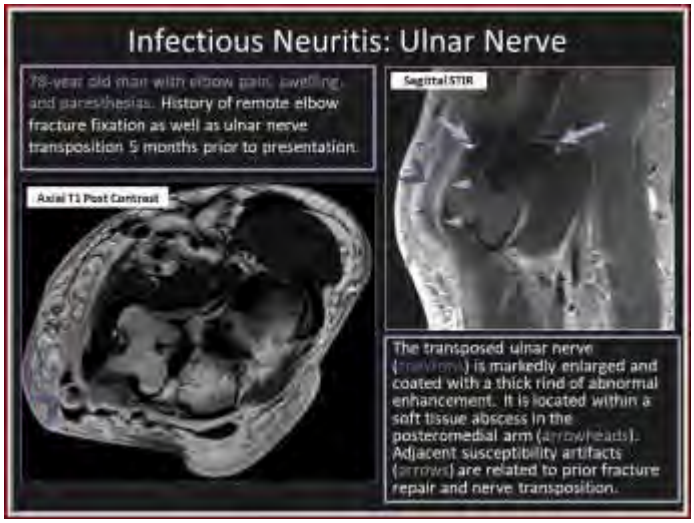

Infectious neuritis of the ulnar nerve.

Traumatic axonotmesis of the radial nerve0

Poster #13

Reverse shoulder arthroplasty; Pre and Postoperative Imaging and Current Concepts.

Michael Davis, MD; Alireza Eajazi, MD; Angel Gomez-Cintron, MD; Michael Tall, MD; Robert Cone, MD
UT Health San Antonio, San Antonio, USA
(Presented by: Michael Davis, MD, UT Health San Antonio)

Purpose: Carefully selected patients such as those with advanced glenohumeral arthropathy with massive rotator cuff tears, pseudoparalysis, and those who have failed conventional arthroplasty have increasingly been undergoing reverse total shoulder arthroplasties (RSA). This procedure reverses the ball-and-socket of the glenohumeral joint and allows control of shoulder motion by the deltoid. Our objective is to review current standards in preoperative imaging assessment, normal postoperative appearances, and complications related to reverse shoulder arthroplasty.

Materials and Methods: After consultation with our institution's shoulder surgeons and review of the literature, standards in preoperative assessment of glenoid morphology and glenoid bone stock are presented including comparison of 2D vs 3D CT assessment and the use of specialized software. The expected postoperative radiographic appearance of reverse shoulder arthroplasty and unique complications are presented with illustrative examples compiled from our practice.

Results: We present a guide to meeting surgeon's expectations with regard to preoperative imaging for reverse shoulder arthroplasty. Normal postoperative findings are illustrated and unique complications are discussed and illustrated with case examples where available.

Conclusion: Radiologists should be familiar with the rationale for reverse shoulder arthroplasty and what orthopedic surgeons expect from preoperative imaging assessment. In this exhibit we review current standards in preoperative assessment as well as the expected postoperative findings and unique complications.

Modality % - Radiography / Fluoroscopy:	40
Modality % - CT:	40
Modality % - MRI:	20
Modality % - US:	0
Modality % - Nuclear Medicine:	0

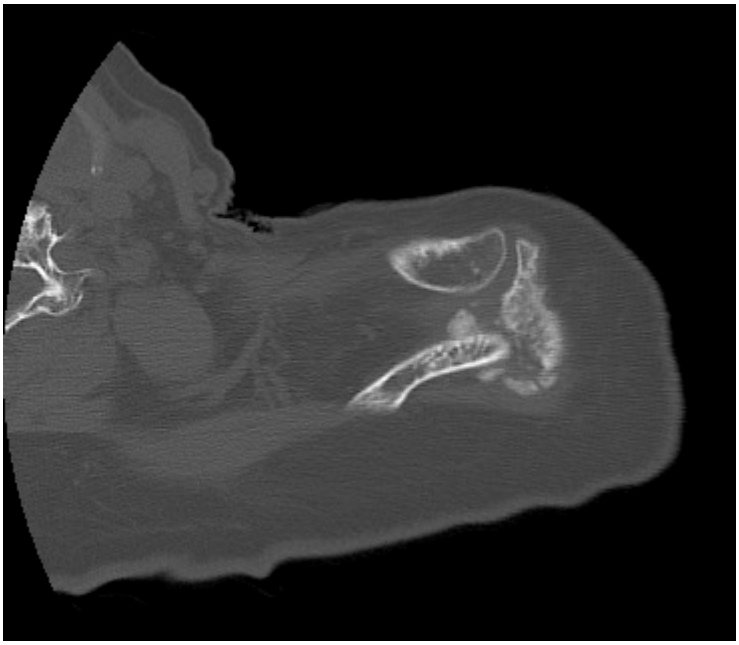

Image 1: Axial CT images demonstrate a characteristic acromial stress fracture

Poster #14

Teres Minor Atrophy and Associated Pathology

Derrick Doolittle, MD; William Aibinder, MD; Joaquin Sanchez-Sotelo, MD, PhD; Doris Wenger, MD
Mayo Clinic, Rochester, MN, USA
(Presented by: Derrick Doolittle, MD, Mayo Clinic)

Purpose: Functional impairment of the teres minor muscle has been shown to affect outcomes following various shoulder procedures, including reverse TSA. Melis et al (2011) reviewed cross sectional imaging of patients with rotator cuff tears and noted that 3.2% of patients had teres minor atrophy. This study sought to assess the incidence of teres minor atrophy in patients undergoing MRI for shoulder pain, and assess for associated pathologies.

Materials and Methods: A retrospective review of 7,376 noncontrast shoulder MRIs performed between 2010 and 2015 at our institution were reviewed through a key word database search. Image review by 2 musculoskeletal radiologists revealed teres minor atrophy in 209 (2.8%) shoulders. All shoulder girdle muscles were reviewed and atrophy was graded based on the Fuchs-Gerber classification (grades 0-2). Images were also assessed for rotator cuff and biceps tendon pathology and osteoarthritis.

Results: The mean age was 60.6 years, with 164 (78%) males. Fatty atrophy of the teres minor muscle was grade 2 in 118 (57%) shoulders. Concomitant deltoid muscle atrophy occurred in 142 (70%) shoulders with 95% classified as grade 1. Full thickness tears of the supraspinatus, infraspinatus, or subscapularis tendons were present in 100 (48%), 51 (24%), and 31 (15%), respectively. There was atrophy in 58% of supraspinatus, 61% of infraspinatus, and 50% of subscapularis muscles. 207 (99%) shoulders had tendinopathy or tear of the biceps tendon. Moderate or severe osteoarthritis was noted in 65 (31%).

Conclusion: Teres minor atrophy is commonly associated with other shoulder pathologies, including deltoid atrophy. Given that concomitant rotator cuff tears and osteoarthritis may necessitate surgical intervention, it is important to recognize that deficits in postoperative external rotation and elevation may be due to teres minor and deltoid atrophy. Further studies aimed at assessing the clinical significance of teres minor atrophy following shoulder surgery is indicated.

Modality % - Radiography / Fluoroscopy:	0
Modality % - CT:	0
Modality % - MRI:	100
Modality % - US:	0
Modality % - Nuclear Medicine:	0

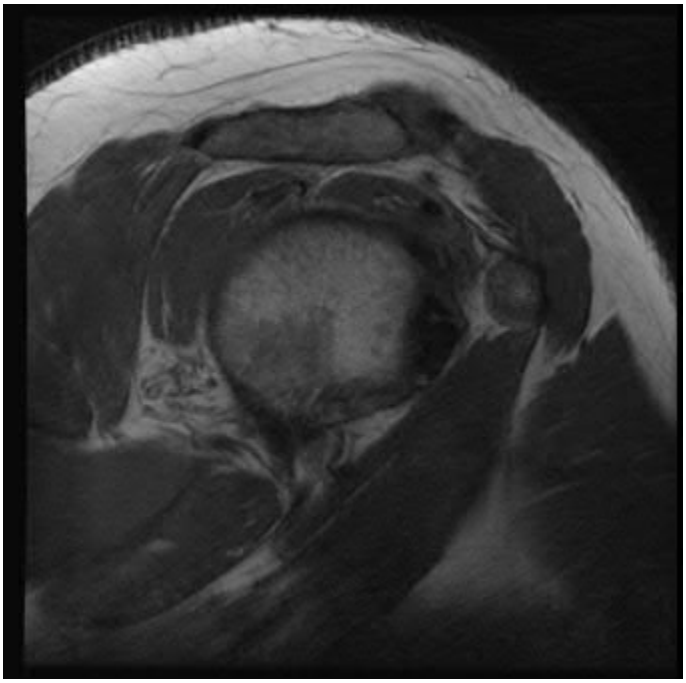

Sagittal T1 image demonstrates grade 2 fatty atrophy of the teres minor muscle.

Poster #15

ROTATOR CUFF REPAIR/RECONSTRUCTION FOR 'UNREPAIRABLE' TEARS

Nicholas Rhodes, MD[1]; Amanda Baillargeon, MD[1]; Christin Tiegs Heiden, MD[1]; Bassem Elhassan, MD[1]; Daniel Wessell, MD[2]
[1]Mayo Clinic, Rochester, MN, USA; [2]Mayo Clinic Florida, Jacksonville, FL, USA
(Presented by: Nicholas Rhodes, MD, Mayo Clinic)

Purpose: To review the non-arthroplasty surgical interventions for "unrepairable" rotator cuff tears.
Materials and Methods: Illustrative cases of "unrepairable" rotator cuff tear were selected. Rotator cuff function and rotator cuff disease are reviewed, with specific attention to new surgical techniques used to repair/reconstruct what were once considered "unrepairable" state rotator cuff tears.
Results: Discuss and illustrate nonoperative and operative management, excluding arthroplasty, of unrepairable rotator cuff tears, with specific focus on surgical intervention, including:
1. superior capsular reconstruction,
2. latissimus dorsi and lower trapezius transfer for posterosuperior rotator cuff tears, and
3. pectoralis major and latissimus dorsi transfers for anterosuperior rotator cuff tears.

Demonstrate the expected imaging appearance of these techniques and review some common postoperative complications that present clinically and/or on imaging.

Conclusion: Massive rotator cuffs tears are commonly encountered in clinical practice. Though not largely utilized, there are a number of important non-arthroplasty surgical interventions for massive rotator cuff tears. These repairs/reconstructions aim to diminish pain and to restore some shoulder function. The musculoskeletal radiologist should understand the rationale behind these surgeries and should be familiar with the postoperative appearance and common complications of these interventions.

Modality % - Radiography / Fluoroscopy:	1
Modality % - CT:	5
Modality % - MRI:	90
Modality % - US:	0
Modality % - Nuclear Medicine:	1

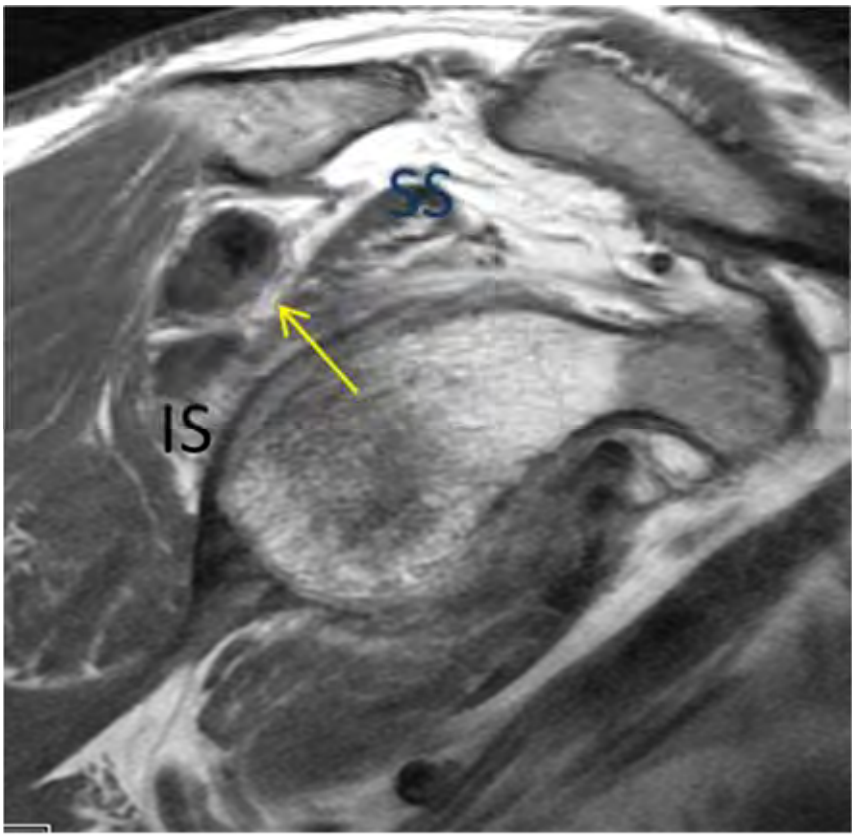

Massive cuff tear with retracted supraspinatus (SS) and infraspinatus (IS) tendons. Low trapezius transfer with augmented Achilles tendon passes posterior to the joint (yellow arrow).

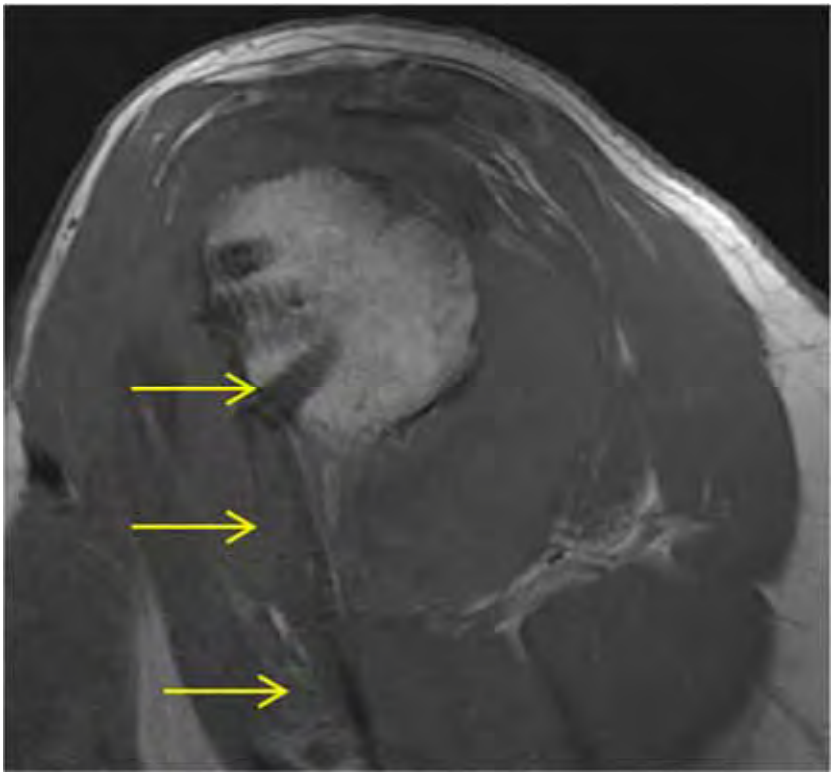

Patient with completely torn subscapularis tendon and partial anterior supraspinatus tear, status post latissimus dorsi (yellow arrows) transfer to the lesser tuberosity.

Poster #16

POST-SURGICAL IMAGING OF ACROMIOCLAVICULAR (AC) JOINT SEPARATIONS

Kimia Kani[1]; Jack Porrino, MD[2]; Hyojeong Mulcahy, MD[3]; Felix Chew, MD[3]
[1]University of Maryland School of Medicine, Baltimore, MD, USA; [2]Yale University School of Medicine, New Haven, CT, USA;
[3]University of Washington / Harborview Medical Center, Seattle, WA, USA
(Presented by: Kimia Kani, University of Maryland School of Medicine)

Purpose: Background information

1. Variety of continuously evolving surgical techniques are available for treatment of AC joint separations.
2. Imaging of postoperative complications

Materials and Methods: Educational goals

The goals of this presentation are to review the following:

1. Preoperative imaging and classification of AC joint separations
2. Surgical options for fixation of the reduced AC joint and repair/reconstruction of the torn soft-tissues
3. Normal postoperative imaging
4. Imaging of postoperative complications

Results: Key issues

1. Rockwood classification of AC joint injuries and its role in management decisions
2. Normal postoperative imaging appearances of: Transarticular AC joint fixations, nonanatomic and anatomic reconstructions of the coracoclavicular (CC) ligament, and flexible CC suspensions
3. Imaging of complications (including postsurgical) of AC joint separations

Conclusion: Familiarity with the various surgical techniques available for treatment of AC joint separations, along with their expected postoperative imaging appearances and complications are necessary for accurate interpretation of postoperative images.

Modality % - Radiography / Fluoroscopy:	80
Modality % - CT:	10
Modality % - MRI:	10
Modality % - US:	0
Modality % - Nuclear Medicine:	0

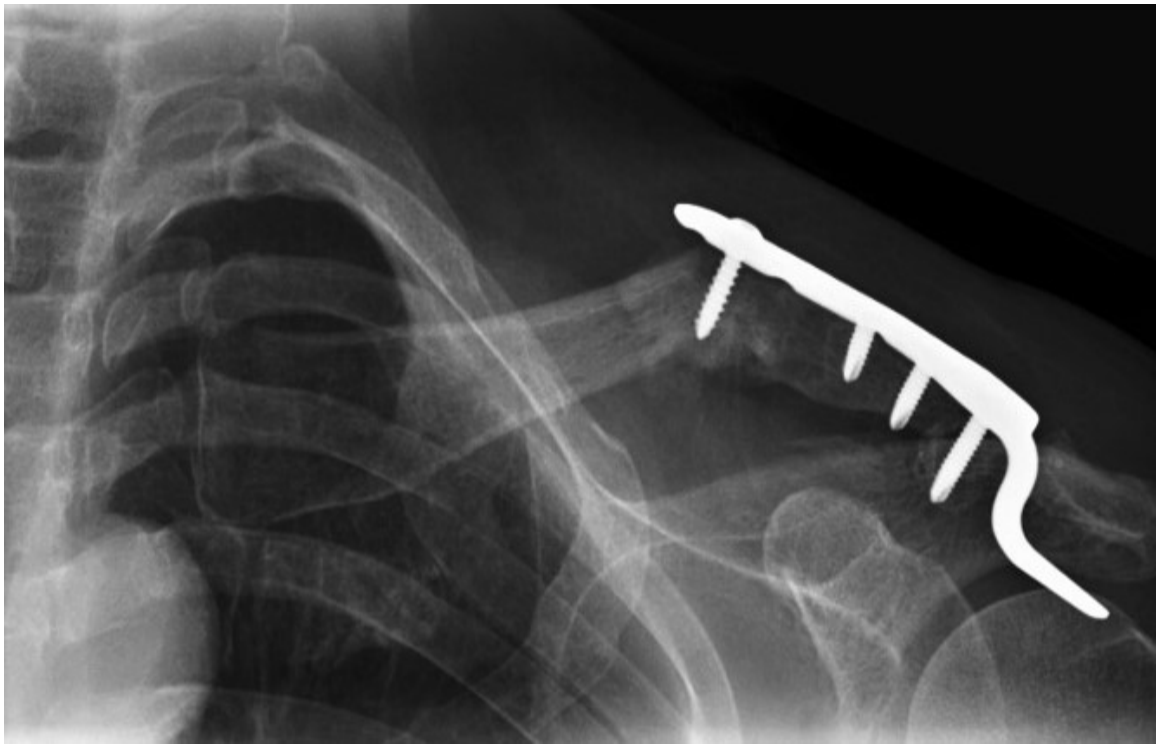

Unhooking of hook plate from acromion + Subacromial impingement + Periprosthetic midclavicular shaft fracture

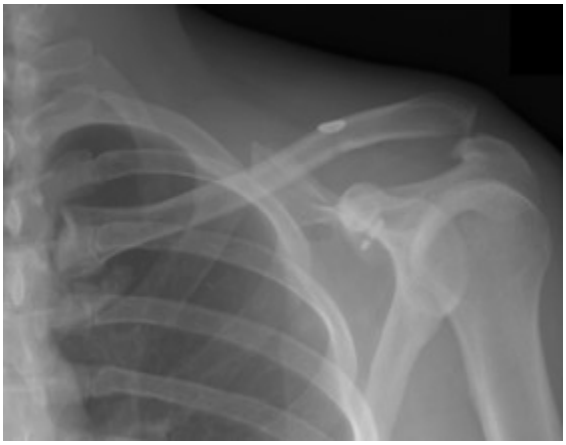

TightRope fixation for type V AC joint separation with persistent AC joint dislocation

Poster #17

AN APPROACH TO THE PAINFUL STERNOCLAVICULAR JOINT: DIAGNOSIS AND INTERVENTION

Gregory Matthews, MD; Maha Torabi, MD; Scott Wuertzer, MD
Wake Forest University School of Medicine, Winston-Salem, NC, USA
(Presented by: Gregory Matthews, MD, Wake Forest University School of Medicine)

Purpose: Describe an imaging approach to pathology of the sternoclavicular joint and present therapeutic interventions to this pathology with an emphasis on ultrasound guidance.

Materials and Methods: We will review the anatomy of the sternoclavicular joint on radiographs, CT, MRI, and ultrasound. We will then present examples of common and uncommon pathology at the sternoclavicular joint and describe an imaging approach to diagnose this pathology. Finally, we will discuss ultrasound-guided interventions at the sternoclavicular joint.

Results: Pathology at the sternoclavicular joint is varied. Osteoarthritis is the most common pain generator, but inflammatory and crystal induced arthropathies can also affect the sternoclavicular joint. Septic arthritis and osteomyelitis typically arise from hematogenous spread. Traumatic posterior dislocations of the clavicular head are uncommon, but prompt diagnosis is critical due to potential impingement on the superior mediastinum. Less common pathology unique to the sternoclavicular joint includes osteitis condensans of the clavicle and SAPHO (synovitis, acne, pustulosis, hyperostosis, and osteitis).

Percutaneous ultrasound-guided access to the joint can easily be obtained by aiming the needle towards the superior half of the medial clavicular head, which is covered by synovium and joint capsule. With a longitudinal approach along the clavicle, the needle tip can be confidently visualized throughout the procedure to provide easy access for intra-articular steroid injection or therapeutic aspiration.

Conclusion: Because the sternoclavicular joint is the only synovial articulation between the upper extremity and the axial skeleton, it can be a source of direct pain around the joint or referred pain to the shoulder, neck, or arm. Pathology in the sternoclavicular joint may be delayed in diagnosis due to these referred pain patterns and/or difficulty visualizing the sternoclavicular joint on conventional radiographs. To accurately diagnose pathology at the sternoclavicular joint in a timely fashion, radiologists should be familiar with the anatomy and pathology, best imaging options, and common image-guided therapeutic techniques.

Modality % - Radiography / Fluoroscopy:	25
Modality % - CT:	25
Modality % - MRI:	25
Modality % - US:	25
Modality % - Nuclear Medicine:	0

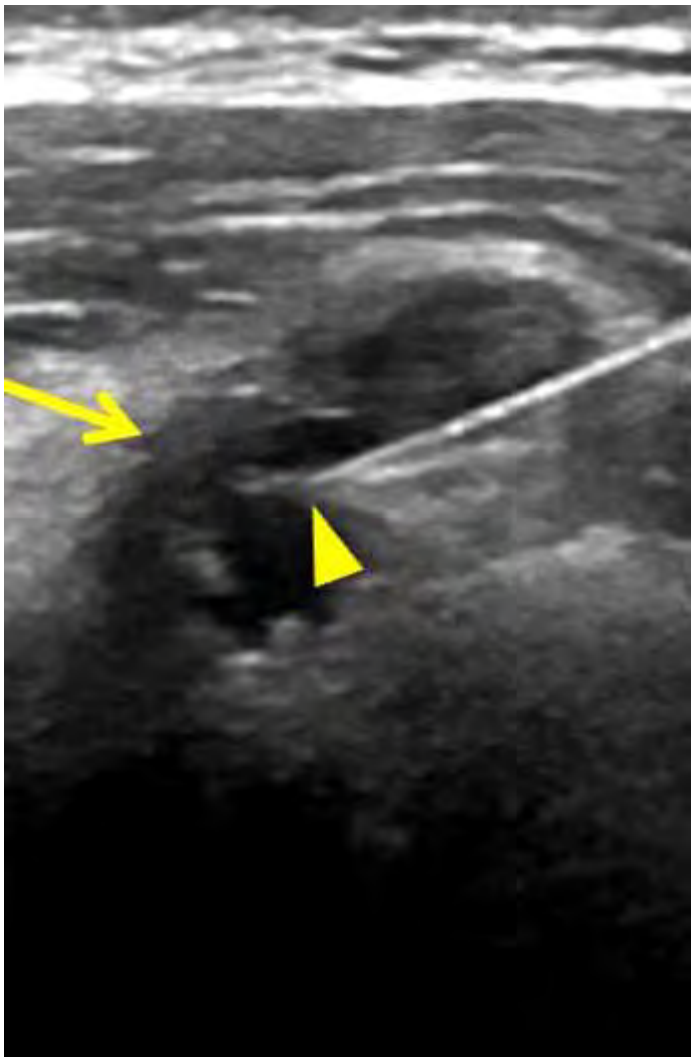

Image obtained during ultrasound-guided aspiration shows the needle tip (arrowhead) within a ganglion (arrow).

Posterior dislocation. Axial CT image in a 20-year-old man shows posterior dislocation of the clavicular head (arrow) with compression of the left brachiocephalic vein (arrowhead).

Poster #18

Post-operative complications of distal biceps tendon repair: an educational multi-modality imaging review

ANESH CHAVDA, BSc, MRCP, FRCR; Isabelle Dupuis, MD.CM, FRCPC; Yara Alhajjar; JEFF PIKE, RCPSC; PARHAM DANESHVAR, RCPSC; MARK CRESSWELL, MBBCh, FRCPC; DARRA MURPHY
ST PAUL'S HOSPITAL, VANCOUVER, BC, Canada
(Presented by: ANESH CHAVDA, BSc, MRCP, FRCR, ST PAUL'S HOSPITAL)

Purpose: Distal biceps tendon ruptures are quite uncommon with an incidence of 0.8-1.8/100,000 per annum. It predominantly affects the dominant arm of young males between the ages of 30-50.

Surgical repair is usually reserved for full-thickness or partial-thickness tears that fail conservative treatment in those classified as active, healthy and likely to engage in subsequent strength and endurance exercise.

Non-anatomic and anatomic repairs have been described both suffering postoperative complications with varying frequency according to the literature (5 - 50%). The most common include neurological, heterotopic ossification (HO), re-rupture, prosthetic/hardware failure, chronic regional pain syndrome, infection, stiffness and weakness.

Our aim is to present an educational poster describing the distal biceps tendon insertional anatomy, a brief review of the surgical techniques and the subsequent complications that can arise following surgical repair through a multi-modality imaging approach.

Materials and Methods: We reviewed both PACS and our local orthopedic database for cases specifically relating to nerve injury, heterotopic ossification and synostosis, distal biceps re-rupture, vascular injury, infection, chronic regional pain syndrome as well as technique specific complications. We have selected the optimal imaging modality to best demonstrate the range of these complications which include radiographs, ultrasound, Computed Tomography (CT) and Magnetic Resonance Imaging (MRI).

Results: We have reviewed the range of complications of distal biceps rupture and repair with local examples and describe the range of imaging modalities that best demonstrate the post-operative appearances. Awareness of the post-repair appearances and range of complications with a view to early diagnosis can help our orthopedic colleagues best manage this particular patient cohort.

Conclusion: We believe this will help clinicians, surgeons and radiologists in the imaging assessment of postoperative distal biceps tendon repair and reconstruction.

Modality % - Radiography / Fluoroscopy:	20
Modality % - CT:	20
Modality % - MRI:	20
Modality % - US:	20
Modality % - Nuclear Medicine:	20

AXIAL CT: BONE WINDOW: demonstrating heterotopic ossification along the proximal length of a distal biceps tendon repair

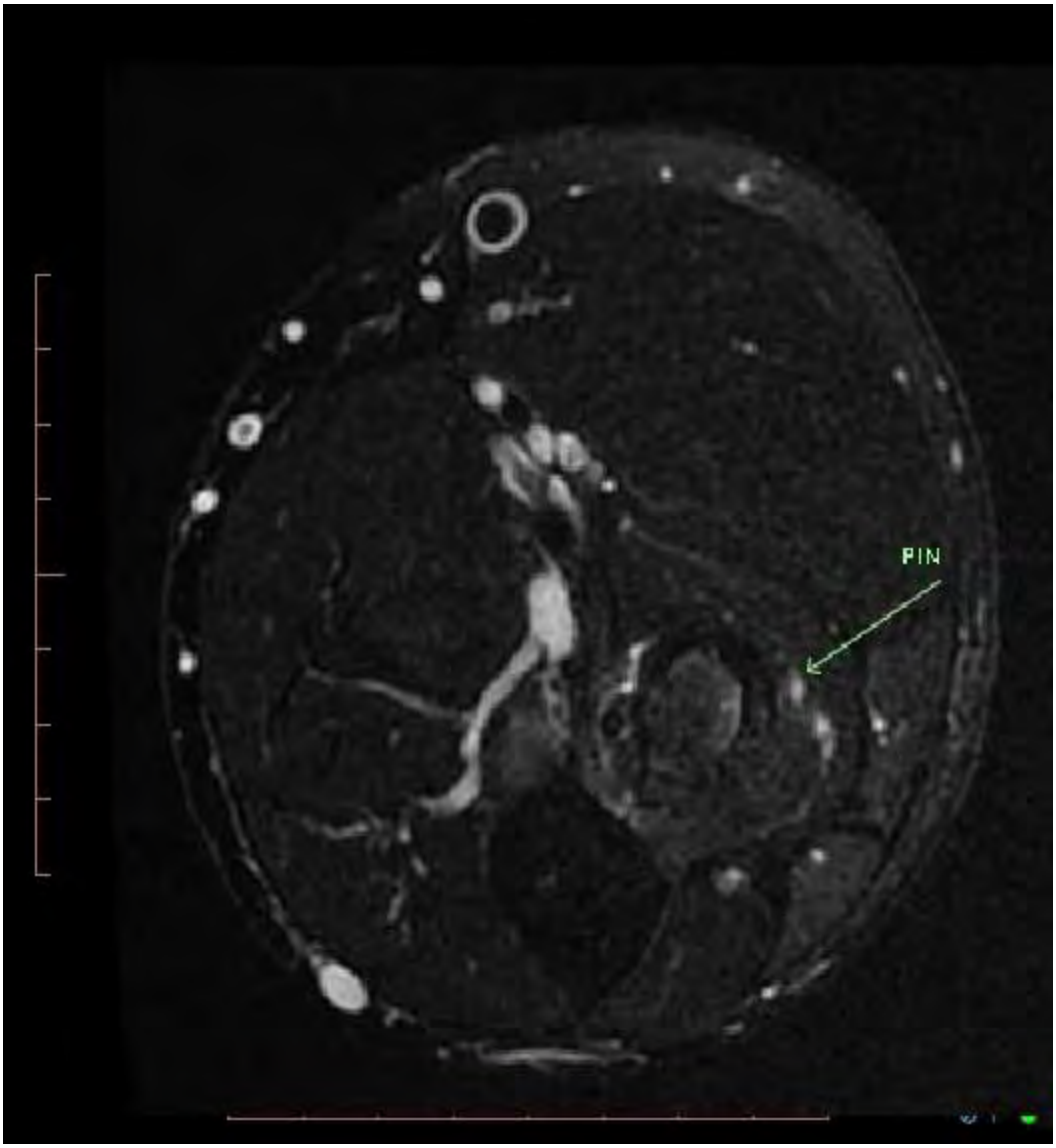

SAGITTAL CT: BONE WINDOW: demonstrating heterotopic ossification along the proximal length of a distal biceps tendon repair

T2FS AXIAL: thickened, hyperintense posterior interosseous nerve suspicious for neuritis, with mild oedema of the supinator, extensor digitorum and extensor digiti minimi suggestive of denervation.

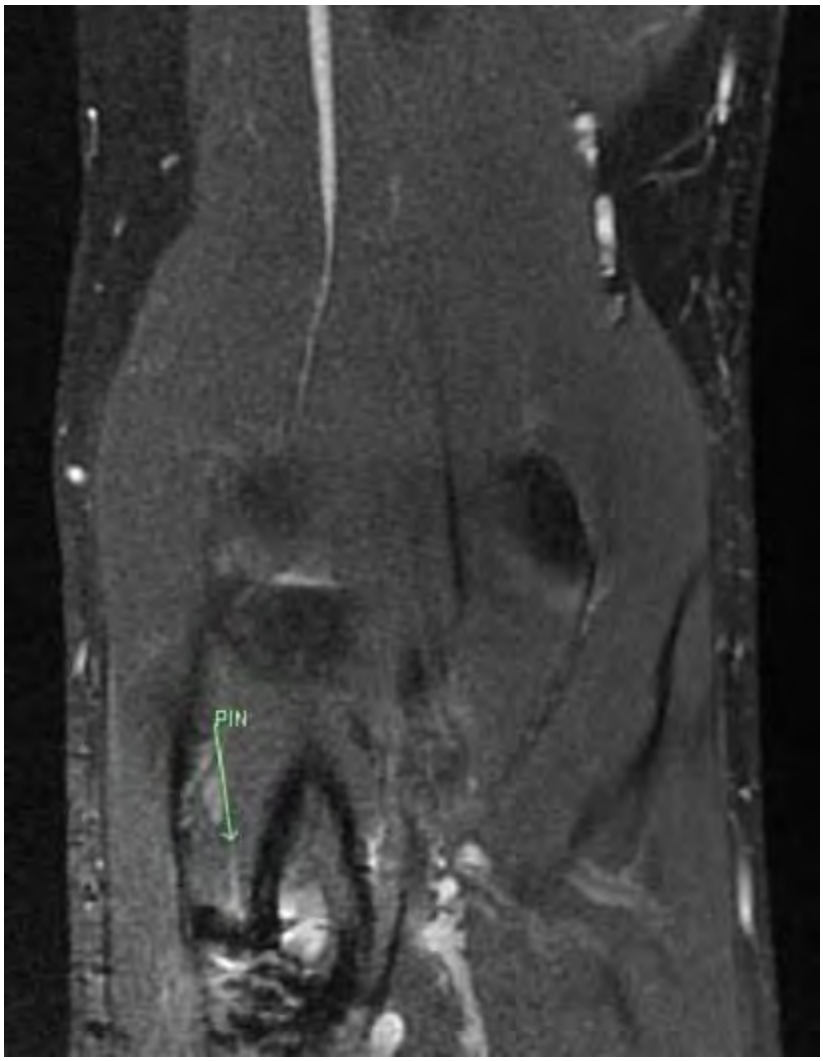

T2FS CORONAL: the posterior interosseous nerve impressed upon by surgical material at the site of distal biceps tendon repair.

Poster #19

GLENOID BONE STOCK AND ROTATOR CUFF PATHOLOGY.

Oganes Ashikyan, MD; Mathew Siebert, BS; Majid Chalian, MD
University of Texas Southwestern Medical Center at Dallas, Dallas, TX, USA
(Presented by: Oganes Ashikyan, MD, University of Texas Southwestern Medical Center at Dallas)

Purpose: We hypothesize that the severity of glenoid bone loss correlates with rotator cuff tendon pathologies and severity of fatty infiltration of the rotator cuff musculature.

Materials and Methods: We retrospectively reviewed 45 CT scans of 44 patients who underwent shoulder CT for primary shoulder pain. Measurements of glenoid bone loss, bone stock, version and joint line medialization were assessed on a 2-D CT image in the axial plane. Measurements were defined by use of the Friedman line to approximate the surface of the paleoglenoid. Glenoid version was measured by Friedman technique. Glenoid morphology was assigned by modified Walch classification. Rotator cuff muscle fatty infiltration was assessed by MRI and each muscle assigned Goutallier score. MRI used to assess rotator cuff tendon tears.

Results: There was a statistical difference in the Goutallier score for the supraspinatus and infraspinatus muscle fatty infiltration between Walch subtypes ($p < 0.05$). There was statistical difference in the severity of subscapularis tendon tear between different Walch subtypes ($p < 0.05$). Degree of anteversion, anterior glenoid and medial glenoid bone loss correlate to subscapularis tendon tear severity ($p<0.05$). Anterior bone loss and joint-line medialization correlate to increased fatty infiltration of the subscapularis muscle ($p<0.05$).

Degree of retroversion correlates to glenoid bone loss at all points and glenohumeral joint-line medialization ($p<0.05$). B2, B3 glenoids have significantly greater bone loss at all points, whereas D type glenoids exhibited greater anterior and middle bone loss compared to other Walch classes.

Conclusion: B2, B3 and D type glenoids are correlated with greater bone loss compared to other Walch sub-types. High-grade tears of the subscapularis tendon correlated to greater pathologic anteversion, and anterior and posterior glenoid bone loss. Anterior bone loss and joint-line medialization was correlated to increased fatty infiltration of the subscapularis muscle. Pathologic retroversion correlates to global increase in bone loss and humeral head medialization.

Modality % - Radiography / Fluoroscopy:	0
Modality % - CT:	100
Modality % - MRI:	0
Modality % - US:	1
Modality % - Nuclear Medicine:	0

Poster #20

USING THE RAVER VIEW AND ACROMIAL INDEX TO PREDICT ROTATOR CUFF TEARS ON RADIOGRAPHS

Adam Zoga, MD, MBA[1]; Christopher Aland, MD[2]; Weilong Shi, MD[2]; Vishal Desai, MD[1]; William Morrison, MD[1]
[1]Thomas Jefferson University Hospital, Philadelphia, PA, USA; [2]Rothman Orthopaedics Institute, Philadelphia, PA, USA
(Presented by: Adam Zoga, MD, MBA, Thomas Jefferson University Hospital)

Purpose: Rotator cuff disease is a common indication for subspecialty orthopaedics referral. MRI and US are definitive diagnosing rotator cuff tear (RCT), but patient selection for advanced imaging remains difficult. Arthroscopic studies have shown osseous hypertrophy at the anterosuperior humeral head is a frequent finding in patients with RCT. We sought to trial a novel radiographic view to allow for measurement of osseous features associated with RTC, assisting with selection for advanced imaging referral.

Materials and Methods: 113 consecutive patients referred to a shoulder surgeon for RCT underwent a novel X-ray view, resting, abduction view in external rotation (RAVER), in conjunction with the standard shoulder series. Osseous prominence was measured at the anterosuperior humerus. An Acromial Index (AI), was calculated by the ratio between the size of the prominence and distance between the acromion and the footprint. MRI referral was based upon the established practice protocol. MRI was correlated the RAVER measurements. Non-parametric tests and logistic regression were used to analyze the data.

Results: 48 (42.9%) subjects underwent MRI, of which 35 had rotator cuff tears. The mean AI in the RCT tear group was 1.15, whereas the mean AI in subjects without MRI or without tear at MRI was lower, 2.53 and 1.82 respectively. AI was significantly associated with RCT tear (p=0.003), independent of gender and age. 3 MSK trainees reviewed 18 cases independently to assess reliability of AI, and an intraclass correlation coefficient was 0.96 (95% CI: 0.92-0.98, p<0.001), showing high concordance and little variation in scoring.

Conclusion: The acromial Index is a reliable radiographic predictor of rotator cuff tears and can be calculated with the addition of a single, novel RAVER view. Once validated, this view and measurement can allow clinicians to more effectively select patients who would benefit from shoulder MRI or US, ultimately improving imaging efficiency and value.

Modality % - Radiography / Fluoroscopy:	70
Modality % - CT:	5
Modality % - MRI:	25
Modality % - US:	0
Modality % - Nuclear Medicine:	0

Resting AP view of the shoulder with 30% abduction and 30% external rotation (RAVER)

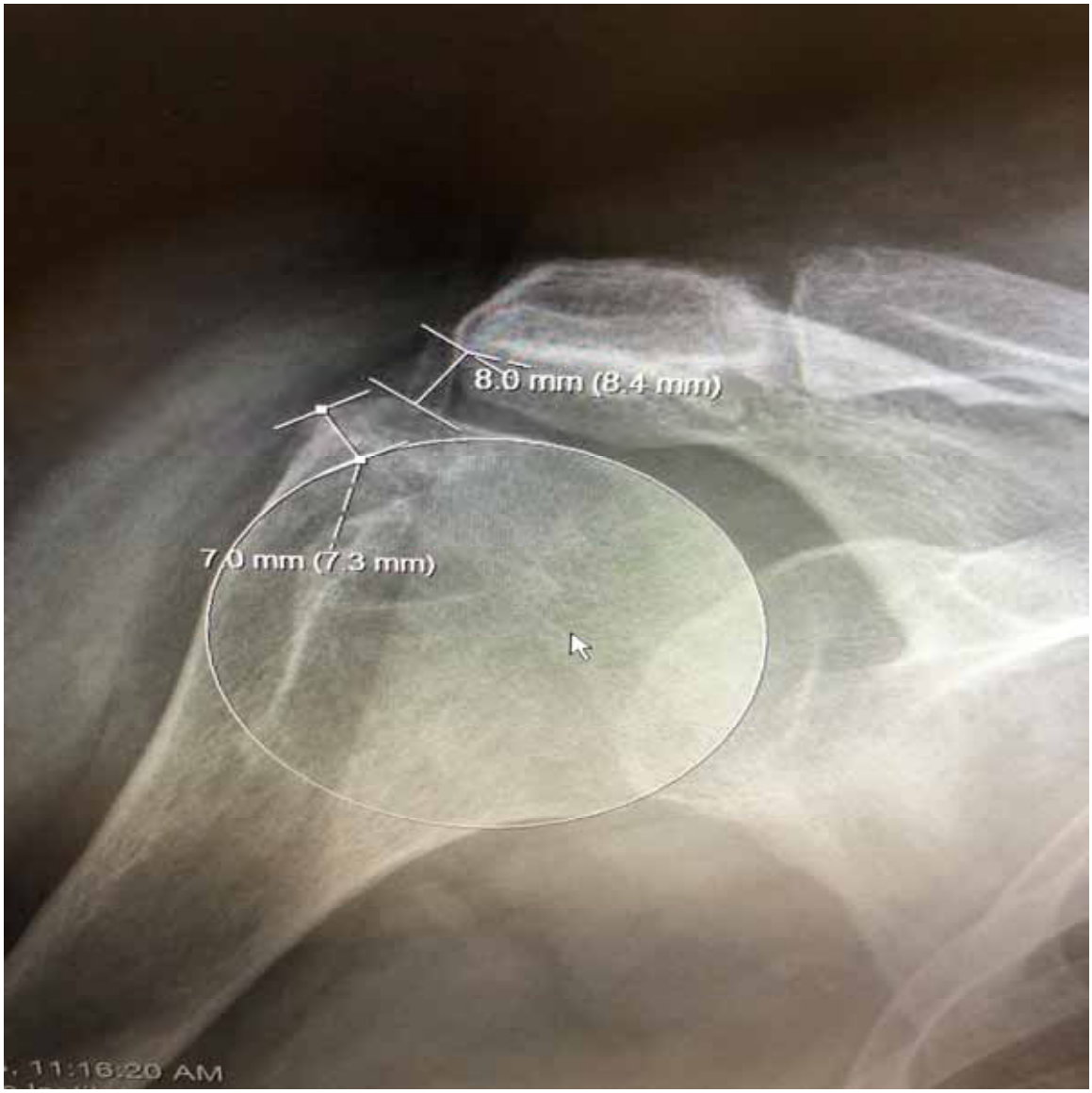

RAVER view showing osseous and Acromial Index measurements associated with rotator cuff tear

Poster #21

A MULTIMODALITY CENSUS OF CARPAL COALITIONS

Aleksandr Rozenberg, MD; Alessandra Sax, MD; Jeffrey Belair, MD; Kristen McClure, MD; Johannes Roedl, MD, PhD; William Morrison, MD; Adam Zoga, MD, MBA
Thomas Jefferson University Hospital, Philadelphia, PA, USA
(Presented by: Aleksandr Rozenberg, MD, Thomas Jefferson University Hospital)

Purpose: Carpal coalitions are less common than tarsal coalitions, and are frequently found incidentally with imaging. Still, coalitions can be symptomatic, and few series have been conducted to establish the prevalence and imaging findings of carpal coalitions across imaging modalities. We endeavored to create the largest known study to date detailing the locations and imaging features carpal coalitions.
Materials and Methods: A report database from upper extremity radiographic, CT, and MRI exams at our institution was retrospectively mined for the word "coalition", and studies were then reviewed by 2 MSK rads. Locations were logged along with any pathology across the coalition, and the ordering indication. Other pathologies potentially related to the coalition were observed.
Results: 430 radiographic exams were found. Lunotriquetral coalition was most prevalent at 88%, with capitohamate in 7%, scapholunate in 2%, hamate-pisiform in 1%, trapezoid-capitate in 1%, and single occurrences in 3 other locations. 71% of x-rays were ordered for recent injury (within one month), and 29% for non-traumatic pain. 114 MRIs were reviewed. Lunotriquetral coalition was most common in 83%, with capitohamate in 2%, hamate-pisiform in 3%, trapezoid-capitate in 6% and 6% at either an os styloideum or os trapezoideum secundareum. 35% of MRIs were ordered for recent injury, and 65% for non-traumatic pain. Edema across the coalition occurred in 33% of MRIs. Common associated pathologies involved the extensor tendons (40%), with the 6th compartment involved the most often (26%), followed by the 2nd (20%), and the 4th (11%). Scapholunate tear was present in 27% of MRs. Flexor compartment tendinosis was present in 21% of exams.
Conclusion: With relative rarity and presumed benignity, the presence of carpal coalition in the medical literature is limited. Coalitions should be recognized at imaging, however, and the most frequent locations should be acknowledged. Some partial coalitions with associated biomechanical instability can be a source of symptoms.

Modality % - Radiography / Fluoroscopy:	70
Modality % - CT:	5
Modality % - MRI:	25
Modality % - US:	0
Modality % - Nuclear Medicine:	0

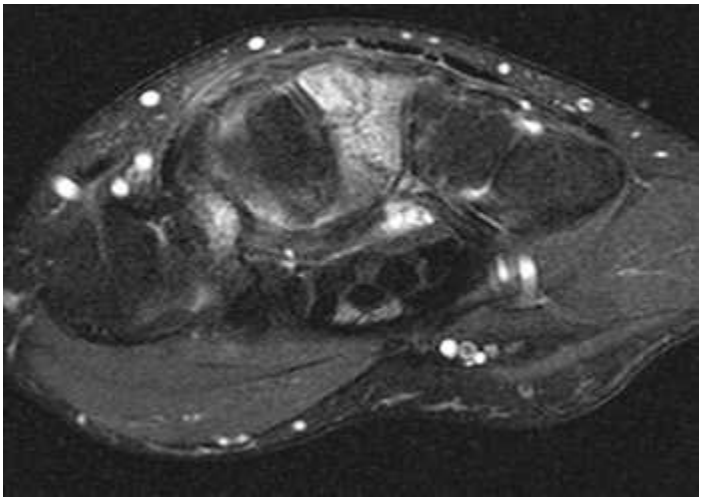

Axial PD FSE fat suppressed image of a symptomatic partial coalition at an os styloideum

Axial PD FSE fat suppressed image of a symptomatic coalition between the trapezoid and the 2nd metatarsal

Poster #22

PREOPERATIVE ULTRASOUND GUIDED BOTULINUM TOXIN A INJECTION FOR COMPLEX VENTRAL WALL HERNIA REPAIR: ONE TERTIARY CARE CENTER'S APPROACH

Christopher Nall, MD; Dana Feraco, DO; Joshua Powell
Beaumont Health System, Royal Oak, MI, USA
(Presented by: Christopher Nall, MD, Beaumont Health System)

Purpose: The purpose of this exhibit is to discuss the utility of administrating botulinum toxin (Botox) as an adjunct to surgical repair of complex abdominal wall hernias. Through presentation of the ultrasound-guided procedural technique and outcome data of one tertiary care center, it is our intention to bring awareness to this newer therapeutic option in an attempt to facilitate the performance of this procedure at other care centers, on a larger scale.

Materials and Methods: The procedure method of ultrasound-guided Botox injections and clinical course at one institution will be discussed. Outcome data including complications, primary fascial closure success, hernia recurrence, and patient population will be presented.

Results: Preoperative ultrasound-guided botulinum toxin A injection is a safe and effective procedure in patients undergoing complex ventral abdominal wall hernia repair which helps facilitate primary closure of large abdominal wall defects.

Conclusion: Awareness of this safe and effective preoperative image-guided procedure will help facilitate performance of this technique at more care centers, increasing the likelihood of primary closure of abdominal wall defects in more patients with large complex ventral hernias.

Modality % - Radiography / Fluoroscopy:	0
Modality % - CT:	30
Modality % - MRI:	0
Modality % - US:	70
Modality % - Nuclear Medicine:	0

Ultrasound image showing administration of Botox into the right inferior oblique muscle.

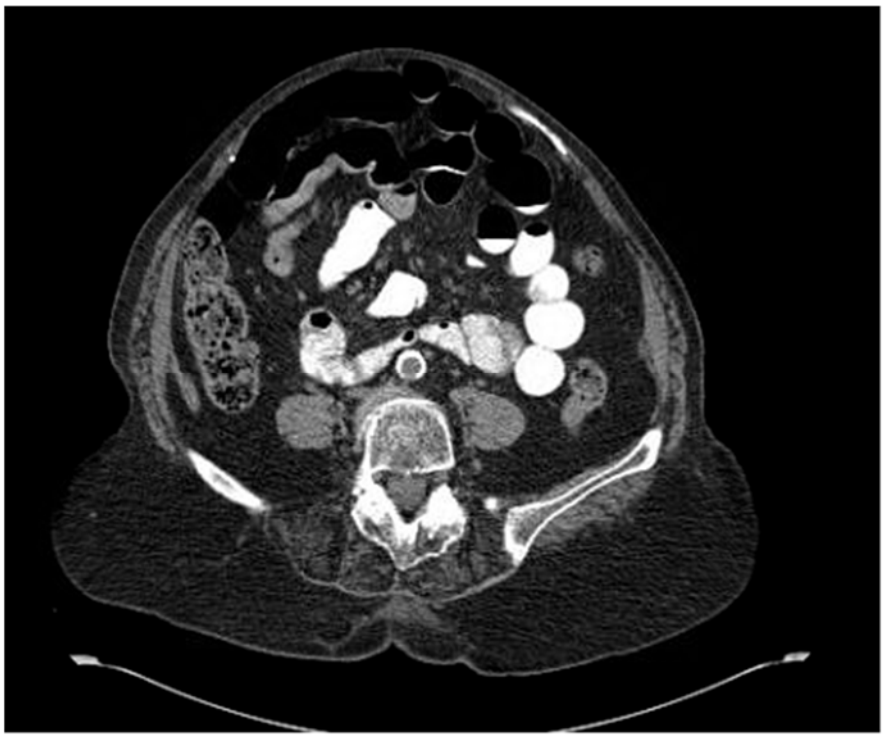

Axial CT showing large ventral abdominal wall defect.

Poster #23

BIOPSY OF SUSPICIOUS OSSEOUS LESIONS IN PATIENTS WITH A KNOWN PRIMARY MALIGNANCY: RATE OF ALTERNATE DIAGNOSIS AND COMPLICATION RATE.

Alexander Grushky, MD[1]; Christopher Nall, MD[1]; Zakaria Aqel, MD[1]; Alyssa Kirsch, MD[1]; Jonathan Im, MS[2]
[1]Beaumont Health System, Royal Oak, MI, USA; [2]Michigan State University College of Human Medicine, Grand Rapids, MI, USA
(Presented by: Alexander Grushky, MD, Beaumont Health System)

Purpose: In patients with multiple suspicious osseous lesions in the setting of a known primary malignancy, we sought to determine the rate at which tissue sampling of these osseous lesions yielded a different diagnosis from the primary malignancy. Secondary objective included determination of the complication rate in these biopsy procedures, including the need for re-biopsy.

Materials and Methods: Medical records for patients undergoing CT guided biopsy of a suspicious osseous lesion were retrospectively reviewed over a 12 month period from 2017 to 2018. There were 78 patients that underwent CT guided biopsy. Inclusion criteria for this study included: known primary cancer diagnosis, greater than three suspicious osseous lesion, and targeted CT guided biopsy performed by a musculoskeletal radiologist. The results of the biopsy lesions were then categorized as matched pathologic diagnosis, alternate pathologic diagnosis, no evidence of malignancy, and non-diagnostic or unsatisfactory sample.

Results: There were a total of 34 out of 80 CT guided biopsies that met the inclusion criteria. Of those included, 74% (n= 25) had matched pathologic diagnosis, 9% (n= 3) had an alternative pathologic diagnosis, 9% (n= 3) had no evidence of malignancy, and 9% (n= 3) had a non-diagnostic or unsatisfactory sample. Alternative diagnosis included: breast cancer with different receptor profile, bone island, and adenocarcinoma unspecified. Of the 34 bone biopsies, no immediate post-procedural complications were identified, and 3% required a re-biopsy (n= 1).

Conclusion: In patients with known primary malignancy and multiple suspicious osseous lesions, CT-guided biopsy of a suspicious osseous lesion represented matched pathologic diagnosis of the primary malignancy in 74% of cases. An alternative diagnosis was obtained in 9% of cases, and there was no evidence of malignancy in 9% of cases. Our results suggest that given the rate of alternative pathologic diagnosis in this patient population, careful consideration should be made when determining the need for biopsy

Modality % - Radiography / Fluoroscopy:	0
Modality % - CT:	100
Modality % - MRI:	0
Modality % - US:	0
Modality % - Nuclear Medicine:	0

T-Loc bone biopsy device shown with the needle tip in a suspicious right sacral osseous lesion.

Poster #24

THROW ME A BONE: EFFECT OF A BONE BIOPSY SKILLS WORKSHOP UTILIZING ANATOMICALLY ACCURATE 3D PRINTED MODELS

Michael Durst, MD; Corey Ho, MD; Dorissa Gursahaney, MD; Amanda Crawford, MD; Melody Carroll, PhD
University of Colorado Denver, Aurora, CO, USA
(Presented by: Michael Durst, MD, University of Colorado Denver)

Purpose: This study assesses the effect of a practicum utilizing low-cost, anatomically accurate 3D-printed models on trainees' bone biopsy skills using a powered device as well as self-assessed preparedness.

Materials and Methods: This study was IRB-exempted. Following a presentation highlighting manufacturer's provided instructions, trainees performed a biopsy on 3D printed models and were graded by a predetermined rubric. Following the initial attempt, a hands-on tutorial was provided with a subsequent graded biopsy attempt. Prior to and following the tutorial, trainees rated the utility of the tutorial, bone model usefulness, and personal anxiety/technical preparedness in performing bone biopsies on a 10-point Likert scale. Self-reported scores and grading of each trainee were compared using Wilcoxon signed-rank test with significance level at 0.05.

(10-point Likert scale: 1= not confident/anxious/useful to 10 = extremely confident/anxious/useful).

Results: 24 trainees completed pre- and post-tutorial surveys, with 83.3% rating the 3D model tutorial 9-10 (extremely useful) and 16.7% rating it 7 to 8 (Mean 9.42, SD 0.88). Assessing the manufacturer's instructions, 95.5% subjects rated it 1 (not useful) to 5 (neutral) and 4.5% rated it 8 (Mean 2.23, SD 1.875). Self confidence increased from an average of 2.096 (SD 1.73) to 7.29 (SD 1.71), $p < 0.001$. Self-described anxiety decreased from an average of 7.08 (SD 2.45) to 4.58 (SD 2.4), $p < 0.001$. Biopsy technique was graded for 21 trainees and a Wilcoxon signed-rank test demonstrated improved initial access, $p = 0.001$, biopsy access $p < 0.001$, sample $p = 0.035$, drill technique $p < 0.001$, and removal, $p = 0.001$.

Conclusion: 3D-printed bone biopsy models can serve as affordable, readily-available, and effective training tools to improve technical skills and confidence in performing biopsies.

Modality % - Radiography / Fluoroscopy:	50
Modality % - CT:	50
Modality % - MRI:	0
Modality % - US:	0
Modality % - Nuclear Medicine:	0

Photo of 3D printed distal femur

Arrow On-Control Powered Bone Access System

Poster #25

ACCURACY OF PREOPERATIVE MRI AND MRA FOR THE ASSESSMENT OF ACETABULAR LABRAL SIZE IN PATIENTS WITH FEMOROACETABULAR IMPINGEMENT (FAI)

Richard Marshall, MD; Daniel Kaplan, MD; Christopher Burke, MD; Soterios Gyftopoulos, MD; Jonathan Vigdorchik, MD; Robert Meislin, MD; Thomas Youm, MD; Mohammad Samim, MD
NYU Medical Center/ Hospital for Joint Diseases Langone Medical Center, New York, NY, USA
(Presented by: Richard Marshall, MD, NYU Medical Center/ Hospital for Joint Diseases Langone Medical Center)

Purpose: Arthroscopic management of acetabular labral tear in FAI includes labral repair, debridement, or reconstruction, with the optimal treatment strategy depending on the size and quality of the labrum. When residual labral tissue is deficient in size, or poor quality (e.g. macerated or calcified), a graft reconstruction may be indicated. Therefore, knowledge of labral size and quality could assist surgeons in the preoperative planning process. Our goal was to evaluate the accuracy of MR imaging for the measurement of labral size using intraoperative arthroscopic measurements as the reference standard.

Materials and Methods: Preoperative MR studies (35 MRI, 16 MRA) of 51 consecutive patients with FAI and labral tear referred to our hip surgeons were analyzed by two MSK radiologists to assess the labral size at 11:30 (superior), 1:30 (anterosuperior), and 3:00 (anterior) acetabular locations. The same measurements were taken during arthroscopy. Inter reader agreement was assessed using simple kappa and intra-class correlation coefficients.

Results: There was no significant difference between MRA and MRI in accuracy of labral size measurements compared with intraoperative findings. With MR, the average labral size was 6.7mm at 11:30, 6.1mm at 1:30, and 6.3mm at 3:00. With arthroscopy, the average labral size was 6.1mm at 11:30, 6.0mm at 1:30, and 5.8mm at 3:00. Correlation between the labral size measurements on MR and arthroscopy was moderate at 11:30 ($r=0.42$, $p<0.001$) and strong at 1:30 ($r=0.66$, $p<0.001$) and 3:00 ($r=0.63$, $p<0.001$). The agreement between readers was substantial for labral measurements in all locations (K: 0.87 at 11:30, 0.79 at 1:30, and 0.78 at 3:00).

Conclusion: Our study shows that MRI can be used to accurately measure the size of the labrum in patients with FAI and labral tear when compared to arthroscopy. Knowledge of labral size may assist surgeons in the preoperative planning process to better assess the need for labral graft reconstruction.

Modality % - Radiography / Fluoroscopy:	0
Modality % - CT:	0
Modality % - MRI:	100
Modality % - US:	0
Modality % - Nuclear Medicine:	0

PD fat saturated MR image of labral measurement at the insertion of the indirect rectus (11:30 position).

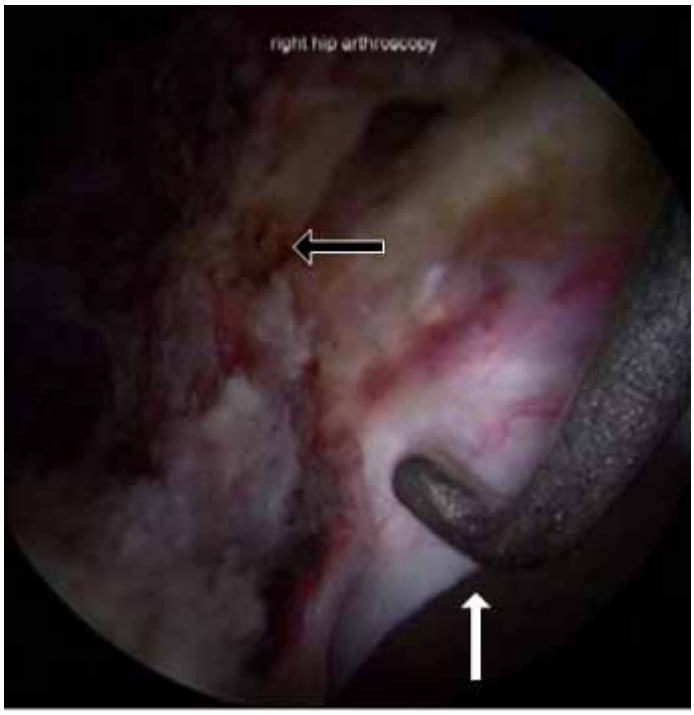

Arthroscopic image of labral (white arrow) measurement at the insertion of the indirect rectus (black arrow)(11:30 position).

Poster #26

SACROILIAC JOINT INFECTIONS IN CHILDREN: MR IMAGING FEATURES

Sara Cohen, MD; David Biko, MD; Christian Barrera, MD; Suraj Serai, PhD; Jie Nguyen, MD
Children's Hospital of Philadelphia, Philadelphia, PA, USA
(Presented by: Sara Cohen, MD, Children's Hospital of Philadelphia)

Purpose: To investigate magnetic resonance (MR) imaging features of sacroiliac joint infections in children with clinical correlation.

Materials and Methods: This IRB-approved, HIPPA compliant study included 41 MR studies with sacroiliac joint infections from 41 children (mean age 8.73 +/- 6.1 years; 20 boys and 21 girls) performed between December 1, 2002 and July 31, 2019. Infections were established using a combination of positive cultures, elevated inflammatory markers, clinical assessment, and response to antibiotic treatment. MR studies were retrospectively reviewed for the presence of bone marrow edema, bony erosions, joint effusion, extracapsular edema, soft tissue abscess, and sciatic neuritis. Pre-treatment radiography was reviewed for the presence of radiographically visible osseous change. Clinical chart review was performed for clinical history and outcomes. Chi-square, Fisher Exact, and Mann Whitney U tests were used.

Results: A bimodal age distribution for infectious sacroiliitis was identified with 39% (16/41) from children $\leq$ 5 and 61% (25/41) from children $\geq$ 8. The mean duration of symptoms was 10.0 $\pm$ 11.0 days and length of hospital stay was 8.4 $\pm$ 5.3 days, which did not differ between the age groups (p=0.20 for symptom duration, p=0.18 for hospital stay). No difference was found between the groups in terms of elevated inflammatory markers and presence of bone marrow edema, bony erosions, joint effusion, and soft tissue abscess. Although the presence of anterior extracapsular edema was not significantly different between the groups (p=0.99), the presence of posterior extracapsular edema was more common in the younger age group (p=0.007). Radiographically visible osseous changes were often not present at the time of diagnosis.

Conclusion: Clinical findings and many of the MR imaging features of infectious sacroiliitis in children did not significantly differ with respect to age. Posterior extracapsular edema was more common in younger children which suggests regional ligamentous and capsular laxity and immaturity.

Modality % - Radiography / Fluoroscopy:	0
Modality % - CT:	0
Modality % - MRI:	100
Modality % - US:	0
Modality % - Nuclear Medicine:	0

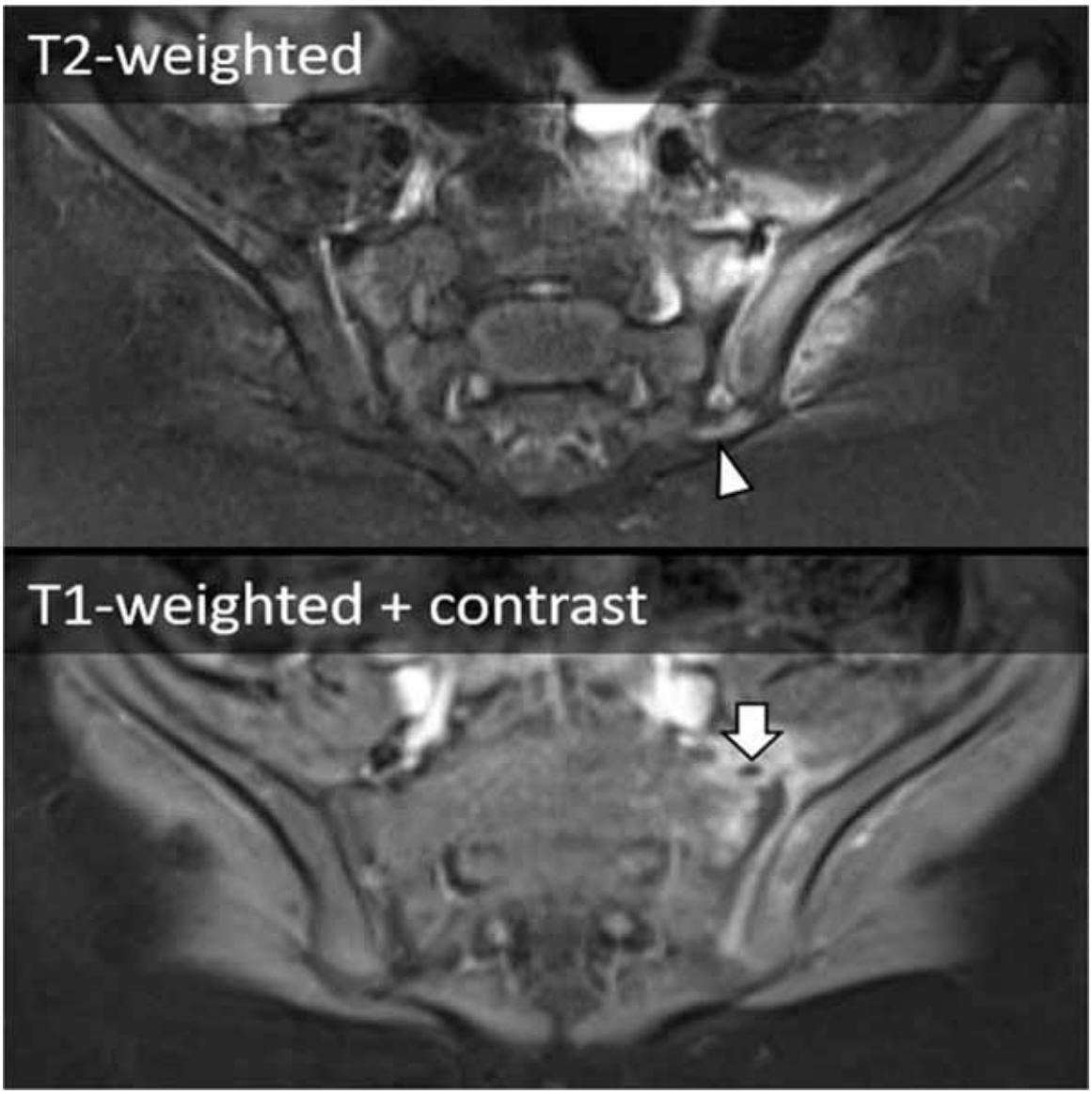

MRI from a 1 year-old boy with 7 days of symptoms shows right sacroiliitis with osteitis, sacral erosion, anterior abscess (arrow), and posterior edema (arrowhead).

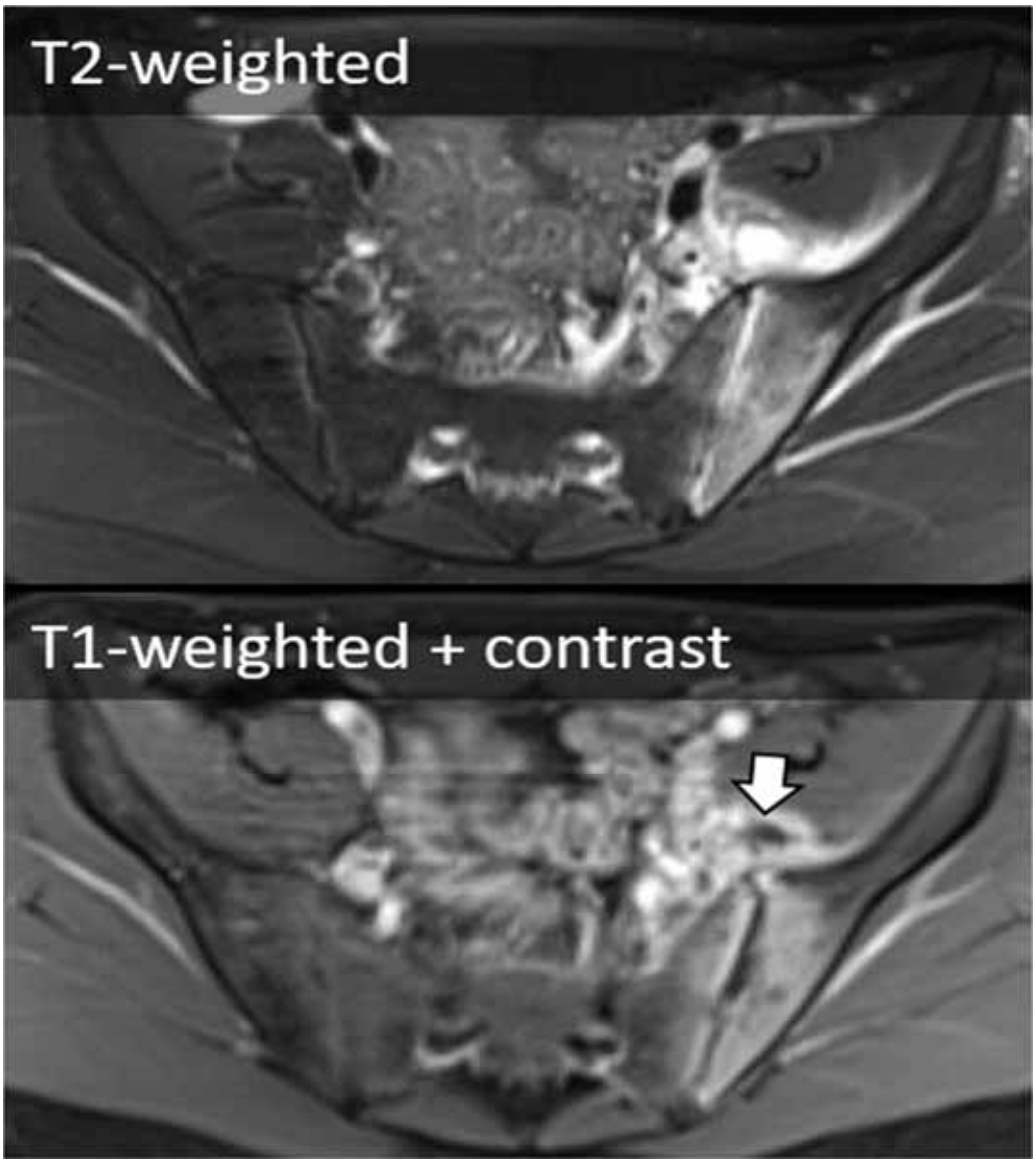

MRI from a 15 year-old boy with 7 days of symptoms shows right sacroiliitis with osteitis and anterior abscess (arrow).

Poster #28

B-CELL PERIPHERAL NEUROLYMPHOMATOSIS: MRI AND 18F-FDG PET/CT IMAGING CHARACTERISTICS

Stephen Broski, MD; Anthony DeVries, MD; Benjamin Howe, MD; Robert Spinner, MD
Mayo Clinic, Rochester, MN, USA
(Presented by: Stephen Broski, MD, Mayo Clinic)

Purpose: To examine the MRI and ^{18}F-FDG PET/CT imaging characteristics of peripheral neurolymphomatosis (NL).
Materials and Methods: All institutional cases of NL with an MRI or ^{18}F-FDG PET/CT from 2000-2017 were retrospectively reviewed. Included cases were biopsy-proven NL or lymphoma patients with clinical and imaging evidence of NL that resolved after chemotherapy. Multiple imaging parameters and clinical characteristics were recorded.
Results: There were 27 cases of B-cell NL in 25 patients (18 M, 7 F; mean age 64.6 +/-10.0 years). 85% (23/27) of cases were biopsy-proven. Most were diagnosed after disease progression or recurrence (20/27, 74%), and presented with isolated nerve involvement (18/27, 67%). Bone marrow biopsy (17/19, 89%) and CSF cytology (16/23, 70%) were usually negative. On ^{18}F-FDG PET/CT, NL presented as a linear or fusiform (23/26, 88%), FDG-avid (average SUVmax: 7.1 +/- 4.5, range 1.5 – 17.0) mass, and on MRI as a T2 hyperintense (21/22, 95%), enhancing (21/22, 95%), linear or fusiform mass (19/22, 86%) with associated muscle denervation (14/22, 64%). FDG avidity was significantly higher in patients with muscular denervation on MRI (mean SUVmax 8.2 +/- 4.6 vs. 4.3 +/- 2.3, p = 0.04).

Conclusion: B-cell NL most commonly manifests as T2 hyperintense, enhancing linear or fusiform neural enlargement associated with muscular denervation on MRI, with intense FDG activity on PET/CT. It is most often an isolated site of disease, presenting after progression or recurrence. A familiarity with the imaging appearance of NL can help refine the differential diagnosis, direct biopsy, and aid in accurate diagnosis.

Modality % - Radiography / Fluoroscopy: 0
Modality % - CT: 0
Modality % - MRI: 50
Modality % - US: 0
Modality % - Nuclear Medicine: 50

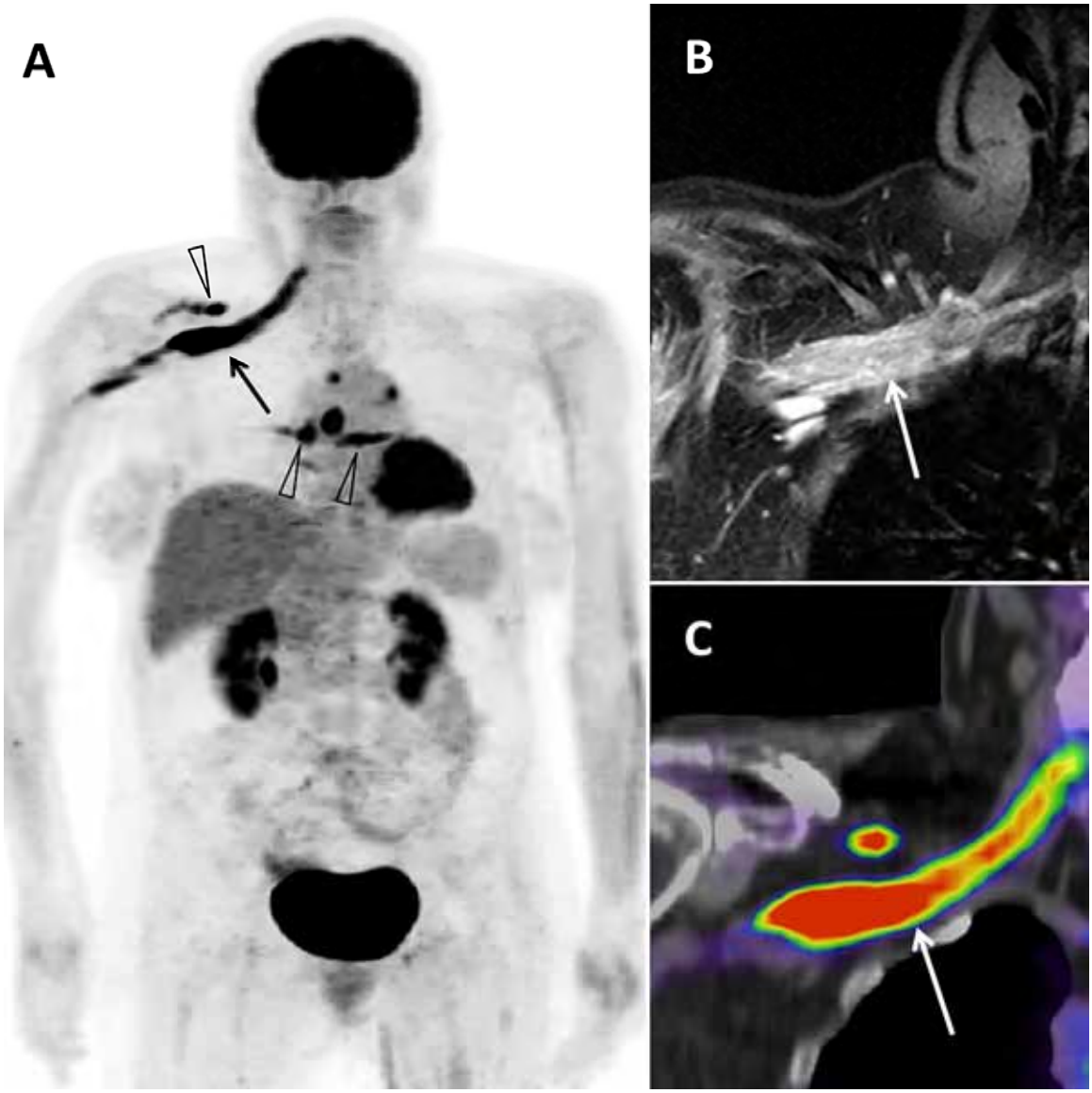

60-year-old male with biopsy-proven B-cell NL of the left brachial plexus with linear thickening extending from the trunks through the cords.

74-year-old male with biopsy-proven diffuse large B-cell NL of the right sciatic nerve with nodular enlargement and enhancement.

Poster #29

FRIENDLY FAT MASQUERADING AS AN AGGRESSIVE FOE ON PLAIN RADIOGRAPHY: A CASE SERIES

Bhumin Patel, MD; Douglas Mintz, MD
Hospital for Special Surgery, New York, NY, USA
(Presented by: Bhumin Patel, MD, Hospital for Special Surgery)

Purpose: To review radiologic appearance of intraosseous fatty lesions seen at a single institution that appear aggressive on radiographs.
Materials and Methods: Over two and a half years, we observed several cases of incidental aggressive appearing lucent lesions on radiographs that were actually fat containing intraosseous lesions. We reviewed patient demographics, presenting symptoms, lesion size and location, and imaging characteristics on MRI.
Results: From September of 2016 to January of 2018, our collection included 5 males and 4 females with an average of 66 (range, 44-85 years). The most common clinical query was to evaluate for degenerative changes (5 patients) and the least common was to evaluate for fracture (1 patient). All lesions initially were detected on radiographs and subsequently underwent magnetic resonance imaging. There were 6 patients (67%) with lesions in the upper extremity and 3 patients (33%) with lesions in the lower extremity. Specifically, most lesions were found in the femur (44%) followed by the tibia (22%). All lesions were located in the appendicular skeleton with 4 (44%) proximal to the knee, 2 (22%) distal to the knee, 2 (22%) distal to the elbow, and 1 (12%) proximal to the elbow. Lesions were an average of 1.5 cm in greatest dimension (range of 1-2.6 cm). No associated soft tissue masses or calcifications were identified. On MRI, all cases followed fat signal characteristics on all sequences.
Conclusion: We present a collection of cases where an incidental aggressive finding led to MRI follow-up that yielded benign fat hiding in a misleading appearance.

Modality % - Radiography / Fluoroscopy:	50
Modality % - CT:	88
Modality % - MRI:	50
Modality % - US:	0
Modality % - Nuclear Medicine:	0

AP of the pelvis demonstrates a partially circumscribed lucent lesion in the proximal right femoral diaphysis.

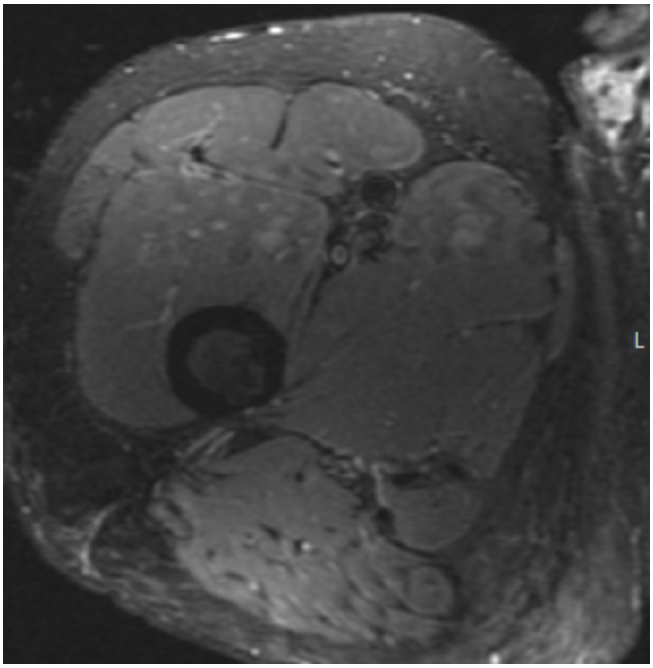

Coronal PD demonstrates a well-defined marrow signal intensity focus corresponding in the proximal femoral cortex that corresponds to radiographs.

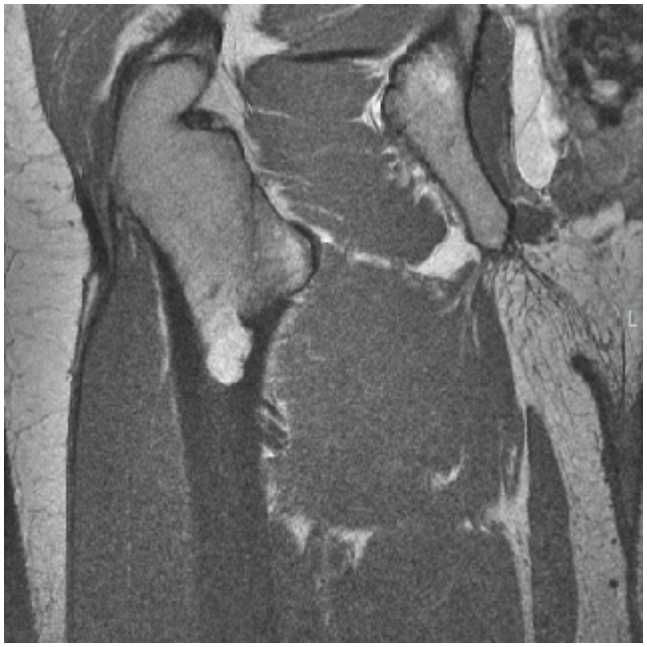

Axial inversion recovery demonstrates loss of signal corresponding to fat within the corresponding focus seen on the PD sequence.

Poster #30

INTRANEURAL LIPOMA: A CASE SERIES

Christin Tiegs-Heiden, MD; Katarina Glazebrook, MB, ChB; Matthew Frick, MD; Tara Anderson, MD; Robert Spinner, MD; Kimberly Amrami, MD
Mayo Clinic, Rochester, MN, USA
(Presented by: Christin Tiegs-Heiden, MD, Mayo Clinic)

Purpose: Intraneural lipoma is an extremely rare soft tissue tumor. These lesions represent an encapsulated lipoma located with a neural structure, without neural elements within the lipoma itself. The most common location for these tumors is in the upper extremity, specifically within the median nerve. They may lead to compression neuropathy. The purpose of this case series is to demonstrate the MRI and ultrasound features of intraneural lipoma.

Materials and Methods: A search of MRI reports in our imaging database using the term “intraneural lipoma” produced 3 cases between the years of 2006 and 2018. All cases were selected for inclusion in this series. The MRI images were reviewed for all cases. One patient also had a comparison ultrasound available for review. The clinical chart was reviewed for each case.

Results: We present three cases of intraneural lipoma. Two of these lesions were located in the median nerve, and one was in the peroneal nerve. On MRI, each lesion was well encapsulated and located within the nerve sheath. Two lesions were located eccentrically within the nerve and one was central. All tumors had signal characteristics equal to that of fat. The lipoma which was imaged with ultrasound demonstrated a well-defined echogenic lesion within the nerve. All patients ultimately underwent excision of the lipoma, and intra-operative photos are available in two cases.

Conclusion: Intraneural lipoma may be encountered by musculoskeletal radiologists. We present this case series to remind radiologists of this rare pathology and to demonstrate its imaging features on both MRI and ultrasound.

Modality % - Radiography / Fluoroscopy:	0
Modality % - CT:	0
Modality % - MRI:	75
Modality % - US:	25
Modality % - Nuclear Medicine:	0

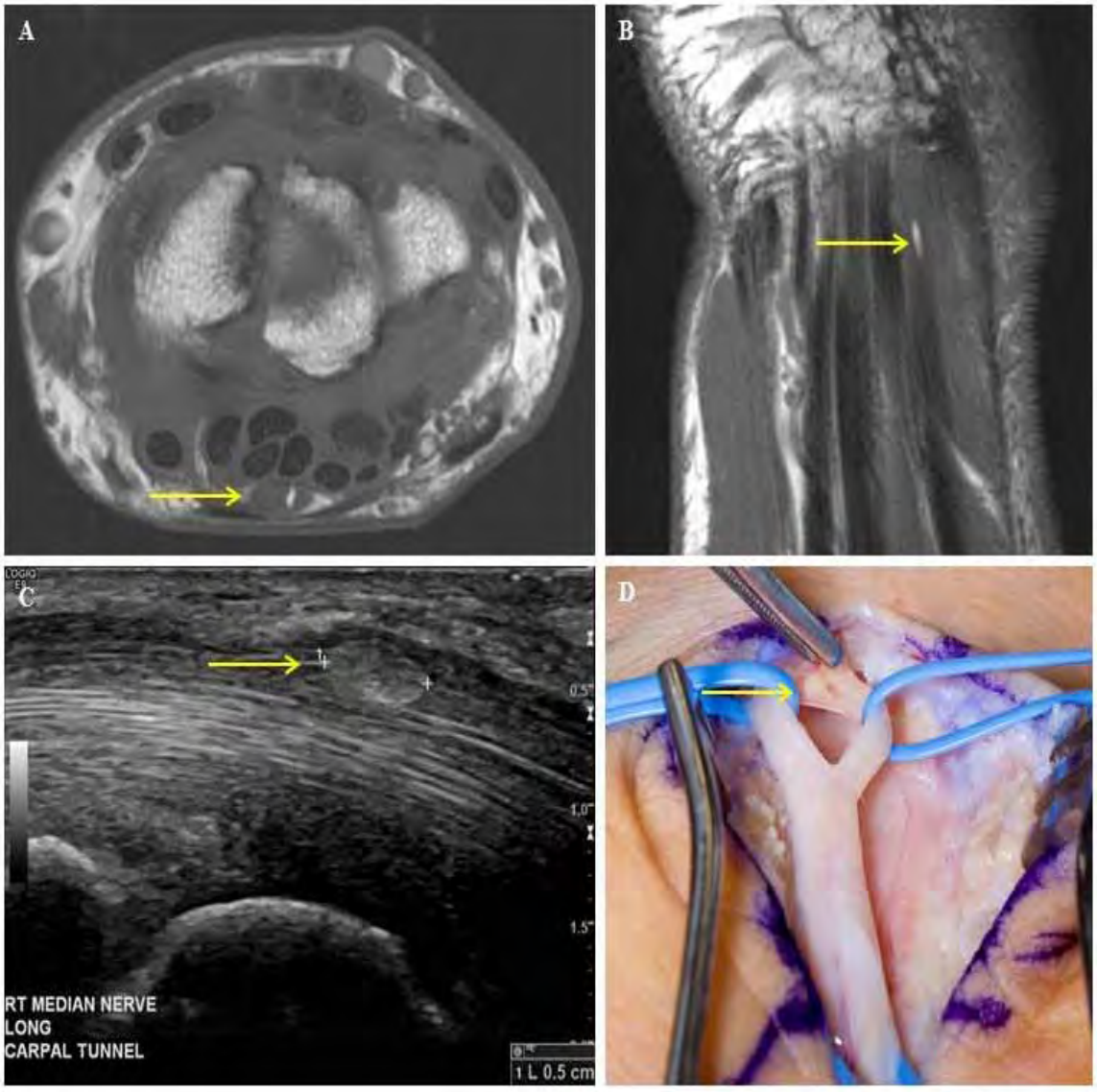

Figure 1 demonstrates a median nerve intraneural lipoma. It is T1 hyperintense on MR images (A, B) and hyperechoic on ultrasound (C). Intra-operative photograph (D).

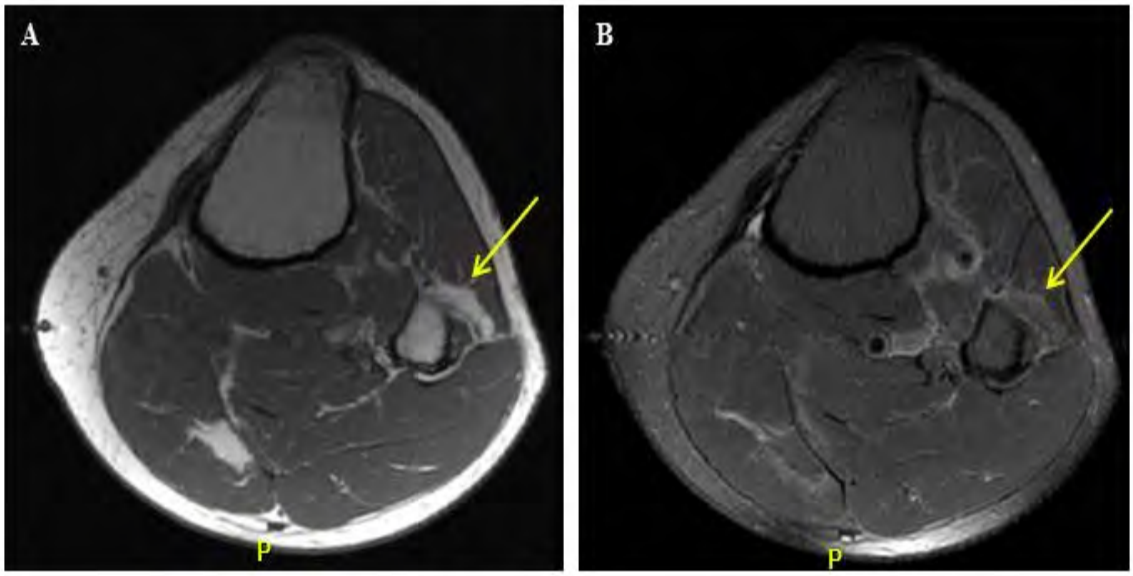

Figure 2 demonstrates an intraneural lipoma eccentrically within the peroneal nerve (arrows). It follows the signal of fat on T1 (A) and T2FS (B) images.

Poster #31

POPLITEAL LYMPH NODES IN PATIENTS WITH OSTEOSARCOMA: ARE THEY METASTATIC?

Shivani Ahlawat, MD; Mark Cleary, MD; Laura Fayad, MD
Johns Hopkins University, Baltimore, MD, USA
(Presented by: Shivani Ahlawat, MD, Johns Hopkins University)

Purpose: To evaluate the prevalence, imaging appearance and significance of popliteal lymph nodes (LN) on magnetic resonance (MR) imaging in patients with distal femoral or proximal tibial osteosarcoma (OS).
Materials and Methods: This IRB approved, HIPAA compliant retrospective study included consecutive patients with OS presenting to our institutional sarcoma center from 05/2016-03/2018. Inclusion criteria were: patients with distal femoral or proximal tibial OS, MR imaging and pathology evaluation at our institution. On MR imaging, tumor size, location, signal characteristics and extra-compartmental extension of the primary tumor and popliteal LN when present. Clinical data including tumor grade (grades 1-3), histology, stage based on chest CTand bone scan, operative notes, as well as follow-up were recorded. Descriptive statistics are provided.
Results: Sixteen patients with OS (age: 20+10 (range10-40) years, 6/16 female) were included (osteoblastic type (n=10), chondroblastic (m=3), surface (n=2), and fibroblastic (n=1)). One patient had a history of total body irradiation for aplastic anemia and another had 2 retinoblastomas. According to pathology, 81% (13/16) OS were classified as high-grade/grade 3. Although 87% (14/16) of the patients had popliteal LNs on MR imaging at presentation (size range: 0.3-3.6 cm), few patients had extra-compartmental spread: intra-articular extension (50% (8/16), skip lesions (25% (4/16)), lung metastases 31% (5/16) and osseous metastases (12% (2/16). Four (25%) patients had popliteal lymph nodes greater than 1cm in mean size: one presumed metastatic due to rapid development, mineralization and avidity on PET-CT, two were pathologically proven to be reactive while one is treated and presumed as non-metastatic. The remainder (75% (12/16)) were less than 1cm in mean diameter and presumed as non-metastatic.
Conclusion: In our single center preliminary evaluation, small popliteal LNs (mean size<1cm) are frequently visible on MR imaging of patients with OS; when large (mean size>1cm), they can rarely be metastatic in etiology (overall prevalence=6%).

Modality % - Radiography / Fluoroscopy:	0
Modality % - CT:	0
Modality % - MRI:	100
Modality % - US:	0
Modality % - Nuclear Medicine:	0

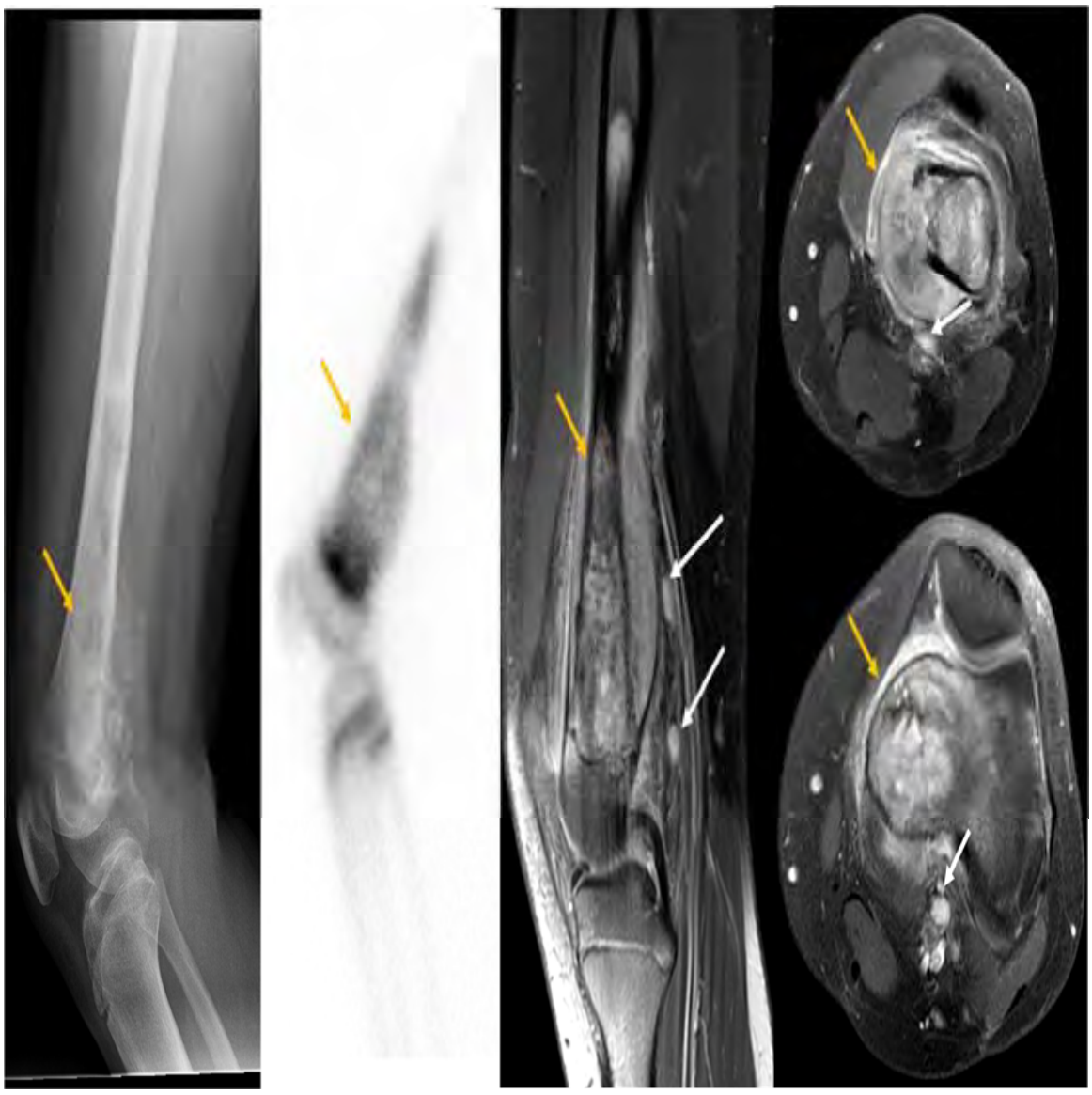

17 year old male with distal femoral grade 3 osteoblastic osteosarcoma with skip lesions and popliteal lymph nodes (arrows).

Poster #32

SCAPULAR AND PERISCAPULAR LESIONS: WHAT THE RADIOLOGIST NEEDS TO KNOW

Terence Farrell, MD, MRCPI, FFRRCSI, FRCRUK[1]; Kristen McClure, MD[2]; DIane Deely, MD[2]; Adam Zoga, MD, MBA[2]
[1]Jefferson Radiology Musculoskeletal Radiology Fellowship, Philadelphia, PA, USA; [2]Thomas Jefferson University Hospital, Philadelphia, PA, USA
(Presented by: Terence Farrell, MD, MRCPI, FFRRCSI, FRCRUK, Jefferson Radiology Musculoskeletal Radiology Fellowship)

Purpose: The scapula is a key component of the shoulder girdle. It has complex anatomy forming predominantly from intramembranous ossification with seven ossification centers and contains 17 sites of muscular attachment. This can make the evaluation of scapular and periscapular lesions more challenging compared to long bones. The extent of scapular and periscapular disease and involvement of critical structures dictates treatment algorithms. The scapula is most often imaged at the edge of the field of view of a shoulder MRI or chest CT and is frequently a forgotten bone making it an important review area on these studies. The purpose of this exhibit is to review normal scapular and periscapular anatomy, identify appropriate MR imaging protocols for the scapula and through a case-based approach demonstrate the array of neoplastic and non-neoplastic scapular pathologies emphasising the impact of involvement of key structures on treatment decisions.

Materials and Methods: Educational goals:

Upon completion of this exhibit the reader should be proficient in normal scapular anatomy, be able to identify common scapular pathologies, be cognizant of the array of less common scapular and periscapular pathologies and understand the importance of scapular involvement in treatment decisions.

Results: Results/ Outline:

1. Review normal scapular and periscapular anatomy
2. Review MRI protocols for imaging scapular lesions
3. Case-based imaging review of scapular pathologies highlighting distinguishing imaging features including

a. Infectious and inflammatory disorders
b. Trauma
c. Tumor-like lesions
d. Neoplasia- malignant and benign

Conclusion: The scapula is an uncommon site of disease often imaged at the edge of the field of view and is an important review area on cross-sectional imaging of the shoulder and chest. Its complex anatomy makes the evaluation of scapular and periscapular pathologies challenging. Awareness of normal scapular anatomy and the imaging spectrum of scapular pathologies is important to improve their diagnosis and guide their management.

Modality % - Radiography / Fluoroscopy:	10
Modality % - CT:	30
Modality % - MRI:	50
Modality % - US:	10
Modality % - Nuclear Medicine:	0

3D CT reconstruction of the thorax in a 65 year old male demonstrating a destructive scapular lesion with a chondroid matrix consistent with a chondrosarcoma.

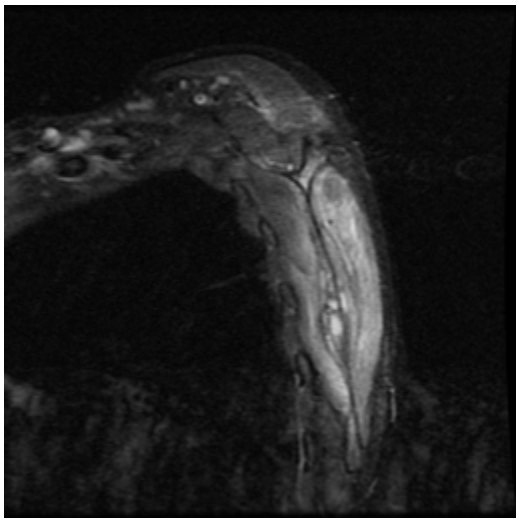

Sagittal STIR MRI of the scapula demonstrating marked periosteal thickening of the scapular body with associated surrounding muscle edema consistent with scapular osteomyelitis.

Poster #33

IMAGING OF EPITHELIOID SARCOMA WITH PATHOLOGIC CORRELATION

Mariam Malik, MD[1]; James Jelinek, MD[2]; Mark Kransdorf, MD[3]; Mark Murphey, MD[1]
[1]American Institute for Radiologic Pathology, Silver Spring, MD, USA; [2]MedStar Washington Hospital Center, Washington, DC, USA; [3]Mayo Clinic, Phoenix, AZ, USA
(Presented by: Mariam Malik, MD, American Institute for Radiologic Pathology)

Purpose: To evaluate the radiologic appearance of epithelioid sarcoma with pathologic correlation.

Materials and Methods: Fifteen pathologically confirmed cases of proximal and distal subtypes of epithelioid sarcoma were retrospectively reviewed. Radiologic studies were independently reviewed by three musculoskeletal radiologists, with agreement by consensus and included radiographs (n=3), ultrasonography (n=3), PET/CT (n=5), CT (n=9), and MRI (n= 12). Evaluation included patient history and demographics, lesion size and location, and intrinsic imaging characteristics on ultrasound, CT and MRI.

Results: Average patient was 34 years old, with male predominance (80%). Symptoms including pain, swelling, or an enlarging mass were present in 50% of patients. All distal and proximal lesions had increased uptake on PET/CT.

All patients with distal lesions presented with skin ulceration of an extremity. Radiographs demonstrated nonspecific soft tissue mass (67%) without calcifications (100%). On MRI, all distal lesions were multifocal and showed infiltrative margins, and underlying bone involvement. All distal lesions demonstrated T1 signal isointense to muscle, and intermediate signal on T2 weighted sequences.

Proximal tumors were solitary and most commonly found in the buttocks or pelvis (50%). The average lesion measured 7.1 cm. Sonograms demonstrated masses with heterogeneous echogenicity (100%). On CT, all tumors were isodense to muscle, and well defined (89%). No calcifications were seen on CT. On MRI, lesions were well-defined (100%) with intermediate signal on both T1 and T2 weighted images. Unlike distal lesions, bone involvement with erosion was unusual (11%). There was only mild surrounding edema in 33% of cases.

Conclusion: The imaging appearance of epithelioid sarcoma varies on the lesion subtype, either distal or proximal. Distal lesions have a suggestive imaging appearance of multifocal subcutaneous lesions with infiltrative margins, bone involvement, and associated surrounding edema. In contradistinction, proximal lesions have a nonspecific imaging appearance of a well-defined soft tissue mass without intrinsic features to suggest diagnosis.

Modality % - Radiography / Fluoroscopy:	8
Modality % - CT:	35
Modality % - MRI:	50
Modality % - US:	5
Modality % - Nuclear Medicine:	2

Oblique radiograph shows nonspecific appearance of large fungating mass centered around the thumb of the right hand.

Post contrast T1 weighted image of the hand demonstrates multifocal areas of enhancement and bone involvement.

Poster #35

CURRENT CONCEPTS IN FOOT AND ANKLE TRAUMA: IMAGING FEATURES, HARDWARE AND COMPLICATIONS

Zachary Ashwell, MD, MS; Hyo-Jeong Mulcahy, MD; Felix Chew, MD
University of Washington / Harborview Medical Center, Seattle, WA, USA
(Presented by: Zachary Ashwell, MD, MS, University of Washington / Harborview Medical Center)

Purpose: The foot and ankle are functionally complex structures, subject to a wide array of trauma with an increasing incidence over the past two decades. Due to the complex anatomy and the importance of adequate fracture reduction, internal fixation can be extremely challenging and complications are common. As such, it is essential that radiologists be familiar not only with diagnosis of the initial fracture but also the normal and abnormal postoperative appearances. Doing so will aid in avoiding diagnostic pitfalls and ensure early and adequate intervention so as to reduce long-term disability.

Materials and Methods: Teaching points/Educational goals:

1. Describe pertinent foot and ankle anatomy.
2. Discuss common and uncommon fracture mechanisms/biomechanics.
3. Review the imaging appearance of foot and ankle fractures, associated fracture classifications and their implications on treatment.
4. Describe surgical approaches, goals of surgery and the expected postoperative appearance of each case of fracture fixation.
5. Recognize the role of various imaging modalities in fracture diagnosis, follow-up and identifying complications.
6. Illustrate examples of common and uncommon hardware failure patterns as well as how and why they occur.

Results: Key issues:

1. Foot and ankle fractures are common but easily missed due to complex anatomy and superimposition of overlying structures.
2. Understanding of foot and ankle biomechanics may aid in initial fracture detection.
3. Knowledge of goals of surgical reduction and fixation will improve the reader's ability to identify normal vs. abnormal postoperative appearance.
4. Many postoperative complications occur in a predictable pattern but are missed due to unfamiliarity with hardware and goals of fracture reduction.

Conclusion: Familiarity with the normal as well as the abnormal postoperative appearance of orthopedic fixation hardware about the foot and ankle is essential to ensure early intervention and to minimize complication rates.

Modality % - Radiography / Fluoroscopy:	40
Modality % - CT:	60
Modality % - MRI:	0
Modality % - US:	0
Modality % - Nuclear Medicine:	0

Lateral and Broden views revealing an abnormally shallow Bohler angle resulting from a Sanders type 2C joint depression type intraarticular calcaneal fracture.

Immediate postoperative radiographs demonstrating congruity of the subtalar joint with restoration of Bohlers angle. Seven month follow up imaging reveals hardware failure with subsidence.

Complicated fractures of the distal tibia and fibula requiring staged repair.

Misinterpreted hardware infection resulting in subsequent multicomponent hardware failure.

Poster #36

IMAGING EVALUATION OF HEEL PAIN

Sailaja Yadavalli, MD, PhD; Onowenerhi Omene, MD
Beaumont Health System, Royal Oak, MI, USA
(Presented by: Sailaja Yadavalli, MD, PhD, Beaumont Health System)

Purpose: Heel pain is seen in patients of all ages raging from the young athlete to the very old, including the middle-aged weekend warrior or a person with sedentary lifestyle. The pain may be quite debilitating whether it results from an acute injury or due to chronic changes with worsening symptoms. Heel pain may relate to abnormalities of tendons, plantar fascia, bursae, nerves, the calcaneus, or the surrounding soft tissues. Causes include trauma, infectious or inflammatory processes, neoplasms, and post-operative changes. It is often difficult to clearly delineate the cause of pain from physical exam alone and therefore imaging has an important role in making an accurate diagnosis and treatment plan.

Materials and Methods: The exhibit will be in a case based format and will discuss the optimal use of various imaging modalities including MRI, CT, US and radiography in the evaluation of heel pain. Cases will include abnormalities related to tendons, plantar fascia, the calcaneus and surrounding soft tissues. Examples discussed in the presentation will include, but not be limited to, tendon and fascial rupture, post-operative changes of Achilles tendon, Haglund's syndrome, xanthomas, plantar fibromatosis, heel and fat pad abnormalities, bursitis, stress injuries of calcaneus, Sever's disease, neoplasms of calcaneus and surrounding soft tissues, osteomyelitis, and enthesitis secondary to inflammatory processes.

Results: MRI is the most preferred modality for imaging evaluation of heel pain. However, ultrasound also plays an important role in many cases given its easy access and versatility for dynamic imaging. In some cases correlation with radiographs or CT exam, where faint soft tissue calcifications are better seen, allows one to reach a definitive diagnosis.

Conclusion: Understanding the various causes of heel pain, optimal imaging, and correlation with history and symptoms is important in assessing heel pain where clinical findings alone are not adequate in reaching a correct diagnosis and treatment plan.

Modality % - Radiography / Fluoroscopy:	10
Modality % - CT:	10
Modality % - MRI:	60
Modality % - US:	20
Modality % - Nuclear Medicine:	0

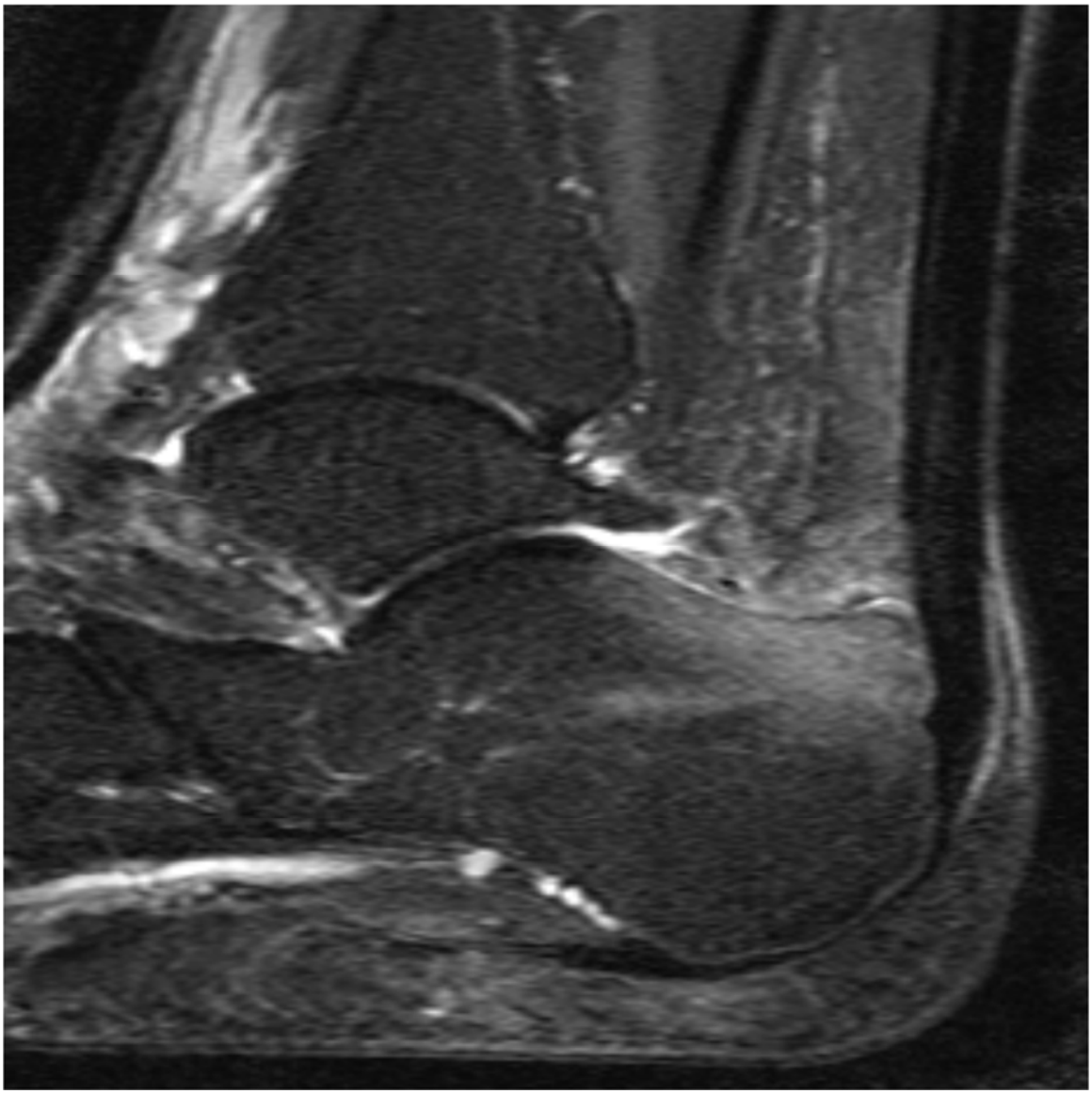

Haglund's Syndrome: Note thickened Achilles tendon with retocalcaneal and retro-Achilles bursitis and prominence of calcaneus with bone marrow edema.

Sever's Disease or Calcaneal Apophysitis: Note bone marrow edema along posterior aspect of calcaneus in the apophysis in a 10 year old patient.

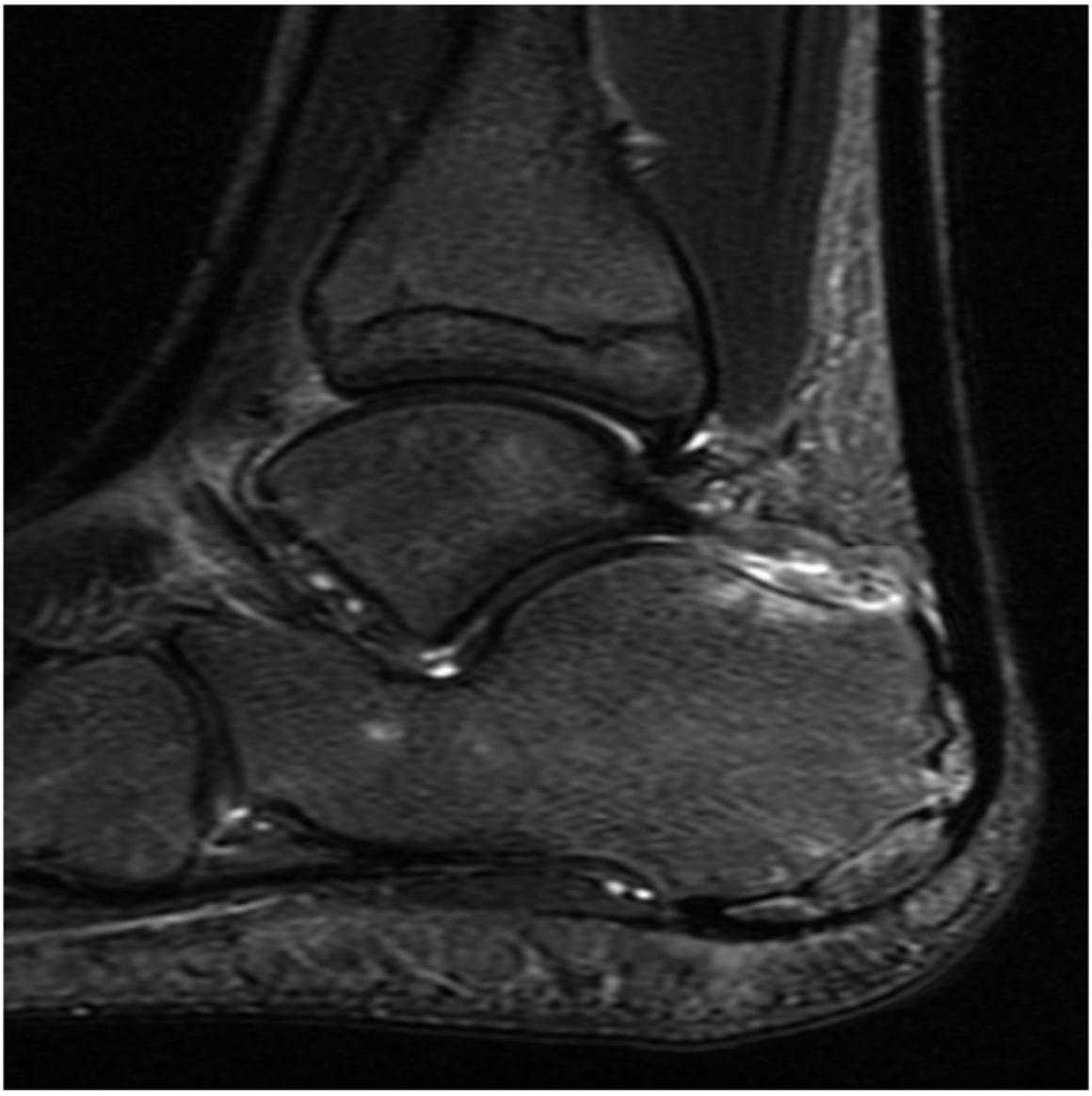

US of Achilles tendon in patient with hypercholesterolemia: Fusiform hypoechoic lesion in thickened Achilles tendon is the typical appearance of a xanthoma.

Poster #37

COMMUNICATION BETWEEN THE NAVICULOCUNEIFORM AND SECOND AND THIRD TARSOMETATARSAL ARTICULATIONS: UNDERAPPRECIATED NORMAL ANATOMY AND HOW IT MAY IMPACT FLUOROSCOPIC GUIDED INJECTIONS

Barry Hansford, MD[1]; Megan Mills, MD[2]; Sarah Stilwill, MD[2]; Anna McGow, MD[2]; Chris Hanrahan, MD, PhD[2]
[1]Oregon Health Sciences University, Portland, OR, USA; [2]University of Utah Medical Center / SOM, Salt Lake City, UT, USA
(Presented by: Barry Hansford, MD, Oregon Health Sciences University)

Purpose: Since second/third tarsometatarsal and naviculocuneiform joints normally communicate, the least arthritic/technically most straightforward joint was injected when a fluoroscopically-guided therapeutic injection was ordered for one or both joints. We hypothesized that pain relief would be equivalent regardless of the joint injected and would result in less radiation and steroid dose compared to patients with both articulations injected.
Materials and Methods: Seventy-eight patients were divided into four joint groups: 1) naviculocuneiform requested and injected (n=15), 2) non-requested naviculocuneiform or second/third tarsometatarsal injected (n=25), 3) both injected (n=23), and 4) tarsometatarsal requested and injected (n=15). Variables recorded included: patient age, gender, fluoroscopy time, steroid amount, pre- and post-procedural pain, arthritis degree and confidence of intra-articular injection. Statistical analysis compared mean pain level change pre- and post-injection, mean fluoroscopy time, and mean steroid amount between groups. The mean OA of the non-requested joint was compared to the requested joint OA in patients whose injected and requested joints did not match (group 2).
Results: Pre- and post-injection pain reduction ($p=0.630$) and post-injection pain ($p=0.935$) were not significantly different. Mean steroid dose ($p<0.0001$) and fluoroscopy time ($p=0.0001$) were significantly increased for the both joint injection group. Within the non-requested naviculocuneiform or second/third tarsometatarsal injection group, there was a significant difference in OA grade between injected (least arthritic) and requested joints ($p= 0.001$).
Conclusion: When faced with challenging naviculocuneiform or second/third tarsometatarsal joint injections, choosing the technically most straightforward joint may result in less radiation and steroid dose without compromising quality of care/pain reduction.

Modality % - Radiography / Fluoroscopy:	90
Modality % - CT:	5
Modality % - MRI:	5
Modality % - US:	0
Modality % - Nuclear Medicine:	0

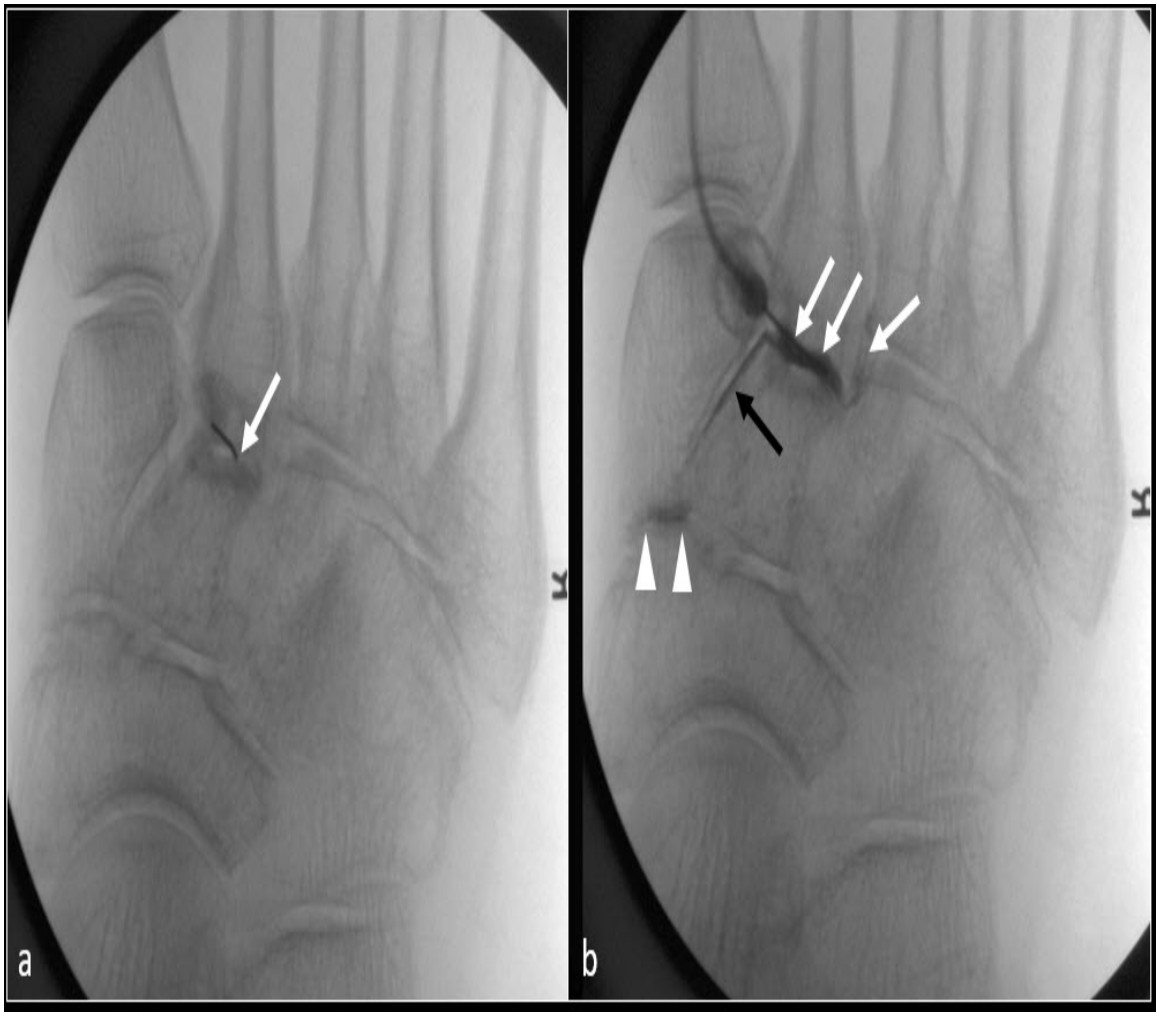

A) AP pre-fluoroscopic image needle in second TMT joint. B) AP post-injection fluoroscopic image contrast communicates with naviculocuneiform joint (arrowheads) via intercuneiform articulation (black arrow).

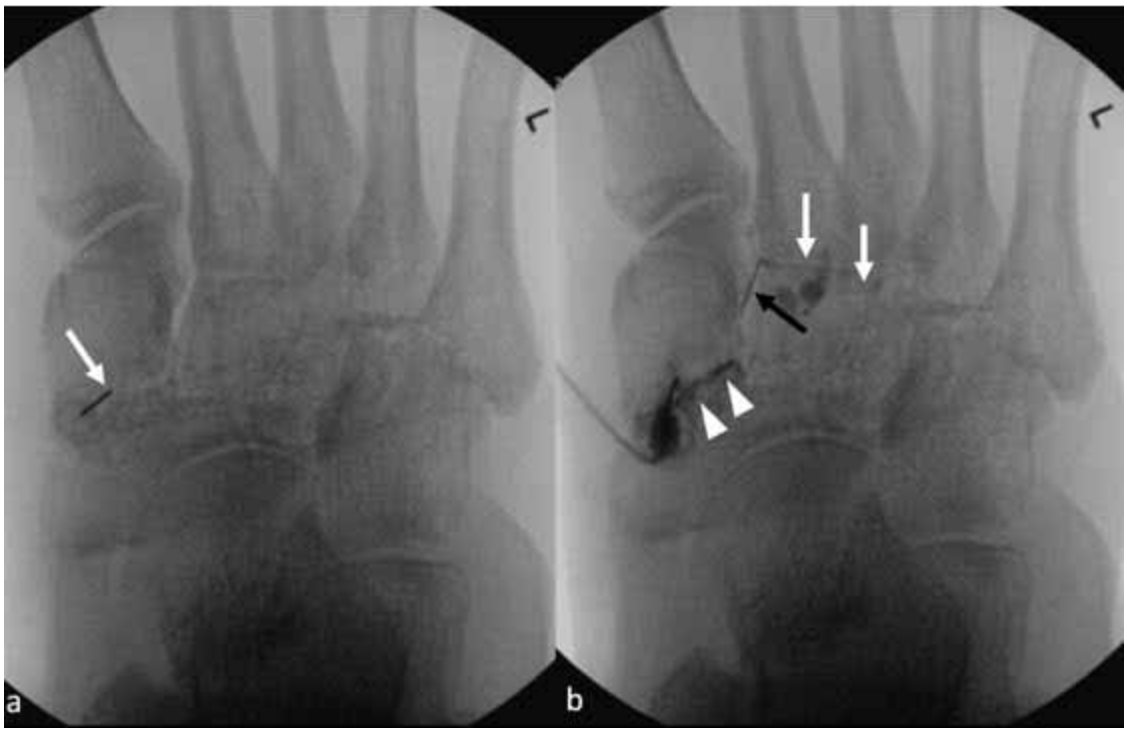

A) AP pre-fluoroscopic image needle in naviculocuneiform joint. B) AP post-injection fluoroscopic image contrast communicates with second/third TMT (white arrows) via intercuneiform articulation (black arrow).

Poster #38

ADDED BENEFIT OF KNEE MRI VERSUS RADIOGRAPHS ALONE IN PATIENTS 60 YEARS AND OLDER

Michael Fox, MD, MBA, FACR[1]; Jeremiah Long, MD[1]; Mark Kransdorf, MD[1]; Jonathan Flug, MD[1]; Ashtyn Chamberland[2]; Adam Schwartz, MD[1]
[1]Mayo Clinic Arizona, Phoenix, AZ, USA; [2]Grand Canyon University, Phoenix, AZ, USA
(Presented by: Michael Fox, MD, MBA, FACR, Mayo Clinic Arizona)

Purpose: Determine if knee MRIs alter management in patients aged 60 and older compared to radiographs alone.
Materials and Methods: Consecutive patients aged 60 and older who had knee radiograph and MRI exams performed within 90 days of each other and no history of malignancy or trauma (within 90 days) were identified. Radiographs included standing (AP, PA flexion, lateral) and Merchant views and were evaluated by an MSK radiologist with 4 years of experience using the Kellgren-Lawrence (KL) and the International Knee Documentation Committee (IDKC) scoring systems. Original MRI report interpretations were used.
Results: 50 patients (mean age 70 (range 60-88); 23F:27M) met the inclusion criteria. Orthopedic surgeons ordered 38% of the knee MRIs (19/50) and 82% of patients were eventually evaluated by orthopedics (41/50). In 14% of patients, radiographs followed the MRI. Mean follow-up after MRI with provider or ortho was 16 days on average (range 0-90) with the MRI performed 23 days (mean) after radiographs (range 0-82).
5 patients had subchondral fractures on MRI (mean age 78.4 (67-88); 3F:2M) and 6 patients (mean age 64.5 (60-70); 3F:3M) had management changed (arthroscopy (n= 5) and symptomatic ruptured popliteal cyst (n=1)). 39 patients did not have a material change in management documented.

Using the PA flexion view, none of the 11 patients (0%) with either a subchondral fracture or a change in management had a KL score of 4, compared to 20.5% (8/39) of the patients with no management change (p=0.10).

Conclusion: 22% of patients over the age of 60 had either a subchondral fracture detected or a change in management based on the MRI findings; all 11 having a PA flexion KL score of 3 or less. A trend suggests that patients with a KL score of 4 do not typically gain additional benefit from an MRI; however, additional numbers are required to confirm.

Modality % - Radiography / Fluoroscopy:	80
Modality % - CT:	0
Modality % - MRI:	20
Modality % - US:	0
Modality % - Nuclear Medicine:	0

Poster #39

ROUTINE KNEE MRI: HOW COMMON ARE PERIPHERAL NERVE ABNORMALITIES?

Shivani Ahlawat, MD; Laura Fayad, MD
Johns Hopkins University, Baltimore, MD, USA
(Presented by: Shivani Ahlawat, MD, Johns Hopkins University)

Purpose: To evaluate the prevalence, MRI appearance, and pattern of peripheral nerve abnormalities visible on routine knee MRI.

Materials and Methods: A retrospective PACS review was performed to identify consecutive patients who underwent knee MRI from 03/2015-03/2018. Clinical data including indication, injury mechanism, operative findings and clinical outcomes were recorded. The MR images were reviewed for the presence or absence of tibial and common peroneal nerve (CPN) abnormality including size, signal intensity, bulbous enlargement, architectural distortion, and discontinuity. Additional findings including presence or absence of meniscal, cruciate and ligament injury were recorded. Descriptive statistics are reported.

Results: The search yielded 8,125 MRI studies, of which 48 patients (age (years):44+19; range:9-77) with 50 knee MRs had abnormalities of the CPN and tibial nerves. Clinical indications were: pain(n=18), trauma(n=17), weakness(n=12), or lump(n=3). An abnormal tibial nerve (n=13/50) exhibited hyperintensity (n=13/13), enlargement(n=4/13), effaced perineural fat(n=2/13), architectural distortion(n=2/13) and skeletal muscle denervation(n=6/13). An abnormal CPN was more common (36/50) and exhibited hyperintensity(n=36/36), enlargement(n=27/36), effaced perineural fat(n=3/36), architectural distortion (n=8/36) and muscle denervation (n=12/36). Spectrum of pathologies included tumors (n=3/50), intraneural ganglion (n=1/50), nerve ischemia after embolization(n=1/50), neuroma(n=4/50), and entrapment(n=6/50). Patients with nerve abnormalities had concomitant ACL injuries(n=16/50), of the CPN(n=13/16) or tibial nerve(n=2/16). A subset of patients with ACL and multi-ligament injuries (n=4/16) had CPN neuromas excluded from the FOV(n=2/4). Treatment included CPN decompression (n=2), and nerve grafting (CPN (n=4) and tibial nerve (n=1)); otherwise, to our knowledge, no peripheral nerve treatment was offered.

Conclusion: Although rare (prevalence=0.6%), peripheral nerve abnormalities (CPN more common than tibial nerve) are visible on knee MRI, and can affect patient management. In patients with multi-ligament injury, a neuroma may extend more proximal than imaged in a routine knee MR FOV and require additional imaging.

Modality % - Radiography / Fluoroscopy:	0
Modality % - CT:	4
Modality % - MRI:	100
Modality % - US:	0
Modality % - Nuclear Medicine:	0

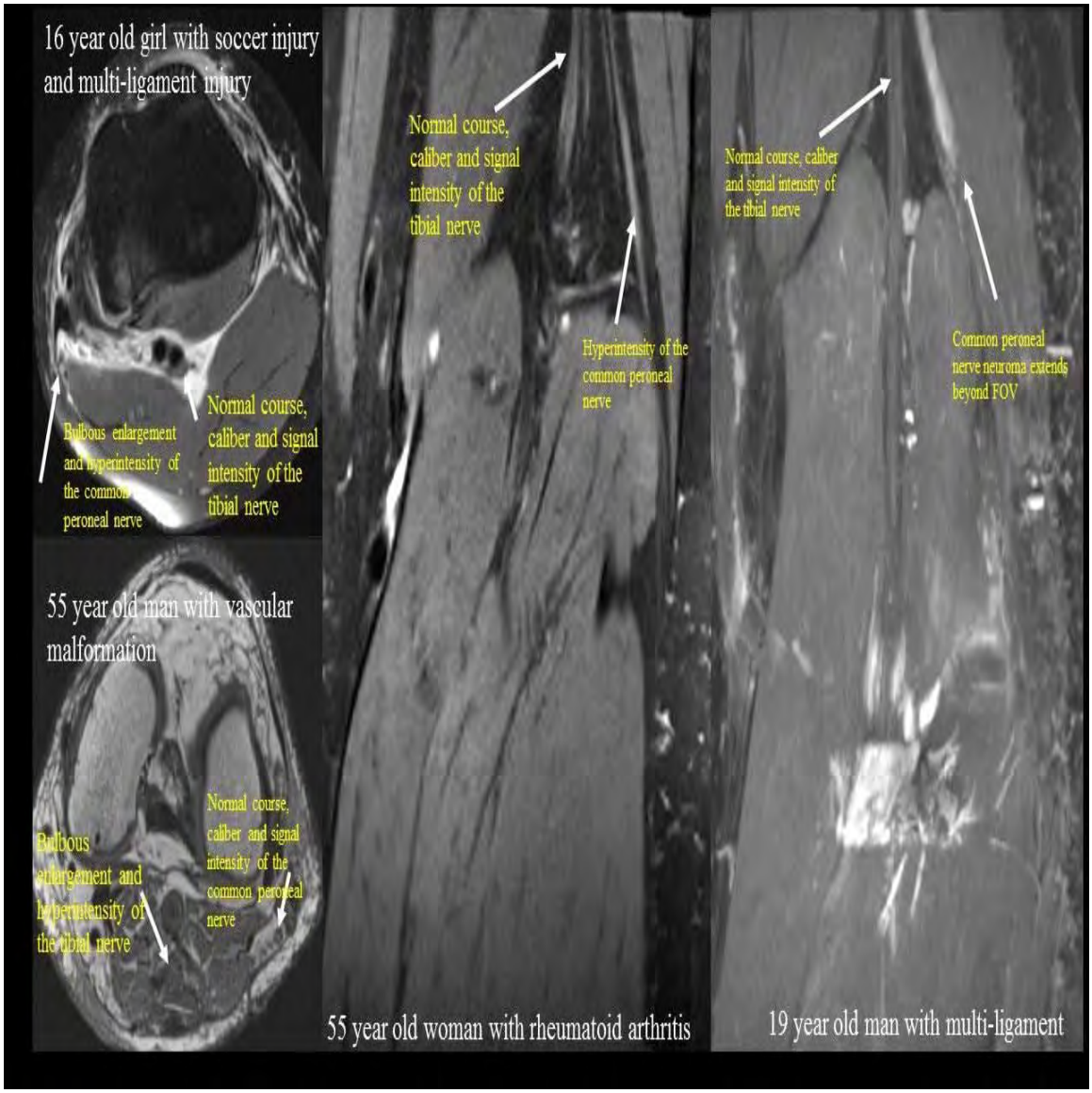

Although rare, radiologists should be aware that clinically-significant peripheral nerve abnormalities occur, and may extend more proximal than identified on typical knee MRI FOV.

Poster #40

INCIDENCE AND SPECIFICITY OF INTRALESIONAL FAT GLOBULES WITHIN MOREL-LAVALLEE LESIONS ABOUT THE KNEE

Justin Friske, MD; Stephen Broski, MD
Mayo Clinic, Rochester, MN, USA
(Presented by: Justin Friske, MD, Mayo Clinic)

Purpose: Differentiation of prepatellar bursitis from post-traumatic degloving injuries (Morel-Lavallee lesions) about the knee can occasionally present a diagnostic dilemma for clinicians and radiologists. Several features have been described as suggestive of MLL including:

-Collection extending beyond the expected location of the prepatellar bursa, including in the transverse dimension to the level of the femoral epicondyles
-Presence of intralesional fat globules within the collection

In our practice it was felt that the presence of intralesional fat globules would be fairly specific however literature documenting specificity was lacking. The purpose of this study was to investigate the frequency and specificity of intralesion fat globules within a prepatellar fluid collection suspected of being either a MLL lesion or prepatellar bursitis.
Materials and Methods: Retrospective search of the medical/radiology database (MRI within 2 years, dictation query of "morel-lavallee" or "prepatellar bursitis").

Data including:
-Location (prepatellar, pelvis/thigh, other)
-Presence of intralesional fat globules
-Transverse dimension extending to the level of the femoral epicondyles
-Size/volume, MRI characteristics, radiologist and clinician interpretation
-Degree of clinical confirmation (surgical, vs sclerotherapy, vs resolution after multiple aspirations, vs none, vs aspiration positive for bursal infection/inflammatory process)
Results: Pending final data collection and analysis. Preliminary data includes 89 individual discrete cases queried under "Morel-Lavallee" and 68 cases queried under "prepatellar bursitis". Preliminary data evaluation suggests that intralesional fat globules are not uncommon for Morel-Lavalle and rare for bursitis. In both cases, findings rarely go on to definitive clinical confirmation with surgery, sclerotherapy, or definitive aspiration due to resolution with time/conservative treatment and relatively mild symptoms/clinical concern.
Conclusion: Preliminary data suggests that intralesional fat globules may be useful for evaluating prepatellar lesions, especially in conjunction with other suggestive features, however data collection and analysis is ongoing.

Modality % - Radiography / Fluoroscopy:	0
Modality % - CT:	5
Modality % - MRI:	90
Modality % - US:	5
Modality % - Nuclear Medicine:	0

T1 weighted image demonstrates prepatellar fluid collection extending medially to the level of the medial femoral epicondyle. Intralesional fat lobules are present.

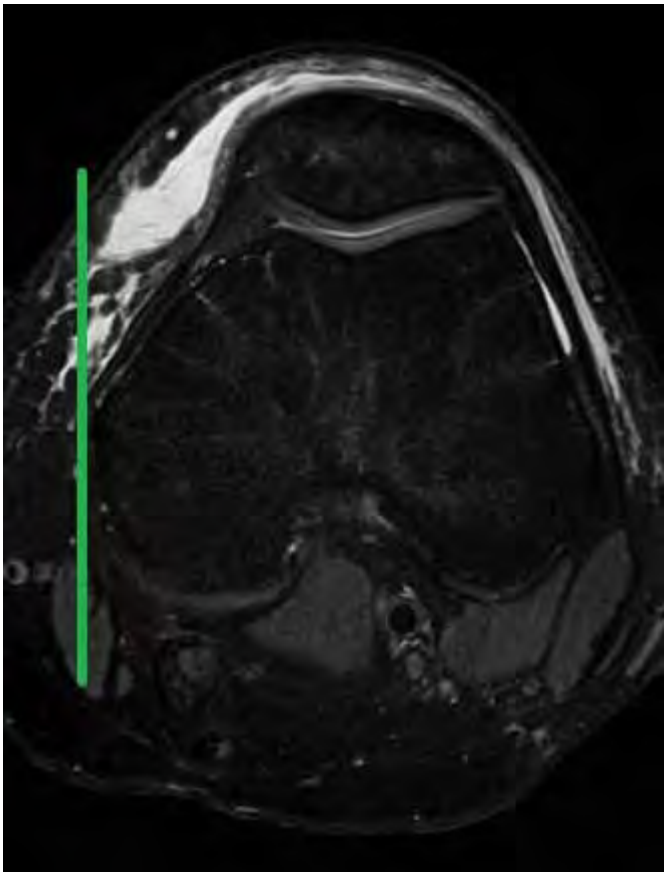

T2 weighted image demonstrates prepatellar fluid collection extending in transverse dimension to the level of medial femoral epicondyle, beyond the expected boundary of the bursa.

Poster #41

MULTIMODAL IMAGING OF ACUTE TRAUMATIC BONE MARROW LESIONS IN THE KNEE: NEW INSIGHTS WITH HIGH RESOLUTION PERIPHERAL QUANTITATIVE CT

Richard Walker, MD[1]; Andres Kroker, MS[2]; Mariya Shtil[2]; Sarah Manske, MS, PhD[1]; Nicholas Mohtadi, MD, MS[3]; Steven Boyd, MS, PhD[1]

[1]Department of Radiology, Cumming School of Medicine, University of Calgary, Calgary, AB, Canada; [2]University of Calgary, Calgary, AB, Canada; [3]University of Calgary Sport Medicine Centre, Calgary, AB, Canada

(Presented by: Richard Walker, MD, Department of Radiology, Cumming School of Medicine, University of Calgary)

Purpose: To describe the temporal changes of traumatic bone marrow lesions (BMLs) in the knee following acute anterior cruciate ligament (ACL) rupture on magnetic resonance imaging (MRI) and high resolution peripheral quantitative computed tomography (HRpQCT).

Materials and Methods: Subjects between the age of 18 and 45 presenting to a specialized acute knee assessment clinic with a clinical diagnosis of an acute ACL rupture between July 2016 and June 2017 were recruited for 1.5T knee MRI at baseline, 4 months and 8 months post injury and HRpQCT at baseline, 2, 4, and 8 months post injury. Subjects with a history of prior knee injury or a contraindication to MRI were excluded.

Results: 49 subjects were enrolled. 39 completed baseline imaging, 31 completed 2-month follow-up and 18 completed either 4-month and/or 8-month follow-up imaging. 3 were excluded due to motion artifact on HRpQCT, resulting in a cohort of 15 subjects (10 female) for longitudinal evaluation of 4 months or longer. Average time between injury and baseline imaging was 31 days. At HRpQCT, preliminary results suggest that trabecular detail (despite 61µm isotropic resolution) was insufficient to confidently identify individual trabecular disruption and confirm microtrabecular fracture at the site of traumatic BMLs. Although the majority of BMLs seen on MRI resolved by the 4-month follow-up scan, HRpQCT confirmed ongoing active remodelling of the subchondral bone at the site of BMLs beyond 4 months.

Conclusion: BMLs in the knee are common following acute traumatic ACL rupture. Despite resolution on MRI by 4 months post-injury, HRpQCT demonstrates active remodelling at the site of BMLs beyond 4 months. Multimodal imaging of BMLs in the knee using MRI and HRpQCT has the potential to provide invaluable insights into the structural changes and physiologic response of bone to acute injury.

Modality % - Radiography / Fluoroscopy:	0
Modality % - CT:	50
Modality % - MRI:	50
Modality % - US:	0
Modality % - Nuclear Medicine:	0

Poster #42

Effect of Patellar Instability on Extensor Mechanism Dysfunction

Jehan Ghany, MD; Vishal Desai, MD; William Morrison, MD; Johannes Roedl, MD, PhD; Jeffrey Belair, MD; Adam Zoga, MD
Thomas Jefferson University Hospital, Philadelphia, PA, USA
(Presented by: Jehan Ghany, MD, Thomas Jefferson University Hospital)

Purpose: Patellar instability or maltracking is a common cause of anterior knee pain and is predominantly a result of structural abnormalities, including trochlear dysplasia, patella alta, patellar tilt/translation, tibial tubercle lateralization, and an increased Q angle. This study investigates the effect of the repeated stress on the patellar stabilizers, particularly the extensor mechanism, in patients with maltracking.

Materials and Methods: A retrospective review of our institutional RIS was performed for patients with patellofemoral maltracking on knee MRI. An age-matched control group without maltracking on MRI was obtained. For each case, the following was reviewed: demographics, degree of quadriceps or patellar tendinosis, presence of tendon tears, and any predisposing anatomic variants such as trochlear dysplasia, patella alta, patellar tilt/translation, and an increased TT-TG distance. The incidence of extensor mechanism dysfunction (tendinosis and/or tear) was compared for patients with and without patellar instability, and the association with each variable was reviewed.

Results: Data collection is in progress. At the time of submission, knee MRI of 100 patients with patellofemoral maltracking and 50 patients without were reviewed. 45% of patients in the maltracking group had quadriceps tendinosis compared to 28% in the age-matched control group ($p<0.05$). 5% of patients in the maltracking group had patellar tendinosis compared to 1% in the control group. Extensor mechanism dysfunction was present in 38% of patients with trochlear dysplasia, 46% with patella alta, 45% with patellar tilt/translation. In the preliminary dataset, there was a trend towards increased TT-TG distance in those with quadriceps tendinosis compared to those without in the maltracking group (17 mm versus 16 mm).

Conclusion: Extensor mechanism dysfunction is associated with patellar instability, specifically quadriceps and patellar tendinosis. The use of imaging to identify patients with patellar instability and risk factors for concomitant extensor mechanism pathology could help focus conservative treatment or classify patients who may benefit from early intervention.

Modality % - Radiography / Fluoroscopy:	0
Modality % - CT:	0
Modality % - MRI:	100
Modality % - US:	0
Modality % - Nuclear Medicine:	0

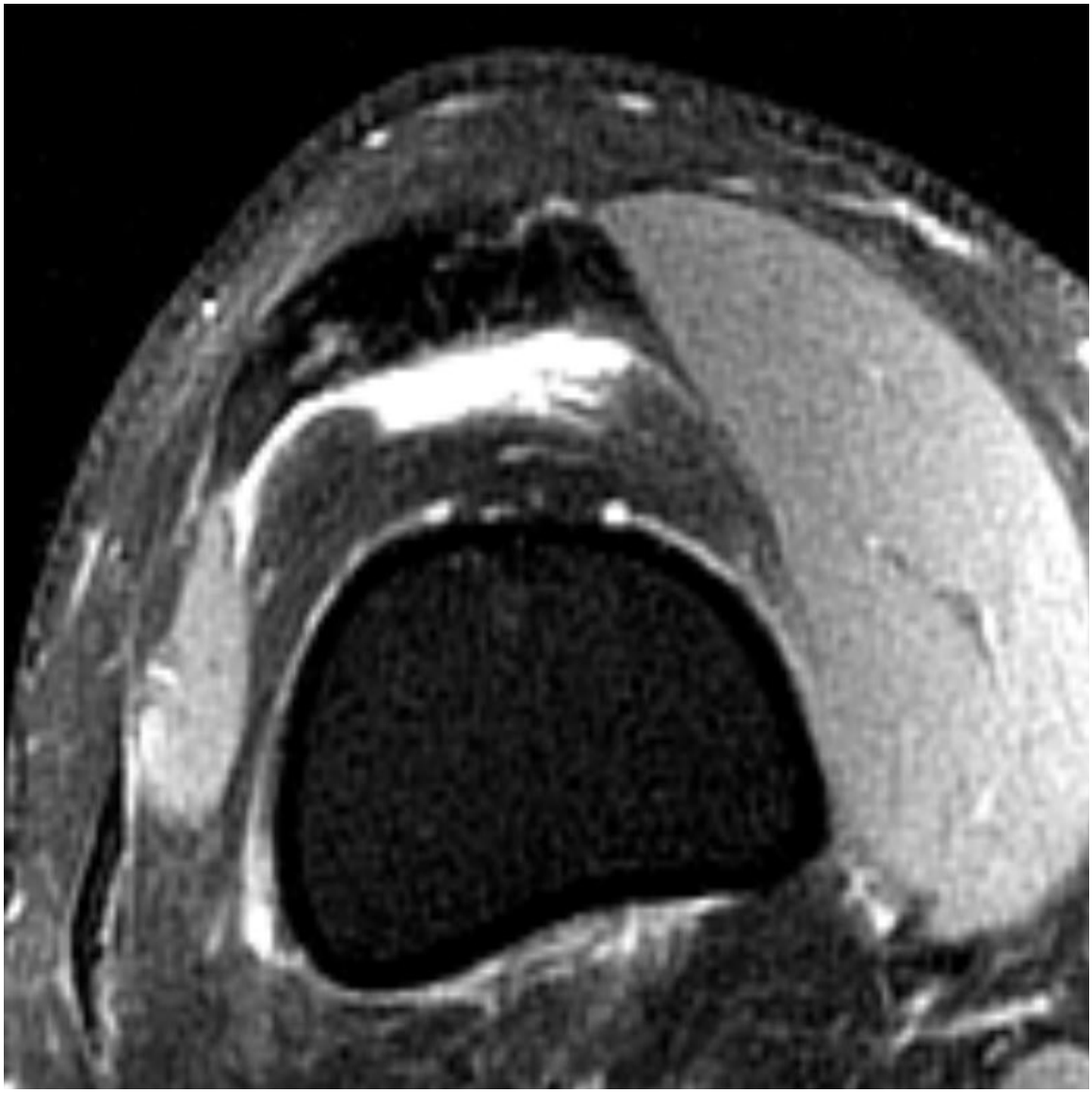

Example of a patient with patellofemoral maltracking by MRI with associated quadriceps tendinosis and peritendinous edema

Poster #43

THE ANTERIORLY DISPLACED ACL STUMP: A FREQUENT FINDING BUT UNCOMMON CAUSE FOR A "LOCKED KNEE"

Richard Walker, MD[1]; Andres Kroker, MS[2]; Peter Salat, MD[1]; Nicholas Mohtadi, MD, MS[3]
[1]Department of Radiology, Cumming School of Medicine, University of Calgary, Calgary, AB, Canada; [2]University of Calgary, Calgary, AB, Canada; [3]University of Calgary Sport Medicine Centre, Calgary, AB, Canada
(Presented by: Richard Walker, MD, Department of Radiology, Cumming School of Medicine, University of Calgary)

Purpose: To describe the relationship between a displaced distal anterior cruciate ligament (ACL) stump and fixed extension deficit of the knee on clinical exam in the setting of acute ACL rupture.
Materials and Methods: A retrospective, blinded chart review of subjects presenting to a local sport medicine centre between July 2016 and June 2017 was performed. Subjects were stratified based on the presence or absence of knee extension deficit ("locked knee") on clinical evaluation.
Inclusion criteria included age between 18 and 45 with clinical evidence of acute ACL rupture, not prior history of knee injury and no contraindication to MRI. All subjects underwent a standardized clinical assessment and a 1.5T knee MRI prospectively interpreted by a musculoskeletal radiologist using a standardized reporting template. Findings on the MRI were correlated with the audit assessment and surgical reports, when available.
Results: 49 subjects were enrolled. 12 were excluded leaving 37 subjects for analysis, including 22 females. Average age was 30.9 years, average time between injury and clinical assessment was 18 days and clinical assessment and MRI 10 days.
All subjects had evidence of an ACL tear and 46% had an anteriorly displaced ACL stump on MRI. Based on the audit, 6 of 37 were considered suspicious for a "locked knee" on clinical evaluation. Of those, MRI demonstrated a displaced distal ACL stump in 2 subjects and both a displaced ACL stump and displaced meniscal tear in 1 subject. No cause for extension deficit was identified on MRI for the remaining 3 subjects. Of note, 14 subjects with an anteriorly displaced ACL stump on MRI did not have clinical evidence of an extension deficit on clinical exam.
Conclusion: In the acute setting, an anteriorly displaced ACL stump was commonly observed on MRI, but an infrequent associated with clinical evidence of a "locked knee" on examination.

Modality % - Radiography / Fluoroscopy:	0
Modality % - CT:	0
Modality % - MRI:	100
Modality % - US:	0
Modality % - Nuclear Medicine:	0

Poster #44

REDUCING UNNECESSARY KNEE MRI IN PATIENTS WITH KNOWN OSTEOARTHRITIS

Dorian Nobbee, MD
University of Calgary, Calgary, AB, Canada
(Presented by: Dorian Nobbee, MD, University of Calgary)

Purpose: Knee MRI is the second most common MRI test in our province. In the setting of chronic pain and documented osteoarthritis, there is no role for the routine use of MRI. A quality improvement project was conducted intending to reduce the number of knee MRI requests in a large Canadian city.

Materials and Methods: A retrospective review of locally performed knee MRIs in patients aged 55 or older with histories that included keywords suggesting osteoarthritis was performed. Every 6th MRI was sampled. Clinical history, prior studies, MRI and final report were reviewed by a senior radiology resident supported by a musculoskeletal radiologist.

A multi-disciplinary team, including Radiology, Rheumatology and Family Medicine, developed a clinical decision support tool to help family physicians and their patients understand that MRI would not assist with management of joint pain and to improve x-ray ordering practices.

At 4 months post-intervention requisitions were sampled and compared using a Fischer exact test.

Results: 1342 MRIs were performed in our pre-intervention population and 237 were sampled. 106/237 (45%, $p<0.05$) were not indicated. The majority 69/106 of studies not indicated had at least moderate osteoarthritis, 28/106 did not have weight-bearing radiographs.

Our clinical decision support tool was the most downloaded tool suggesting the tool was being used by referring primary care physicians. At 4 months post-intervention all requisitions in our population were collected over 1 week. 31 requisitions were assessed, 24/31 were indicated resulting in a 22% decline in inappropriately requested studies ($p=0.02$). The proportion of studies with preceding weight-bearing radiographs also increased from 80% to 92%.

Conclusion: After implementation of our clinical support tool there was a statistically significant decline in the number of inappropriately requested knee MRIs. The intervention will be continuously assessed for a sustained improvement.

Modality % - Radiography / Fluoroscopy:	50
Modality % - CT:	0
Modality % - MRI:	50
Modality % - US:	0
Modality % - Nuclear Medicine:	0

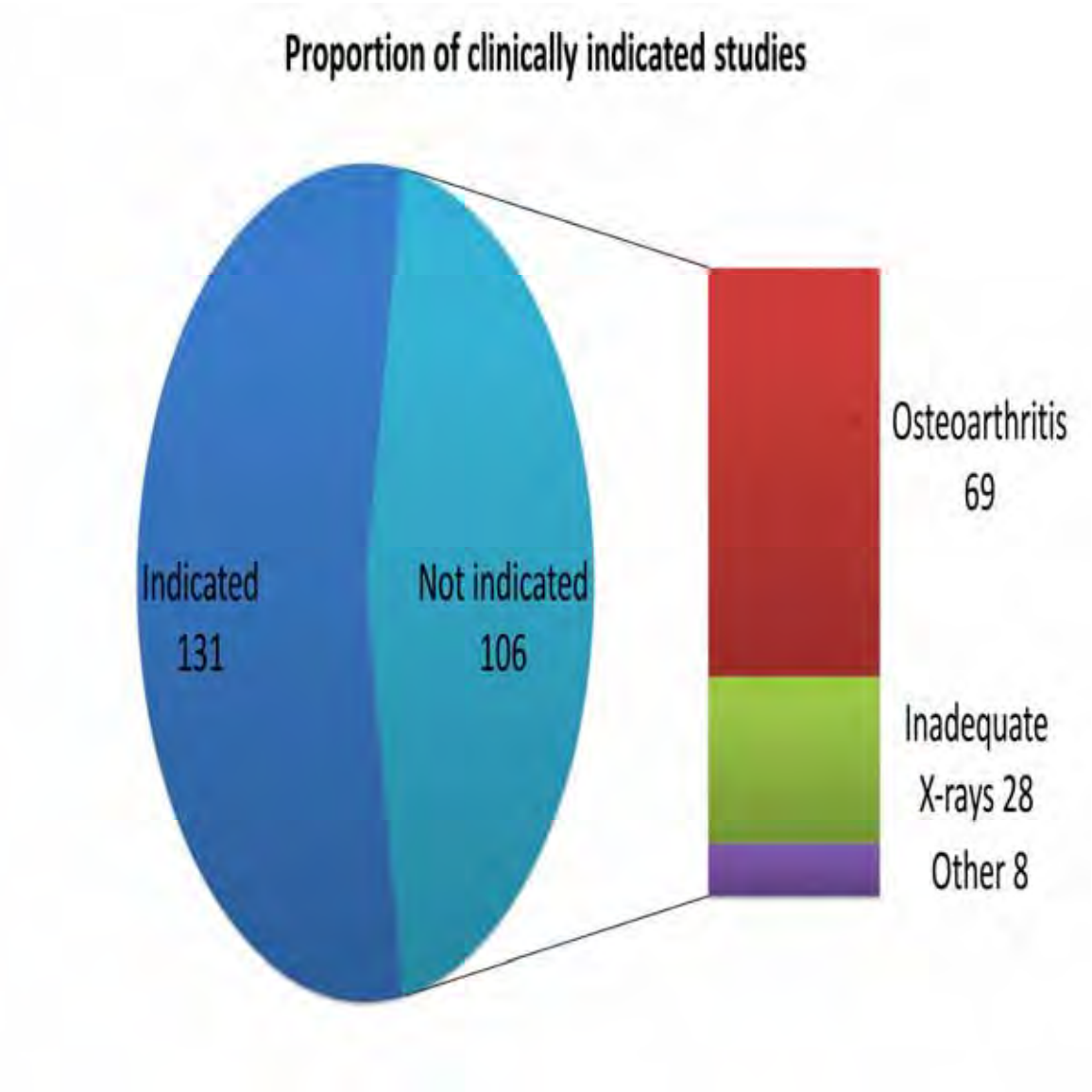

Pre-intervention distribution of indicated and non-indicated studies.

2019 MODALITY CHARTS

Society of Skeletal Radiology

42nd Annual Meeting

March 10-13, 2019

Podium/Poster Number	Modality %: Radiography / Fluoroscopy	Modality %: CT	Modality %: MRI	Modality %: US	Modality %: Nuclear Medicine
Podium 1	15	15	65	0	5
Podium 2	0	100	0	0	0
Podium 3	0	100	0	0	0
Podium 4	0	0	100	0	0
Podium 5	0	0	100	0	0
Podium 6	0	0	1	0	0
Podium 7	0	100	0	0	0
Podium 8	0	100	0	0	0
Podium 9	100	0	0	0	0
Podium 10	10	0	89	0	0
Podium 11	0	0	100	0	0
Podium 12	0	0	100	0	0
Podium 13	0	0	0	100	0
Podium 14	0	0	100	0	
Podium 15	90	5	5	0	0
Podium 16	0	0	100	0	0
Podium 17	0	0	40	60	0
Podium 18	0	0	0	100	0
Podium 19	33	33	29	0	0
Podium 20	0	100	0	0	0
Podium 21	0	33.3	33.3	33.3	0
Podium 22	0	0	0	100	0
Podium 23	80	0	0	20	
Podium 24	5	20	0	75	0
Podium 25	100	0	0	0	0
Podium 26	10	10	80	0	0
Podium 27	0	0	30	70	0
Podium 28	100	0	0	0	0
Podium 29	50	0	50	0	0
Podium 30	0	0	100	0	0
Podium 31	0	0	100	0	0
Podium 32	0	0	100	0	0
Podium 33	50	0	50	0	0
Podium 34	33	33	33	0	0
Podium 35	20	80	0	0	0
Podium 36	0	100	0	0	
Podium 37	0	0	100	0	0
Podium 38	0	0	100	0	0
Podium 39	100	0	0	0	0
Podium 40	90	5	5	0	0
Podium 41	100	0	0	0	0
Podium 42	0	0	100	0	0
Podium 43	0	50	0	0	50
Podium 44	20	10	70	0	
Podium 45	0	0	100	0	0
Podium 46	0	0	100	0	0
Podium 47	10	30	60	0	0
Podium 48	5	15	75	5	
Podium 49	0	0	100	0	0
Podium 50	10	0	90	0	0
Podium 51	0	0	100	0	0
Podium 52	100	0	0	0	0
Podium 53	0	0	100	0	0
Podium 54	0	0	100	0	0
Podium 55	1	0	0	100	0
Podium 56	100	0	0	0	0
Podium 57	0	0	2	0	0
Poster 1	100	0	0	0	0
Poster 2	10	45	45	0	0
Poster 3	80	10	10	0	0
Poster 4	80	10	10	0	0
Poster 5	70	28	2	0	0
Poster 7	10	0	90	0	0
Poster 8	0	0	50	50	0
Poster 9	0	0	50	0	50
Poster 10	0	0	50	50	0
Poster 11	0	0	100	0	0
Poster 12	0	0	100	0	0
Poster 13	20	0	40	40	0
Poster 14	40	40	20	0	0
Poster 15	0	0	100	0	0
Poster 16	1	5	90	0	1
Poster 17	80	10	10	0	0
Poster 18	25	25	25	25	0
Poster 19	20	20	20	20	20
Poster 20	0	100	0	1	0
Poster 21	70	5	25	0	0
Poster 22	70	5	25	0	0
Poster 23	0	30	0	70	0
Poster 25	0	100	0	0	0
Poster 26	50	50	0	0	0
Poster 27	withdrawn				
Poster 28	0	0	100	0	0
Poster 29	0	0	50	0	50
Poster 30	50	88	50	0	0
Poster 31	0	0	75	25	0
Poster 32	0	0	100	0	0
Poster 33	10	30	50	10	0
Poster 34	withdrawn				
Poster 35	8	35	50	5	2

Podium/Poster Number	Modality %: Radiography / Fluoroscopy	Modality %: CT	Modality %: MRI	Modality %: US	Modality %: Nuclear Medicine
Poster 36	10	10	60	20	
Poster 37	90	5	5	0	0
Poster 38	80	0	20	0	0
Poster 39	0	4	100	0	0
Poster 40	0	5	90	5	0
Poster 41	0	50	50	0	0
Poster 42	0	0	100	0	0
Poster 43	0	0	100	0	0
Poster 44	50	0	50	0	

AUTHOR INDEX

Society of Skeletal Radiology

42nd Annual Meeting

March 10-13, 2019

Author Index

X

Y

Z